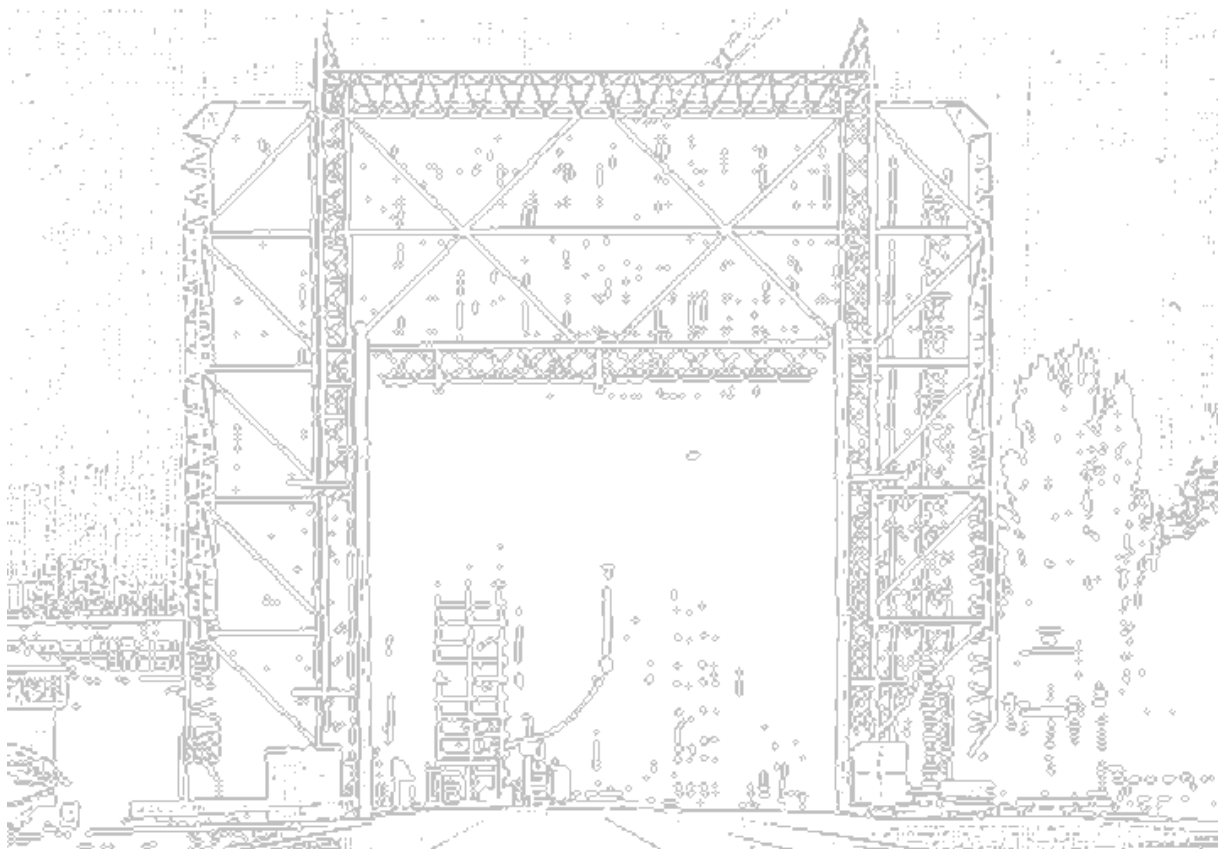


Technische Universität Graz

DISSERTATION



Institut für Hochspannungstechnik und Systemmanagement

Oil-cellulose insulation systems for HVDC applications

Contributions to ageing behaviour, electrical conductivity and charging
tendency

Dissertation

zur Erlangung des Grades eines
Doktors der technischen Wissenschaften

genehmigt von der
Fakultät für Elektrotechnik und Informationstechnik
an der
Technischen Universität Graz

vorgelegt von

Dipl.-Ing. Thomas JUDENDORFER

1. Begutachter: O. Univ.-Prof. Dipl.-Ing. Dr. Dr. h.c. Michael MUHR
 2. Begutachter: Prof. Dr.-Ing. Ernst GOCKENBACH, Leibniz Universität Hannover, Deutschland
- Supervisor: Dr. Wolfgang EXNER, WICOR Holding AG, Schweiz

Institut für Hochspannungstechnik und Systemmanagement
Technische Universität Graz

Vorstand: O. Univ.-Prof. Dipl.-Ing. Dr. Dr. h.c. Michael MUHR

Graz, im April 2012

Oil-cellulose insulation systems for HVDC applications

Öl-Zellulose Isolationssysteme für HGÜ-Anwendungen

Contributions to ageing behaviour, electrical conductivity and charging tendency

Beiträge zum Alterungsverhalten, der elektrischen Leitfähigkeit sowie zum Aufladungsverhalten

© 2012 by Thomas Judendorfer, use for non-commercial and educational purpose permitted

Annotation: Please note that within this thesis the *dot* "." is used as digit grouping symbol whereas the *comma* "," is used as decimal symbol.

Important Note: Measurement data and results are basically valid for the investigated samples only. **Under no circumstances any of these values should be the sole basis for a design process!** Due to possible variability in the manufacturing process and/or in the material composition, materials can differ strongly from the ones tested within this work. Even an identical material data sheet is not a guarantee for having actually the same materials. In a design process it is therefore recommended to repeat the necessary measurements for the materials which are intended to be used.

Abstract

The transmission of electrical energy with direct voltage and direct current (DC) respectively was considered and also applied (with comparable low voltages) already since the beginning of high voltage engineering. With the need of transporting large amounts of electrical energy (*bulk power transport*) over long-distances between several 100 and more than 1.000 km, HVDC transmission schemes are increasingly interesting.

The electrical design of HVDC equipment (converter transformers, bushings, cables, insulators,...) is significantly different from a pure AC design. When designing AC equipment, basically only the relative permittivities ϵ_r are relevant for the electrical field distribution and in succession also for the stress onto the insulation system. When considering an oil gap and a pressboard layer of same thickness, in a general approach the oil gap would be stressed twice as much as the cellulosic component due to field displacement. At DC stress these relations are strongly different, as now the electrical conductivities σ are relevant for the electrical field distribution. Typically, the cellulosic components are stressed (up to a factor of 100 or more) higher than the oil gaps.

Unfortunately, the electrical conductivity σ of typical insulating materials is, in contrary to the relative permittivity ϵ_r , dependent on many factors. This bears a challenge in terms of safe insulation system design. One of the main parameters is temperature, but also electrical field strength, moisture content and ageing condition can pose an influence.

In the scope of this work pressboard and various insulating oils (based on mineral oils) are investigated. The focus is on the topics "electrical conductivity", "ageing behaviour" and "charging behaviour".

The **electrical conductivity of Transformerboard T IV** (WEIDMANN) **and** the **insulating oils** Nynas Nytro 4000X, Shell Diala GX and Nynas Nytro 10XN in dependence of the above mentioned parameters is determined. To do so, customized test cells have been designed and constructed and also commercial available test cells have been utilized.

The **influence of ageing** onto the electrical conductivity is researched. For this reason, artificial ageing of samples at laboratory scale at 135°C has been conducted. Ageing durations between 1 and 32 weeks were considered. Furthermore, the influence of a combined thermal-electrically ageing is studied.

In large power transformers, the **electrostatic charging tendency (ECT)** plays an important role. Exemplary, the charging behaviour of unaged and aged pressboard samples is investigated with a set-up based on the spinning-disc principle.

Space charges can have a significant influence onto the electrical field and stress distribution respectively within an insulating material. With an electro-acoustic method (PEA), the space charge distribution in pressboard (T IV) and paper samples was investigated at different temperatures and for varied ageing conditions.

Keywords: Oil-cellulose insulation systems, high voltage direct current (HVDC), thermal and combined ageing, electrical conductivity, electrostatic charging tendency (ECT), space charges

Kurzfassung

Die Übertragung von elektrischer Energie mit Gleichspannung (DC¹) wurde schon seit Beginn der Hochspannungstechnik in Betracht gezogen und für (heutzutage verhältnismäßig) kleine Spannungen auch angewandt. Erst durch die Notwendigkeit, große Mengen elektrischer Energie (*Bulk Power Transport*) über weite Entfernungen (mehrere 100 bis zu über 1.000 km) zu übertragen sowie durch die Verfügbarkeit von geeigneten Leistungshalbleitern erfreut sich die HGÜ-Technologie wieder steigender Beliebtheit.

Die Auslegung von elektrischen Betriebsmitteln für HGÜ-Systeme (Konvertertransformatoren, Durchführungen, Kabel, Isolatoren,...) unterscheidet sich signifikant von jener für reinen Wechselspannungsbetrieb (AC). Wird nach Wechselspannungskriterien dimensioniert, so sind die (relativen) Permittivitäten ϵ_r für die Verteilung des elektrischen Feldes und damit auch für die Beanspruchung des Isolationssystems verantwortlich. Bei typischen Öl-Zellulose-Isolationssystemen führt dies dazu, dass üblicherweise die Ölstrecken durch Feldverdrängung etwa doppelt so hoch belastet werden wie die Zellulosekomponenten Papier und Pressboard. Hinsichtlich einer Gleichspannungsbeanspruchung verschiebt sich dieses Verhältnis jedoch grundlegend, da hier die elektrischen Leitfähigkeiten σ der einzelnen Materialien für die Verteilung des elektrischen Feldes ausschlaggebend sind. Typischerweise werden hier nun die Feststoffkomponenten (bis zum Faktor 100 und mehr) stärker belastet als die flüssige Komponente des Isolationssystems.

Unglücklicherweise sind elektrische Leitfähigkeiten σ von Isolierwerkstoffen im Gegensatz zur (relativen) Permittivität ϵ_r von vielen Faktoren abhängig, was eine sichere Auslegung des Isolationssystems deutlich erschwert. Die Temperatur hat hierbei maßgeblichen Einfluss auf die elektrischen Leitfähigkeiten. Weiters können die elektrische Feldstärke, der Feuchtegehalt und auch der Alterungszustand für diesen Materialparameter von Bedeutung sein.

Im Rahmen dieser Arbeit werden daher Pressboard und verschiedene Isolieröle auf Mineralölbasis untersucht. Es werden dabei die Themenbereiche "Elektrische Leitfähigkeit", "Alterungsverhalten" sowie "Aufladungsverhalten" behandelt.

Mittels selbst entwickelten und gebauten sowie kommerziell erhältlichen Messaufbauten wurde die **elektrische Leitfähigkeit von Transformerboard T IV (WEIDMANN) sowie den Isolierölen** Nynas Nytro 4000X, Shell Diala GX und Nynas Nytro 10XN in Abhängigkeit der o.a. Parameter untersucht. Ebenso wurde der **Einfluss der Alterung** auf die elektrische Leitfähigkeit dieser Materialien ermittelt. Zu diesem Zweck wurden beschleunigte Alterungsversuche im Labor bei 135°C durchgeführt, wobei die Materialien zwischen 1 und 32 Wochen in Wärmeschränken verblieben. Zusätzlich wurde noch der Einfluss einer kombinierten thermisch-elektrischen Alterung untersucht.

Die **elektrostatische Aufladungsneigung (ECT)** des Öl-Zellulose-Isolationssystems spielt besonders bei größeren Leistungstransformatoren eine wichtige Rolle. Beispielhaft wurde das Aufladungsverhalten von Transformerboard T IV in Kombination mit drei unterschiedlichen Isolierölen in verschiedenen Alterungszuständen mittels einer Spinning-Disc-Anordnung untersucht.

Raumladungen (space charges) beeinflussen die elektrische Feldverteilung in einem Isolierstoff maßgeblich. Mittels einer elektroakustischen Methode (PEA) wurde die Raumladungsverteilung in Transformerboard T IV und Isolierpapier bei verschiedenen Temperaturen und Alterungszuständen ermittelt.

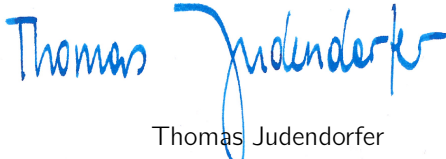
¹Die Abkürzung "DC" steht eigentlich für *direct current*=Gleichstrom; wird jedoch auch synonym für die, den Gleichstrom verursachende Gleichspannung verwendet. Sinngemäß gilt dies auch für AC (*alternating current*=Wechselstrom).

Schlüsselwörter: Öl-Zellulose-Isolationssystem, HGÜ, Thermische und kombinierte Alterung, Elektrische Leitfähigkeit, Elektrostatische Aufladungsneigung (ECT), Raumladungen

EIDESSTATTLICHE ERKLÄRUNG

Ich erkläre an Eides statt, dass ich die vorliegende Arbeit selbstständig verfasst, andere als die angegebenen Quellen/Hilfsmittel nicht benutzt, und die den benutzten Quellen wörtlich und inhaltlich entnommenen Stellen als solche kenntlich gemacht habe.

Graz, im April 2012


Thomas Judendorfer

STATUTORY DECLARATION

I declare that I have authored this thesis independently, that I have not used other than the declared sources / resources, and that I have explicitly marked all material which has been quoted either literally or by content from the used sources.

Graz, April 2012


Thomas Judendorfer

Vorwort

» Keine Schuld ist dringender, als die, Dank zu sagen.* «

Marcus Tullius Cicero, 106 v.Chr. - 43 v.Chr.

Diese Arbeit entstand während meiner Tätigkeit am Institut für Hochspannungsmanagement und Systemtechnik der Technischen Universität Graz im Zeitraum von 2008 bis 2012. Obwohl man selbst natürlich eine Unmenge an Zeit und Energie in die Arbeit investiert, ist es ein Irrglaube, derlei Projekte alleine (erfolgreich) abwickeln zu können. In diesem Sinne möchte ich allen Kollegen, Mitstreitern und Freunden danken, die an dieser Arbeit mitgewirkt haben:

Herrn O.Univ.-Prof. Dipl.-Ing. Dr.techn. Dr.h.c. Michael MUHR sei in seiner Funktion als Institutsvorstand und als Betreuer und Begutachter für die Ermöglichung und Förderung dieser Arbeit herzlichst gedankt. Mein aufrichtiger Dank gilt ebenfalls Herrn Oberrat Dr. Werner LICK für die Anregung zu dieser Arbeit sowie für seine fachliche Unterstützung.

Ganz besonders danken möchte ich der Firma *WEIDMANN Electrical Technology AG* (Rapperswil, CH) und ihren Mitarbeitern, die diese Arbeit großzügig fachlich und finanziell unterstützt und gefördert hat. Die zahlreichen Besprechungen und Diskussionen haben wesentlich zum Gelingen dieser Arbeit beigetragen. Insbesondere sind hier die Herrn Dipl.-Ing. ETH Christoph KRAUSE, Dr.-Ing. Wolfgang EXNER sowie Dr.-Ing. Ugo PIOVAN zu nennen. Herrn Dipl.-Ing. Dr. Stefan JAUFER sowie Hans-Peter GASSER und Frau Kochuthresia KIRIYANTHAN sei ebenfalls für ihre vielen fachlichen Inputs sowie ihre Geduld, mir unter anderem die Untiefen der Chemie und die der Laborpraxis näher zu bringen, gedankt.

Der Firma *Nynas AB* (Nynäshamn, SE) bzw. *Nynas-Technol Handels-GmbH* (Graz, AT) und ihren Mitarbeitern Dipl.-Ing. Gerfrid NEWESELY, Dr. Herbert FRUHMANN sowie Martin STERNER möchte ich für die technischen Hilfestellungen und Diskussionen sowie die unkomplizierte Unterstützung und Zurverfügungstellung von Isolieröl danken. In diesem Zusammenhang bedanke ich mich bei Herrn Dipl.-Ing. Dr.techn. Priv.-Doz. Robert SCHWARZ, Dipl. Ing. Dr. Georg PUKEL, Dipl. Ing. Dr. Christoph KUEN sowie Herrn Dr.-Ing. Ruthard MINKNER für ihre Unterstützung.

Herrn Ao.Univ.-Prof. Dipl.-Ing. Dr.techn. Rudolf WOSCHITZ sei für seinen Support und die Vorarbeit auf dem Gebiet der elektrischen Leitfähigkeit herzlichst gedankt. Für die vielen Anregungen und Ratschläge möchte ich mich bei Herrn Univ.-Doz. Dipl.-Ing. Dr.techn. Christof SUMEREDER bedanken. Ohne die Unterstützung im Öllabor durch Bettina WIESER, Bernhard HEINE sowie Alexander PIRKER hätte ich wohl noch eine Vielzahl von dielektrischen Messungen vor mir.

Den Kollegen der institutseigenen Werkstätte - Anton SCHRIEBL, Gerald MUSTER, Matthias KAINZ und Markus RAPPOLD - die mich bei den Versuchsaufbauten und einer Vielzahl von Spezialanforderungen immer mit Rat und Tat unterstützt haben, sei an dieser Stelle ebenso gedankt. Ohne den Support von Herrn DI Christian AUER in Elektronikbelangen hätte ich sicher wesentlich mehr "Lehrgeld" bei den Schaltungsentwicklungen zahlen müssen und das eine oder andere Gerät wäre wohl im Betrieb "abgeraucht". Erst durch

*Dieser Ausspruch wird Cicero nur *zugeschrieben* und ist somit nicht direkt in seinen Werken zu finden.

die Hilfe von Herrn DI Jürgen PLESCH bei der Programmierung und Abfrage der Messgeräte war die Datengewinnung in dieser Qualität möglich.

Allen Damen und Herren am Institut für Hochspannungstechnik, die mich direkt und indirekt bei der Durchführung dieser Arbeit unterstützt haben, möchte ich an dieser Stelle meinen herzlichen Dank aussprechen. Das angenehme Arbeitsklima hat sicher ebenfalls wesentlich zum Gelingen beigetragen.

Für die Hilfe und den Support bei den (chemischen) Isolierölmessungen möchte ich meinen Dank an Dipl.-Ing. Ernst PAGGER und Joachim THEUERMANN von der *VERBUND-Umwelttechnik GmbH* (St.Andrä, AT), sowie an Dipl.-Ing. Dr. Marlene FRITZ und Ing. Herta LUTTENBERGER (beide *TU Graz*, Institut für Chemische Verfahrenstechnik und Umwelttechnik) richten.

Der Firma *Pamminger Maschinenbau GmbH & Co.KG.* (Linz, AT), insbesondere den beiden Herren Thomas FALTNER und Aleksandar MARINKOVIC sei für Ihre Geduld und Ihre Unterstützung bei der Herstellung der Prüfgefäße gedankt.

Mein ganz besonderer Dank gebührt auch den Damen und Herren am Institut *High Voltage Technology and Management* am Department of Electrical Sustainable Energy der *TU Delft* (NL) für die Unterstützung und den Support bei den Raumladungsmessungen (PEA). Erst durch ihre Hilfe konnte dieser Teil der Arbeit zustandekommen. Daher möchte ich mich bei allen Kollegen herzlichst bedanken, insbesondere bei Prof. Dr. Johan J. SMIT, Dr. Peter H.F. MORSHUIS sowie Herrn Dr. Thomas ANDRITSCH.

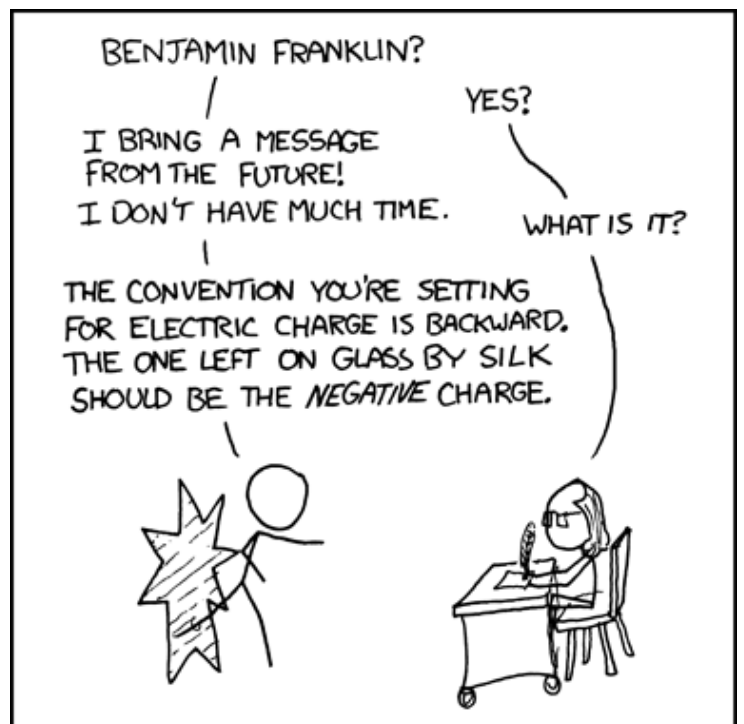
Nicht zuletzt gilt mein herzlichster Dank meinen Eltern, meiner Familie und meinen Freunden. Einerseits für ihre Unterstützung, insbesondere in schwierigen Zeiten und andererseits für ihr Verständnis, mich in den letzten 4 Jahren wenig oder praktisch nur im Büro gesehen zu haben.

Meiner Freundin Susanne danke ich für ihre Geduld und Ihr Verständnis, insbesondere was die Vielzahl der versäumten Wochenenden betrifft.

DANKE! THANK YOU! BEDANKT! GRAZIE! TACK! DZIĘKUJĘ! 谢谢!

Graz, im April 2012

Thomas Judendorfer
Thomas Judendorfer



WE WERE GOING TO USE THE TIME MACHINE TO PREVENT THE ROBOT APOCALYPSE, BUT THE GUY WHO BUILT IT WAS AN ELECTRICAL ENGINEER.

Contents

1	Introduction	1
1.1	Transmission of electrical energy at high voltages	1
1.2	HVDC-High voltage, direct current: Theory and applications	2
1.3	Problem description	9
1.4	Main goals and scope of work	11
2	Basics of oil-cellulose insulation systems for HVDC applications	13
2.1	Introduction	13
2.2	Cellulose: Insulation paper and pressboard	15
2.3	Insulation oils	18
3	Ageing behaviour of oil-cellulose insulation systems	21
3.1	Basics	21
3.2	Ageing processes of cellulose	24
3.3	Ageing processes of insulation oil	27
3.4	Ageing models	28
4	Electrical conductivity and charging behaviour	31
4.1	Basics of electrical conductivity	31
4.2	Electrical conductivity of solids: Pressboard	37
4.3	Electrical conductivity of liquids: Mineral insulation oils	40
4.4	Electrical conductivity and oil-cellulose insulation systems	43
4.5	Measurement of electrical conductivity	48
4.6	Charge and charging behaviour	52
4.7	Electrostatic charging tendency (ECT)	55
5	Accelerated ageing and measurement set-ups	59
5.1	Investigated materials and their preparation	59
5.2	Set-ups for accelerated ageing	66
5.3	Electrical conductivity measurement set-ups	70
5.4	Electrostatic charging tendency measurement set-up	73
5.5	Space charge measurement set-up	73
6	Experimental results	75
6.1	General	75

6.2	Electrical conductivity of pressboard	76
6.3	Electrical conductivity of mineral insulating oils	85
6.4	Material parameters after ageing: Pressboard	92
6.5	Material parameters after ageing: Insulating oils	94
6.6	Electrostatic charging behaviour of oil-cellulose insulation systems	97
6.7	Space charges in cellulose	101
7	Conclusions	107
7.1	Electrical conductivity and ageing behaviour	107
7.2	Charging tendency	109
7.3	Recommendations and consequences	110
7.4	Further steps and outlook	111
8	Summary	113
	List of Figures	115
	List of Tables	119
	References	121
	Appendices	135
A	Investigated materials and their preparation	A.1
B	Ageing vessels for thermal ageing	B.1
C	Ageing vessels for combined ageing	C.1
D	Ageing diagnosis: Pressboard	D.1
E	Ageing diagnosis: Mineral insulating oils	E.1
F	Summarized list of equipment and materials used	F.1

Glossary

1.4301	<i>stainless steel</i> (outdated identifier: X5CrNi18-10 or AISI 304, V2A)
AC	A lternating C urrent
BRICS	B rasil, R ussia, I ndia, C hina and S outh Africa
CAS#	C hemical A bstracts S ervice; <i>unique numerical identifiers for chemicals</i>
CDM	C harge D ifference M ethod
CIGRÉ	C onseil I nternational des G randes R éseaux É lectriques
DC	D irect C urrent
DP	D egree of P olymerisation; <i>average length of cellulose macro-molecules</i>
EC#	E uropean C ommission number; <i>coding for chemicals within the EU</i>
ECT	E lectrostatic C harging T endency
EMC	E lectro M agnetic C ompatibility
ENTSO-E	E uropean N etwork of T ransmission S ystem O perators for E lectricity
EOL	E nd O f L ife
FEM	F inite E lement M ethod
FDS	F requency D omain S pectroscopy
FKM	A basic term for <i>fluoroelastomers</i> (sometimes also labelled as FPM) <i>within this work, FKM sealings have been made from Viton[®]</i>
GIL	G as I nsulated L ine
GIS	G as I nsulated S witchgear
GDT	G as D ischarge T ube
GPIB	G eneral P urpose I nterface B us (or G eneral P urpose I nstrumentation B us)
HF	H igh F requency
HV	H igh V oltage
IEC	I nternational E lectrotechnical C ommission
IEV	I nternational E lectrotechnical V ocabulary; see http://www.electropedia.org
IPA	I so P ropyl A lcohol, also: 2-Propanol
IR	I nfra R ed, wavelengths in the range between 780 nm and 1 mm
KFT	K arl- F ischer- T itration
LV	L ow V oltage

NMR	N uclear M agnetic R esonance
OHL	O ver H ead L ine
OIP	O il- I mpregnated P aper
PB	P ress B oard
PCB	P oly C hlorinated B iphenyls
PDC	P olarisation- D epolarisation C urrent
PE	P oly E thylene
PEA	P ulsed E lectro- A coustic (method)
PP	P oly P ropylene
PR	P olarity R eversal
PTFE	P oly T etra F luoro E thylene, <i>a synthetic fluoropolymer with excellent dielectric and chemical properties; best known as Teflon™ (Brand name of DuPont)</i>
pu	p er u nit
PWP	P ressure W ave P ropagation
RIP	R esin- I mpregnated P aper
RVM	R eturn V oltage M easurement
T III	Transformerboard (shapeable board from WEIDMANN) Pressboard with <i>low density</i> (0,9 g/cm ³) Specified as B 4.1 according to IEC 60641-3-1 (VDE 0315-3-1 [152])
T IV	Transformerboard (Hot-Press-Dried Board from WEIDMANN) Pressboard with <i>high density</i> (1,1 ... 1,2 g/cm ³) Specified as B 3.1 according to IEC 60641-3-1 (VDE 0315-3-1 [152])
UCTE	U nion for the C o-ordination of T ransmission of E lectricity since 2009 superseded by ENTSO-E
UV	U ltra V iolet, wavelengths in the range between 1 and 400 nm
VDEW	V erband D er E lektrizitäts W irtschaft e.V., since 2007 as Bundesverband der Energie- und Wasserwirtschaft e.V. (BDEW) ("Federal Association of the Energy and Water Industry", Germany)
VI	V iscosity I ndex
XLPE	Cross- L inked P oly E thylene

Symbols and constants

A	Area [m ²] (Pre-exponential) rate factor (for ageing processes)
α	Polarizability of a medium/material
a	Lattice parameter Barrier distance in potential energy barrier model
c	Speed of light (in vacuum), $c = 299.792.458$ [m/s] (Exact Value ^A)
C	Capacitance ^B [F]
C_D	Diffusion coefficient [m ² /s]
χ	Electric susceptibility
d	Diameter or distance [mm]
D	Electric flux density [$\frac{A \cdot s}{m^2}$]
E	Electrical field strength [kV/mm] \equiv [MV/m]
E_a	Activation energy [J] \equiv [W · s] or [kJ/mol]
E_f	Fermi energy [eV]
ϵ_0	Vacuum permittivity = $8,854187817(\dots) \cdot 10^{-12}$ [$\frac{A \cdot s}{V \cdot m}$] \equiv [F/m] (Exact Value ^C)
ϵ_r	Relative permittivity of a material
η	Degradation rate Dynamic viscosity ^D [$\frac{kg}{m \cdot s}$] \equiv [$\frac{N \cdot s}{m^2}$] Dynamic viscosity [Poise]
f	Frequency [Hz] \equiv [1/s]
G	Electrical conductance [S]
h	Planck constant ^E , $h = 6,62606957 \cdot 10^{-34}$ [J · s]

I	Electrical current [A]
i	Complex number ($i^2 = -1$)
J	Current density [A/m ²]
k	Ageing rate or chemical reaction rate
k_B	Boltzmann constant ^F $k_b = 1,3806488 \cdot 10^{-23}$ [J/K] or $k_b = 8,6173324$ [eV/K]
κ^{-1}	Debye length
λ	Wave length [m]
μ_0	Vacuum permeability (also known as magnetic constant) $\mu_0 = 4\pi \cdot 10^{-7} = 1,2566370614(\dots) \cdot 10^{-6}$ [$\frac{V \cdot m}{A \cdot s}$] \equiv [N/A ²] (Exact Value ^G) (Ion) mobility [$\frac{m^2}{s \cdot V}$]
n	Number of elements, charge carriers, etc.
ν	(Kinematic) viscosity [m ² /s]
N_A	Avogadro constant ^H , $N_A = 6,02214129 \cdot 10^{23}$ [1/mol]
n_B	Refractive index
ω	Angular velocity [1/s] or [rad/s]
P	(Real) Power (or active power) ^I [W] Probability
Q, q	Electrical charge ^J [C]
R	Electrical resistance ^K [Ω] (Molar) Gas constant ^L , $R = 8,3144621$ [$\frac{J}{mol \cdot K}$]
ρ	Specific resistivity ^M [$\Omega \cdot m$] Density [kg/m ³]

ρ	Kinematic viscosity [$\frac{\text{m}^2}{\text{s}}$]
ρ_{SD}	Space charge density [C/m^3]
S	Complex power [$\text{V} \cdot \text{A}$]
σ	Electrical conductivity ^N [S/m] or [$\frac{1}{\Omega \cdot \text{m}}$]; sometimes also κ or γ are used
T	Temperature [$^{\circ}\text{C}$]; temperature intervals are given in [K]
t	Time [s]
τ	Time constant, for RC elements $\tau = R \cdot C \equiv [\Omega \cdot \text{F}] = \left[\frac{\text{kg} \cdot \text{m}^2}{\text{A}^2 \cdot \text{s}^3} \right] \cdot \left[\frac{\text{A}^2 \cdot \text{s}^4}{\text{kg} \cdot \text{m}^2} \right] = [\text{s}]$
Φ	Work function of a material [eV]
U	Electrical voltage ^O [V]
U_{BDS}	Impulse voltage breakdown strength [V]
u	Dipole moment ^P [$\text{C} \cdot \text{m}$]
ν_0	Oscillation frequency (of a molecule)
ν_D	(Drift) velocity [m/s]
z	Ionic strength of an electrolyte [mol/m^3]

^AExact value; value taken from <http://physics.nist.gov/cgi-bin/cuu/Value?c>

^B $1\text{F} = \frac{\text{A} \cdot \text{s}}{\text{V}}$

^CExact value, also known as electric constant; value taken from <http://physics.nist.gov/cgi-bin/cuu/Value?ep0>

^D $1\text{mPa} \cdot \text{s} = 0,001 \frac{\text{N} \cdot \text{s}}{\text{m}^2}$

^EValue taken from <http://physics.nist.gov/cgi-bin/cuu/Value?h>

^FValue taken from <http://physics.nist.gov/cgi-bin/cuu/Value?k>

^GExact value, value taken from <http://physics.nist.gov/cgi-bin/cuu/Value?mu0>

^HValue taken from <http://physics.nist.gov/cgi-bin/cuu/Value?na>

^I $W = \frac{\text{kg} \cdot \text{m}^2}{\text{s}^3}$

^J $C = \text{A} \cdot \text{s}$

^K $\Omega = \frac{\text{kg} \cdot \text{m}^2}{\text{A}^2 \cdot \text{s}^3} = \frac{\text{J} \cdot \text{s}}{\text{C}^2}$

^Lvalue taken from <http://physics.nist.gov/cgi-bin/cuu/Value?r>

^M $1\Omega \cdot \text{mm}^2/\text{m} = 10^{-6}\Omega \cdot \text{m}$

^N $1\text{S}/\text{m} = \frac{\text{A}^2 \cdot \text{s}^3}{\text{kg} \cdot \text{m}^3}$

^O $1\text{V} = \frac{\text{kg} \cdot \text{m}^2}{\text{A} \cdot \text{s}^3}$

^PThe electrical dipole moment is sometimes given in the unit "Debye" which is equal to $3,33564 \cdot 10^{-30} [\text{C} \cdot \text{m}]$

» *There are no foolish questions and no man becomes a fool until he has stopped asking questions.* «

Charles Steinmetz, 1923

1.1 Transmission of electrical energy at high voltages

Electrical and electrostatics phenomena have been known since ancient times, like the ability of amber to attract small objects, as reported by Thales of Miletus (*624 BC, †546 BC). It took more than two thousand years, until a technologically very simple, first “transmission” line was built in 1729 by the physicist Stephen Gray. He used it to demonstrate that static electricity could be also transferred over certain distances. Although the theory behind was completely unknown during that time, eventually his set-up achieved lengths¹ of around 150 m and he successfully transmitted electricity [10].

The first **transmission line** in that sense was built much later: In 1882, the famous engineer Oscar von Miller built a nearly 60 km long overhead transmission line. This line was operated with 2 kV (DC) to transfer electrical energy from Miesbach to Munich on the occasion of the first electro-technical exhibition in Germany [40, 62]. With the development of two- (1887) and three-phase (1888) alternating current systems and equipment by Nikola Tesla and Michail Ossipowitsch Doliwo-Dobrowolski respectively, electrical energy started its triumphal way into modern society. Shortly afterwards, already the first long-distance transmission line was going to be built. In 1891, electricity was transferred over 169 km on an AC overhead transmission line running at 25 kV [40]. And since then, the operating voltage of (long-distance) transmission lines increased steadily (see Figure 1.1) - and nearly all of them used alternating current (AC).

But also **DC transmission systems** have been considered ever since. This was logical insofar, as the first electrical machines and generators were DC equipment. Already in 1899, a 225 km long DC overhead transmission line (upgraded in 1912 to 125 kV and 19,3 MW) was built between Lyon and Moûtiers by René Thury [4, 78]. Although it was working well with hydro power generation, there have been some technical issues with steam turbines. So eventually this technology vanished temporarily from the scene. A further attempt of DC transmission has been made in Germany in 1940 which led to the installation of a DC cable line in Berlin (15 MW, 100 kV), between the suburbs of Charlottenburg and Moabit (Figure 1.2, a). This project should lay the path for a much more powerful system (60 MW, 400 kV) which was planned as a cable

¹The actual length is not given in [10], but is stated in Britannica Online at: <http://www.britannica.com/EBchecked/topic/242640/Stephen-Gray>, visited on 12.07.2011

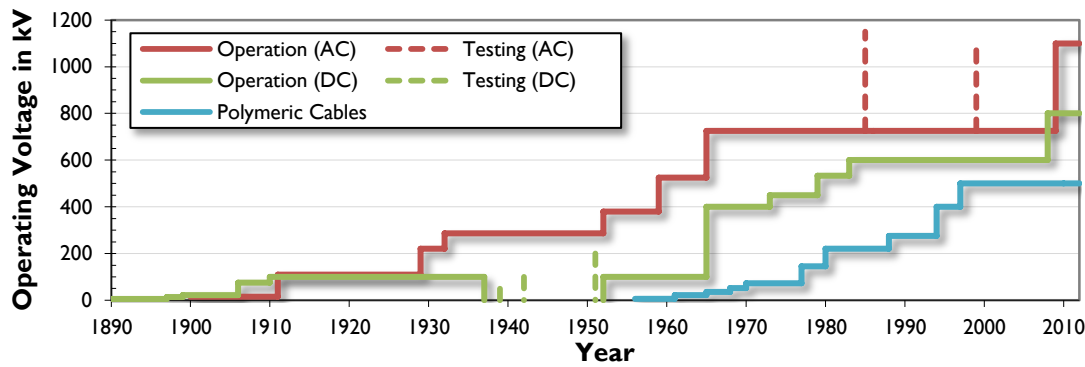


Figure 1.1: Evolution of transmission voltages (adapted from [45, 75, 76, 86])

line from Elbe (near Dessau) to Marienfelde (near Berlin) by Siemens and A.E.G. In 1942, a similar project (100 kV, 400 A) was planned by Brown Boveri and the Badenwerk [62]. However, these projects were not finished due to World War II and the remains of the former project have been transported to the USSR (Russia) as reparations [78].



Figure 1.2: a) AC/DC Test installation in Berlin (1942) between suburbs of Charlottenburg and Moabit²
 b) Valve hall of Gotland 1 Line³ c) Pulling the Gotland cable ashore⁴

It was not before the invention of powerful mercury-arc valves that HVDC transmission could be used on industrial scale. One of the first demonstration schemes was installed in 1939 on the occasion of the regional exhibition in Zurich: An experimental set-up was built to transfer electrical energy from a power plant in Wettingen to the exhibition site in Zurich, a distance of 30 km. This was achieved with a system voltage of 50 kV and a nominal current of 30 A [62]. The famous and often quoted 96 km long **HVDC Gotland cable connection** in 1954 with 100 kV and 20 MW (200 A), which went in operation in 1956, marked the start of modern HVDC transmission schemes [83]. Furthermore, the Gotland connection was also the first usage of a HVDC (mass-impregnated) cable [13]. This link has been upgraded several times and is still in operation nowadays. Since then, voltage and power ratings of HVDC links increased steadily, as indicated by Figure 1.1. Currently, HVDC links with voltage ratings of ± 800 kV and power ratings of 6.000 MW are available.

1.2 HVDC-High voltage, direct current: Theory and applications

The efficiency of electrical energy transmission increases with increasing operational voltage at the same nominal power, as the electrical current can be reduced simultaneously (and so are the losses). As a rule

²Siemens Press Picture, © by Siemens

³© ABB Press Picture, available at [http://www04.abb.com/global/gad/gad02007.nsf/Images/B719955F34122CE6C125776000287684/\\$File/L31115_W_720.jpg](http://www04.abb.com/global/gad/gad02007.nsf/Images/B719955F34122CE6C125776000287684/$File/L31115_W_720.jpg), accessed on 1.10.2011

⁴© ABB Press Picture; from ABB Brochure, available at [http://www05.abb.com/global/scot/scot221.nsf/veritydisplay/1948be2b1f349d61c12576f700210126/\\$file/abbtechnologiesthatchangedtheworld_lowresolution.pdf](http://www05.abb.com/global/scot/scot221.nsf/veritydisplay/1948be2b1f349d61c12576f700210126/$file/abbtechnologiesthatchangedtheworld_lowresolution.pdf), accessed on 1.10.2011

of thumb, the operational voltage of an AC transmission scheme is approximately the line length in km, at which an efficient transmission of electrical energy is possible [47]. Now, there are certain limits in terms of maximum voltages and distances at AC lines. For the following theoretical examples on **AC lines**, no compensation (of reactive power) is considered.

First, the maximum line length must not exceed a quarter of the (electromagnetical) wavelength ($\lambda/4$). This is based on the fact that in a $\lambda/4$ conductor, a short-circuit condition is transformed in a no-load case and vice versa. This is beneficial in signal transmission applications but not in the case of electrical power transmission. For an operational frequency of $f = 50$ Hz and when assuming a wave propagation equal the speed of light (c), the wavelength (λ) is calculated as following:

$$\lambda = \frac{c}{f} \rightarrow \lambda = \frac{299.792.458 \text{ m/s}}{50 \text{ Hz}} \approx 5.996 \text{ km} \quad (1.1)$$

So, the theoretical line length limit is a fourth of this value, approximately 1.499 km. Actually, this applies only to overhead lines, as the speed of (wave) propagation is approximately the speed of light there. For cables, the propagation speed is much lower (around 50% of the speed of light, depending on the dielectric materials used). Therefore, the theoretical line length limitation is even lower for cables than for overhead lines. However, for practical applications, the actual line length limit is smaller than these theoretical limits stated above. This is due to the fact that at lines, which have a length equal to $\lambda/4$, the phase shift between both line ends is 90° , which is unacceptable. To comply with power quality regulations, phase shift should be in the region of around $<40^\circ$ [41], which results in a maximum (uncompensated) line length of around 500 km at AC then. Actually, this depends also on the operational voltage and power, as Figure 1.4 indicates.

Obviously, these disadvantages do not occur when using **direct current** to transmit electrical power. Furthermore, at AC transmission systems, there are losses due to reactive power. These losses are not present at DC transmission schemes. So there is also no need for compensation equipment which is necessary at AC transmission schemes, if they reach certain length limits.

With DC interconnection schemes it is also possible to connect two AC systems which are not running at the same frequency: These are either typically $50 \Leftrightarrow 60$ Hz interconnections (e.g. in Japan) or connections of system blocks which have different frequency controlling (as this was the case in the past with the UCTE⁵ \Leftrightarrow Eastern Europe interconnections for example). Furthermore, short-circuit power of the two coupled networks do not influence each other at a DC interconnection - Therefore, there are no issues with network stability in such cases. On the contrary, though, DC interconnections can increase network stability as the power flow between the two network areas can be regulated.

These are all reasons, why HVDC transmission schemes are getting more and more popular. Especially in the so-called BRICS countries⁶, the distances between electricity generation and load centers are often in the region of several hundred kilometers or more. A transmission technology with low line losses and small land consumption is surely beneficial, which all can be provided by HVDC technology.

In Figure 1.5, the actual transmissible power of different transmission technologies is compared. For AC, a 3-phase system and for DC a bipolar system is assumed. The data has been adapted from [50]. Different colours show the spread of typically transmissible power for each technology.

Now, the transmission of 5 GW over a distance of 1.400 km is investigated exemplary: This could be achieved with different solutions. Assuming a 30 years lifetime for each OHL transmission scheme, according to [127], total costs⁷ would be as following:

⁵The UCTE merged into ENTSO-E in 2009

⁶BRICS = Brasil, Russia, India, China and South Africa; Together they have more than 40% of the worlds population and around 24% of the worlds GDP (2009 data from <http://diepresse.com/home/wirtschaft/international/650188/Aus-den-BRICStaaten-werden-die-BRICSStaaten>)

⁷Total costs consist of line costs, station costs and losses

- 765 kV AC transmission (100% costs)
- 500 kV DC (83% costs)
- 800 kV DC (64% costs)

HVDC transmission characteristics⁸

Advantages

- Reduced losses compared to AC systems
- Reduced number of necessary conductors compared to AC⁹
- Working voltage is equal to rated voltage¹⁰
- No issues with reactive power
- No skin effect
- No (theoretical) limitations of transmission line length
- System-inherent redundancy at bipolar systems (Operation with only one pole and halved power)

Disadvantages

- Expensive converter stations necessary
- Presently, only point-to-point connections feasible¹¹
- Insulation system design is more challenging than for AC systems
- Less operational experience than for AC systems

The transmission of large amounts of electrical energy over long distances (> 500 km) with HVDC is beneficial in several ways, as it is also shown in Figure 1.3. In terms of economics, ecological terms and land usage, HVDC is therefore the preferred option. Other examples can be found in [5].

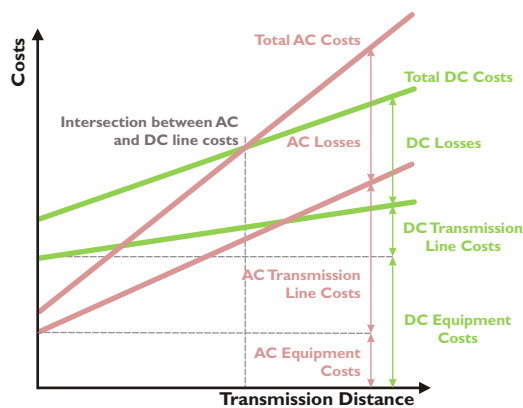


Figure 1.3: Comparison of AC and DC transmission line costs (adapted from [86, 136])

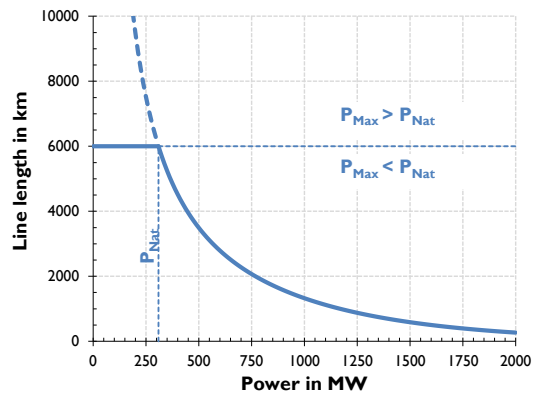


Figure 1.4: Transmissible power with a 1100 kV (uncompensated) AC Overhead line (adapted from [75])

In electrical energy generation and transmission, insulation systems for HVDC are needed in converter stations, high voltage (overhead) lines, bushings and cables. With a focus on the oil-cellulose insulation system, some of them are briefly described below.

⁸Data compiled from [5, 41, 47, 62]

⁹Only 1 conductor (ground return) or 2 conductors (metallic return) are needed instead of 3 conductors for AC 3-phase systems.

¹⁰This is an advantage over AC systems: They need to be designed (=insulated) according the peak value of the AC line voltage (of one phase); power transmission is according to the root mean square (RMS) value however.

¹¹According to [4], there are 2 multi-terminal HVDC schemes currently in operation: Sardinia-Corsica-Italy and Quebec-New England. However, for a large-scale application of multi-terminal applications, DC circuit breakers are necessary [120].

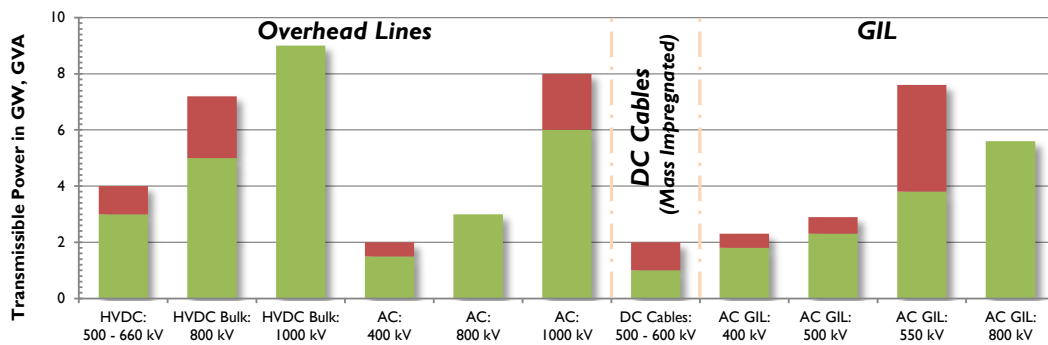


Figure 1.5: Transmissible Power with different line technologies (adapted from [50])

1.2.1 HVDC converter transformers and transmission systems

Transformers have been subjected to strong research and development since they have been developed in 1884¹² [82] and used in energy transmission schemes from then on. Voltage levels and unit power have been increased also rapidly ever since. Although there is one limitation which has been constant also for a long time: Transportation and the transportation profile respectively is defined by limits of railway and road transportation. So the rated power per unit size also increased dramatically during the last decades. Designing a transformer with low losses over the whole operational conditions, which is furthermore cost-effective and possesses a long lifetime is therefore challenging. Requirements tighten when it comes to HVDC converter transformers. Their application and stress differs strongly from standard AC power transformers.

But, and this is similar to standard power transformers, **HVDC converter transformers** are of high importance in terms of asset management: For example, for a typical bipolar 800 kV station (12 pulse conversion), 12 (single phase) converter transformers are used per pole, totalling in 24 transformers per station and 48 for the complete transmission scheme (spare transformers not included)¹³. So, several transformers are used within one converter station. They are quite expensive and long manufacturing and delivery times have to be taken into account for construction or replacement. Of course, this also applies to the bushings (on the transformer side and also the wall bushings on the DC side).

The operational duty and operational stress differs from an AC transformer: HVDC converter transformers have to withstand AC stress on the line side and a mixed stress (AC and DC superimposed) on the valve side. Furthermore, harmonics are more severe at HVDC converter transformers due to the converter/rectifier equipment which results in higher thermal and mechanical stress [77, 120].

Insulation design of a HVDC converter transformer is strongly different from **AC power transformers**: In AC power transformers, most of the electrical field stress is within the oil gaps. As the dielectric withstand behaviour of oil is lower than of cellulosic material and the permittivity is also around 50% lower than the one of paper and pressboard, insulation design is focusing on oil and oil gaps respectively. Solid insulation is used additionally for field grading (angle rings, shielding rings, etc.). As the permittivity of cellulose is around twice as high as the one of oil ($\epsilon_{Oil} \approx 2,0$; $\epsilon_{Board} \approx 4,4 @90^{\circ}C$), the introduction of more solid material is countereffective, as the oil gaps are stressed even more when overall dimensions are kept the same. Therefore it aspired to use only as much solid material as required.

At **DC stress** the situation is exactly the opposite: As the cellulose has a much higher specific resistance than oil ($\sigma_{Oil} \approx < 10^{-13} S/m$; $\sigma_{Board} \approx < 10^{-15} S/m @20^{\circ}C$), the electrical field is mainly concentrated within the pressboard and the paper. So, to avoid breakdown or high dielectric stress, more cellulosic material is

¹²In [46], the first transformer is dated 1883, made by Gibbs and Gaulard to transfer electrical energy over 40 km for lighting purposes with 2000 V AC

¹³If a typical star-star and star-delta transformer scheme is assumed, at least 2 transformers are needed as spare (per station).

introduced [22, 77, 120] for field grading purposes. The electrical field plots for AC, DC and polarity reversal (PR) stress are pictured in Figure 1.6. The scale is the same for all 3 plots (from 0 to 30 kV/mm) to enable a better comparison. The differences between these different stresses can be clearly observed. In reality, the stress which acts onto an insulation system consist of displacement field, (steady-state) DC fields and transients.

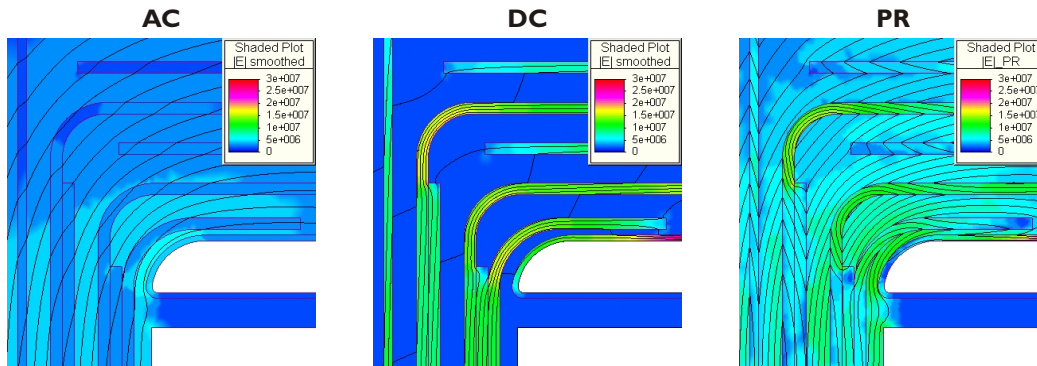


Figure 1.6: Electrical field plot of a converter transformer (end distance) during AC, DC and PR stress (from [122])



Figure 1.7: a) Active part of an HVDC converter transformer during manufacturing¹⁴b) Assembled HVDC converter transformer¹⁵

1.2.2 Bushings

Bushings are insulation systems which have a centre conductor that is insulated from the device itself and its surroundings. So it is possible to conduct current (up to 40 kA) at HV potential (up to 1000 kV) through grounded walls or enclosures. This is needed at transformers, switchgear, HVDC converter station halls, etc. Historically, bushings are often made of porcelain. Inside, oil-impregnated paper (OIP, Figure 1.8) or resin-impregnated paper (RIP, Figure 1.9) is used in most cases as insulation material. Nowadays, RIP is more common, as this technology has several advantages over other technologies (OIP), for example no oil is needed inside the bushing, reduced weight and prolonged service intervals etc. [27]. This does also apply for gas-filled bushings.

Although bushings are quite simple in terms of composition, the design of the insulation system is challenging. There are several possibilities to control the electrical field strength within the bushing (field

¹⁴297 MVA, 550 kV HVDC converter transformer, Siemens Press Picture, © by Siemens, available at http://www.siemens.com/press/pool/de/pressebilder/2009/corporate_communication/2009-12-cop15/300dpi/SOAXX20091223-19_300dpi.jpg

¹⁵ABB press picture, available at [http://www04.abb.com/global/seitp/seitp202.nsf/0/157263868a5c511ac1257839002ac96c/\\$file/Transformator+800+kV+UHVDC+.jpg](http://www04.abb.com/global/seitp/seitp202.nsf/0/157263868a5c511ac1257839002ac96c/$file/Transformator+800+kV+UHVDC+.jpg), last accessed 24.01.2012

grading): geometrical, resistive, refractive, capacitive and non-linear field grading [65]. The length is defined by the voltage level, whereas the current defines the diameter of the conductor and the bushing respectively. Besides electrical specifications, further requirements could be low weight and high mechanical stability. This is even more urgent for HVDC bushings, as they have quite large lengths to fulfil electrical parameters (HV insulation, creepage lengths,...). Furthermore, the current sites for UHV DC application are often subjected to a higher-than-average pollution, which results in further increased necessary creepage lengths [129].

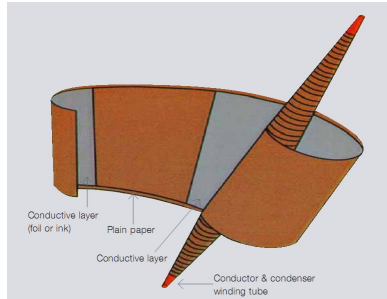
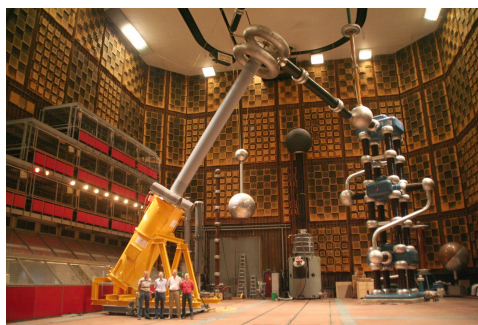


Figure 1.8: Schematic view of a HV condenser bushing core [58] **Figure 1.9:** Modern RIP HV bushing manufacturing [129]

Figure 1.10 shows two gas-filled bushings for HVDC applications: A HVDC converter transformer bushing and a wall bushing.



a) **Figure 1.10:** HVDC bushings for 800 kV systems during testing at Graz University of Technology: a) Transformer bushing¹⁶ b) Wall bushing¹⁶

1.2.3 Cables

Up to now, high voltage cable systems have a niche existence when compared to overhead lines in terms of installed systems length [21]. This is also shown in Figure 1.1. Advanced engineering and materials were needed to handle this complex HV insulation system safely. However, cables are used for special applications like sub sea power transmission ever since. Furthermore, they are also increasingly used in ecological sensitive areas or areas with no/reduced availability of transmission routes, e.g. cities or airports. Finally, they are used for the supply of a multitude of industrial (DC) applications like electrostatic precipitators, microscopes or medical equipment like X-Ray or NMR apparatus.

The **maximum operational voltage**, which is currently in use at AC cable systems, is 525 kV [115]. However, there are plans for 1200 kV cable systems available for quite some time [89]. Most frequently, the system voltage of 400 kV is used for AC systems these days. Cross-linked polyethylene (XLPE) is nowadays the standard insulating material for (AC) high voltage cables (see Figure 1.11, left). This is due to the stable manufacturing process of XLPE cables and environmental issues with oil filled cables, which have been used widely previously. However, in the beginning of XLPE cable application, several failures were caused by treeing and partial discharges. But since these quality issues have been solved, XLPE cables are used successfully in medium and high voltage networks since the late 1970's [65, 102].

¹⁶Image copyright by Graz University of Technology, © Dr. Werner Lick

However, for HVDC applications, the situation is slightly different. XLPE insulated cables have a serious disadvantage when they are used in HVDC applications: Because of the (comparable) high volume resistivity of this polymer (around $10^{16} \Omega \cdot \text{m}$), space charges can be accumulated in the dielectric [11, 13]. If a switching action or polarity reversal is conducted with space charges present in the dielectric, serious overvoltages and dielectric stress can occur [13]. Therefore, it was not before 1999 until a polymeric insulated cable was used for HVDC cables [13]. However, system voltages for HVDC cables based on XLPE are currently limited to 320 kV. Nowadays, up to 1,2 GW can be transmitted with such a single cable system ($\pm 320 \text{ kV}$, $2.500 \text{ mm}^2 \text{ Al-conductor}$) [9].

For higher system voltages/operational currents, mass-impregnated/paper insulated cables are still used (see Figure 1.11, right). They have superior dielectric properties but the accumulation of electrical charge within the dielectric is significantly smaller when compared to XLPE insulated cables. Furthermore, it seems that there is only little influence of oil and paper type as well as electrode material, as indicated in [56]. Independently of the insulation technology used, HVDC cables have some advantages over HVAC cable systems, as already stated on page 4.

The (currently) longest HVDC cable link is the NorNed project, which links Norway with The Netherlands. The link is 580 km long, of which 420 km is carried out as cable line, and can transmit 700 MW at $\pm 450 \text{ kV}$ system voltage [110].

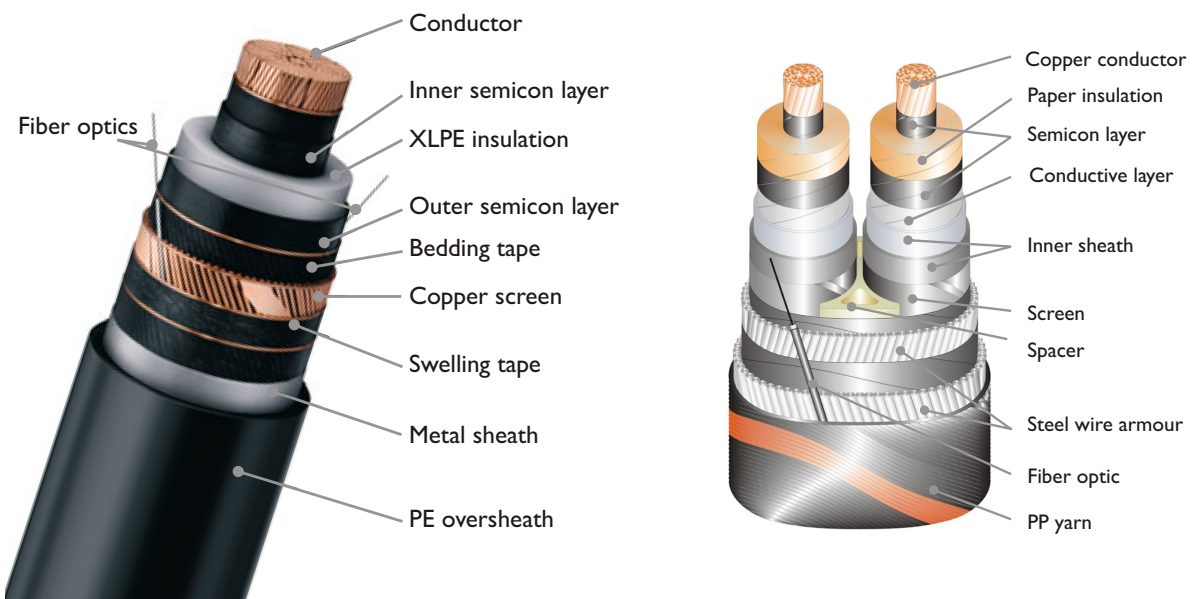


Figure 1.11: Insulation system of a XLPE (left, adapted from [110]) and a mass-impregnated, paper insulated HV cable (right, adapted from [1])

1.3 Problem description

When insulation systems are stressed with DC fields or mixed electrical stress¹⁷, the electrical conductivities of the used insulation materials play a vital role in the distribution of electrical field stress within the insulation system. As accurately formulated in [84]:

- **DC** in its pure form **does not occur**, or if it occurs it is rare
- The physical phenomena, like field configuration and breakdown mechanisms **differ considerable from** those of **AC**
- DC is used for other applications which ask for **other standards of reliability** than for AC

On the contrary, at pure AC stress only the (relative) permittivities ϵ_r are responsible for electrical field distribution (for instance, see Figure 1.12 and [71, 84, 114]). This important material parameter is well known for the materials which are relevant in the sense of (high voltage) electrical engineering. Furthermore, relative permittivity is quite constant over time (=ageing), temperature and within the frequency range of power systems. The dependence of the relevant factor for AC ([relative] permittivity ϵ_r) and DC (conductivity σ) behaviour is shown in the table below [44]:

Table 1.1: Dependence of (relative) permittivity ϵ and electrical conductivity σ on several factors [44]

Dependence on factor	Permittivity ϵ	Conductivity σ
Material	high	high
Electrical field strength E	low	medium
Frequency f	low	"low"
Temperature T	low	high

For decades, **AC apparatus** design engineers had to focus on the oil gaps in oil-board insulation systems, as the oil gaps have been the (electrically) weaker parts [143]. This situation is also intensified, as the ratio of $\epsilon_{\text{Pressboard}}$ to ϵ_{Oil} is somewhere in the region of 2. Simplified, this means that the oil is stressed electrically two times more at equal material thicknesses than the pressboard due to field displacement.

For the design of **HVDC equipment**, the electrical conductivity is the dominating parameter. Typically, the ratio of σ_{Oil} to $\sigma_{\text{Pressboard}}$ is higher than 50 at 20°C. In these cases, the solid insulation (pressboard) is stressed strongly by the electric field whereas the stress in the oil is comparable low (at steady state). However, relative permittivities are still important at DC but only during transient stages. This leads to completely different electrical field distribution within an insulation system.

In the following example, a HV bushing is stressed with AC (Figure 1.12) and with a DC-step voltage (Figure 1.13). The transition from AC behaviour (Laplacian¹⁸ field distribution) to a DC behaviour, according to a Poissonian¹⁹ field distribution, can be clearly observed.

Furthermore, as seen in Table 1.1, **electrical conductivity** depends strongly on the material type and temperature but also on the electrical field strength. It may furthermore change with ageing. For insulation systems of large high-voltage power transformers²⁰ or HVDC bushings this has **serious outcomes**:

The electrical conductivity of typical mineral insulating oils which are used currently in transformers, can differ by the factor of 10 (or even more) already when new. Conductivity measurements of used insulation oils from large AC power transformers show a large spread of electrical conductivity, as pictured in Figure 1.14. For typical insulation oils, the change in electrical permittivity between 20 and 105°C is in the region of a few percentage points. In terms of electrical conductivity, the conductivity at 20°C is around 20 up to (or even more) than 100 times lower than the conductivity at 105°C.

¹⁷A combination of AC stress (may also contain substantial harmonic content) and superimposed DC stress

¹⁸Pierre-Simon Laplace (*1749, †1827) Mathematician and Astronomer

¹⁹Siméon Denis Poisson (*1781, †1840) Physicist and Mathematician

²⁰In this case, this will affect HVDC converter transformers.

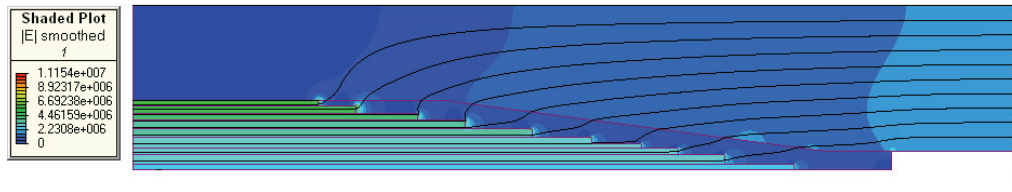


Figure 1.12: FEM model of a HV bushing²¹ for AC application; Electrical field plot with an applied voltage of 230 kV AC (RMS)

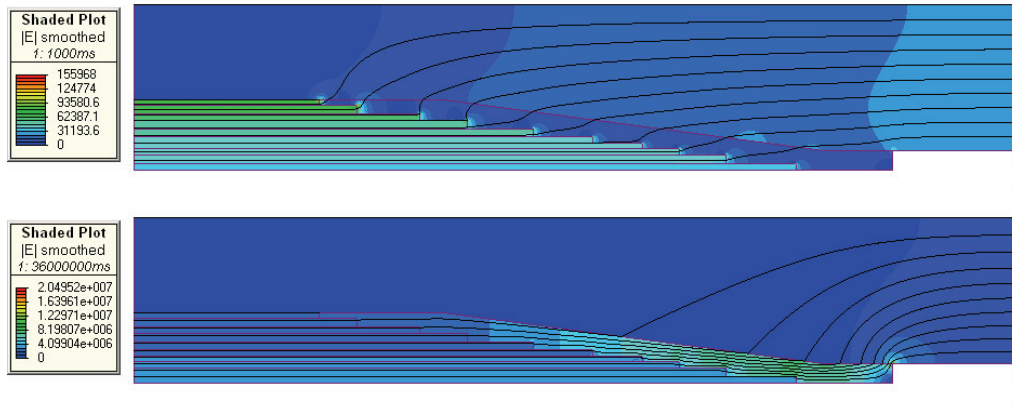


Figure 1.13: AC Bushing²¹ as in Figure 1.12 but with applied step voltage of 326 kV DC. Electrical field plot at 1 ms (top) and 10 h (bottom) after step voltage application

This can lead to undesired situations in terms of electrical field distribution: Electrical field distribution between oil and cellulose (pressboard and paper) depends on equipment operational temperature. Also, the usage of different oils during design, equipment testing and operation lead to different electrical stresses in each case [16]. Ageing (and moisture content) will also contribute to this problem. For equipment design this is very unpleasant as the electrical conductivity (and therefore electrical field distribution) is not easily manageable for all operational conditions.

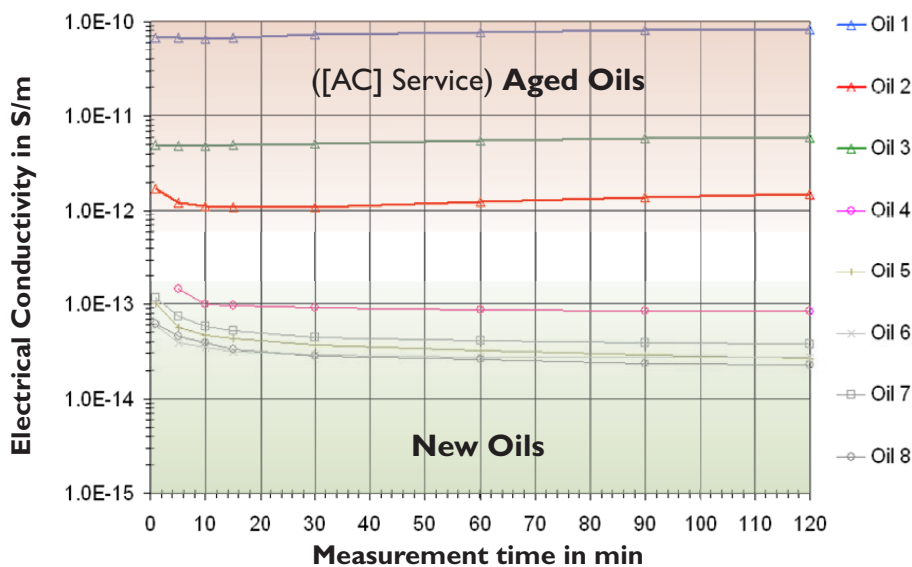


Figure 1.14: Electrical conductivity of various insulation oils, measured at 20°C and $E = 1 \text{ kV/mm}$ (adapted from [16, 59])

²¹FEM-Model adapted from data supplied by Infolytica Corp, available at <http://www.infolytica.com/en/applications/ex0108/>

Present standards and test procedures for the determination of electrical conductivity for oil and pressboard do not replicate the actual needs and furthermore **do not reflect reality good enough**. Such shortcomings in terms of measurement time, -set-up and -methods have been identified also by [71, 123] for example. In general, the test voltages and hence the electrical field stress is too low to get reasonable results²².

For example, the IEC 60093 [52] (VDE 0303-30 [148]) defines typical measurement voltages of 100 V, 500 V or 1000 V. Concerning the measurement time, the standards define a typical time of 1 min, although longer times can be necessary for specific resistances of $10^{10} \Omega \cdot \text{m}$ or higher. As it is known from previous investigations and from the literature (e.g. [59, 71, 90, 114]), it can take several hours or even day(s) to get “stable” current readings for such high resistivities. As the specific resistances of mineral oil and cellulose are comparable high, the resulting current amplitudes at conductivity measurements are quite low (in the range of pA or less). Therefore, great care has to be taken to yield reliable and reproducible results.

These problems are already known for several decades and different methods for the evaluation of electrical conductivity are currently used. They differ in measurement times, electrical field strengths and so forth. For example, **voltage-current measurement** over time, **return voltage measurement (RVM)**, **Polarisation-Depolarisation Current method (PDC)** or **Charge difference method (CDM)** could be used, just to name a few. As the approach differs for these methods, a comparison of electrical conductivity values of different materials could be difficult, especially when they have been conducted with different methods in different laboratories (and probably under different conditions). This is very inconvenient, as it also hinders progress in this research area. A CIGRÉ task force²³ was set up recently to define “at least” a practical standard procedure on electrical conductivity measurements for insulating liquids/oils.

Charging behaviour is an important property for an insulation system. Failures and outages due to electrostatic charging of oil-cellulose insulation systems have been reported in the 1970s and 1980s and are well documented in literature [15, 26]. The **electrostatic charging tendency (ECT)** was identified as main cause for many failures of large high voltage power transformers during or shortly after commissioning. The combination of certain oil-cellulose types and especially the relatively high velocity of the insulation oil due to forced cooling (OD, OF)²⁴ are the key parameters.

Recently, problems due to charging have been identified also at transformers which have been in service for quite a long time and with artificially aged materials respectively [81, 96, 144]. This is in contradiction to the main findings of past ECT research, as problems only happened directly at or shortly after energization there. However, possible problems in terms of ECT due to (oil) ageing have already been reported in literature [96, 144].

1.4 Main goals and scope of work

As it was already described, electrical conductivities play an important role in HVDC equipment design. Although HVDC equipment has been used successfully for several decades by now, knowledge lacks still behind AC system design. A multitude of investigations has been carried out in the past with focus on different parameters and influences to bring some light to this topic. However, the influence of oil-cellulose **ageing onto electrical conductivity** is not covered in relevant literature to a larger extent. Especially the influence of (DC) electrical ageing is not well-investigated.

Therefore, the main goal of this research work is the **determination of electrical conductivity of both mineral oil and pressboard at different ageing conditions**. Electrical conductivity of oil and pressboard

²²When compared to operational conditions

²³CIGRÉ joint working group (JWG) A2/D1-41: “HVDC transformer insulation - Oil conductivity”

²⁴OD...Oil directed; OF...Oil forced

is determined by voltage-current measurements over time. Furthermore, several methods have been applied to assess the ageing condition (moisture content, degree of polymerisation (DP), etc.). Ageing was induced artificially by increased temperature (135°C) and furthermore through application of electrical stress ($U = 10 \text{ kV}$)²⁵. The samples had to be aged artificially in the laboratory as on the one hand no (HVDC equipment) service aged samples have been available. On the other hand, the comparability between samples of different origin would be quite limited anyway. Test cells for artificially ageing of samples and conductivity measurement of pressboard needed to be designed and manufactured.

Also, little is known about the (space) **charge distribution within pressboard** at DC applications. Reasonable knowledge exists about the electrical field and space charge distribution in oil gaps at oil-cellulose insulation systems and in general for a multitude of polymeric materials. Many measurements have been made with different technologies (mostly laser-based systems) at oil gaps. In terms of space charge distribution in the cellulosic insulation part, several works are described in literature, but most of them focused on (thin) insulation paper only [11, 56, 84]. Furthermore, generally these investigations covered only new samples. Therefore, measurements have been conducted on aged samples within this work as well.

Finally, the **electrostatic charging tendency** (ECT) is also investigated for different oil-pressboard combinations and also for different ageing conditions. This topic is of interest, as it has been reported in literature recently that the electrostatic charging tendency of aged cellulose samples has increased when compared to new ones. A test cell based on the spinning disc principle (spinning disc apparatus, [73, 124, 164]) is used within this work.

Outline of the thesis

This thesis is composed of 8 chapters. After a short introduction of the broader topic and the problem description in this chapter, the basics of oil-cellulose insulation systems are described in **Chapter 2**. Here, both oil and cellulose properties and manufacturing processes are pictured.

Chapter 3 gives an overview about the ageing behaviour of oil-cellulose insulation systems. Major ageing factors and selected ageing models, which are described in relevant literature, are described there.

The theory of electrical conduction is covered in **Chapter 4**. Basic principles as well as influencing factors for the electrical conductivity of oil, pressboard and oil-cellulose insulation systems are discussed. Furthermore, the charging behaviour of oil-cellulose insulation systems is described in this chapter. Measurement methods for electrical conductivity and charging behaviour (space charges and electrostatic charging tendency) are also covered.

In **Chapter 5** the practical set-ups for the ageing tests within this work are described. Moreover, the general approach for the measurements and material diagnosis is detailed there. The designed and manufactured test cells as well as the measurement processes and procedures are covered in this chapter.

The results of this work are pictured in **Chapter 6**. This chapter is structured into the divisions *electrical conductivity* and *ageing behaviour* of oil and pressboard respectively and *charging behaviour* of oil-cellulose insulation systems.

Conclusions and outcomes are given in **Chapter 7**. Practical consequences are discussed and an outlook for further work and projects is given. The work itself is summarized in **Chapter 8**.

²⁵This results in an electrical field strength of $E = 10 \text{ kV/mm}$ at the investigated disc-shaped samples (with a thickness of 1 mm).

Basics of oil-cellulose insulation systems for HVDC applications

» *Electric and magnetic forces. May they live for ever, and never be forgot (...)* «

Oliver Heaviside, 1912

2.1 Introduction

Cellulose paper is perfectly qualified as a solid insulating material for high voltage applications. This is due to a very low electrical conductivity, appropriate electrical permittivity and its chemical properties. Furthermore, it is a cheap and renewable material and can be easily manufactured in several ways (moulding, wrapping, bending, sawing, grinding, milling, etc.) [17, 106]. Although there are other (synthetic) insulating materials available, the oil-cellulose insulation system is still the preferred HV insulation for power transformers. The dielectric strength of pure cellulose is very low, as it contains large amounts of air and moisture. Therefore, (mineral) oil is used as the second part in this insulation system to create superior insulation systems [160].

According to [87], the long-term maximum admissible electrical field strength for high-density pressboard is in the region of 40 kV/mm (DC). Breakdown will occur in the region of more than 100 kV/mm (DC), according to [107].

Although in actual high voltage equipment, cellulose is, amongst others, used in the form of paper and pressboard, all investigations within the scope of this work have been carried out with **high-density pressboard only**²⁶.

2.1.1 Historical development

The combination of oil and cellulose is a long proven and successful teamwork as insulation system for high voltage equipment. In the beginning of transformer history, the insulation system was made only from simple asbestos and paperboard assemblies in air [106]. But already since the 1920's paper is used as electrical insulation material in transformers (as a replacement of cotton) [38]. With increasing unit power, oil was introduced to improve both cooling and insulation properties. A breakthrough in insulation system

²⁶The only exception is the usage of K-Buffer paper as reference samples for space charge measurements.

design was achieved with the invention of Transformerboard in the late 1920's [106]. Nowadays, transformers tend to be optimized for several different and often diametrical requirements. Commonly, the stress on the oil-cellulose insulation system has increased when compared to past designs. This can be only achieved successfully - especially in the long-term - if the underlying physical and chemical processes are understood [143].

2.1.2 Oil-cellulose insulation systems

Besides its primary function of providing electrical insulation, an insulation system has to fulfil specific requirements in terms of mechanical and chemical stress as well as regarding thermal and lifetime considerations [12, 24, 61]. In a more general way, an insulation system consists of two or more insulating materials, which are used for a galvanic separation of electrical conducting bodies/materials against ground potential [65]. In the oil-cellulose insulation system, the advantages of both oil and cellulosic components are combined to successfully achieve this task:

Cellulose is a material with a low electrical conductivity and is chemically inert (in its purest form) [160]. However, in its original state it contains substantial amounts of moisture and air, which results in a comparable low dielectric strength.

So, **oil** is used to eliminate air and other gases within the cellulose and improve its dielectric strength. Furthermore, it improves the heat dissipation characteristics of the whole insulation system significantly [24]. On the other hand, cellulose (pressboard) is used to fulfil electrical and mechanical requirements. Pressboard is used to separate large oil gaps into smaller gaps with higher dielectric strength (barrier package) [143].

Although many different synthetic materials have been developed within the last decades, for example aramid fibres (Nomex[®]²⁷) and silicone oils, the insulation system of large power transformers is still based on mineral insulating oils and cellulose products (paper and pressboard). As already noted, this is due to the good (electrical) properties of this insulation system and to the comparable low costs of this solution [14]. Basically, one has to distinguish two different types of oil-cellulose insulation [82]:

- Paper insulation: oil-impregnated paper (OIP)
- Oil-Barrier Insulation: Oil ducts separated by pressboard

So, the insulation system of a transformer always utilizes both, as indicated in Figure 2.1 (b). Paper is used to insulate the conductor wires and pressboard products improve the dielectric strength of oil ducts. Further, such products like angle rings and spacers are used for field grading purposes and they can also fulfil mechanical duties.

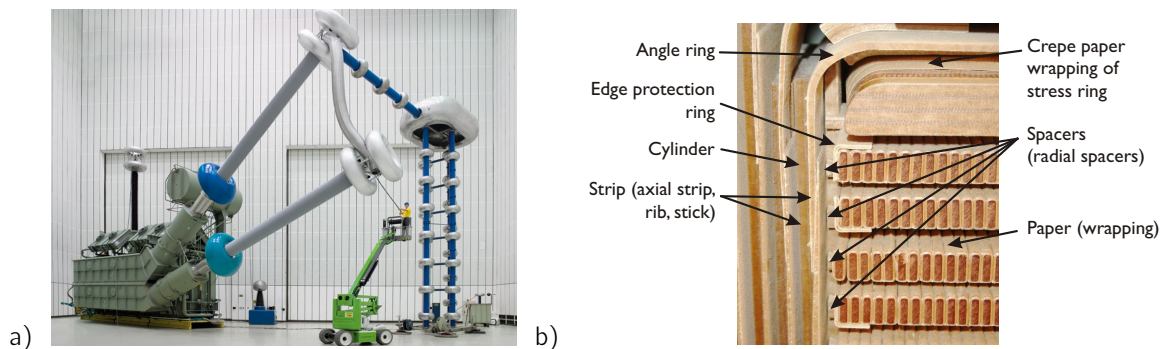


Figure 2.1: a) 800 kV HVDC Converter transformer during HV-test (with 940 kV)²⁸ b) Cross-sectional view of a 220/400 kV (AC) transformer[17]

²⁷Nomex[®] is a registered trademark of DuPont and is the brand name of a material based on aromatic polyamides.

²⁸Siemens Press Picture, © by Siemens

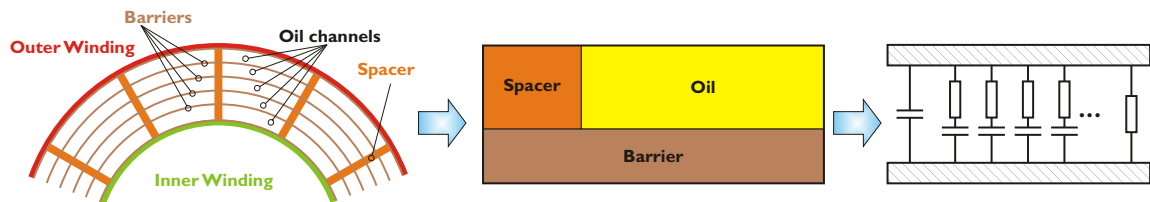


Figure 2.2: Schematic insulation system of a power transformer (adapted from [43, 65]): Section of insulation duct with cylindrical barriers and axial spacers (left); Simplified insulation system model (middle) and Network schematic (right)

2.2 Cellulose: Insulation paper and pressboard

2.2.1 Basics

Cellulose is the most abundant “bio-polymer” and also the most prominent (renewable) raw material worldwide with a yield of around 10^{11} to 10^{12} tons per year. Although cellulose is already used by mankind for several thousand years, the industrial use as a chemical raw material has started only around 150 years ago. The most common form of cellulose is the so-called “hemi-cellulose”, a combination of lignin and cellulose and other polysaccharides [79].

Cellulose itself is a polar compound with pronounced hydrophilic properties. Chemically, cellulose is a **polysaccharide** (long carbohydrate molecule), consisting of H (hydrogen), OH (hydroxyl groups) and C (carbon). Cellulose monomers consist of glucose, which is also known as grape-sugar. However, the basis for cellulose is not the complete glucose molecule $C_6H_{12}O_6$ but reduced by one water molecule (H_2O), which therefore results in $C_6H_{10}O_5$. Actually, the cellulose monomer is not flat but it has a spatial extent, which is only partially accounted in Figure 2.3.

The cellulosic macromolecule consists of several hundreds or up to around 1.000 to 1.500 of such single monomers, linked together via oxygen bridges between the 1st and the 4th carbon atom. The number of these connections is called **degree of polymerisation (DP)**. New wooden cellulosic fibres have a DP of around 2.000, new pressboard (dried and oil impregnated) somewhere in the region below 1.200. The DP is also well suited to describe the mechanical strength of cellulose [48]. In earlier days, often tensile strength was used to describe this property. However, tensile strength is difficult to measure correctly and reproducible. Furthermore, cellulose can experience a drop in tensile strength even in no-load conditions, as described in [34, 126].

Although the cellulose molecule itself seems to be quite simple, one has to distinguish between **three structural levels** [79]:

- Molecular level of a single macromolecule
- Supramolecular level of packing
- Morphological level

Crosslinking takes place between the hydroxyl groups which forms micelles (crystalline regions). For further details about cellulose and its (chemical and physical) properties see [17, 79, 80].

2.2.2 Manufacturing process

The first patent for machine-made paper dates back to 1799, where paper is manufactured in a continuously process [82]. Today, paper is still manufactured that way, whereas board can not be manufactured

²⁹The C atoms at the quadruple linking points within a monomer are not pictured here.

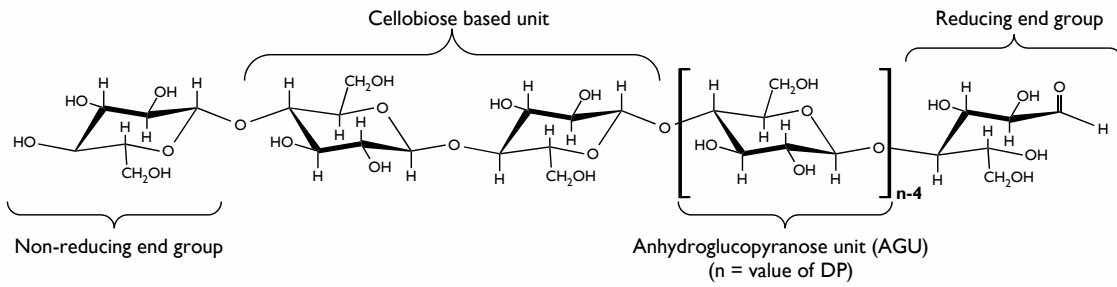


Figure 2.3: Cellulose in its structural form²⁹(D-glucopyranose with 1,4 β-linkages; adapted from [79, 121])

continuously, due to the large thickness of up to 8 mm [106], as shown in Figure 2.4.

Pressboard can be manufactured today in dimensions up to 6,3 x 3,2 m with a thickness of up to 8 mm. If a thicker material is needed, single sheets can be glued together³⁰ to reach a thickness of up to 120 mm.

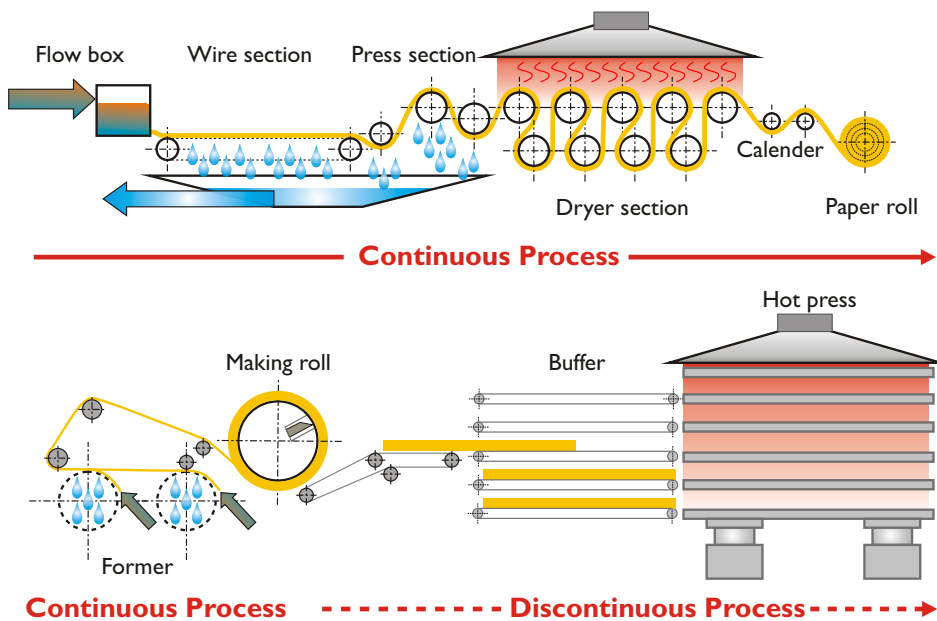


Figure 2.4: Schematic production of paper (above) and pressboard (below); adapted from [82]

Paper and pressboard are manufactured in the “kraft”-process, where unbleached sulfate cellulose is used as a raw material. Unprocessed cellulose contains alpha cellulose, hemi-cellulose and lignin in a larger content. Lignin is also removed in the process. After refining, the pulp contains around 80% cellulose, 10 to 20% hemi-cellulose and 2 to 6% lignin. Cellulosic insulation, as it is used in power transformers for example, is used either in the form of paper or pressboard. Both are manufactured from the same base material and also the manufacturing process is similar, as described below. The main differences can be found in the final production steps and in the addition of stabilisers to protect the cellulose from ageing. The final product (Figure 2.5) can either be paper or pressboard, which can be seen as a “thick insulation paper of the highest quality” [106]. Details about the manufacturing process can be found also in [106].

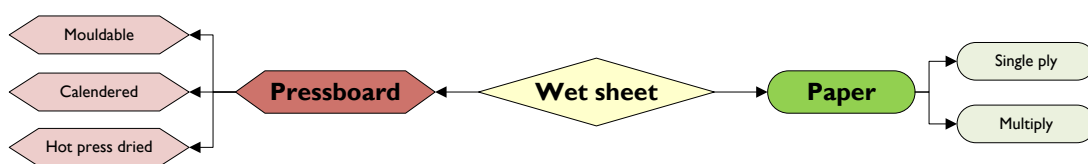


Figure 2.5: Cellulosic insulation products (adapted from [17])

³⁰The glue is based on casein or polyester.

2.2.3 Paper

Insulation paper is the standard insulation material for conductor insulation. As it is very thin (thicknesses of several $100\ \mu\text{m}$), it can be easily wrapped around any conductor shape. Insulation paper can be divided into 2 categories:

- Kraft paper (non-thermally stabilized paper)
- Thermally stabilized paper (Upgraded paper)

Standard paper, which is often referenced as kraft paper is widely used as insulating material, e.g. in winding insulation. Thermally stabilized paper (or upgraded paper) is a chemically treated paper. The reason for this chemical conditioning is the achievement of higher operating service temperatures and/or prolonged lifetime. According to IEC 60076-7 (VDE 0532-76-7 [158]), the degradation rate is reduced this way. There are two methods to achieve this. First, the degradation rate can be reduced, if the water-forming products are (partly) removed from the paper. Secondly, the addition of stabilizers can also lead to a significant improvement of lifetime. According to IEC 60076-7 (VDE 0532-76-7 [158]), a paper is thermally stabilized if the tensile strength is equally or higher than 50% of the original value after 65.000 h ageing in a closed vessel at 110°C or any other time/temperature combination according to:

$$\text{Time (h)} = e^{\left(\frac{15.000}{\Theta_h + 273} - 28,082\right)} \approx 65.000 \cdot e^{\left(\frac{15.000}{\Theta_h + 273} - \frac{15.000}{110 + 273}\right)} \quad (2.1)$$

Θ_h is used as the hot-spot temperature in $^\circ\text{C}$ in the formula above. Thermally stabilized papers are therefore high-quality products and can allow higher operational temperatures of electrical equipment simultaneously with a prolonged lifetime.

2.2.4 Pressboard

The manufacturing process of pressboard has some similarities with the paper process, as seen in Figure 2.4. Transformerboard is the well-known name for high-quality pressboard, manufactured from high-grade sulfate cellulose. Today, pressboard can be manufactured in a variety of thickness ranges and different sheet sizes. Also moulded insulation parts can be manufactured nowadays. High density pressboard, which was used for this work, is standardized in IEC 60641 (VDE 0315-3-1 [152]).

2.2.5 Material preparation

Cellulosic insulation material (paper and pressboard) has a very low dielectric strength when new and untreated (breakdown in the region of several kV/mm only [24]) due to high moisture and air content. Before it can be used as a dielectric, it has to be dried to remove the residual moisture and impregnated to fill the enclosed voids. Moisture inside the cellulose reduces its dielectric strength and increases ageing rate. Furthermore, enclosed air bubbles can start partial discharges due to ionization of the gas voids. Result products of these discharges (like ozone) can also accelerate cellulose and oil degradation rates [24]. It has to be noted, that a "perfect" preparation can never be achieved, so there will be always a small amount of moisture and enclosed air bubbles present all the time. In typical industrial applications, moisture contents of much below than 1% can be reached with vacuum and kerosine drying processes. In fact, moisture contents of around 0,2% are possible when these processes are applied carefully.

Generally speaking, with increasing equipment voltage and dielectric stress respectively, the requirements on the material preparation process increase: For low voltage and even medium voltage applications, drying (evacuation) and impregnation process can be shortened in comparison to cellulose for high voltage equipment.

2.3 Insulation oils

Mineral oil has proven his reliability as electrical insulation fluid for more than 100 years by now. In combination with cellulose it is still used as the main insulation in high-voltage transformers. This is due to the superior dielectric properties, cost effectiveness as well as the possibility to utilize insulating oils as cooling liquid due to its good thermal properties. Furthermore, it can be (and it is still) used as arc extinguishing medium in switchgear equipment. The requirements onto insulation liquids are obviously depending on the electrical equipment, in which the liquid (mineral oil) is going to be used. In the beginning of electrical engineering, air has been used as insulating and cooling medium. Later, mineral and oil based liquids have been utilized. From the 1930's until the late 1980's insulating liquids based on polychlorinated biphenyls (PCB, CAS 1336-36-3; e.g. *chlordiphenyls*, *askarels*) have been widely used in transformers and capacitors. **PCBs** have superior chemical properties, are non-flammable and also possess good electrical properties with a high dielectric strength and a low electrical conductivity. Nevertheless, they have been prohibited totally since 1989 due to their strong negative effects onto the environment and because they are harmful to health [37]. Also, other alternative liquids like oils based on silicone oils and oils based on esters have been developed. However, for large power transformers and HV applications in general, mineral oil is still the standard insulating liquid.

In general, a **distinction between polar and non-polar insulating liquids** can be made. Polar materials and liquids respectively have a constant dipole moment, which result in a displacement of positive and negative charge centres, even when no external influences (electrical field, temperature, pressure,...) are present. A typical characteristic of polar liquids is their high (relative) permittivity, e.g. pure water $\epsilon_r = 81$ [57]. Insulation oils are however mostly of a non-polar type.

2.3.1 Insulation oils for transformers

For transformers and bushings, the most important properties are high dielectric strength, low viscosity (and pour point), high specific heat and thermal conductivity [6]. Low dielectric losses and a high electrical resistivity are also important parameters for an undisturbed equipment operation. On the other hand, the dielectric requirements onto insulation oils for transformers are not that high when compared to other equipment, like in oil-filled cables for example (see Table 2.1). This is due to the fact that the electrical stress during standard operating conditions is comparable low (in the region of several kV/mm). New and clean insulation oil has a dielectric withstand voltage between 30 to even more than 40 kV/mm³¹.

According to IEC 60422 (VDE 0370-2 [154]), there are 4 basic requirements on insulating oils:

- **High dielectric strength** to withstand the dielectric stress during operation
- **Low viscosity** to allow the oil to circulate freely inside the transformer and to enable unhindered heat exchange
- Good **low temperature properties** to enable cold-start of the transformer
- **Oxidation stability** to achieve long equipment operational times

Finally, the insulation must be compatible with all other construction materials used in electrical equipment, e.g. cellulose, steel, copper and so on. For example, issues like corrosion (e.g. due to corrosive sulphur) can lead to problems during equipment operation [20, 100, 109]. During the last decades, insulation oils which are not based on raw mineral oils have been developed. Namely, these are silicone and

³¹This corresponds to a breakdown voltage of around 70 to 100 kV/mm on a 2,5 mm electrode gap, when tested according to IEC 60156 (VDE 0370-5 [156])

Table 2.1: Important properties of insulation liquids for various electrical equipment [161]

Equipment	Important properties of insulation liquids
Bushings	Electrical
Cables	Electrical, gassing characteristics, permittivity, thermal stability
Capacitors	Electrical, gassing characteristics, permittivity, thermal stability
Electronics	Fire resistance, electrical, thermal characteristics
Switchgear	Carbon formation, arc extinguishing
Transformers	Chemical stability, thermal characteristics, (fire resistance in special cases)

ester based oils. Biological degradable oils have entered the scenes. Such oils have a higher flash point than mineral oils, which is advantageous for uses in urban applications. Furthermore, due to their biodegradability, they can be used also in ecological sensitive areas [65].

Table 2.2: Important properties³² of mineral insulation oils [161]

Physical properties	Chemical Properties	Electrical properties
Auto-ignition temperature	Contaminants	Breakdown strength
Coefficient of thermal expansion	Hydrocarbon analysis	Contaminants
Contaminants	Neutralisation value	Dielectric dissipation factor
Density	Nitrogen content	Impulse strength
Fire point	Oxidation stability	Permittivity
Flash point	Saponification value	Volume resistivity
Interfacial tension	Stability to electrical stress (Gassing)	
Molecular weight	Sulphur content and staining	
Pour point	Thermal stability	
Refractive index	Water content	
Solvent power		
Specific heat		
Thermal conductivity		
Vapour pressure		
Viscosity		

2.3.2 Oil composition

Oil quality improved radically since its first usage in high voltage engineering. So, with better insulation liquids available, also the (electrical) stress could be increased. In the 1930's around 3,5 litres of oil were used per kVA in transformers. This value already dropped below 0,25 litres per kVA in the 1980's [113]. Mineral oil is still the most widely used dielectric liquid for high voltage applications. Petroleum crude stocks are the basis for the refinery process to manufacture such oils. Such crude oils consists of many different and individual hydrocarbon compounds. The amount and type of such hydrocarbons varies with the source of the crude oil and therefore later does also the final insulation oil [125]. In detail, final oils can differ strongly in composition and refining processes, oil molecules (aromates, naphtenes and paraphines), sulphur compounds, inhibitors, passivators, etc. [17].

A classification of crude petroleum is given in Table 2.3. However, commonly mineral oil based insulating liquids are classified into three main categories [6]:

- Alkanes (**paraffines**)
- Cycloalkanes (naphtenes, **naphtenics** or cycloparafins)
- **Aromatics**

³²Those parameters, which have been investigated within the scope of this work are highlighted in the table

To transfer crude oil into high quality insulation liquids, the crude stock needs to be refined. Refining must be made carefully and extensively to achieve clean insulation oils with the desired electrical and chemical properties. The main oil parameters are listed in Table 2.2.

Even with modern refining processes (solvent hydrorefining), current insulation liquids are not perfect insulators: They still have a measurable electrical conductivity and dielectric losses. Furthermore, they are still vulnerable to ageing processes and chemical reactions [113, 160].

These three types differ in their configuration as described below [6, 14, 37, 109, 125, 160]:

Paraffinic oils containing mostly straight chained hydrocarbons. Such components are often referenced as alkanes. Carbon atoms are single bonded with linear chains or one or several side branches, for example n-hexane and 2,3-dimethylbutane (linear and branched alkanes respectively with low molecular weight). They have a high viscosity index³³ and a high pour point. A (high) paraffinic content of an insulating oil prevents therefore its ability to flow at low temperatures. This could poses a problem for the “cold-start” of a transformer during winter season, especially at higher latitudes.

Naphtenic oils contain large numbers of iso-paraffins and saturated cycloparaffines (cycloalkanes). They are arranged in one or more ring structures with single bonded carbon atoms (cyclized 5,6 or 7 carbons). Two or more of such ring structures can be bonded together to form a naphthene molecule. Naphtenic molecules may also have linear or branched paraffinic/alkane side chains.

A low viscosity index is typical for naphtenic oils, which is why they offer good cooling properties. Furthermore, they have a low pour point and good dissolving properties.

Aromatic oils have one or more (unsaturated) ring structures. The carbon atoms are double bonded within these structures, and there are roughly the same number of carbon and hydrogen atoms within one structure, e.g. like in the simplest hydrocarbon *benzene* (C₆H₆). Mono-aromatic hydrocarbons contain only discrete benzene ring structures, whereas poly-aromatic hydrocarbons contain 2 or more benzene rings fused together. Aromatic ring structures may have also alkyl side chains and/or naphthenic ring substituents. Aromatic oils are resistant to electric discharges and oil decomposition due to such processes respectively. However, aromatics are in general more reactive than saturated hydrocarbons (alkanes) due to the unsaturated bonds. Therefore they are often removed during refining.

Currently, there are no specified limits for the concentration of various hydrocarbons in transformer oils³⁴.

Table 2.3: Classification of crude petroleum [161]

Class	Petroleum
1	Paraffinic
2	Paraffinic-Intermediate
3	Intermediate-paraffinic
4	Intermediate
5	Intermediate-naphtenic
6	Naphtenic-intermediate
7	Naphtenic
8	Paraffinic-naphtenic
9	Naphtenic-paraffinic

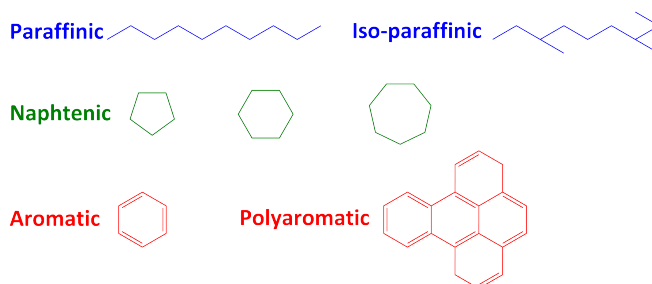


Figure 2.6: Structures of hydrocarbons present in a typical mineral insulation oil (adapted from [113])

³³The viscosity index describes the temperature behaviour of the viscosity of a material, but not the viscosity itself. It is mainly used to characterise lubricating oils but it is also common for insulating oils [161]. A low viscosity index means that the viscosity changes strongly with temperature.

³⁴However, there are other, for example health-related levels: For instance, a note of possible carcinogenic effects can be omitted if the content of DMSO (*Dimethyl sulfoxide* (CH₃)₂SO) extractable compounds (PAHs = *Polycyclic aromatic hydrocarbons*) is less than 3% (e.g. shown in [112]). All three investigated oils comply with this regulation according to their safety datasheets [111, 112, 132]. Such general limits would be impractical nevertheless, as it is very difficult (if not currently impossible) to analyze all molecules within a typical insulation oil, which can go up easily to several hundred different compounds [125].

Ageing behaviour of oil-cellulose insulation systems

» *The strongest of all warriors are these two - Time and Patience* «

Leo Tolstoy, 1869

3.1 Basics

Ageing can be defined as all irreversible chemical and physical processes which are taking place within material in the course of time, according to [29]. In general, the term »ageing« is used to describe a degradation of material properties. However, there are also possibilities, where material properties can be actually improved, for example post-condensation or cross-linking at plastics (polymers) [64].

Temperature is by far the most important ageing factor for oil-cellulose insulation systems and generally also (within a technical temperature range) for nearly all insulation materials. Increasing the operational temperature of any equipment will reduce the lifetime in one way or the other. Basically, it can be distinguished between **chemical and physical ageing processes** [64]:

Chemical ageing processes

Chemical ageing processes are characterized by modification of chemical composition, molecule structure and/or molecule size of one material or at least of one material at multi-component systems.

Physical ageing processes

These are processes during the course of ageing which cause changes and modifications of structure, molecular order state, shape, texture, (measurable) physical conditions and/or concentration ratio of components (at multi-component systems), as long as they are not caused by chemical processes.

In terms of the **causation of ageing**, one can distinguish **two causes** [64]:

Ageing caused by external factors

Physical or chemical (external) interactions of the environment with a material (*exogenic ageing*).

Internal (chemical) reactions of a material, which lead to ageing (*endogenetic ageing*). It is not necessary that an external factor is interacting with the material, the ageing process is purely caused by the material itself.

For electrical/high voltage equipment, the ageing factors/processes are often grouped in the so called TEAM-Stresses:

- Thermal ageing
- Electrical ageing
- Ambient ageing
- Mechanical ageing

It rarely happens that one single ageing factor is present only, in most cases it is a combination of several or all stresses mentioned above. This is described as “**multi-factor ageing**”. The impact of multi-factor ageing is generally more severe than only the “sum” of single effects and ageing factors, as different stresses can interact with each other. These interactions can be generally of a cumulative or an alleviative nature. Generally, multi-factor ageing runs faster as single-factor ageing and therefore the total ageing is accelerated. For example, due to high temperatures inside the equipment, cellulose deteriorates, which releases water. Presence of (additional) water can accelerate ageing significantly.

Oil-cellulose insulation systems are subjected to **ageing processes from the very beginning**. As ageing can not be reversed, the only countermeasures are a slowdown of the ageing processes or the reprocessing of the materials. The former can be achieved by keeping the transformer dry and at moderate operational temperatures for example. **Transformer loading guides** [34, 51] can give guidance here.

Basically, the reprocessing is only possible for the insulation oil, as it can be either exchanged or treated on-line. With the on-line treatment process it is possible to filter particles and remove moisture from the oil. Acidity levels can be reduced and other ageing by-products can be removed when such on-line driers are equipped with fuller’s earth cartridges. In fact, if the oil is treated and dried on-line, moisture can also migrate from the cellulosic materials to the oil, but such a drying effect takes a very long time and for an efficient process the transformer needs to operate at elevated temperatures (above 60°C).

It is not very common to reprocess the cellulosic part (*active part*) of a transformer as it is usually necessary to transport the transformer back to the manufacturer/a workshop, which is very expensive. However, it is now also possible to service the active part directly on-site [98], which is a time-consuming and complex process nevertheless. Therefore it is extremely important to keep the cellulosic insulation in good condition to achieve long equipment lifetime.

The ageing behaviour of oil-cellulose insulation system was subject of many research works during the last decades. Various parameters have been analysed and diagnostic methods have been defined to access the ageing condition of the materials. However, there are still some **black-spots concerning the ageing behaviour**: For example, there is still no consistent ageing model, which can describe all parameters which influence ageing (TEAM stress). Many models are just focusing on the temperature, although several multi-factor ageing models have been developed [103].

Furthermore, there has not been that much research concerning the influence of electrical fields on the ageing process of oil and cellulose as this is the case for pure thermal influences. Especially the influence of pure DC fields has not been documented in that sense in literature, according to present knowledge. Target of this task is to increase the level of knowledge concerning the ageing of pressboard and insulation oils used presently with the influence of temperature and presence of electrical (HV)DC fields. Factors, which are influencing the **ageing of oil-cellulose insulation systems**:

- Temperature and duration (keyword: *thermal cycling*)
- Moisture content
- Gas content (mainly presence of oxygen)
- Electrical stress (operational voltage, partial discharges, short-currents,...)
- Other (material composition/quality/preparation,...)

These main factors are also pictured in Figure 3.1 and are described briefly in the following sections.

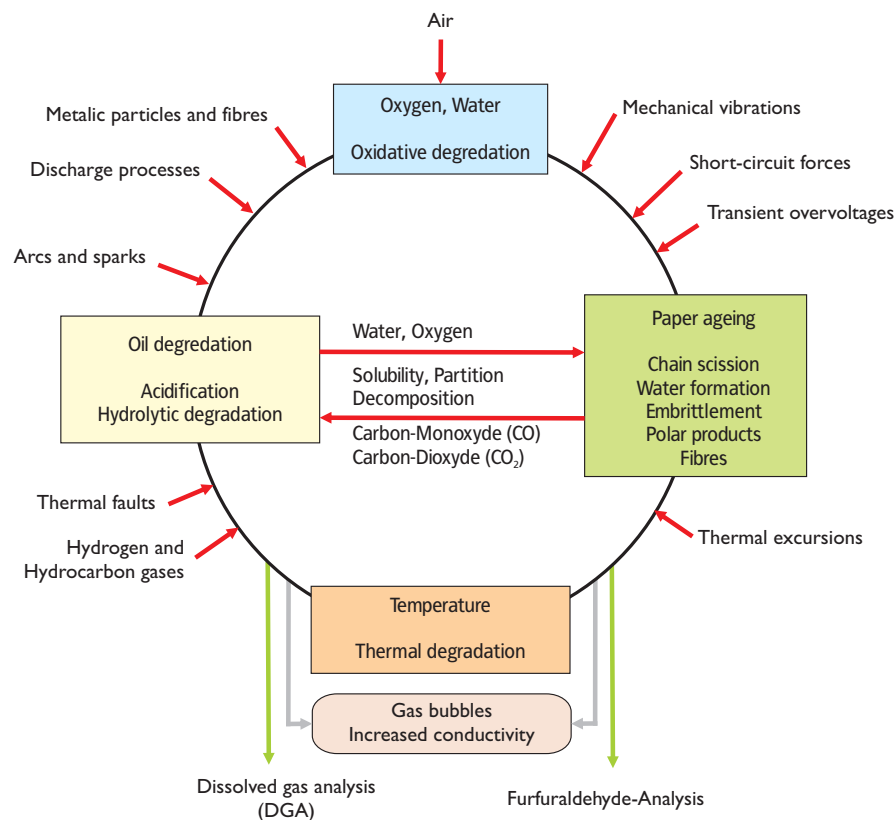


Figure 3.1: Factors influencing performance and degradation of transformer oil/paper insulation and resulting breakdown mechanisms (adapted from [36])

3.1.1 Temperature and the influence of duration

The ageing of oil-cellulose insulation systems is strongly linked to temperature. Vincent M. Montsinger already established a direct relationship between operating temperature and ageing rate in the 1930s [104]. This is also considered in transformer loading guides (e.g. in the IEC transformer loading guide [51]), as an increase in transformer operating temperature by 6 K (steady-state operation; within the temperature range of 80°C to 140°C) results in a reduction of lifetime by 50%. However, there are also other models to describe the influence of temperature - The IEEE transformer loading guide [34] uses the Arrhenius law for example.

3.1.2 Moisture content

Moisture has an important influence on the ageing of the whole oil-cellulose insulation system. If moisture (water) is present in the insulation system, it increases the ageing rate and also the losses (due to an increased $\tan(\delta)$). Furthermore, it reduces the electrical strength of the insulation system dramatically [17]. Basically, **there are three possibilities for moisture being present** in the insulation system:

- Residual moisture (in “dry” condition: around 0,2% for cellulose and <1 ppm for oil)
- Moisture ingress due to construction of insulation system or non-functional/defective sealing
- Ageing of either oil or cellulose or both

The largest part of the moisture (water) is stored in the cellulose, as the following example shows: A modern HVDC converter transformer (240 MVA and 450 kV DC)³⁵ has an oil weight of 130 t and a cellulose

³⁵ Converter transformer used at the NorNed Transmission Project, the data has been taken from http://www2.nynas.com/start/article.cfm?Art_ID=2706&Sec_ID=65

weight of 11 t. When the new and unaged condition of such a transformer is assumed, the moisture levels should be less than 1% in the cellulose and around (or below) 5 ppm in the oil (see [154]). The following image picts this distribution:

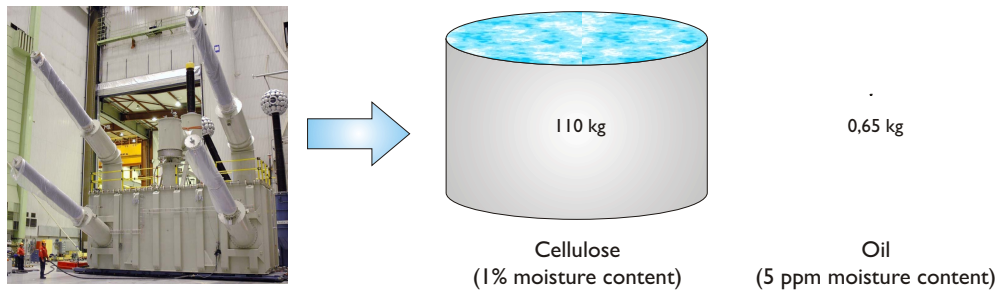


Figure 3.2: Distribution of water content between cellulose and oil for a new transformer³⁶

So, simplified 0,65 kg of water is stored in the oil and 110 kg inside the cellulose. For aged transformers, the situation can get worse: If moisture content of 3% and 15 ppm are assumed respectively, this results in a total water content of 330 kg in the cellulose and 1,95 kg in the oil.

The influence of moisture and oxygen content on the ageing process was investigated first-time in an extensive way in [38] and later in [135].

3.1.3 Gas content and ambient influences

It was already shown in the late 1940s in a large ageing experiment with model transformers [126] that preventing the transformers from ambient air³⁷ is the best way to significantly slow down ageing processes. Such increased ageing would be caused on the one hand due to the presence of oxygen (oxidative ageing) and on the other hand due to the possible ingress of moisture.

3.1.4 Other influences

Generally, the material composition of an ageing sample or all materials present within a transformer can influence the ageing process. For example, plywood is a common material in transformers, which can have a significant influence. Plywood releases acids into the oil [17, 82], especially when operated and artificially aged respectively at elevated temperatures. This can have large influence on the ageing process of the whole oil-cellulose insulation system. In many cases, there are voids within the plywood. Such voids can be the starting point for discharges and dielectrically issues for example [82]. So this might pose a problem for dielectric strength and may therefore have an influence in combined (thermal+electrical) ageing experiments.

3.2 Ageing processes of cellulose

The causes for the cellulose ageing are quite well known nowadays. However, as it is never a single influence of a single factor or material, it is next to impossible to predict (remaining) lifetime accurately. Furthermore, the single ageing processes can influence/interact - and in the worst case also boost - each other. The **main ageing processes of cellulose** are [64]:

³⁶Transformer image taken from [138]

³⁷Or apply at least controlled breathing

- Depolymerisation due to hydrolysis and oxidation
- Hydrolysis in an acid environment
- β -elimination in an alkaline environment
- Formation of crosslinks
- Cornification

3.2.1 Introduction

It is generally understood, that temperature is the main ageing factor for cellulosic materials. Two general approaches are used to describe this process: On the one hand, Montsinger's Law [104] is used (e.g. in the IEC transformer loading guide [51]). Otherwise, in the IEEE loading guide, the Arrhenius law is used [17, 34].

However, both approaches take **chemical reaction kinetics** into account to describe the ageing of cellulose. The main effect of cellulose ageing is a reduction of mechanical strength (tensile strength). Such a parameter decrease can be described basically with chemical reaction kinetics [64]:

$$\text{Reaction rate} = \frac{dC}{dt} = -k \cdot C^n \quad (3.1)$$

C Concentration (in a homogeneous system)

t Time

k Rate constant

n Order

Paper and pressboard will turn brownish at ageing and lose their mechanical strength. Initially, this is not an instant problem, but at mechanical stress situations, e.g. at a short-circuit the cellulose can be severely damaged. This goes in connection with the loss of dielectric strength [38]. The mechanical properties are directly linked to the (average) length of the cellulose molecules. As Figure 3.3 shows, there are typically three stages of ageing in terms of DP value. At a DP of less than around 400 mechanical strength decreases steadily. At a DP of around 250 the tensile strength has already decreased by 50% when compared to the unaged material.

Table 3.1: Duration needed (in years) to reduce the DP of paper from 1.300 to 150 in variation of temperature (from [38])

Temperature in °C	115	110	105	100	95	90	85	80
Duration in years	14	26	50	95	180	350	650	1200

The three main ageing processes for cellulose are **Hydrolysis**, **Oxidation** and **Pyrolysis**, which are described briefly now in the following sections.

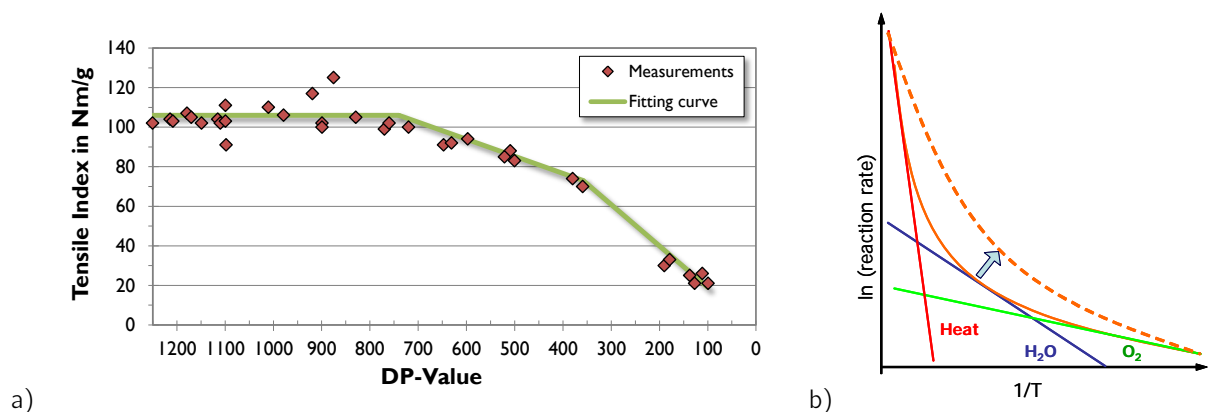


Figure 3.3: a) Correlation between degree of polymerisation (DP-Value) and tensile strength (adapted from [17]) b) Ageing rates of cellulose due to the three main ageing factors [17]: Hydrolysis (H_2O), Oxidation(O_2), Pyrolysis (Heat)

3.2.2 Hydrolysis

With rising moisture content of the cellulose, **water can contribute substantially to cellulose ageing**. At the beginning of equipment life, moisture content levels are low: <0,5% in cellulosic materials and around 10 ppm (or less, e.g. <5 ppm) moisture content in the oil. During operation, water can enter the insulation system, e.g. through leaky sealing or diffusion. Furthermore, water can be formed by cellulose ageing itself, which could be caused by temperature for example. But besides the water content, the organic acid content also influences the reaction kinetics and ageing rate respectively, as summarized in [17]. The reaction kinetics at hydrolysis is often determined with [64]:

$$\frac{1}{DP_n(t)} - \frac{1}{DP_n(0)} = k \cdot t \quad (3.2)$$

$DP_n(0)$ (Average) Degree of Polymerisation (Unaged material)

$DP_n(t)$ (Average) Degree of Polymerisation (after ageing duration t)

k Rate constant

This formula is valid for cellulosic material, which is aged in acid/alkaline liquids in a temperature range between 120 and 200°C [64]. Hydrolysis may be also influenced by low molecular weight acids from oils [17].

3.2.3 Pyrolysis

Thermal degradation - or *pyrolysis* - effects cellulosic material in the range of around **200°C upwards**. Stressing cellulose with such temperatures results in a strong reduction of the degree of polymerisation for example. Therefore, cellulosic insulation material should not be used at continuous (!) operational temperatures of more than around 140°C, otherwise an (accelerated) ageing process takes place [17]. For such high temperature applications, different materials like for example Nomex® could be used.

3.2.4 Oxidative decomposition

The presence of oxygen in an oil-cellulose insulation system can also add to cellulose degradation. Especially in free-breathing transformers, where according to [17], oxygen levels can reach typical values of around 20.000 ppm and approximately 30.000 ppm if the oil is completely saturated. If the **oxygen content can be kept below** 2.000 ppm (e.g. through the means of a sealed transformer) the **ageing rate** can be significantly **reduced** [17]. If the oxygen content is even lower (< 300 ppm), cellulose ageing is slowed down by a factor of around 40 when compared to the free-breathing system [88]. However, these are values gained in laboratory experiments - Practical ageing rates in open transformers are considerable smaller (about 2 to 3 times higher than at closed systems) [17].

3.2.5 Combined stress

In practical applications, all these processes do not occur alone or serially (one process follows an other) - They are all taking place simultaneously to a certain degree. This is also indicated in Figure 3.3 b). The effect of increased water content is demonstrated by the arrow [17]. Multi-ageing factor models are therefore very complex and not easy to handle. In a basic approach, the total ageing rate η could be described as following:

$$\eta_{\text{Total}} = \left(A_{\text{Oxidation}} \cdot e^{\frac{-E_{\text{Oxidation}}}{R \cdot T}} + A_{\text{Hydrolysis}} \cdot e^{\frac{-E_{\text{Hydrolysis}}}{R \cdot T}} + A_{\text{Pyrolysis}} \cdot e^{\frac{-E_{\text{Pyrolysis}}}{R \cdot T}} \right) \cdot t \quad (3.3)$$

The influence of oxidation, hydrolysis and pyrolysis on a real ageing process depends strongly on the temperature and “ambient conditions” (oxygen, water and acid content). Furthermore, there can be autocatalytic reactions and processes which influence each other [17]. Generally, ageing rate increases with rising temperature. According to [17], Hydrolysis doubles for each 6-7 K and Oxidation doubles for each 8-9 K temperature increase. However, the actual temperature step for a lifetime halving depends on several factors, as it will be shown for different ageing models (see Section 3.4).

In fact, **chemical reaction rate doubles for a temperature increase between 2 to 25 K** [48]. This depends on the activation energy E_a , which is given for cellulose aged in oil between 85 and 120 kJ/mol [36, 48]. An average value of 111 kJ/mol was determined in [36].

3.2.6 Countermeasures

The usage of thermally upgraded papers is in fact not a “real” countermeasure against ageing processes. Due to chemical modifications, thermally upgraded paper has a slower decomposition rate (see Section 2.2.3 and equation (2.1) respectively) than normal kraft paper. The ageing rate can be reduced by a factor between 1,5 and 3 [17]. However, their ageing processes might differ from kraft paper in certain properties, e.g. in generation of moisture and acids.

3.3 Ageing processes of insulation oil

3.3.1 Basics

The main ageing mechanism of (mineral oil based) insulating liquids is due to oxidation. Water, low molecular weight acids and larger acids and sludge can be formed, when oils are in contact with oxygen [6]. Sludge can alter thermal properties of oils which can lead to increases losses. Generally, dielectric losses ($\tan(\delta)$) caused by the oil are much lower than the overall losses, so the influence of oil ageing is negligible there [6]. The influence of oxidation at room temperature is low, however with rising temperature also the oxidation rate increases [14]. The presence of an electric field, due to operation or partial discharges, can accelerate the ageing rate and degradation of oil respectively [145].

3.3.2 Countermeasures

Ageing can be avoided (or actually only slowed down) by adding antioxidants and/or metal passivators. Possible passivators can be for example [6]:

- 2,6 DTBP: 2,6-Di-tert-butylphenol (CAS: 128-39-2)
- DBPC: Butylated hydroxytoluene (CAS: 128-37-0)

DBDS (DiBenzilDiSulfide; CAS: 150-60-7) was used in the past as antioxidant additive in lubricants and it was found also in commercially available insulating oils. However, it is now known for its corrosive nature³⁸, especially to metal surfaces and particularly to copper, which is why it is not allowed in new oils, according to new standards e.g. IEC 60296 (4th edition, 2012).

³⁸see exemplary <http://www.seamarconi.com/modules.php?name=Encyclopedia&op=content&tid=25>

3.4 Ageing models

A lifetime of at least 25 years is anticipated for electrical equipment [14]. However, lifetimes of 40 years or more are desirable and already have been already achieved or exceeded in the past. For a theoretical investigation of this topic, several different ageing models have been developed. Although it is not practicable to determine remaining lifetime, a basic approximation of typical lifetimes based on material data is possible. A good introduction into ageing models can be found in Annex I in [34] and in [103].

3.4.1 Ageing model according to Arrhenius

The Arrhenius equation is based on the collision theory, which is a simple mechanical theory to describe chemical reactions [117]. With the Arrhenius equation, which is named after the Swedish Physicist and Chemist Svante August Arrhenius³⁹, it is possible to describe the dependence of temperature onto the chemical reaction rate:

$$k = A \cdot e^{\left(\frac{-E_a}{R \cdot T}\right)} \quad (3.4)$$

- k Reaction rate constant
- A Ageing factor (frequency factor)
- E_a Activation energy [J/mol]
- R Gas constant $R = 8,314$ [J/ (K · mol)]
- T Temperature [K]

This is a zero-order equation: For example, if the ageing rate of cellulose is investigated, it assumes that all chemical bonds might break with equal possibilities. This results in a linear ageing factor A , which is not correct as the ageing factor and ageing rate respectively depends also on the temperature, which will be shown later. As it was shown by [35], especially at progressed ageing (with low DP values), zero order models have a large deviation from actual results.

3.4.2 Ageing model according to Montsinger

Vincent M. Montsinger described a fundamental correlation between equipment lifetime and operational temperature already in the 1920s which has been reported in 1930 [104].

$$k = A \cdot e^{-0,088 \cdot x} \quad (3.5)$$

- k Reaction rate constant (originally named Y...time in years)
- A Ageing factor (frequency factor), constant; $A = 7,15 \cdot 10^4$ [104]
- x (Hotspot) Temperature [°C]

The data and ageing constants respectively have been determined through laboratory experiments in the 1920's on insulation paper samples. This resulted in the often quoted result of lifetime halving by each temperature increase of 8 K. It is already indicated there [104] that if an equipment lifetime of 40 (in fact 46 years) is going to be achieved, the maximum hotspot temperature must be equal or less than 70°C. However, as already found in the 1940's the model and the results have some deficiencies [34]: Most important the ageing rate is not constant but temperature dependent.

³⁹Svante August Arrhenius (*1859, †1927) Physicist (and chemist), Nobel laureate in Chemistry in 1903

3.4.3 Ageing model according to Dakin

Based on the Arrhenius chemical reaction rate theory, a modification to this theory was done by Dakin [28, 34]. Main critics of earlier theories and therefore main driver of this work was the fact that the lifetime halving with temperature increase between 7 and 10 K itself is temperature dependent. This was not accounted before. With this model it is now possible to account that issue.

$$K_0 = A \cdot e^{\left(\frac{B}{\Theta + 273}\right)} \quad (3.6)$$

K_0 Reaction rate constant

A, B . . . Empirical constants

Θ Temperature [°C]

A good overview about different values for the B constant can be found in [34], wherein a value of $B = 15.000$ is suggested.

3.4.4 Ageing models defined in equipment standards

Several “equipment standards” about the operation of transformers have evolved during the last decades, e.g. transformer loading guides. Here, they should be discussed only briefly for the sake of completeness. The major drawback of the ageing models defined in equipment standards is that they still only take the impact of temperature and therefore thermal ageing into account. As it is was shown before, ageing is a much more complex process. Therefore, such models can represent reality only simplified. But already the definition of a single temperature within the equipment, e.g. the “**hot-spot temperature**” of a large power transformer is difficult to make. Firstly, it is not an easy task to define a single “hot-spot” temperature and secondly, there can be large temperature gradients inside the equipment which should be also considered. Generally, only the highest temperature (“hot-spot temperature”) is used for calculations. This is also physically justified, as the higher the temperature, the faster the ageing process is taking place. So this is also an advantage of such methods as only minimal input data is needed. One of the more severe problems of this approach is the utilized ill-defined end-of-life (EOL) criteria, e.g. the 50% of tensile strength, which dates back to Montsinger’s experiments.

Nowadays, the IEEE Standard C57.91 [34], IEC 60076-7 and VDE 0532-76-7 [158] use quite similar approaches for defining a relative service life consumption.

3.4.5 Discussion

The question still arises **when the end-of-life (EOL) is reached?** As already noted in [126], tensile strength might not be the best indicator for this, as transformers with a tensile strength of much lower than 50% can still behave fine during service. However, their ability to withstand short circuits or impulse overvoltages might be low - They could even run on “borrowed time” [126] already, as the remaining lifetime can not be determined safely.

Therefore it was recommended to use the degree of polymerisation instead of the loss of tensile strength as an ageing indicator [34]. Furthermore, there is still a good agreement within certain limits between the degree of polymerisation and tensile strength, as shown in [34, 48].

There is a slight uncertainty in literature, which DP value corresponds to end-of-life. Typically, ranges between 100 and 300 are reported [34, 48, 135]. However, there are reports of HV transformers with DP values less than 100 which are still in service [34]. Within the scope of this work, a DP of less than 300 is considered as EOL.

Electrical conductivity and charging behaviour

» *A hypothetical theory is necessary, as a preliminary step, to reduce the expression of the phenomena to simplicity and order before it is possible to make any progress in framing an abstractive theory.* «

William John Macquorn Rankine, 1855

4.1 Basics of electrical conductivity

Basically, all materials - with the exclusion of metals - are in some sort dielectrics. Therefore, all these materials can be attributed with a relative permittivity ϵ_r and an electrical conductivity σ [23]. Although (ideal electrical) insulators are supposed to have no electrical conductivity at all, as their resistivity⁴⁰ is not infinite in reality. In a perfect insulator ($\sigma = 0$) there would be no conduction current at all. However, in every real dielectric there will be a (small) conduction current, as $\sigma \neq 0$. The magnitude of this current is dependent on several factors, like for example, electrical field strength and temperature. If purely electrical conduction is considered, materials can be therefore classified into 3 categories [63]:

- Superconductors (Resistivity equals zero below a certain transition temperature)
- Conductors: Metals and semiconductors
- Insulators

The **electrical conductivity**⁴¹ itself can be classified into three categories, which will be briefly listed here [63]:

- Intrinsic conductivity
- Extrinsic conductivity
- Injection-controlled conductivity

A material, which posses **intrinsic conductivity**, have charge carriers generated in the material itself by its chemical structure only. Exemplary, this is the case in metals due to free electrons in their valence shells. Copper for example has one free electron per atom, so the total electron concentration is around

⁴⁰In some references, the specific resistance (resistivity) ρ is given in $\frac{\Omega \cdot \text{mm}^2}{\text{m}}$, which equals $10^{-6} \Omega \text{m}$.

⁴¹According to [63] the conductivity covered here (electrical conductivity) can be called *dark electrical conduction*. There, charge carriers are generated by all means other than optical excitation. Otherwise, such conduction needs to be referred as *photoconduction*.

10^{23} per cm^3 [63]. For typical insulating materials intrinsic conductivity is negligible due to its very low value [99].

Extrinsic conductivity is caused by impurities in a materials. However, the origin of such impurities is not important for the conductivity process. Extrinsic conductivity can vary strongly with temperature.

Conductivity can be also caused by charge **carrier injection**. Generally, this is a phenomena which occurs at high (local) electrical field strengths. The charge carriers are hereby mainly injected from metallic electrodes.

Furthermore, electrical **insulators also conduct heat** (thermal energy) **and sound** (mechanical energy). In general, a very low electrical conductivity (=a very large *resistivity*) of 10^{-13} S/m (or more) is desirable for electrical insulators. Nevertheless, there are applications, where such a low electrical conductivity can lead to different problems, e.g. static electrification. Because of high resistivities and therefore very slow relaxation processes, charge could be accumulated at insulators and reach problematic levels. Such processes could happen in DC GIL/GIS spacers or in power transformers - This phenomena is known as electrostatic charging (see Section 4.7).

4.1.1 Definition of electrical conductivity

As shown before, the electrical conductivity of a material describes the ability to conduct electrical current. To begin with, **Ohm's Law** can be applied for electrical conductors:

$$U = R \cdot I \rightarrow \text{Potential [V]} = \text{Resistance } [\Omega] \cdot \text{Current [A]} \quad (4.1)$$

Under the preconditions that R and the specific resistivity ρ are constant and do not vary with time and that the material is **isotropic and linear**, ρ can be defined with equation (4.1) as given in [14]:

$$\rho = \frac{R \cdot A}{d} \rightarrow \frac{U \cdot A}{I \cdot d} \rightarrow \frac{\mathbf{E} \cdot d \cdot A}{\mathbf{J} \cdot A \cdot d} \rightarrow \rho = \frac{\mathbf{E}}{\mathbf{J}} \quad (4.2)$$

It is therefore important that the above mentioned parameters are constant over (measurement) time to receive a correct result and conductivity value respectively. In detail, a thermodynamic equilibrium is necessary, which means that the mobility and density of free carriers need to remain constant [49]. The electrical conductivity σ is the reciprocal of the specific resistance ρ . If this is applied to (4.2), the electrical conductivity σ can be described in the well known form of current density \mathbf{J} and electrical field strength \mathbf{E} .

$$\mathbf{J} = \sigma \cdot \mathbf{E} \quad (4.3)$$

The current density \mathbf{J} is therefore an important parameter, as it defines the distribution of electrical charges [23] with a medium (insulating material). As it will be shown later, the current density can be expressed also as the result of moving charge carriers (charge carrier density n^{42}) with a charge q and a velocity v :

$$\mathbf{J} = n \cdot q \cdot v_D \quad (4.4)$$

The velocity of charge carriers can be directly linked to their mobility μ [23]:

$$v_D = \mu \cdot \mathbf{E} \quad (4.5)$$

⁴²Number of charge carriers per cubic meter

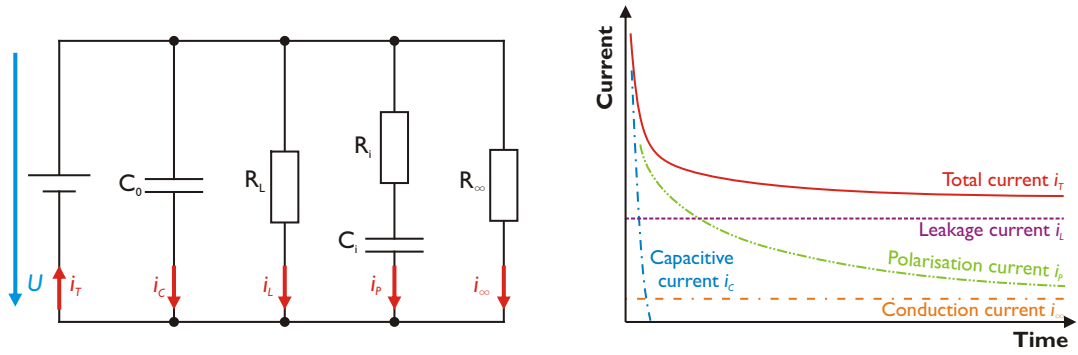


Figure 4.1: Schematic of an insulation system and time trend of currents after voltage application (polarisation; adapted from [32])

Now, if a medium contains i dissociable particulate material, which are generating a volume charge density q_i of free carriers with a mobility μ_i , the electrical conductivity can be expressed as [49, 63]:

$$\sigma = \sum \mu_i \cdot q_i \quad (4.6)$$

The (insulation) material can then be simplified as RC-circuit (Figure 4.1). The conduction current can be expressed by:

$$I_\infty = \frac{U}{R_\infty} \quad (4.7)$$

To describe the (AC) losses of such a material, the dielectric loss factor $\tan(\delta)$ is introduced [25]:

$$\tan(\delta) = \frac{1}{\omega \cdot R \cdot C} = \frac{\sigma}{\omega \cdot \epsilon} \quad (4.8)$$

However, these are very basic relationships as they implies some preconditions:

- A linear relation between the electrical current and the electrical field
- Thermodynamic equilibrium of the material [49]
- A linear and isotropic material

Especially for oil and cellulose (as for all polymers), the relation between electrical field and current is not straightforward. Therefore, these basic equations can not be directly utilized in most cases. If an electrical field is applied to such a material, it **“charges up”** and is **polarised** respectively [14]. This current is the sum of the charging, polarisation and insulation (=conduction) current⁴³, as it is shown in Figure 4.1.

So Ohm's Law (4.1) can be easily applied when considering that $\nabla \cdot \mathbf{J} = 0$, which is true for a pure resistive behaviour [11]. But, electrical conductivity can be influenced by **space charges**. Therefore, a more general approach is taken with **Maxwell's Law** [63] to draw a relationship between the electric field \mathbf{E} and space charge density ρ_{SD} :

$$\rho_{SD} = \nabla \cdot \mathbf{D} = \nabla \cdot \epsilon \cdot \mathbf{E} \quad (4.9)$$

Here, ρ_{SD} is used as the space charge density, ϵ as permittivity and \mathbf{D} as electric flux density. Now, with (4.3) one could determine electrical conductivity, however the more general approach for the current density \mathbf{J} and electrical conductivity σ respectively is given by [11, 61]:

$$\mathbf{J} = \sigma \cdot \mathbf{E} + \epsilon \cdot \frac{\delta \mathbf{E}}{\delta t} + C_D \nabla \rho \quad (4.10)$$

⁴³And a possible leakage current

To sum up, the **electrical current density** can be described as the sum of three single currents: **conduction current, displacement current and convection current** due to space charges.

$$\mathbf{J} = \sigma \cdot \mathbf{E} + \frac{\partial \mathbf{D}}{\partial t} + \rho_{SD} \cdot \mathbf{v} \quad (4.11)$$

A so called “resistive” behaviour (Poisson⁴⁴ field distribution) of a dielectric is reached only through the transition from a “capacitive” behaviour (Laplacian⁴⁵ field distribution with no space charges, see also Figure 4.1). The time needed for this transition, the so called **transition or conduction relaxation time**⁴⁶, can be described with permittivity ϵ and specific resistivity ρ or electrical conductivity σ as [23, 134]:

$$\tau_c = \epsilon \cdot \rho = \frac{\epsilon}{\sigma} \quad (4.12)$$

4.1.2 Dielectric properties of materials

The proportionality factor between electrical field strength \mathbf{E} and the electric displacement field \mathbf{D} is the permittivity ϵ :

$$\mathbf{D} = \epsilon \cdot \mathbf{E} = \epsilon_0 \cdot \epsilon_r \cdot \mathbf{E} \quad (4.13)$$

The (relative) permittivity ϵ_r is one of the most important parameters for insulating materials. Basically it describes the ratio of the capacitance of a given set-up with a specific material to the capacitance with the same set-up and air (more precise: vacuum) as a dielectric [24]. Generally, as it can be seen from (4.13), permittivity describes the quantity of electrical flux which is caused by an electrical field. Permittivity is also related to **electric susceptibility** χ , which describes the ability of a material to response to electrical fields:

$$\epsilon = \epsilon_0 \cdot \epsilon_r = (1 + \chi) \cdot \epsilon_0 \rightarrow \chi = \epsilon_r - 1 \quad (4.14)$$

In general, ϵ_r depends on frequency, temperature and at some materials also on the electrical field strength. With rising temperature, ϵ_r generally decreases as the entropy (disorder) increases concurrently. With increasing thermal (=Brownian⁴⁷) motion, the affinity of molecules to follow an electrical field decreases which results in a decrease of permittivity on the material level.

In fact, ϵ_r is a complex parameter and can be separated into a real (ϵ'_r) and an imaginary part (ϵ''_r):

$$\epsilon_r = \epsilon'_r + i\epsilon''_r \quad (4.15)$$

The real part ϵ'_r is related to the stored energy within a material. Dielectric losses are attributed to the imaginary part ϵ''_r . Polarisation P is the sum of all (N) average dipole moments $\vec{u} = \alpha \vec{E}$ [63]: $P = (N) \langle \vec{u} \rangle$, which are caused by different polarisation mechanisms. The main polarisation mechanisms are described in detail in [23, 25, 63, 163] and pictured in Figure 4.2 below. The time constants of the different mechanisms can be seen there as well.

⁴⁴Siméon Denis Poisson (*1781, †1840) Mathematician, geometer and physicist

⁴⁵Pierre-Simon (Marquis de) Laplace (*1749, †1827) Mathematician and Astronomer

⁴⁶The conduction relaxation time is sometimes referenced as “Maxwell time”.

⁴⁷Robert Brown (*1773, †1858) Botanist

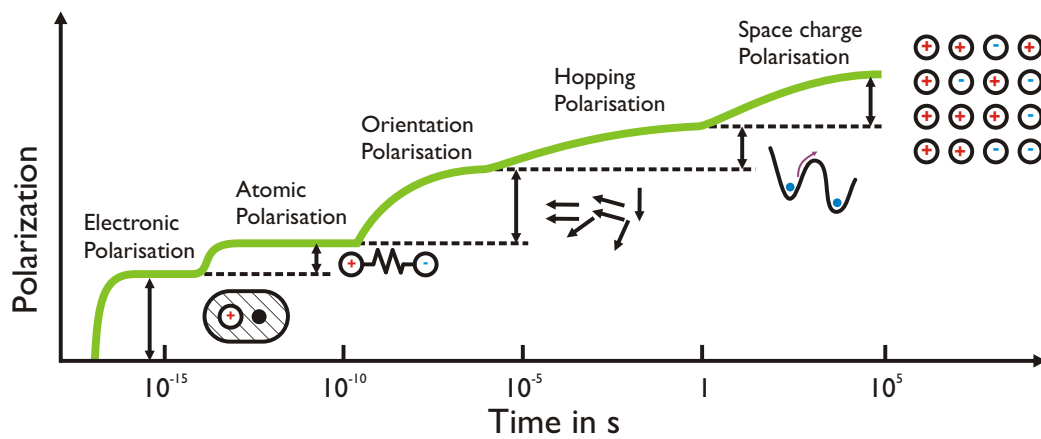


Figure 4.2: Polarisation mechanisms caused by a step-function of the electric field E (adapted from [63])

Electronic and atomic polarisation

Electronic polarisation is caused by a movement of an “electron cloud” in atoms against the (positively charged) atomic nucleus. This polarisation process is dominant at monoatomic gases. In noble gases, the (electronic) polarisation is low, whereas group I elements have the highest polarizability α_e [23, 63]. Due to the low inertia of electrons, electronic polarisation can be found up to frequencies of around 10^{15} Hz, which is in the UV range. Models for the description of α can be found, for example, in [23, 25].

Atomic polarisation describes a process, where atoms or ions are moved which causes a deformation of molecules. In polymeric materials, the change of bond angle or bond distance can cause atomic polarisation [7]. Due to the large(r) inertia, atomic polarisation occurs only at frequencies below the IR range (10^{13} Hz). Electric polarisation is a frequency and temperature dependent mechanism and a linear phenomena. It can cause the [63]:

- Displacement of charges (positive and negative); atoms or molecules
- Orientation of dipoles
- Separation of mobile charge carriers

Electronic polarisation is by far the dominant process of these two. Atomic polarisation is only around 10% of the value of electronic polarisation in non-polar molecules.

Ionic polarisation

Polarisation is induced by charged atoms in certain solids. The magnitude of polarisation is dependent on the structure of the material, which results in values of α_i which are similar to those at electronic polarisation for many materials but can be also much higher (e.g. in ferroelectrics) [23].

Dipolar/Molecular/Orientalional polarisation

Molecular polarisation, which is sometimes referenced as orientational polarization is caused by permanent dipole moments of molecules. Therefore, it occurs only in polar materials and molecules respectively. It can be described with [63]:

$$\alpha_0 = \frac{u_0^2}{3 \cdot k \cdot T} \quad (4.16)$$

Generally (at “standard” conditions), the influence of oriental polarisation is much larger than the one of electronic and atomic polarisation [63].

Interfacial/Space charge polarisation

Interfacial or space charge polarisation occurs when charge carriers with opposite charge signs are separated in the bulk or at dielectric interfaces (space charges) due to an applied electrical field. These charges locally modify the electrical field distribution. Hopping polarisation also falls into this category: Due to the movement of localized charges (e.g. in charge traps) through jumping over (hopping) or tunnelling through a potential barrier, polarisation can occur. These mechanisms are typical for ionic crystals (ions) and in glass and amorphous semiconductors (electrons) [63].

Polarisation of materials

Basically, one can distinguish between **3 types of polarisation** in dielectric (non-ferroelectric) materials:

- Nonpolar materials: $\alpha = \alpha_e$
- Polar materials: $\alpha = \alpha_e + \alpha_i$
- Dipolar materials: $\alpha = \alpha_e + \alpha_i + \alpha_o$

So, in dipolar materials, the total polarisation is the sum of electronic polarisation α_e , ionic polarisation α_i and orientation polarisation α_o . If charge can be trapped within such a material, space charge polarisation also would be needed to consider α_d . Actually, this is further the sum of hopping (α_h) and interfacial (α_c) polarisation [63].

Relaxation processes at different temperatures are often characterized as α , β and γ relaxations with distinctive (loss) peaks at certain temperatures. In a metal (conducting material), the permittivity is $\epsilon = \infty$ at static fields and possesses a finite value at time varying (=AC) fields [63]. More details and the derivation of these formulas can be found there as well.

4.1.3 Electrical double layers

At the interface of a solid and a liquid phase an electric double layer is formed, which was described first by Helmholtz⁴⁸ [6]. This theory was evolved over time by Gouy⁴⁹ and Chapman⁵⁰ and was eventually improved by Otto Stern⁵¹ to the **Stern double layer**. A double layer can form at the liquid-metal interface even without the application of voltage [14].

The double layer effects the electrical and mechanical properties of the interface. The layer close to the solid interface (Stern layer) will not be effected by a flow of the liquid. Ions, which are located in this layer are attached to the (solid) interface and are not removed by liquid flow. On the contrary, ions can move freely in the outer layer (diffuse Gouy-Chapman layer). The liquid in this layer can be convected [23]. This will be of special importance for electrostatic phenomena like ECT (see Section 4.7).

The Debye⁵²-length κ^{-1} is defined as »the distance over which the potential developed by separating a charge density from the background charge of the opposite polarity is equal to the thermal voltage $k_b \cdot T/e$ « [6, 134]:

$$\kappa^{-1} = \sqrt{\frac{\epsilon_r \cdot \epsilon_0 \cdot k_B \cdot T}{2 \cdot N_A \cdot e^2 \cdot z^2}} \quad (4.17)$$

⁴⁸Hermann Ludwig Ferdinand von Helmholtz (*1821, †1894) Physician and Physicist

⁴⁹Louis Georges Gouy (*1854, †1926) Physicist

⁵⁰David Leonard Chapman (*1869, †1958) Physical chemist

⁵¹Otto Stern (*1888, †1969) Physicist and Nobel laureate in physics in 1943

⁵²Peter (Petrus) Debye (*1884, †1966) Physicist and physical chemist, Nobel laureate in Chemistry in 1936

The potential difference ζ describes the potential of the diffuse layer to the undisturbed bulk of the liquid and is referenced as **electrokinetic potential or ζ potential**. More details can be found in [2, 91, 101, 134]. This theory can be also applied for describing interface phenomena on the particle level, for example between nanoparticles and host material [3].

4.2 Electrical conductivity of solids: Pressboard

The conduction process in solids is governed by ionic, electronic or hole conduction. The basic relationships of electronic conduction are shown in the section below. A simplified approach to explain electrical conductivity in materials (solids) is the band model: If there are electrons present in the conduction band⁵³, they can account to electrical conductivity. This is directly the case for metals. Here, the conduction band is fully or partially occupied (e.g. in alkali metals).

Such sharp borders in energy levels, as also pictured in Figure 4.3 are only present in single atoms or crystals with a large lattice parameter a . However, if such atoms are part of a solid or the lattice parameter is significantly reduced, these sharp levels migrate to wider bands due to atom interdependency. Especially the outer energy levels are effected by this process [31, 63]. In Figure 4.4, the development of energy bands and energy band gaps in variation of atom number is shown exemplary.

Where an electron is located depends on the solution(s) of the wave function Ψ [2]. Non-imaginary solutions are corresponding to energy levels and band gaps respectively. Whether an electron can be found in a certain energy level is described by the Fermi⁵⁴-Dirac⁵⁵ distribution function [31]:

$$P(\mathbf{E}, T) = \left[1 + e^{\left(\frac{E - E_f}{k \cdot T} \right)} \right]^{-1} \quad (4.18)$$

Here, E_f is the Fermi energy. At a temperature of $T = 0\text{K}$, all electrons are below the energy level of E_f . The "highest" energy band, which is filled at absolute zero is also called **valence band** and the first unoccupied band is the **conduction band** (see also Figure 4.3). The **band gap** is a kind of forbidden zone, where no electrons can be placed (imaginary solution of the wave function). At temperatures of $T > 0\text{K}$, energy bands have a probability of 50% to be filled when $E = E_f$. The work function Φ describes the difference between vacuum level and Fermi level⁵⁶ and is therefore a quantity to describe the energy necessary remove an electron of a molecule.

Now, a **classification in conductors, semiconductors and insulators is possible** with the knowledge of the **position of the valence band and the conduction band** in terms of energy levels:

In **insulators and semiconductors** the valence band is fully filled with electrons and the next level (conduction band) is separated from the valence band by a **band gap** as described above. At an ideal insulator it is not possible for any electron to reach the conduction band which results in a conductivity σ of zero. In practical insulating materials it is certainly possible for electrons to reach the conduction band. However, the energies necessary are comparable high: For Polyethylene (PE), activation energies of $E_a = 8,8\text{eV}$ and for Polytetrafluorethylene $E_a = 8,4\text{eV}$ are reported in literature, e.g. [99]. This is why only very few electrons are present in the conduction band and the (electrical) conductivity of such materials is low.

⁵³However, this theory is only a simplification. Intentionally it was developed to explain conduction mechanisms in inorganic semiconductors and has been developed further for other materials. So it is not possible to explain every detail about conductivity and molecular structure with such a theory (yet) [31].

⁵⁴Enrico Fermi (*1901, †1954) Physicist, Nobel laureate in physics 1938

⁵⁵Paul Dirac (*1902, †1984) Theoretical physicist and Nobel laureate in physics (1933), shared with Erwin Schrödinger

⁵⁶Actually, this is also the minimum quantum energy $h \cdot \nu_{min}$ for photoemission to occur [31].

In semiconductors it is also possible for electrons to reach the conduction band in significant numbers, e.g. at higher temperatures. For example, silicon is an insulator at absolute zero as it is not possible for electrons to cross the “forbidden zone” - the band gap - as all electrons are in a covalent bond. But at elevated temperatures electrons can move due to thermal lattice vibrations and therefore reach the conduction band. This is only possible when the energy of an electron is higher than the energy defined by the Fermi level. In an intrinsic semiconductor, the Fermi level is (energy wise) always in the middle between valence and conduction band.

In **pure conductors** (=metals) the situation is a bit more complex. Generally, there are two possible types of conductors: The conduction band⁵⁷ generally overlaps the valence band⁵⁸ which enables an easy exchange of electrons. The overlapping and the amount of electrons present in the outer shell (conduction band) defines the electrical conductivity of a material. In metals, the Fermi level is also within the conduction band, which enables electrons to enter the valence band easily.

Metals in the group 11 in the periodic table (copper, silver (silver) and gold⁵⁹) have superior electrical conductivity⁶⁰, as they have just one s-electron in the outer shell/orbital and strongly overlapping energy bands.

More details on the fundamentals of electrical conductivity in solids can be found in [31, 39, 63, 134].

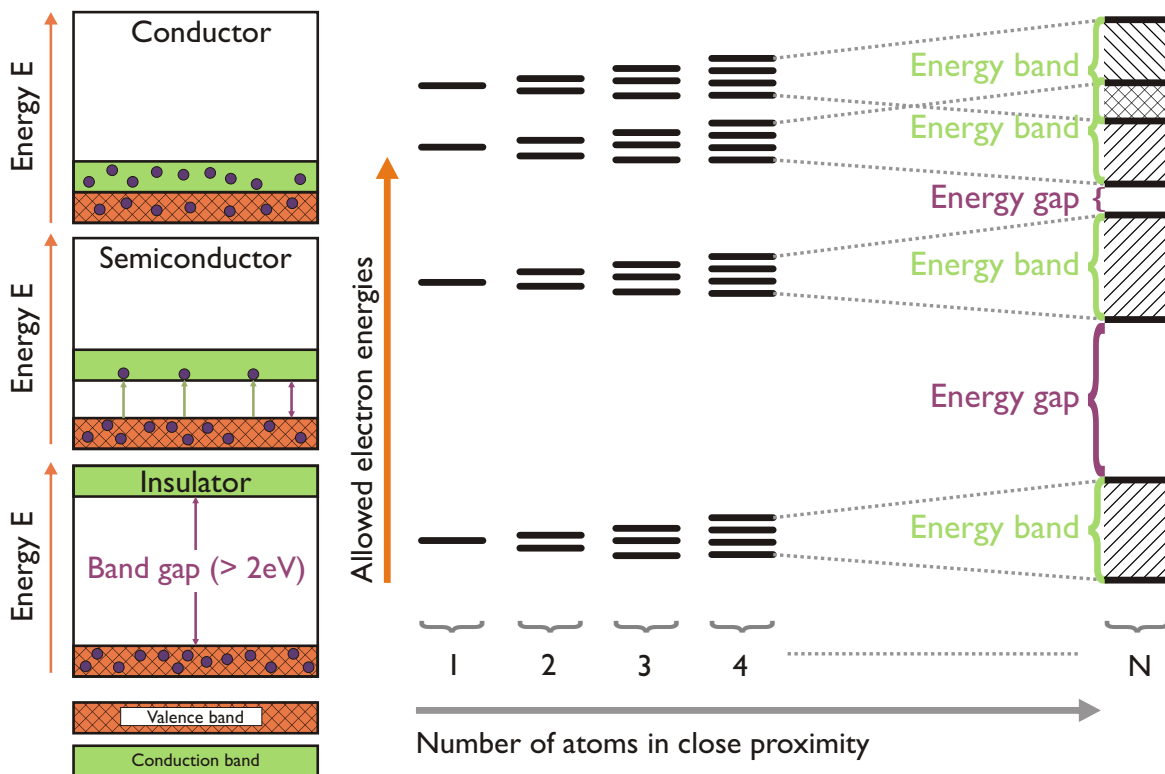


Figure 4.3: Simplified band model of electrical conductivity in solids (adapted from [63])

Figure 4.4: Discrete electron energy states with energy bands and gaps in variation of atom proximity (adapted from [31])

⁵⁷p-band in metals

⁵⁸s-band in metals

⁵⁹For the sake of completeness also roentgenium (atomic number 111) is mentioned, as it falls into this group. However, it is a very unstable isotope and has no practical use here.

⁶⁰ $\sigma_{Cu} = 59,59 \cdot 10^6 \text{ S/m}$, $\sigma_{Ag} = 63,01 \cdot 10^6 \text{ S/m}$, $\sigma_{Au} = 45,17 \cdot 10^6 \text{ S/m}$ at 20°C [94]

Generally, the **electrical conductivity of a solid** can be expressed as the sum of all present charge carriers [31]:

$$\sigma = \sum_i^N \sigma_i = \sum_i^N |n_i \cdot e_i \cdot \mu_i| \quad (4.19)$$

σ Electrical conductivity [S/m]

n Charge carrier concentration [$1/\text{m}^3$]

e Charge of the carrier [C], e.g. elementary charge e

μ Charge carrier mobility [$\frac{\text{m}^2}{\text{V}\cdot\text{s}}$]

As already shown before, electrons are mostly responsible for the conduction process in metals. In insulating materials, mainly other processes are responsible for the electrical conductivity, like for example ionic conduction. The mobility μ of a charge carrier can be expressed by [31]:

$$\mu = \frac{v_d}{E} \quad (4.20)$$

μ Carrier mobility [$\frac{\text{m}^2}{\text{V}\cdot\text{s}}$]

v_d Drift velocity [m/s]

E Electrical field strength [V/m]

Although in liquids and especially in solids the mobility of charge carriers is low and their charge is small, there are large variations in electrical conductivity between different materials. The reasons for the big spread can be found in the charge carrier concentration n which can range from basically nearly zero at insulators to more than one per atom, which equals a carrier concentration of around $n = 10^{29} \text{ m}^{-3}$ [31].

The **effective charge carrier mobility** can be determined experimentally, as described in [11]:

$$\mu_{\text{eff}}(x) = -2 \cdot \frac{\frac{\partial E(x, t)}{\partial t}}{\frac{\partial E^2(x, t)}{\partial x}} \quad (4.21)$$

Generally speaking, electrical conduction may be the result of both electronic and ionic conduction [63]. Both are described below, however ionic conduction is a dominant conduction process for oil and pressboard.

4.2.1 Ionic conduction

Electrical conductivity is besides others, dependent on temperature, frequency and on the involved charge carriers. Ionic conductivity mechanisms are quite typical for solids (but also for liquids). Ionic conduction and ionic transport respectively is connected with mass transport, which is why there is a finite conductivity at metallic electrodes, as such can only provide electrons or recombination sites for holes [31]. Basically, one can distinguish between **intrinsic** and **extrinsic ionic conduction** [63].

The former describes a conduction process, where the ions are present in the materials, whereas at the latter ions are not part of the chemical structure of the solid (polymer) but are due to impurities or other materials present. Intrinsic ionic conduction also increases with temperature. Ionic conduction is defined as the summarized influence of k different ionic species with their mobility μ_k and concentration n [63]:

$$\sigma_{\text{ion}} = q \cdot \sum_k \mu_k \cdot n_k \quad (4.22)$$

The ionic conductivity is furthermore temperature dependent according to the following relationship [61, 63]:

$$\sigma_{\text{ion}} = \sigma_{\text{ion}-0} \cdot e^{\left(-\frac{E_a}{k \cdot T}\right)} \quad (4.23)$$

A theoretical treatise about the ionic mobility and conduction of an NaCl crystal is given in detail in [63]. Suchlike ionic conduction takes place only in ionic solids. For non-ionic solids the conduction process is always of extrinsic nature and depends further on the type and concentration of the ionic impurities [63]. Water, for example, is always a source for ions. It is however interesting to note that the single presence of water does not necessarily imply ionic conduction processes [31].

4.2.2 Tunnelling and hopping of charge carriers

Two conduction processes which are important for electrons and holes are **tunnelling** and **hopping processes**. The former describes a process, in which an electron can tunnel through a potential barrier to a neighbour molecule [63]. This can be explained by quantum mechanics, as it is only possible to determine the probability at which position a charge carrier (an electron) is located [31].

Hopping describes a process in which a charge carrier “jumps” over a potential barrier to reach a neighbouring molecule. This theory was readily applied for ionic conduction in the past but it can be also extended to electrons.

In certain materials, energy levels can exist within the forbidden zone (band gap). They are called traps or trapping centres. A distinction in terms of “depth” of such traps can be made energy wise, whereas different levels exist for the classification into “shallow” and “deep” traps [99]. Generally, “shallow” traps paired with a short residence time of charge carriers (electrons) at these traps can contribute to electrical conductivity in such a way that it will rise. Hopping is generally a thermal dependent process as with increasing temperature it is easier for charge carriers to overcome potential barriers [31, 61].

The question, if the charge carrier reacts in a tunnelling or hopping behaviour is dependent on the distance between to molecules. According to [31, 63], with distances larger than 10 \AA^{61} the chances for hopping are higher than for tunnelling and can be generally expressed through [12, 63]:

$$P_H = v_j \cdot e^{\left(\frac{-\Delta E_a}{k \cdot T}\right)} \quad (4.24)$$

P_H Probability of hopping

v_j Attempt-to-escape jump frequency

E_a Activation energy [J]

k Boltzmann constant

T Temperature [K]

4.3 Electrical conductivity of liquids: Mineral insulation oils

The processes and principles which define the electrical conductivity of insulation liquids (and (mineral) insulation oils) are by far the most complex of the three insulation material types (gases, liquids and solids). It is subsequently different from the conduction processes in solids and cellulose respectively. Several different processes and mechanisms which contribute to electrical conduction are pictured in Figure 4.6. The most

⁶¹ $10 \text{ \AA} = 10^{-9} \text{ m}$

important contribution to conductivity in (new and clean) insulation liquids is **ionic conduction** [160]. Such **ions** are generated through dissociation⁶², especially due to contamination or impurities. The dissociation energy in liquids is generally smaller as in gases which results in a larger quantity of ions when compared to the latter [61]. This is also the reason why water, even if purified is only a poor insulator: Due to spontaneous dissociation an equilibrium between H^+ and OH^- ions exists. This leads to an electrical conductivity of around 10^{-5} S/m [61]. However, the relative permittivity of typical (purified and clean) insulation oils is low when compared to (purified) water ($\epsilon_r \approx 80$ at 20°C), which hinders dissociation [61].

Furthermore, **electrons** can contribute to the electrical conductivity of liquids, however this contribution is small, as the electron life time is much shorter than 10^{-4} s [49] due to their (high) mobilities [14]. These electrons are often generated by ionisation or due to injection from the cathode [61].

Finally, **charged particles** (e.g. colloids) could also make a contribution to the total electrical conductivity. These influences are pictured in Figure 4.6. Similar to highly resistive solids, it can take several hours or even days until a steady-state current is reached after voltage application. Yet, insulation liquids can hardly store any charge, nevertheless the build-up of space charge in oil gaps is possible. The magnitude of initial polarisation current and the steady state (insulation/conduction) current can be influenced by the degree of refinement and purification [160].

Such space charge is generally concentrated around the electrodes, as ions of the opposite sign accumulate there [160]. But, when compared to solid materials, the depolarisation current is relatively small, which backs up this fact. Space charge recombines in the bulk of the insulating liquid, leading to small depolarisation (=discharge) currents with - when compared to solids - short time constants.

Especially for new insulation oils at low temperatures (20°C), the changeover from AC (Laplace; no space charges present) to DC (Poisson) behaviour and conductivity respectively can be (often) clearly observed at the **transit time** τ . This transit time [95, 142] depends on the electrode gap d , the electrical field strength E and the ion mobility μ , as described in (4.25):

$$\tau = \frac{d}{\mu \cdot E} \quad (4.25)$$

τ Transit time [s]

d Electrode gap [m]

E Electrical field strength [V/m]

μ Ion mobility [$\text{m}^2/\text{V} \cdot \text{s}$]

Generally, the charge carrier mobility of liquids can be defined as a function of temperature [61, 63] when neglecting the influence of (external) electric fields:

$$\mu = \frac{v_0 \cdot a^2}{6 \cdot k \cdot T} \cdot e^{\left(-\frac{E_a}{k \cdot T}\right)} \quad (4.26)$$

The difference between initial and long-term electrical conductivity can be somewhere in the range between a factor of 10 to 100 or even more at ambient temperatures, yet this is only valid for pure and dry insulating oils. For insulating oils which have been purified only poorly (and for those which may contain larger amounts of water), the difference between initial and long-term electrical conductivity is very low.

Because the saturation character of the polarisation current is similar to those of ionized gases, it is generally accepted that the processes which lead to conduction in highly refined and purified insulation liquids are similar to those in dense, ionized gases [160].

However, field emission, as thought in the past, is not responsible for charge injection and space charge generation at technically usable field strengths (in the sense of HV engineering). In [134] a threshold level of 10^9 to

⁶²An - in terms of HV engineering applied here - negligible source can be (natural) radiation.

10^{10} V/m is stated which is necessary for field emission, e.g. according to Fowler-Nordheim⁶³, to take place:

$$J = K_1 \cdot \frac{|E|^2}{\Phi} \cdot e \left(-K_2 \cdot \frac{\Phi^{3/2}}{|E|} \cdot \nu \right) \quad (4.27)$$

J Current density [A/m²]

K_1, K_2 Constants (material dependent)

E Electrical field strength [kV/mm]

Φ Work function (of the emitting electrode metal) [eV]

ν Correction factor (function of E and Φ) ≈ 1

However, in [65] it is stated, that field emission processes might already take place at lower field strengths ($E = 1 \dots 10$ kV/mm). This can be justified in such a way that due to surface effects (e.g. surface roughness) the local field strength can be increased and can therefore reach levels high enough to allow emission. Actually, this can be seen as a motivation to use electrodes with very low surface roughness and materials with a high(er) work function to reduce such processes to a minimum.

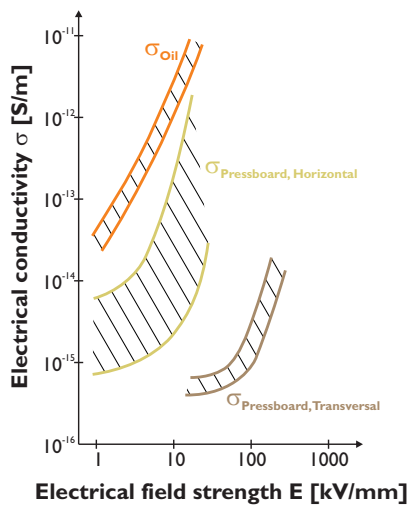


Figure 4.5: Electrical conductivity of pressboard and oil in variation of material density, composition and field strength (adapted from [85])

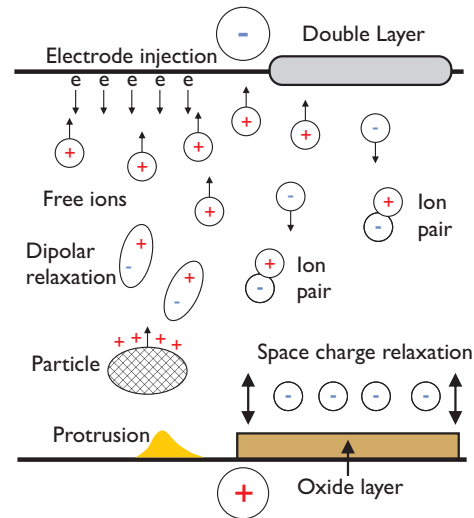


Figure 4.6: Conduction mechanisms in liquid dielectrics (adapted from [6])

Simplified, the **ionic mobility** μ can be described with [49]:

$$\mu = \frac{e}{6 \cdot \pi \cdot \eta \cdot \alpha} \quad (4.28)$$

μ Ionic mobility [m²/V · s]

η Dynamic viscosity of liquid [N · s/m²]

α Radius of ion [m]

There is a direct relationship between viscosity and electrical conductivity, which is also described in literature [61, 139, 160]. In general, the relationship $\eta \cdot \mu$ can be assumed as constant, which is known as **Walden's rule**⁶⁴ [49, 128, 134]. According to [101, 134], the mobility μ of positive and negative ions can be linked to viscosity as follows:

$$\mu_+ = \frac{1,5 \cdot 10^{-11}}{\eta} \quad \mu_- = \frac{3 \cdot 10^{-11}}{\eta} \quad (4.29)$$

⁶³Ralph Howard Fowler (*1889 ,+1944) Physicist and astronomer; Lothar Nordheim (*1899 +1985) Theoretical physicist

⁶⁴Paul Walden (*1863, +1957) Chemist

When considering typical kinematic viscosities η (see Section 5.1.4 on page 64) of around $\eta_{20} = 0,015 \frac{\text{N}\cdot\text{s}}{\text{m}^2}$ at 20°C and $\eta_{90} = 2 \frac{\text{N}\cdot\text{s}}{\text{m}^2}$ at 90°C, this results in (positive) ion mobilities of $\mu_{+,20} = 1 \cdot 10^{-9} \frac{\text{m}^2}{\text{s}\cdot\text{V}}$ and $\mu_{+,90} = 7,5 \cdot 10^{-9} \frac{\text{m}^2}{\text{s}\cdot\text{V}}$ respectively. The difference between AC and DC conductivity⁶⁵ can be also explained with ion mobility, as demonstrated in [14].

At higher field strengths of around $E = 10 \text{ kV/mm}$, the electrical conductivity of insulation oils is significant different from that predicted by Ohm's law. This is caused by additional dissociation [118], which can be described with [61]:

$$\sigma = \sigma_0 \cdot e^{\left(\frac{\sqrt{e^3 \cdot E / (\epsilon_0 \cdot \epsilon_r)}}{k \cdot T} \right)} \quad (4.30)$$

However, field-enhanced dissociation can be neglected up to field strengths of $E = 0,1 \text{ kV/mm}$ [49].

4.4 Electrical conductivity and oil-cellulose insulation systems

Typical oil-cellulose insulation systems can be simplified described with an RC circuit as shown in Figure 2.2 and 4.1. There, the electrical conductivity can be attributed to an ohmic resistance (R_∞ ... insulation resistance), which describes the steady-state behaviour. However, to simulate the actual (transient) behaviour, additional processes need to be considered. For example, polarisation processes are commonly replicated through several RC elements in serial connection. When a step DC-Voltage is applied to a dielectric (e.g. oil-cellulose insulation system), a typical response like the one in Figure 4.7 and 4.1 arises. Such a trend can be classified into 3 stages [114]:

In the first few milliseconds after voltage application a **capacitive current** flows, as the (uncharged) dielectric is charged up. The involved charge can be described with:

$$Q = \int i(t) \cdot dt = C \cdot U \quad (4.31)$$

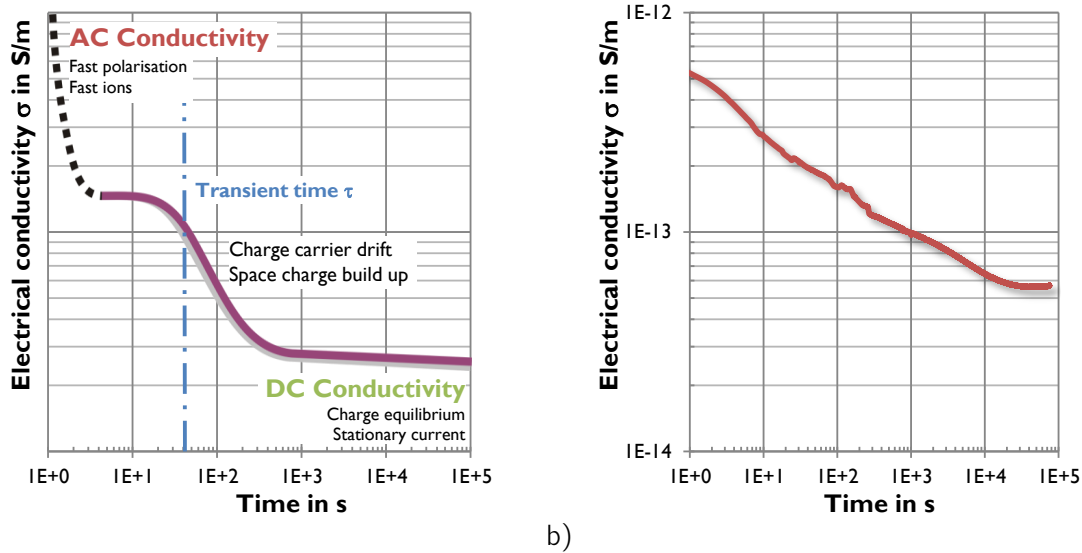
The time constant $\tau = R \cdot C$ is governed by the capacitance of the dielectric and the external resistance (HV source, cabling, etc.). Commonly it is difficult to determine the peak value of this current and the transient time trend within the first milliseconds because current measurement devices (e.g. electrometer) need a certain settling time. Further, the voltage and the current might also experience small deviations from their intended values due to switching actions.

After this initial behaviour, **polarisation processes** governs the current in an intermediate stage. This stage can last for several hours or even days until a steady-state is reached and all polarisation processes have been decayed. Time constants for varied polarisation processes are indicated in Figure 4.2 and can have values between $<10^{-15}$ and $>10^5$ seconds. The **polarisation current** during this stage is expressed by:

$$i(t) - I_0 = \sum_{i=1}^n I_i \cdot e^{-\frac{t}{t_i}} \quad (4.32)$$

Here, I_i and t_i do not depend on time but are rather descriptions of single polarisation processes. The time dependent current $i(t)$ decreases asymptotically to the steady-state current I_0 , which is actually the **conduction current**. Although this behaviour can be modelled with the described RC elements, it still has some shortcomings. Especially the influences of temperature and electrical field strength can not be neglected, especially when considering oil or oil-cellulose insulation systems [95]. For a better description of the actual processes, non-linear models need to be developed [66, 95].

⁶⁵Generally, the conductivity is expected to be lower at AC (power frequency) than at DC [14]

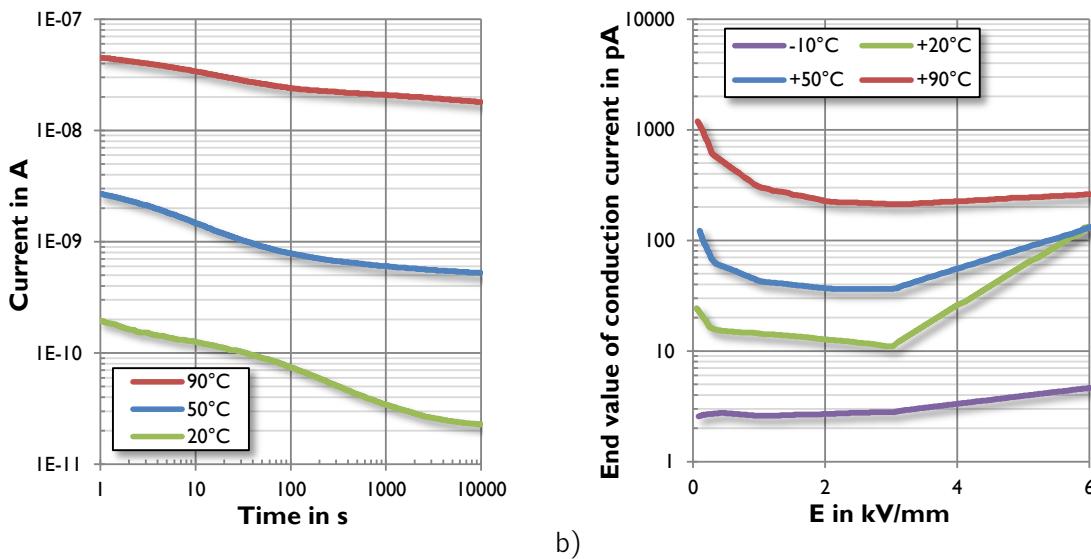


a) b) **Figure 4.7:** Conductivity-time characteristics: a) Theoretical behaviour b) Actual measurement (Shell Diala GX at 22°C, $E = 1$ kV/mm)

4.4.1 Temperature

Temperature has a vital influence onto electrical conductivity. For oil and cellulose an increase of temperature generally results in an increased electrical conductivity. This increase can be explained by an elevated charge carrier mobility and further by the increase of available charge carriers, e.g. due to thermal activation. The relationship is described in (4.23).

The influence of temperature onto the (conduction) current can be seen in Figure 4.8 below. Temperature variations of around 30 K can influence the conductivity of OIP already by one order of magnitude. For practical applications, this effect can be overlapped by field effects as shown in Figure 4.8 b). The deviation of conduction currents of OIP samples (measured with $E = 6$ kV/mm) between 20 and 90°C is less than factor of 3 [66].



a) b) **Figure 4.8:** Influence of temperature onto electrical conductivity and polarisation currents respectively: a) Time trend of the electrical current at OIP samples with moisture content of 1,8%, measured with $E = 0,1$ kV/mm (adapted from [72]) b) End values of the current of an insulation oil at varied field strength (adapted from [66])

4.4.2 Electrical field strength

For certain insulation materials and within certain ranges, the **electrical conductivity depends significantly on the applied electrical field strength**. In terms of insulation design, this can be harnessed when it comes to **equipment protection** like for over-voltage protection due to non-linear material properties (e.g. zinc oxide). On the other hand, this can be also problematically, as the field distribution within an insulation system will change at different stress levels. A general dependence of electrical conductivity onto electrical field strength is shown in Figure 4.9 below. Here, the determination of electrical conductivity is assumed to be made at constant temperature and within a constant interval after voltage application. Then, four characteristic areas (A to D) can be classified:

In the range of low electrical field strengths, the electrical conductivity does not show a dependence of electrical field strength. This can be classified as **ohmic behaviour** ("A"). Conduction is dominated by ionic or polarisation processes [12]. **Electronic conduction processes** are overlapping **ionic conduction** and conductivity increases, which is shown as area "B".

With increasing field strength, **electronic conduction** is dominating the conduction mechanism, which leads to a further increase of electrical field strength ("C"). However, the border between area "B" and "C" is often difficult to find.

If no discharge processes occur, the conductivity experiences a **saturation effect** when the field strength is raised further ("D").

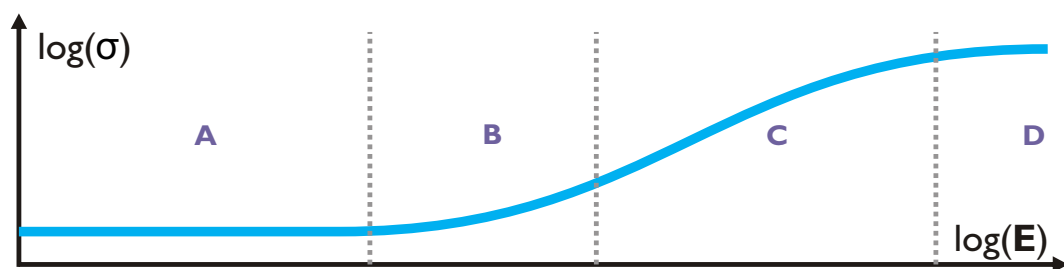


Figure 4.9: Electrical conductivity and influence of electrical field strength (adapted from [12, 99])

For the determination of material parameters (e.g. electrical conductivity), it is therefore interesting to know if there is a strong dependence on field strength. Here, this is especially interesting for pressboard and (mineral) insulation oil. Several conductivity values of both materials are documented in literature, however a direct transfer to the materials investigated here might not be possible or useful. Exemplary, some results of [95] are summarized here: The (steady-state) conductivity σ of new, mineral oil-impregnated T IV **Transformerboard** at room temperature (20°C) at an electrical field strength E in the range between 1 to 30 kV/mm appears as follows:

Table 4.1: Electrical conductivity of Transformerboard at varied electrical field strength (from [95])

Field strength E in kV/mm	1	10	30
Conductivity σ in S/m	7E-15	5E-15	8E-15

These values have been determined by CDM measurements (see Section 4.5.3). The electrical conductivity is quite constant over a fairly large electrical field strength range.

For **insulation liquids** and especially for mineral insulating oil, this is not the case. Above a certain field strength (in the region between 3 and 6 kV/mm, according to [95]), additional charge carriers are generated and the measured electrical conductivity is increased. In [71], field dependency of electrical conductivity of oil was investigated between $E = 1$ kV/mm and $E = 6$ kV/mm at 20, 50 and 90°C with CDM measurements. Between 20 and 50°C the oil conductivity was within one order of magnitude with an increase in oil conductivity at 6 kV/mm. At 90°C, even a slightly falling conductivity with increasing field strength was observed. The dependence of electrical conductivity onto electrical field strength of three different insulation oils [95] is summarized in Table 4.2 below.

Table 4.2: Electrical conductivity in S/m of three different insulation oils at varied electrical field strength (adapted from [95])

Field strength E in kV/mm	0,1	0,3	1	2	3	4	6	10
Oil 1	5,6E-14	2,6E-14	1,3E-14	2,1E-14	4,3E-14	3,9E-14	1,3E-13	-
Oil 2	5,0E-15	3,8E-15	2,6E-15	2,3E-15	2,2E-15	4,4E-15	7,3E-15	-
Oil 3	5,0E-14	3,2E-14	2,0E-14	1,9E-14	-	1,6E-14	2,0E-14	2,5E-13

For the determination of electrical conductivity of oil as well as of pressboard the measurement field strength has to be chosen carefully. Within this work, for pressboard a value of $E = 3 \text{ kV/mm}$ and for oil $E = 1 \text{ kV/mm}$ was chosen generally.

4.4.3 Moisture content

The presence of water inside insulating materials is disadvantageous as it increases losses and electrical conductivity and can significantly reduce electrical strength. Increased moisture content can be a sign of ageing and it can furthermore increase ageing rates, as demonstrated in the previous chapter. The end value (steady-state) of electrical conductivity can therefore be used as a diagnosis parameter for oil-cellulose insulation systems, which is also applied in practice (e.g. in PDC measurements).

Moisture content and electrical conductivity of mineral oils

The electrical conductivity of oil generally rises with increasing water content. However, this effect is strongly dependent on temperature, as it influences the solubility of water in transformer oil. Generally, the water solubility of oil increase with rising temperature. Depending on oil type, around 20 to 40 ppm of water are in solution at 20°C. Higher water contents will result in a suspension of water and oil at this temperature.

Generally it can be expected that with an increased moisture content in oil the electrical conductivity will rise. But this is also a temperature related effect as it depends how much water is dissolved (in solution) and which quantity is in suspension [139]. This effect is also demonstrated in Figure 4.10. It can be seen that at temperatures of around 70°C and above the conductivity of oil increases, more or less independently of moisture content. Basically, this has to reasons: Firstly, water which is present in solution does not ionize and therefore does not contribute (significantly) to electrical conductivity [139]. Secondly, conductivity rises with increasing temperature as demonstrated already in Section 4.4.1. These two overlapping mechanisms govern the conductivity as seen in Figure 4.10. The minimum conductivity is reached when all water is in solution, which is temperature and moisture content dependent.

Moisture content and electrical conductivity of cellulose

Basically, the electrical conductivity of cellulose rises with increasing moisture content. It is known from the literature that the behaviour of pressboard and paper is different with increasing moisture content though [69]. This can be explained through the microscopic composition of both materials. In OIP, several layers exists which all contain small oil films. If the conductivity of these oil layers is increased, either by increasing moisture content or/and using an oil with higher conductivity, the conductivity of the paper increases significantly as well. Pressboard does not show such a strong increase up to a certain moisture level. However, if the moisture content is raised to higher levels (e.g. >3%), the electrical conductivity of both OIP and PB increases steadily, which is also shown in Figure 4.11. The oil conductivities have been in the range of $<10^{-14} \text{ S/m}$ for oil (A) and $>10^{-13} \text{ S/m}$ for oil (B) [68].

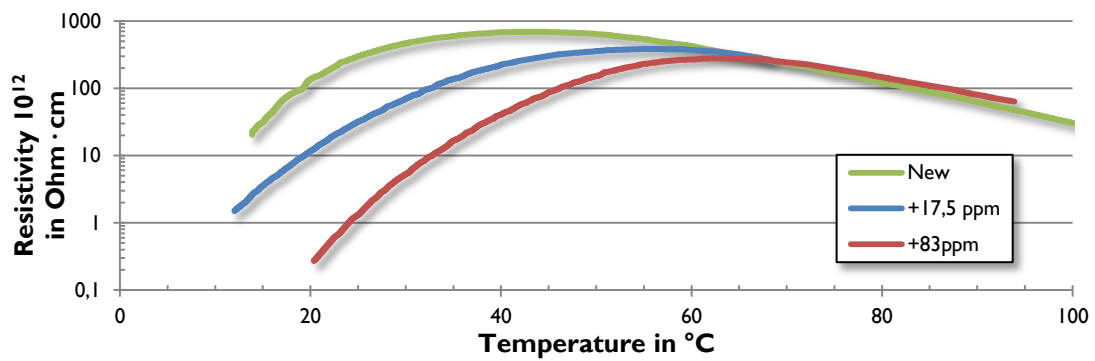


Figure 4.10: Electrical conductivity of a mineral insulating oil with varied moisture content (adapted from [139]). Results have been gained at a set-up with an electrode gap of 5 mm and an applied voltage of 5 kV 1 minute after voltage application

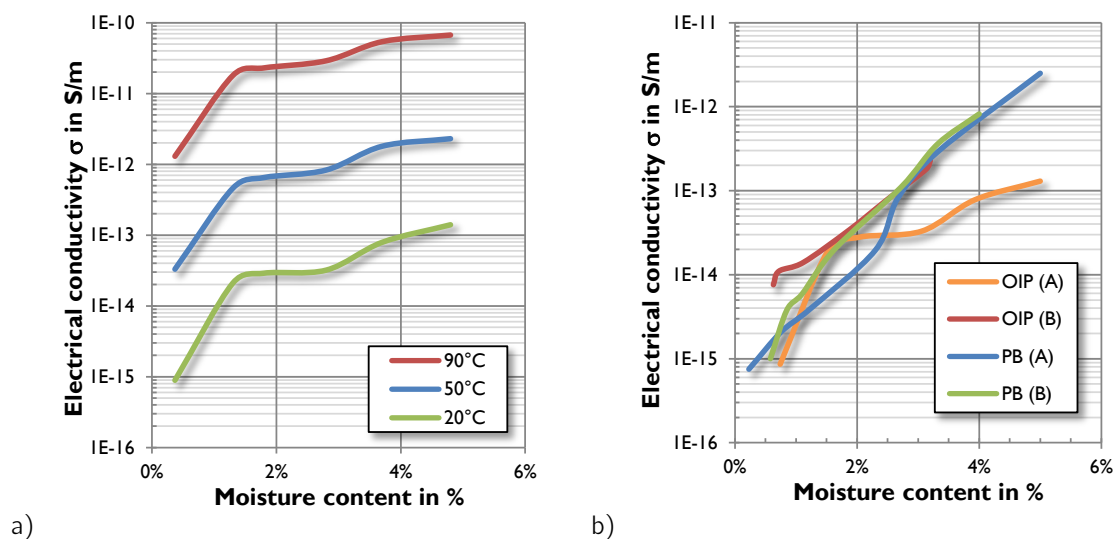


Figure 4.11: Influence of moisture content on electrical conductivity of cellulose: a) OIP at varied temperatures, measured with $E = 0,1$ kV/mm (adapted from [66]) b) Electrical conductivity of OIP and pressboard with a highly resistive (A) and a lower resistive (B) oil, measured at 20°C and $E = 0,1$ kV/mm (adapted from [69, 72])

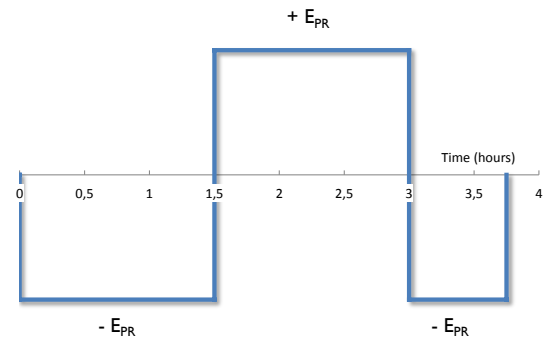
4.4.4 Impact of electrical conductivity

The electrical conductivity also influences AC operation of electrical equipment, as the dielectric loss factor $\tan(\delta)$ is directly proportional to the electrical conductance, as seen in (4.8). The contribution of polarisation to the dielectric loss factor at power frequencies is quite low. However, if there are impurities in the oil, or if the oil has a high viscosity (> 100 mm²/s), dipole behaviour can also contribute to dielectric loss [14]. As already demonstrated before, the electrical conductivity defines the electrical field strength during DC stress. So, variations in electrical conductivity due to temperature, ageing, contaminants, etc. can lead to a changed field distribution. Further, transition times⁶⁶ are comparable long and can be in the region of hours or even days. On the contrary, a typical polarity reversal test for HVDC equipment (e.g. IEEE C57.129 [33]) defines the intervals given in Table 4.3.

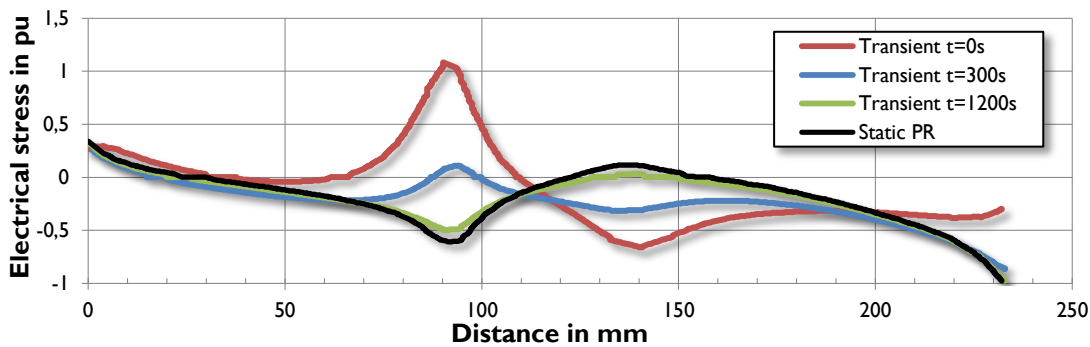
⁶⁶Time needed to reach the steady-state conductivity region which is ideally governed by conduction current only.

Table 4.3: Time intervals for typical PR test

1.	Negative Voltage for 90 minutes
2.	Polarity reversal within 2 minutes
3.	Positive voltage for 90 minutes
4.	Polarity reversal within 2 minutes
5.	Negative voltage for 45 minutes
6.	Voltage Switch off, end of test

**Figure 4.12:** Voltage trend during typical PR-Test [33]

Therefore, current equipment testing procedures need to be critically scrutinised, which is already discussed in [16] for example. In Figure 4.13, the transient stress along a barrier surface at polarity reversal is plotted. Although the electrical stress is quite constant over time at certain points there are places where it varies strongly with time and magnitude. In [16] it is further recommended to use a higher test voltage and a slightly longer time for the second polarity reversal. However, issues caused by different oil conductivities can not be solved with this approach, which is also found in [16]. More research results are definitely necessary before making any changes to that procedure.

**Figure 4.13:** Transient creep stress on bushing barrier surface at polarity reversal (adapted from [122])

4.5 Measurement of electrical conductivity

The determination of electrical conductivity can be made with several different methods and measurement set-ups. They are described in the following section. All these methods are based on the measurement of the electrical current, which flows through the investigated material. However, there are also other methods which employ different set-ups, e.g. as described in [14].

As described in section 4.1.1, Ohm's Law (4.1) can be used to determine electrical resistance R by measuring voltage and current. However, care has to be taken, as Ohm's Law is only valid under certain preconditions. It is widely used for "ohmic resistances", but for a general approach, the following factors need to be remembered:

Commonly, it can be applied for DC, as long as temperature and pressure (onto the investigated material) are constant during measurement time. Furthermore, a linear relationship between voltage and current must be given, otherwise errors might occur (field strength depended resistivities). In materials with a high resistivity, measurement time plays also an important role, as it was demonstrated in section 4.4.2.

Generally, the standardized methods are not qualified to determine the electrical conductivity in that sense which is needed for HVDC equipment design. Time and voltage-dependent polarisation and charging processes are neglected, which is why it is proposed in [71] to call the electrical conductivity, which is determined with such methods, “**apparent conductivity**”.

4.5.1 Measuring specific resistivity according to IEC 60093 (for solids)

The standard IEC 60093 [52] (VDE 0303-30 [148]) covers the determination of volume and surface resistivity of solid insulating materials. Within this work, the electrical conductivity of pressboard is of interest, so only volume resistivity is covered here.

Generally, the standard names the following factors as of importance for the measurement: » *Amplitude of applied voltage, time duration of voltage application, type and shape of electrodes, temperature and moisture of the surrounding atmosphere⁶⁷ and of the sample itself*«. Furthermore, the standard indicates, that for specific (volume) resistivities of less than $10^{10} \Omega \cdot m$, the current can reach a stable state around 1 minute after voltage application. Other, pre-defined times are 2, 5, 10, 50 or 100 minutes.

At higher specific resistivities, it can take much longer (hours or even days) to reach a steady-state. Therefore, the recommended measurement time of 1 minute after voltage application is not really useful for the determination of the electrical conductivity of pressboard. Typical voltage amplitude for measurements can be either 100, 250, 500, 1.000, 2.500, 5.000, 10.000 or 15.000 V, whereas the most common ones are 100, 500 and 1.000 V.

To determine the specific resistivity, a special measurement set-up has to be made. It is important to use a guard or shielding electrode to exclude surface currents from the measurement. Schematic electrodes and the measurement set-up are shown in the figure below in Figure 4.14.

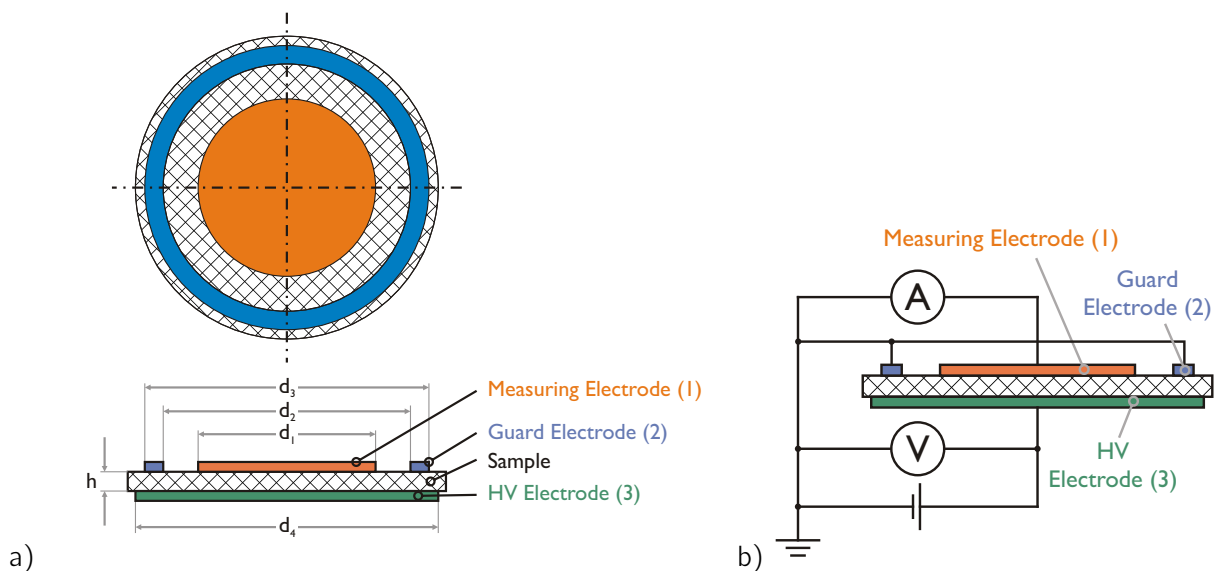


Figure 4.14: Determination of specific resistance of solid materials according to IEC 60093: a) Electrode geometry b) Measurement set-up

The measurement itself is typically based on the simultaneous measurement of voltage and current. There are also other methods possible, like the usage of bridge circuits. Within this work, the former method is applied (with digital voltmeter and electrometer). The **specific resistivity** is then determined by:

⁶⁷If apparatus is not completely sealed and/or sample is in contact with ambient atmosphere before starting the measurement.

$$\rho = R_x \cdot \frac{A}{h} \quad (4.33)$$

ρ Specific resistivity (volume resistivity) [$\Omega \cdot m$]
 R_x Measured resistivity [Ω]
 A (Used) Area of measurement electrodes [m^2]
 h (Average) Thickness of sample [m]

The **effective area of the electrodes** can be calculated as following:

$$A = \frac{\pi \cdot (d_1 + g)^2}{4} \quad (4.34)$$

A Area of electrodes [m^2]
 d_1 Diameter of measurement electrode [m]
 g Gap between measurement electrode and guarding electrode [m]

The actual electrode diameter might differ from this value by a distance of Δ (due to flux line fringing), as noted in [8]:

$$\Delta = d \cdot \left\{ \frac{2}{\pi} \cdot \ln \left[\cosh \left(\frac{\pi}{4} \cdot \frac{g}{d} \right) \right] \right\} \quad (4.35)$$

d Thickness of sample [m]
 g Gap between measurement electrode and guarding electrode [m]

The **correction factor** B^{68} is then calculated by [8]:

$$g \cdot \left(1 - \frac{2 \cdot \Delta}{g} \right) = B \cdot g \rightarrow B = \frac{g - 2 \cdot \Delta}{g} \quad (4.36)$$

However, the influence of this correction is small for the investigated configuration: When applying the dimensions of the used set-up for pressboard (see section 5.2.2 and Appendix C) and using (4.35) and (4.36), this would result in a diameter increase of +0,290 mm or +0,35%. Eventually, the electrode area and therewith also the determined resistivity (4.33) increases by +0,6%. Therefore this method was not applied and the standard formula (4.34) was used instead within this work.

4.5.2 Measuring specific resistivity according to IEC 60247 (for liquids)

According to IEC 60247 [53] (VDE 0380-2 [157]), the specific DC volume resistivity is defined⁶⁹ as the »ratio of the DC electric field strength to the steady state current density within an insulating material, after a given time of electrification«.

It has to be noted that this standard was not specifically designed to determine the specific resistivity (or the electrical conductivity) for HVDC applications but to get informations about the (intrinsic) oil quality instead. Actually, it states even that the "actual" specific resistance can't be measured with the method described in the standard. To do so, one has to measure for example at quite low voltages (electrical field strengths) and directly after voltage application. Such a method is described in IEC 61620 [55] (VDE 0370-16 [153]) but will not be covered further in this work. For HVDC applications this is not vitally important, as the actual field strengths during operation are definitely higher than 0,25 kV/mm. Therefore, such a method has only a limited use in these applications anyway. However, the question has to be raised, **how electrical conductivity is defined and what is the usage of this parameter?**

⁶⁸B = increase of measurement electrode diameter

⁶⁹see also IEC 212-11-16 at <http://www.electropedia.org/iev/iev.nsf/display?openform&ievref=212-11-16>

At insulation oils the polarisation processes can be neglected when determining electrical conductivity. But, and this is also the case at solids, it can be **misleading to determine only one single conductivity value**, which is typically determined 60 seconds after voltage application. Due to charge carrier drift processes, the current falls steadily after voltage application. Therefore it is very likely that there is no steady-state reached after 60 seconds in low-conductivity insulating liquids. This could furthermore lead to a large spread in conductivity determination with such a method, as only the 1-minute values are compared, which could be determined at different charging states or even with different set-ups.

The measurement set-up for liquids itself is similar to the methods for solid insulation material (IEC 60093 [52]). The specific resistivity is determined by measuring the current and the voltage, 60 ± 2 s after the application of voltage. Thereby, the electrical field strength has to be 250 V/mm^{70} . So, the specific resistivity is determined by:

$$\rho = K \cdot \frac{U}{I} \quad (4.37)$$

ρ Specific resistivity [$\Omega \cdot m$]
 U Measured Voltage [V]
 I Measured Current [A]
 K Cell constant [m]

The **cell constant** can be determined from the capacitance (C_{Empty} in pF) of the empty test cell as following⁷¹:

$$K = 0,113 \cdot C_{Empty} \quad (4.38)$$

The measurement depends (exponentially⁷²) on temperature, (non-linear) on electrical field strength (and also polarity) and (non-linear) on measurement time. In terms of accuracy, the standard allows deviations of up to 35% ⁷³ between subsequent measurements.

4.5.3 Determination of electrical conductivity with PDC measurements

As PDC measurements [65, 66, 72, 95, 131] are very common these days, the principal approach is briefly described here: However, this is actually a measurement method and not a concrete and single measurement set-up. The electrical conductivity of insulators with a high specific resistivity (and polarizing behaviour) decreases over measurement time. To assess the DC conductivity (or "actual conductivity") with voltage-current measurements, one has to wait until the current has stabilized.

With the **determination of the step-responses** through the measurement of the polarisation and depolarisation currents (PDC method), it is possible to determine the electrical conductivity after comparable short measurement times already. The current is measured during the application of a DC voltage (polarisation) and also after voltage turn-off (depolarisation). Peaks due to capacitive displacement currents within the first second(s) are usually omitted.

Simplified, an (oil-cellulose) insulation system can be described with a number of parallel RC elements (see Figure 2.2 and 4.1). The polarisation current i_p can then be expressed as following [95]:

⁷⁰For routine measurements, an electrical field strength between 50 and 250 V/mm can be chosen (see Appendix C in [157]).

⁷¹This is an approximation of $1/(\epsilon_0 \cdot 10^{12}) \approx 0,113 \rightarrow \frac{1}{\epsilon_0} \cdot C = \left[\frac{\text{V} \cdot \text{m}}{\text{A} \cdot \text{s}} \cdot \frac{\text{A} \cdot \text{s}}{\text{V}} \right] = [m]$

⁷²Basically, specific resistance is indirectly proportional to temperature

⁷³The allowed 35% difference is to be calculated from the higher specific resistivity.

$$i_{\text{pol}}(t) = \sum_j i_j(t) + i_{\infty} = U \cdot \sum_j \left(\frac{1}{R_j} \cdot e^{-\frac{t}{\tau_j}} \right) + \frac{U}{R_{\infty}} \quad \text{for } t < t_c \quad (4.39)$$

i_{pol}	Polarisation current [A]
i_j	Measured currents (exponentially decreasing) [A]
t	Time [s]
τ_j	Time constant [s], $\tau_j = R_j \cdot C_j$
U	Applied (polarisation) voltage [V]
R_{∞}, R_j	Resistance [Ω]
t_c	Charging time [s]

So, R_{∞} needs to be determined correctly to receive the electrical conductivity. First, the depolarisation current needs to be achieved:

$$i_{\text{depol}}(t) = - \sum_j \left(\frac{u_{c_j}(t_c)}{R_j} \cdot e^{-\frac{t-t_c}{\tau_j}} \right) \quad (4.40)$$

i_{depol} ..	Depolarisation current [A]
u_c	Voltage in [V]

The insulation resistance R_{∞} is not present in depolarisation measurements as it is short-circuited. For very long polarisation and depolarisation times ($t + t_c \gg \tau_j$), the exponential terms in (4.39) and (4.40) can be neglected. The sum of polarisation and depolarisation current is then the approximation for the insulation current:

$$i_{\text{pol}}(t) + i_{\text{depol}}(t + t_c) \approx \frac{U}{R_{\infty}} \Rightarrow I_{\infty} \quad (4.41)$$

A slightly modified approach is taken with the **charge difference method (CDM)** [69]: First, the polarisation and depolarisation currents are integrated over time to obtain the electrical charges. By subtracting these polarisation and depolarisation charges, the steady-state conductivity can be determined. This has the advantage that the current does not even have to reach steady-state levels. The conductivity can be determined through the slope of the charge time trend. Furthermore, disturbances could be filtered out from the measurement data, as long as they are influencing both the polarisation and depolarisation currents accordingly. This would classify that method also for on-site measurements.

4.6 Charge and charging behaviour

Charge and charging behaviour are processes which play an important role for DC equipment. **Charges on the surface** (*surface charges*) and **in the bulk** (*space charges*) of a material can **significantly influence electrical field distribution** and can lead to a notable increase of electrical field stress. This is especially true for (high resistive) solids and partly also for liquids. Therefore, the knowledge about space charge behaviour is important in terms of dielectric strength and insulation design.

The distribution (temporal and spatial) of the electric field within an material is strongly dependent on the shape of the electrodes⁷⁴ and on space charges. Space charges can occur, if the travelling of free charge carriers is hindered. In other words: Space charges within a dielectric (in the bulk) can be directly connected to the electrical conductivity. If the electrical conductivity and therefore the mobility of charge carriers is high enough, no space charges can occur inside a dielectric, as demonstrated below (4.42). In such a case,

⁷⁴Electrode shape defines an uniform or non-uniform electrical field (distribution).

the charge carriers just drift to the electrodes and are not trapped within the material.

Further, (space) charge generation might be influenced by ageing condition, as indicated in [134]. There, it was noticed that charging process is eased when used oils are investigated. In fact, this backs up the theory of electrochemical charge injection mechanisms.

4.6.1 Surface charges

Generally, surface charges are only found on dielectric interface layers. The cause of such surface charges can be externally applied voltages (at the electrode) or space charges in the bulk of the material [97]. So their influence can be overlaid by space charge effects. Especially in space charge measurements, like the PEA method, care has to be taken to distinguish surface from space charges [97].

The precondition for the formation of charge at an interface is described by Maxwell-Wagner theory [84]:

$$\nabla \frac{\epsilon}{\sigma} \neq 0 \quad (4.42)$$

This results in the accumulation of (space) charge, according to:

$$\rho_{SD} = \sigma \cdot \mathbf{E} \cdot \nabla \frac{\epsilon}{\sigma} \quad (4.43)$$

4.6.2 Space charges

As seen in (4.9) and (4.10), the space charge density ρ_{SD} is dependent on the electrical field strength \mathbf{E} . As demonstrated in [11], ρ_{SD} can be expressed as

$$\rho_{SD} = \nabla \epsilon \frac{\mathbf{J}}{\sigma} = \mathbf{J} \cdot \nabla \frac{\epsilon}{\sigma} = \mathbf{J} \cdot \left(\epsilon \cdot \nabla \frac{1}{\sigma} + \frac{1}{\sigma} \cdot \nabla \epsilon \right) \quad (4.44)$$

The precondition for the generation of space charges is the same as given by the Maxwell-Wagner theory (4.42): A gradient of ϵ/σ is necessary for space charges to evolve. Generally speaking, the term $\epsilon \cdot \nabla 1/\sigma$ is much larger than $1/\sigma \cdot \nabla \epsilon$, therefore (4.44) simplifies approximately to:

$$\rho_{SD} \approx \mathbf{J} \cdot \epsilon \nabla \frac{1}{\sigma} \rightarrow \rho_{SD} \approx \mathbf{E} \cdot \sigma \cdot \epsilon \cdot \nabla \frac{1}{\sigma} \quad (4.45)$$

So, space charges and charge injection is influenced by material type (σ, ϵ), electrical field strength (\mathbf{E}) and polarity, electrode material and temperature [56]. Further, the accumulation and distribution of space charges can vary in the bulk of the material. Such deviations and non-uniform distributions can be caused exemplarily by (local) field (\mathbf{E}) or temperature gradients or by non-linear/anisotropic material properties [31].

The presence of a small oil film on a material may govern the charge injection process in such a way, that the electrode material becomes negligible [11].

The polarity of space charges is described in the terms “**homocharges**” and “**heterocharges**”. The former is used to describe charges, which are of the same polarity as the adjacent electrode. Homocharges can enhance the electrical field in the bulk of a (insulating) material significantly and reduces the field on the electrode-material interface at the same time. Heterocharges, which have the opposite polarity, reduces the field in the bulk but can increase the electrical field at the dielectric interface. Generally, heterocharges are therefore more critical as it stresses the interface more severe [11]. It is possible to influence field distribution

when shaping the electrodes accordingly. In [99], the optimisation in terms of reducing the normal component of \mathbf{E} is discussed.

Time constants

Generation and decay of space charges is governed by three processes [11]: **Charge injection, transportation and recombination**. All of them have different time constants, so that observed space charge processes can be described as a superposition of single processes and time constants [11]:

$$\rho = \sum_{i=1}^n q_i \cdot \left(1 - e^{-\frac{t}{\tau_i}} \right) \quad (4.46)$$

Often, space charge generation processes can be divided in two processes which can be described with exponential functions with different time constants: First, a fast build-up of space charge, where most of the charge is formed, occurs with a time constant τ_1 . For reaching a steady state, a slower process with τ_2 is relevant [11].

4.6.3 Measurement methods

Several different methods exist to measure the space charge distribution within a dielectric material. A good introduction about various methods for determining charge distribution in insulating materials is given in [141]. For this work, an electro-acoustic method (PEA) is used, which is described below. For further details see [18, 105, 140].

Pulsed electro-acoustic method (PEA)

The principle of the PEA method (Figure 4.15) is quite simple [140]: A sample is stressed by short electrical pulses with amplitudes of several hundred volts and a pulse width in the ns-region. Through these pulses, charge packets (space charges), which are generated by means of an externally applied electrical field, are mechanically stimulated. This leads to acoustic (pressure) wave travelling through the bulk of the sample. These waves can then be detected with a pressure-sensitive sensor (piezoelectric transducer) [11, 18, 105]. However, complex signal processing needs to be applied to gain space charge data from the raw measurement data [97]. The **PEA method** has **several advantages** over other methods [11]:

- Less signal processing when compared to thermal step method (TSM)
- Higher reproducibility than laser-induced methods
- Electrical decoupling of measurement and charging circuit

The practical set-up used for the measurements within this work is pictured in Figure 4.15 b).

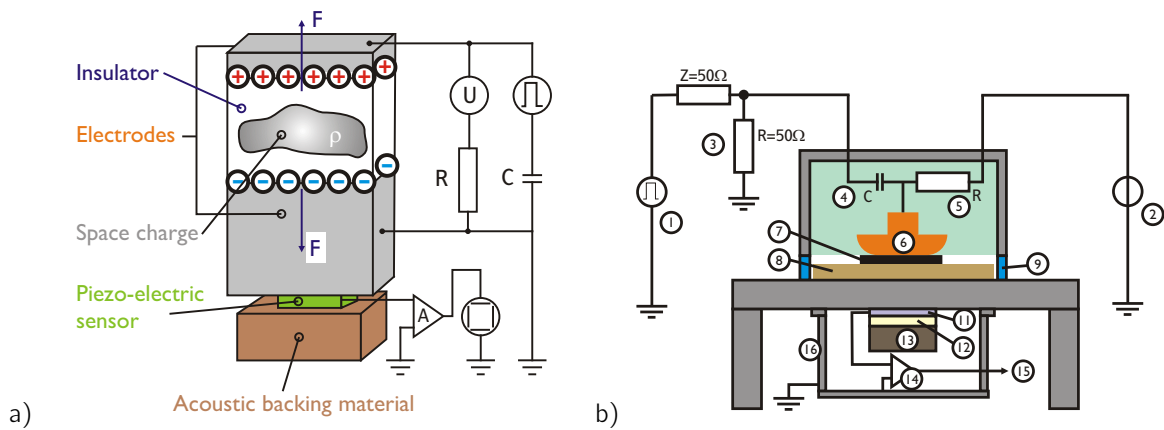


Figure 4.15: Space charge measurement with PEA method: a) Schematic principle (adapted from [11])
b) Measurement set-up used at TU Delft

- | | | | |
|-------------------------|--------------------|--------------------------|-----------------------|
| 1. Pulse Generator | 5. Series resistor | 9. Conductive tape | 13. Acoustic absorber |
| 2. HV DC Generator | 6. HV electrode | 10. Delay block | 14. Signal amplifier |
| 3. Terminating resistor | 7. Semicon rubber | 11. Piezoelectric sensor | 15. Signal output |
| 4. Coupling capacitor | 8. Sample | 12. Acoustic matching | 16. Metal shielding |

4.7 Electrostatic charging tendency (ECT)

The static electrification phenomena or **electrostatic charging tendency (ECT)** and therewith connected problems have been reported in Japan in the 1970's for the first time [15]. Later on, problems with static electrification have been also reported from the United States (1983) [26], South Africa (1986) and Australia (1987) [37]. Obviously, due to the movement of one insulating material (streaming oil) over a second one (cellulosic insulation), the **insulation system builds up charge**. In unfavourable cases, this charge build-up can lead to severe consequences: Discharges of oil gaps of roughly 1 m width have been reported [26].

In the beginning of research, the problem was attributed to a limited number of transformer manufacturers, one oil type and a specific transformer design (shell-type) [26]. Later, it was discovered, that the similarity of all failed transformers was a forced oil cooling (OD or OF type⁷⁵) systems. Due to the flowing of an insulating liquid (with a low electrical conductivity) past an insulating solid, charge separation occurs at the interface [37]. Roughly speaking, each transformer with an oil-cellulose insulation system and forced oil circulation is therefore subjected to static electrification in one way or another due to the relative movement of two insulating materials. According to [26, 37], the following parameters can therefore be relevant for static electrification:

- Oil temperature
- Oil moisture content
- Oil flow rate
- Turbulence of oil flow
- Contaminants
- Surface conditions
- Charging tendency of oil
- Energization/Electrical field strength
- Dielectric strength of moving oil
- Migration of moisture
- Particulate matter
- Charge injection
- Pumps
- Orifice effects

⁷⁵According to IEC 60076-1, this describes the following transformer cooling methods: OD...oil directed, OF...oil forced. In other publications the term FOA is used to describe «forced oil and air» cooling.

4.7.1 Basics

Due to thermal effects, oil circulates inside the tank of power transformers. In large power transformers, oil is often forced to flow through cooling ducts and winding sections to improve the cooling process. As noted before, charge separation occurs at the interface between oil and insulating materials - like pressboard - during this process.

Generally, the solid acts as an absorber for ions and a net charge of the opposite sign is generated in the liquid. As indicated in [23], the sign of the net charges can not be predicted easily and is determined by the material pairing and their energetic levels (Fermi level). If this process is investigated at the microscopic level, the system itself is electrically neutral: On one material excess charges and on the other the same amount of charge, but with opposite sign, are deposited. If now the solid is insulated or floating in relation to ground potential, high surface potentials can occur as not all charges can recombine. Basically, **three recombination processes** can take place [91]:

- Tunnel process
- Gas discharge process
- Relaxation process

A tunnelling process (hopping of charge carriers) is only possible within a small electrode distance (< 1 nm). Gas discharges can occur, if the local electrical strength is exceeded through charge carrier movement paired with an increasing potential difference. Relaxation processes are only governed by relaxation time constant τ which is dependent on material parameters, mainly on the electrical conductivity σ . The consequences of such charging processes can lead to partial discharges or even dielectric breakdown. Furthermore, excessive electrostatic (dis-)charging can lead to the generation of acetylene gas [144]. A good introduction and more details can be found in [15, 23, 37, 91].

As it was already found in [26] in 1988, oil type and oil quality respectively can have a large influence on the electrostatic charging tendency of an oil-cellulose-insulation system. Oil refinery process might also influence ECT behaviour. Generally, a clean and new oil with a low content of polar molecules should exhibit a low ECT [113]. Charge density, which can be measured with a Mini-static tester can be a good parameter to estimate the ECT of various insulation oils [119]. In [96], artificial ageing experiments on oil samples with a closed circuit ECT evaluation have been conducted. It could be shown, that charging levels (ECT) increase with ageing time [116]. The increase is also influenced by inhibitors as shown in [113]. However, if only the oil is investigated, the assessment of the ECT of an insulation system can be ill-defined, as shown in [144].

4.7.2 Diagnostic methods

Basically, three different approaches are known to estimate the electrostatic charging tendency of oil and cellulosic materials directly through electrical current measurements. They are described briefly below. Within this work, a spinning disc apparatus is used, as this set-up is a good compromise in terms of complexity and significance of the results. The biggest advantage of this method is the fact that oil and pressboard could be tested at the same time in one device (which is in principle quite simple).

Mini-static tester

The mini-static tester poses a quick and comparatively easy method to assess the electrostatic charging tendency of insulation oils [119]. The test itself was developed in 1972 for petroleum fuels and was adapted later for ECT investigations [26].

The working principle is quite simple: Oil is forced to flow through a filter, which is insulated from ground. Due to the movement a charge separation is taking place, which can be measured with an electrometer. So a qualitative comparison between different oils is possible. This is actually also the biggest disadvantage of this method: Only the oil is tested against a standardized filter⁷⁶. Possible combination effects of oil and pressboard can not be assessed with this method.

Furthermore, this method is influenced by a multitude of parameters, as shown in [26]: Type of sample bottle, sampling method, effects of storage time, light, moisture, temperature, agitation, type of filter (and filter material), flow pressure, number of measurement runs and measurement set-up. Therefore, testing conditions need to be evaluated carefully and comparison between different investigations may be only on a qualitative basis. However, this is basically true for all ECT investigation methods, as none of them uses a standardized method.

Spinning disc apparatus (SDA)

A spinning disc apparatus (SDA) was proposed in 1989 [73] and was steadily improved ever since [124]. The first design consisted of a metal disc, which spins in an oil-filled vessel. The vessel itself is insulated from ground (potential) via Teflon discs. Due to the rotary movement of the disc, the double layer at the disc (especially on the edges) is ruptured and free electrostatic charge is generated. The ECT can be determined by measuring the charging current.

The current will be influenced by the materials itself but also by the set-up and the measurement conditions: Sample/Disc diameter, vessel volume and diameter, temperature, moisture contents and rotational speed influence are main parameters. This method has the advantage, that pressboard can be easily tested in combination with oil as well, as shown in [124].

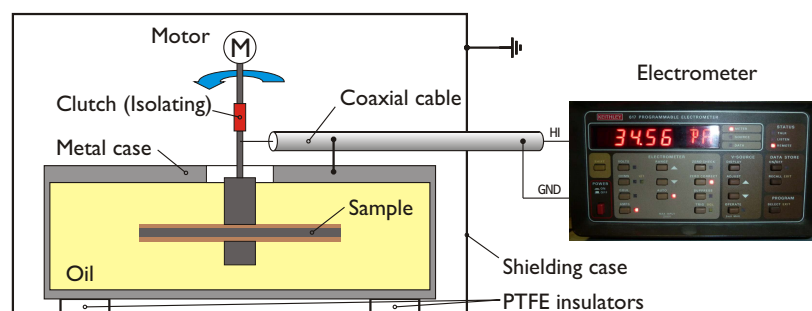


Figure 4.16: Schematic spinning disc apparatus set-up

Channel model (Oil duct model)

A test set-up, which involves full-size cooling ducts of a power transformer (“channel model”) is by far the best method to simulate operational conditions, which are similar to real-life operation. The influence of both oil and pressboard in variation of temperature, oil flow speed and surface properties can be investigated conveniently [108]. The complexity and needed resources for the successful construction and operation are far beyond the scope of this work. Furthermore, even with such a sophisticated set-up it is difficult to draw conclusions between flow rate, temperature and materials. However, it could be demonstrated on new samples, that if the surface roughness is low (as for Transformerboard T IV and aramid fibre boards, e.g. Nomex), no significant ECT could be determined at technical relevant flow rates [108].

Other methods

A different method for ECT evaluation is reported in [144]: Here, a stacked system, consisting of a potential measurement electrode, which is covered by pressboard samples on two sides, is used. Adjacent to

⁷⁶A Whatman 541 filter has been used in several investigations.

the two pressboard stripes, two oil ducts are formed, which are in turn covered by pressboard and grounded electrodes. Now, the electrostatic charging tendency (accumulated charge on the pressboard) can be related to a measured potential of the electrode covered by the pressboard samples. It could be shown, that the measured potential of aged pressboard was 3 times the potential of new (unaged) samples [144].

Accelerated ageing and measurement set-ups

» *An expert is someone who knows some of the worst mistakes that can be made in his subject, and how to avoid them.* «

Werner Heisenberg, 1971

5.1 Investigated materials and their preparation

The following chapter gives an overview of the investigated pressboard and mineral insulating oil samples and their preparation. Material properties of unaged pressboard and insulating oils are described and discussed. Furthermore, the measurement set-ups are pictured.

5.1.1 Investigated pressboard

Pressboard serves as a vital component in oil-cellulose insulation systems, as it is used e.g. for field grading. Especially for DC applications, ageing behaviour in connection with electrical conductivity needs to be understood well. Although paper is also an important component in such insulation systems, e.g. as main conductor insulation, it is not covered within this work. The only exception is K-Buff paper, which is used for comparative reasons for space charge measurements (see Section 6.7.3). The pressboard samples had been used in two different forms and for two different applications respectively:

Disc-shaped samples

Disc shaped samples with a diameter of 140 mm and a thickness of 1 mm have been used for all electrical tests. They have been machined (grinded) to a thickness of 1 mm to receive an even surface. This was considered as important because the samples are comparably thin⁷⁷ and so the sieve structure could have a non-negligible influence if the pressboard is used in unmachined condition due to surface effects (e.g. surface charges, undefined surface properties, etc.). Surface structure can have also an influence on dielectric strength, as described in [133].

⁷⁷Especially when compared to practical applications, e.g. in a power transformer. Thicknesses of several millimetres (or more) are common there.

Spacers

Small pieces of T IV pressboard (25x25x1 mm) have been used as simple spacers for all the thermal ageing samples. They have been placed at the bottom of the glass vessel (4 pieces) and between the disc-shaped samples (6 pieces). The latter was primarily to prevent the samples from sticking together and to allow oil to flow between the discs. Furthermore, these spacers have been used for moisture determination, as they had been processed the same way as the samples to enable this. In that way, no sample had to be “destroyed” purely for moisture content determination.

The two different surface structures are pictured in Figure 5.1 below. On the macroscopic scale⁷⁸ the difference between machined and original surface can be clearly observed. On the microscopic scale⁷⁹ no significant difference between both types could be observed with an optical microscope.

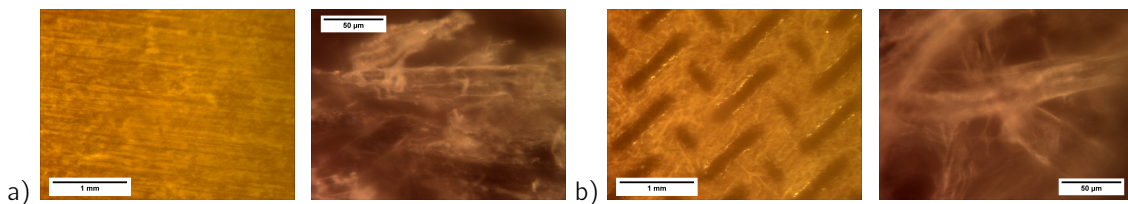


Figure 5.1: Magnified views of unimpregnated pressboard samples: a) Machined sample (disc-shaped) b) Unmachined (ungrinded) material (spacer)

5.1.2 Properties of unaged pressboards

The relative permittivity ϵ_r and the dielectric loss factor have been determined for unaged samples with a digital bridge-vector set-up with an electrode set-up in the style⁸⁰ of IEC 60093 (Tettex 2904) and IEC 60554-2 (VDE 0311-20 [150]). These values are representative only for the investigated samples - Relative permittivities of typical, high density pressboard (which is often thicker as 1 mm) are above these values.

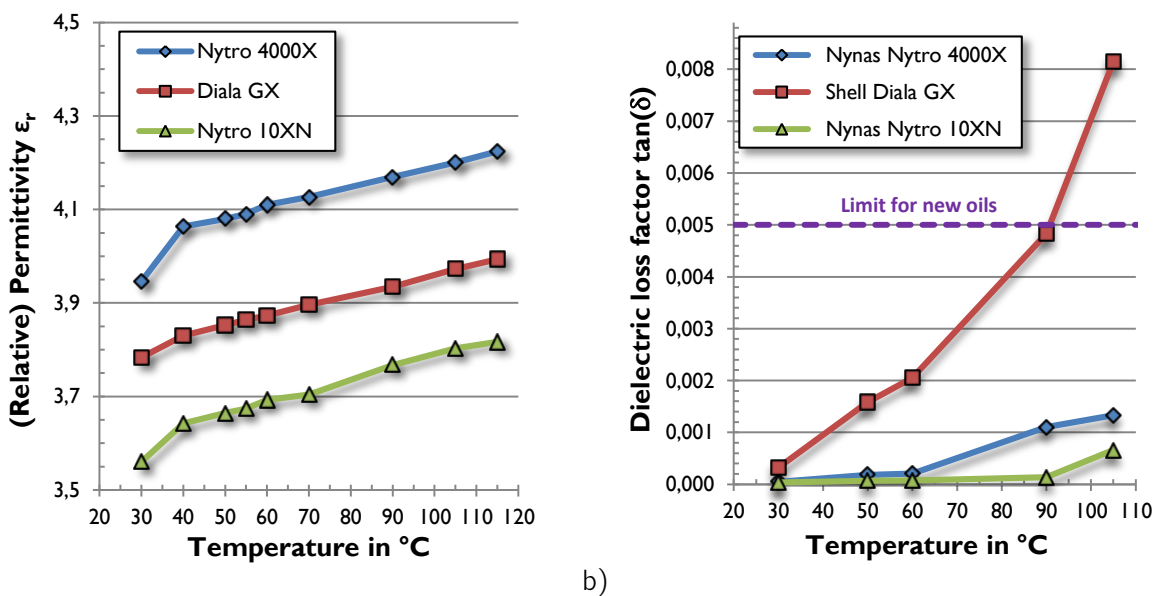


Figure 5.2: Properties of unaged pressboard samples with varied impregnation oil type and temperature: a) Relative permittivity ϵ_r b) Dielectric loss factor $\tan(\delta)$

⁷⁸Here: millimetres

⁷⁹Here: several μm

⁸⁰Test cell was heated to 115°C under vacuum. Afterwards heating has been switched off and measurements have been conducted at decreasing temperature. The samples have been subjected to dry air during that time.

The rise of capacitance and relative permittivity respectively with temperature may be explained with changed dimensions of the electrodes due to thermal expansion. This is also suggested in [160]. However, this was not the case here - The dimensional change of the electrodes between 20 and 100°C was below 0,2%, which was determined experimentally and is furthermore baked up to the low thermal expansion coefficient of (stainless) steel. **Influences due to uneven samples during measurement can be also excluded**, as a weight of 17 kg was used, which should be sufficient for the investigated samples. It is assumed that due to the thin samples and the oil film at the boundary layer, **these boundary layer and surface effects influence the measurement** that way. This is important all that more, as the pressboard is comperable thin and so the influence of a boundary layer has naturally a stronger influence. In [63], it is demonstrated that the **overall electrical properties** of the simplest capacitor model (Maxwell-Wagner [25]) - which equates basically the setup here - **are vitally influenced by the properties of the boundary layer** between both materials.

The rise of the dielectric loss factor $\tan(\delta)$ in the range of 70°C can be explained with the increasing conductivity [160].

5.1.3 Investigated mineral insulating oils

Three different types of mineral insulating oils are used within the scope of this work. Namely, these are:

1. **Nynas Nytro 4000 X**
2. **Shell Diala GX**
3. **Nynas Nytro 10 XN**

For better differentiation of the samples, the oil types have been **colour-coded** as shown above. Furthermore, and this was also kept throughout all the work in the laboratory, **numbers and IDs** starting with "1" indicate Nynas Nytro 4000 X, "2" was used for Shell Diala GX and "3" for Nynas Nytro 10 XN. This was helpful (in terms of quality assurance) to avoid mixing different oils and also eased the cleaning process of vessels and containers, because specific containers have been used for only one oil type each. In terms of supply, all three oils have different "origins":

- **Nynas Nytro 4000 X** was supplied from (unused) storage in the High Voltage Laboratory of TU Graz and partly from Siemens Transformers Austria (STA, Weiz).
- **Shell Diala GX** was taken also from the High Voltage Laboratory storage of TU Graz. However, this oil has been already used for high voltage testing (only little breakdown stresses at room temperature) and was kept under vacuum when not utilized.
- **Nynas Nytro 10 XN** was directly supplied from Nynas AB and therefore acutally the only "new" oil within the scope of this work.

The **electrical parameters** that are given below have been acquired with a BAUR DTL⁸¹. Before a measurement series and after changing from one oil type to a different one, the test cell has been cleaned thoroughly and flushed at least 10 times with the new oil before a measurement was made. Between subsequent measurements (with the same oil type), the test cell has been flushed once here.

All measurement results are **average values**. The column "n" states the number of single measurements which have been made to calculate each averaged value. The test cell itself was frequently disassembled during this project, cleaned thoroughly and calibrated afterwards. The mean value of the **empty cell capacitance** C_{Empty} was 71,57 pF, with a standard deviation σ of 1,09 pF.

The **viscosity** of all three oils has been determined at the Institute of Chemical Engineering and Environmental Technology at Graz University of Technology with a Stabinger Viscometer SVM 3000 (Anton Paar).

⁸¹Measured with 500 V DC (ρ) and 2000 V AC ($\tan(\delta)$, ϵ_r) with the standard electrode configuration (gap of 2 mm).

Nynas Nytro 4000 X

The Nynas Nytro 4000 X is an inhibited, severely hydrotreated (mineral oil based, naphthenic) insulating liquid. It is the successor product of the Technol US 4000 in Austria. The also well known Technol US 3000 was replaced by the Nynas Nytro 4000 A, which is also severely hydrotreated but is just trace inhibited. The material data sheet of Nynas Nytro 4000 X is given in the Appendix on page A.3.

Shell Diala GX

Shell Diala GX is a mineral oil (naphthenic) based, inhibited insulating liquid. According to the material datasheet, which can be found in the Appendix on page A.4 in extracts, inhibitor(s) are for oxidation stability only.

Nynas Nytro 10 XN

The Nynas Nytro 10 XN is an inhibited, highly refined (mineral oil based) electrical insulating liquid. It is specifically designed, besides all "general" electrical requirements, for low temperature applications. Therefore, it has the lowest guaranteed pour point (-45°C) of all three investigated oils. Material data sheet is in the Appendix on page A.5.

5.1.4 Properties of unaged mineral insulating oils

Relative permittivity ϵ_r

The relative permittivity of all three oils is linear decreasing with temperature; the Shell Diala GX has the highest relative permittivity ($\epsilon_r = 2,16 @ 90^{\circ}\text{C}$) of all three oils. The reduction in the relative permittivity from 30 to 90°C is in the region of 4,4 to 5,5%⁸². The separations of the relative permittivities of the three oils are large enough to securely distinguish the three investigated oils by measurement of ϵ_r only. However, a distinction is also possible with the measured specific resistivities (if the oils are unaged and dried).

Dielectric loss factor $\tan(\delta)$

The dielectric loss factor is an important parameter for oil and insulation system condition respectively. The lowest dielectric loss factor was observed for the Nynas Nytro 10XN. This is not surprising, as this is the only "real" new oil in this investigation. A **comparable high** $\tan(\delta)$ was determined for the Shell Diala GX. However, the $\tan(\delta)$ at 90°C is still below the limit defined in IEC 60296 [54] for new oils. However, according to this standard, such an oil can not be considered as "new" as it has been already in contact with "other" materials (e.g. pressboard, copper, etc.).

⁸²related to the value at 30°C

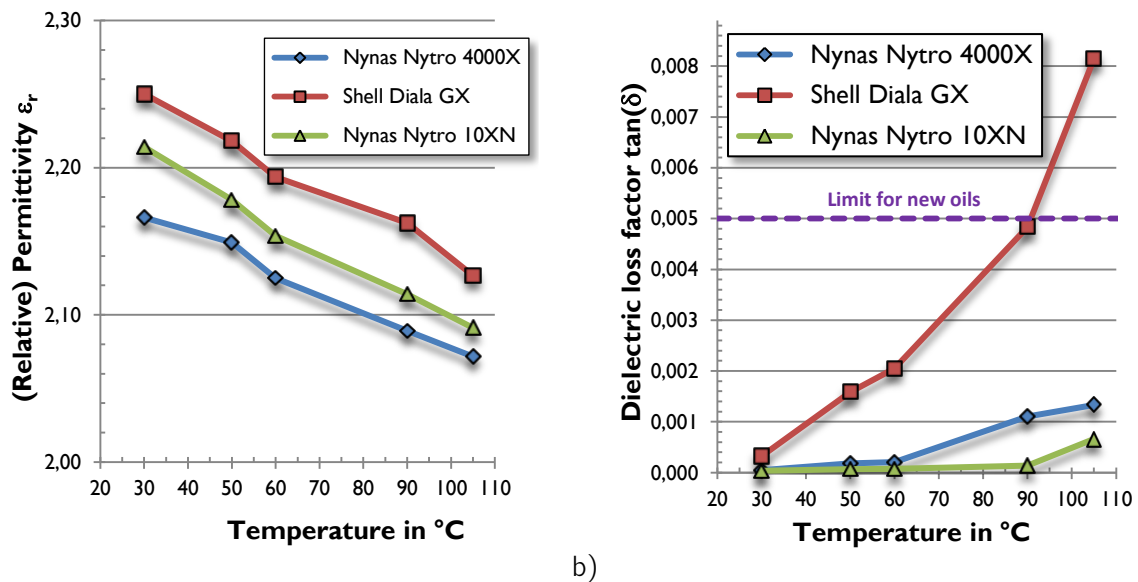


Figure 5.3: a) Relative permittivity ϵ_r and b) dielectric loss factor $\tan(\delta)$ of the (unaged) investigated mineral oils

Electrical conductivity

The (specific) electrical conductivity can also serve as a parameter for condition evaluation of a material. In fact, the BAUR DTL determines the specific resistivity of insulating liquids at a field strength of 250 V/mm (Applied voltage: 500 V, Electrode gap: 2 mm). This field strength is much lower than typical service stresses, so these values have to be interpreted with caution. The values given here are determined automatically by the apparatus around 1 min after DC voltage application, conforming with IEC 60247.

Table 5.1: Electrical properties of Nynas Nytro 4000 X (unaged)

Temp.	n	ϵ_r	$\tan(\delta)$	ρ_+ [Ωm]	ρ_- [Ωm]	σ_+ [S/m]	σ_- [S/m]
30 $^{\circ}\text{C}$	10	2,17	0,00015	1,79E13	>2,00E13	5,59E-14	5,00E-14
50 $^{\circ}\text{C}$	10	2,14	0,00038	4,30E12	5,60E12	2,33E-13	1,79E-13
60 $^{\circ}\text{C}$	16	2,13	0,00030	2,11E12	2,71E12	4,73E-13	3,70E-13
90 $^{\circ}\text{C}$	23	2,09	0,00120	2,51E12	2,73E11	3,98E-12	3,66E-12
105 $^{\circ}\text{C}$	12	2,07	0,00143	1,55E12	1,75E11	6,44E-12	5,71E-12

Table 5.2: Electrical properties of Shell Diala GX (unaged)

Temp.	n	ϵ_r	$\tan(\delta)$	ρ_+ [Ωm]	ρ_- [Ωm]	σ_+ [S/m]	σ_- [S/m]
30 $^{\circ}\text{C}$	10	2,25	0,00043	1,17E12	1,56E12	8,57E-13	6,41E-13
50 $^{\circ}\text{C}$	10	2,22	0,00169	2,94E11	3,58E11	3,40E-12	2,80E-12
60 $^{\circ}\text{C}$	14	2,19	0,00215	2,92E11	3,20E11	3,43E-12	3,13E-12
90 $^{\circ}\text{C}$	13	2,16	0,00493	1,41E11	1,45E10	7,11E-12	6,89E-12
105 $^{\circ}\text{C}$	12	2,13	0,00825	5,15E10	5,96E10	1,94E-11	1,68E-11

Table 5.3: Electrical properties of Nynas Nytro 10XN (unaged)

Temp.	n	ϵ_r	$\tan(\delta)$	ρ_+ [Ωm]	ρ_- [Ωm]	σ_+ [S/m]	σ_- [S/m]
30 $^{\circ}\text{C}$	10	2,21	0,00014	>2,00E13	>2,00E13	<5,00E-14	<5,00E-14
50 $^{\circ}\text{C}$	10	2,18	0,00017	>2,00E13	>2,00E13	<5,00E-14	<5,00E-14
60 $^{\circ}\text{C}$	11	2,15	0,00017	1,00E13	1,41E13	9,99E-14	7,10E-14
90 $^{\circ}\text{C}$	10	2,11	0,00024	1,64E12	1,83E12	6,10E-13	5,46E-13
105 $^{\circ}\text{C}$	17	2,09	0,00076	3,27E11	4,02E11	3,06E-12	2,49E-12

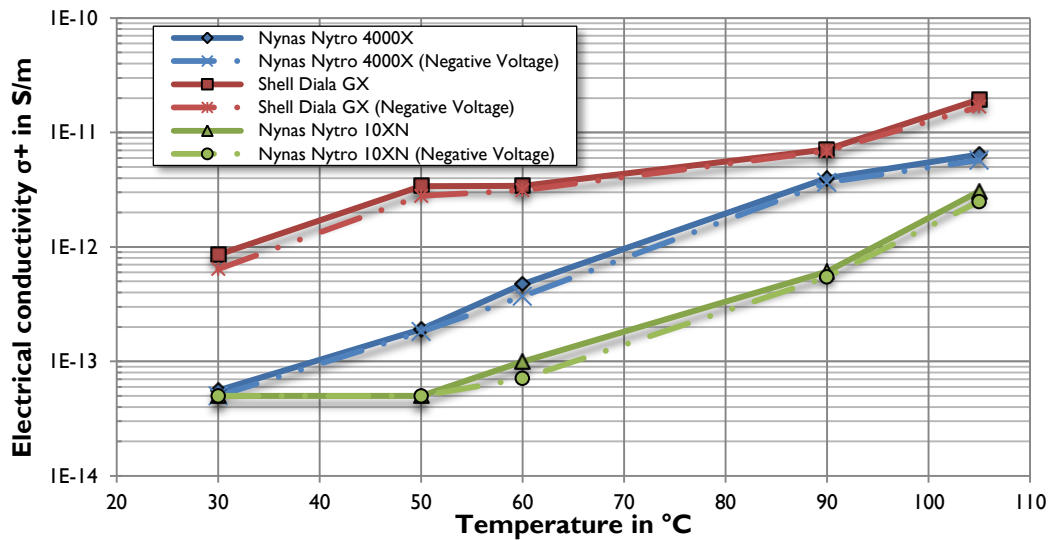


Figure 5.4: Electrical conductivity of (unaged) investigated mineral oils

Viscosity and density

The viscosity of all three oils has been measured in the temperature range between 20 and 90°C. The kinematic viscosity at 40°C is given also in the data sheet for all three oils - These values correspond well with the measured values.

The Nynas Nytro 10XN has the lowest viscosity of the three investigated oils. This is reasonable, as this oil is specifically recommended for low temperature applications. According to the product data sheet, this is due to the naphthenic characteristics and composition of the oil respectively.

It can be derived from [2] that these oils are hydrocarbons of higher order, as the (kinematic) viscosity can be calculated from molecule structure as following⁸³:

$$\eta = 1,095 \cdot 10^{-4} \cdot e^{\left[\frac{0,0046 \cdot n \cdot k_B \cdot T + 0,00154 \cdot (n + 86,5)}{k_B \cdot T} \right]} \quad (5.1)$$

η Kinematic viscosity [Poise]

k_B Boltzmann constant $k_B = 8,6167 \cdot 10^{-5}$ [eV/K]

T Temperature (absolute) [K]

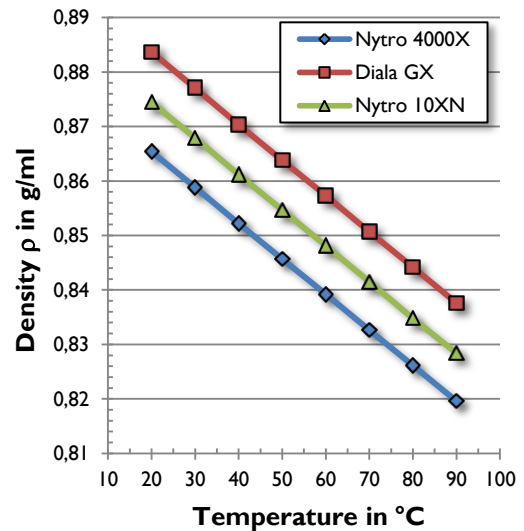
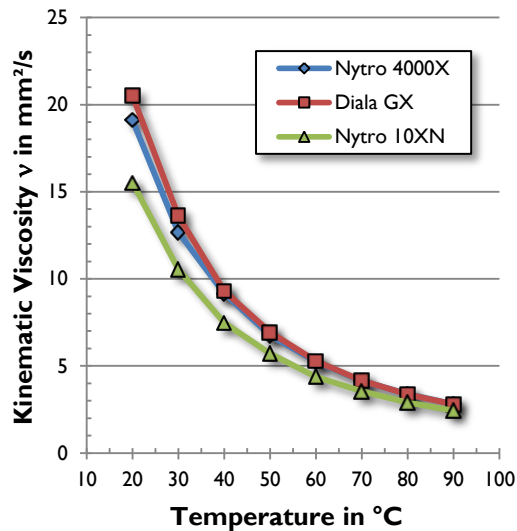
When assuming values for n , say $n = 28$, this results in a kinematic viscosity at 20°C of $\eta = 0,134$ [Poise] which is around the viscosity of 10XN at this temperature ($\rightarrow \eta = 13,44 \eta_{10XN} = 13,57$ [mPa · s]). However, these are only basic assumptions - As it is stated in [2], large deviations between theoretical and practical values can occur. Therefore, other relationships might be more useful which are also described there accordingly.

The density falls linearly with temperature for all three oils as expected (see Figure 5.5). The **decrease in density** between 30 and 90°C is in the range of **5%** for all three oils, which **corresponds well with the decrease of relative permittivity** (see Figure 5.3). Also in case of density, values given in the data sheets could be confirmed, although the value for the Nytro 4000X is slightly lower than the typical value.

⁸³The formula is taken directly from [2] - Therefore different units (International System of Electrical and Magnetic Units) are used for η and k_B

Table 5.4: Viscosity and density of investigated oils

Oil	Kinematic viscosity ν		Density ρ	
	measured	typical (data sheet)	measured	typical (data sheet)
Nynas Nytro 4000 X	9,1 mm ² /s	9,2 mm ² /s	0,865 kg/dm ³	0,872 kg/dm ³
Shell Diala GX	9,3 mm ² /s	8,0 mm ² /s	0,884 kg/dm ³	0,886 kg/dm ³
Nynas Nytro 10XN	7,4 mm ² /s	7,6 mm ² /s	0,874 kg/dm ³	0,877 kg/dm ³



a)

b)

Figure 5.5: a) Kinematic viscosity ν and b) density ρ of (unaged) investigated mineral oils

5.1.5 Ageing sample composition

To receive reliable data from laboratory ageing tests it is necessary to **replicate the real operation and set-up with the utmost effort**. In terms of ageing sample composition this means that the same (or similar) materials need to be used in the same quantities (weight, volume and ratio of volume:surface). An ageing sample used within this work consisted therefore of:

Pressboard

(A) 7 discs (T IV), \varnothing 140 mm, thickness 1 mm, machined

Spacers

(B) 10 pieces (T IV), 25x25x1 mm, un-machined

Oil

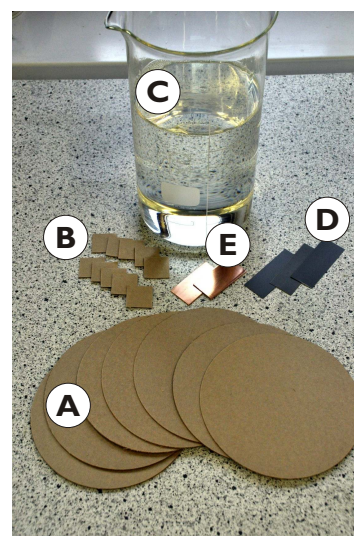
(C) 1,6 l (dried/reprocessed)

Steel

(D) 3 stripes, 64x25 mm

Copper

(E) 2 stripes, 49x25 mm

**Figure 5.6:** Composition of an ageing sample

However, it was not possible to fulfil all parameters here: With a board density of 1,22 kg/dm³ and oil density of 0,88 kg/dm³, a sample consists of 0,139 kg cellulosic material and of 1,408 kg oil respectively. This results in an oil:board ratio of 10,13, which lies in the typical range of around 10 to 12. However, when

taking the dimensions of a real HVDC converter transformers into account [19], the ratio volume:surface is around 5 there whereas only a value of 0,6 could be achieved with the given set-up and restrictions.

For the investigated sample composition, varied water content⁸⁴ will lead to the following, absolute moisture content levels:

Table 5.5: Water content in oil and pressboard for ageing sample ratios

Moisture content board	0,2%	0,5%	1%	2%	3%	4%
Water (absolute) in g	0,25 g	0,63 g	1,25 g	2,51 g	3,76 g	5,02 g
Moisture content oil	5 ppm	10 ppm	15 ppm	20 ppm	25 ppm	30 ppm
Water (absolute) in g	0,00716 g	0,01432 g	0,02148 g	0,02864 g	0,03580 g	0,04296 g
Ratio Board:Oil	35	44	58	88	105	117

5.2 Set-ups for accelerated ageing

The accelerated ageing in the laboratory was divided into 2 parts: pure thermal ageing (main part) and combined thermal and electrical ageing. For the **thermal ageing part**, test vessels are needed, which:

- can sustain temperature (up to 135°C) and the presence of mineral oil
- do not limit other experiments and tests (e.g. limitations of sample size)
- are (relatively) gas tight

Ageing vessels need to fulfil numerous requirements, which are often diametral. Therefore, several compromises had to be made. First of all, the test vessels should not be too complex and be able to easily accommodate the test samples. This already posed a serious problem: To make useful measurements (electrical conductivity, breakdown strength, etc.) disc-shaped samples need to have a sufficient diameter. Eventually a diameter of 140 mm was chosen for this work. So this is a big difference to most of the ageing tests which have been reported in literature so far. For small scale accelerated ageing tests, small glass vials are used which can not be applied here for self-evident reasons. For larger samples, standard laboratory glassware (borosilicate glass 3.3) with standard closures (GL45 screwing) have been used in many cases. Although slightly larger diameters (up to GL80) are available from stock, they are still too small for the planned application.

The customised test cell should be large enough to accommodate the samples and small to accommodate as much vessels as possible into the thermal ovens. Therefore, the dimensions (and the available area) inside the thermal ovens had to be considered. Furthermore, in terms of materials, they should not influence the ageing processes. Finally, the overall costs should be low. In terms of material, costs have a strong influence. On the other side, the vessel materials should not influence the ageing process at all. If they still have an influence, then it should be preferably the same way than it would be in reality.

Example: The tank in a real transformer is made from sandblasted steel which is often coated with an "anti-corrosion-paint" ("primer"). So, either the vessels are made from this material or from an inert material, like stainless steel. The former solution is disadvantageous in terms of temperature stability, as such a paint has a maximum constant operating temperature in the same region as the planned artificial ageing temperature (135°C). The latter solution is very expensive in comparison though.

⁸⁴Moisture levels have been chosen arbitrarily.

5.2.1 Vessels for thermal ageing

A technically simple and non-complex solution was found with Pyrex laboratory glass dishes, which are covered with a stainless steel sheet. The vessel is sealed with a FKM gasket. To ensure gas tightness as good as possible, the sealing and the steel cover are glued to the glass dish. For further details on these vessels see Appendix B.

Vessel size and electrical conductivity measurement

Several different versions have been evaluated for the thermal ageing vessels. As a first approach, standard laboratory bottles from borosilicate glass have been analysed. Although such bottles have superior properties in terms of chemical and temperature resistance, price and availability, the small opening hinders the usage of large pressboard samples as described above. And such samples are needed for an useful electrical conductivity measurement for example. Standard bottles (GL45) have an inner bottle neck diameter of around 30 mm only⁸⁵. This is not satisfactory, as the achievable current during electrical conductivity measurements is very small at practical set-ups (see Figure 5.7). This is demonstrated in the following example. The specific resistivity with a standard set-up according to IEC 60093 [52] can be determined with (4.33). The following assumptions are made:

- Rectangular-shaped pressboard sample; width: 30 mm, thickness: 1 mm
- Specific resistivity of pressboard (ρ): $10^{16} \Omega \cdot \text{m}$ ("worst case" measurement wise)
- Electrode diameter (d_1): 11 mm
- Air gap (g) between measurement and guard electrode: 3 mm
- Measurement voltage (U): 3 kV (resulting in a field strength of 3 kV/mm)

The effective electrode area can be determined with (4.34), and amounts in this example:

$$A = \frac{\pi \cdot (d_1 + g)^2}{4} = \frac{\pi \cdot (11 + 3)^2}{4} = 153,94 \text{ mm}^2 \quad (5.2)$$

The current is then estimated with (4.33) and (4.1):

$$R_x = \frac{\rho \cdot h}{A} \rightarrow I = \frac{U}{R} = \frac{U \cdot A}{\rho \cdot h} = \frac{3.000 \cdot 153,94 \cdot 10^{-6}}{10^{16} \cdot 0,001} = 46,18 \text{ fA} \quad (5.3)$$

This situation is undesirable, as such a set-up leads to very small (steady state) currents. The background noise - due to leakage currents, disturbances, etc. - of typical set-ups can be in the region of some tenth up to several pA, so the signal-to-noise ratio is quite low in such a case, if the desired current can be measured at all. Furthermore, such a set-up is limited in terms of maximum voltage (and field strength respectively), as the creeping distance between HV and guard electrode is very short on the narrow end of the board (see Figure 5.7). Although the guard electrode actually needs to be reduced in size for a practical set-up, such a configuration will not yield usable results.

However, if larger samples ($\varnothing 140 \text{ mm}$) and electrodes ($\varnothing 84 \text{ mm}$, airgap $g=3 \text{ mm}$) are used, the current is estimated (when keeping the same preconditions as in the example before; $U = 3 \text{ kV}$, $\rho = 10^{16} \Omega \text{m}$, sample thickness $h=1 \text{ mm}$, resulting electrode area according to (4.34): $A = 5.944,68 \text{ mm}^2$) with (4.33):

$$I = \frac{3.000 \cdot 5.944,68 \cdot 10^{-6}}{10^{16} \cdot 0,001} = 1,783 \text{ pA} \quad (5.4)$$

⁸⁵Although larger bottles are available (GL80), the sample sizes would be still limited heavily.

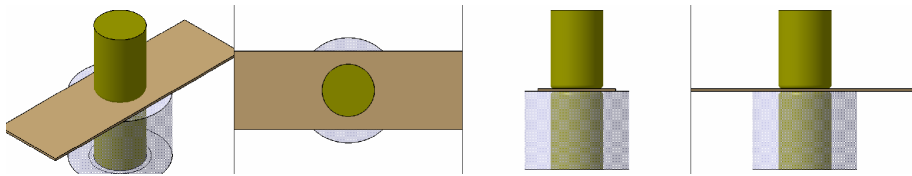


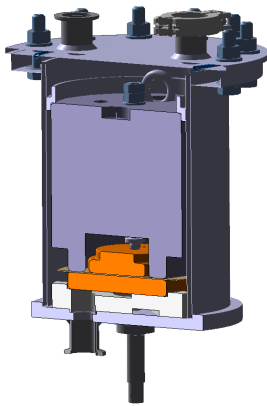
Figure 5.7: Schematic set-up for electrical conductivity measurement

So the current is nearly 39 times higher than in the previous example, although it is still “small”. The usage of larger samples has the further advantage that such samples could also be used for other investigations like dielectric withstand tests (see Section 6.4.3, page 93), ECT evaluation (see Section 6.6, page 97) and space charge measurements (see Section 6.7, page 101) for example.

Eventually, a cost-effective solution had been found, which can accommodate such samples and which can be placed into the thermal ovens in a space efficient way. These vessels consists of a standard laboratory glassware dish and a stainless steel cover with a vacuum flange for oil filling and sample taking. More details are given in Appendix B.

5.2.2 Vessels for combined ageing and conductivity measurement

The design of a vessel for combined ageing - the concurrent application of thermal and electrical stress is more complex than for the thermal ageing vessels. Furthermore, it should be possible to measure the electrical conductivity of the sample without interaction or even open the test vessel during accelerated ageing. Several different versions have been evaluated. Eventually, a design with a vessel made completely from stainless steel (1.4301) evolved, of which 8 vessels have been built. The vessel is described in detail in Appendix C.



a)



b)

Figure 5.8: a) Schematic of conductivity measurement cell; b) Practical set-up

This design poses the possibility to use it for the combined ageing tests (application of thermal and electrical stress at the same time or without the need to open the cell) and also for the measurement of electrical conductivity.

Conductivity measurement

Assuming a specific board resistivity of $\rho = 5 \cdot 10^{15} \Omega \cdot \text{m}$, the steady state current with this set-up under the given preconditions can be estimated with (4.33):

$$I = \frac{3.000 \cdot 5.944,68 \cdot 10^{-6}}{5 \cdot 10^{15} \cdot 0,001} = 3,57 \text{ pA} \quad (5.5)$$

5.2.3 Accelerated ageing equipment

The whole accelerated ageing tests took place in a Portakabin, which was placed in the open-air high voltage test field of the Institute of High Voltage Engineering and System Management at Graz University of Technology. This was done on the one hand for practical reasons (available floor space) and on the other hand for safety and security reasons. The container is equipped with according safety equipment and a temperature monitoring system. Furthermore, fans have been installed during the course of the project to keep the air temperature within the container below 40°C, especially during the summer months.



Figure 5.9: Delivery of Portakabin



Figure 5.10: Inside view of ageing container

Thermal ovens for sample ageing

Two thermal ovens (Heraeus UT6200) have been used specifically for thermal ageing. In each oven, 16 ageing vessels can be accommodated at the same time. Although these ovens have a forced convection, there is quite a large spatial temperature difference inside the oven ($\pm 5^{\circ}\text{C}$). However, it has to be noted, that the ovens have been loaded very tightly which also hinders the air flow considerable. A relocation of samples during the ageing process was not considered. On the one hand, it would be necessary to remove the temperature sensors and on the other hand it is difficult to achieve the same “average” ageing temperature for all samples anyway.

For the combined (thermally and electrically) ageing of samples, two slightly larger thermal ovens (Mettmert UFP600) have been used. However, these two ovens also have been used to accommodate pure thermal ageing samples in the beginning of the work (up to 9 samples per oven).



Figure 5.11: Thermal ovens with ageing vessels: a) Heraeus UT6200 with thermal ageing vessels; b) Mettmert UFP600 with combined ageing vessels

5.2.4 Temperature monitoring systems

Temperature has an important influence on ageing and is also considered as the dominant ageing factor, especially in absence of other processes (e.g. corrosive sulphur etc.). As noted before, the spatial temperature distribution within the thermal ovens has quite a large spread: All ovens have been set to 135°C, but the temperature at the bottom of the oven could be as low as 130,7°C, whereas at the top shelf up to 140,5°C at maximum could be measured, nota bene not simultaneously.

Two approaches had been followed: Direct sample temperature measurement for thermally aged samples and measuring vessel temperature at combined ageing test cells:

Temperature measurement at thermally aged samples

30 out of 32 thermally aged samples have been monitored with a customized, 30 channel measurement system. Pt100 temperature sensors are mounted directly at the ageing vessel to determine the oil temperature directly (see Figure 5.11, a). Sensor tips are covered with a PTFE foil to minimize the influence of the sensor onto the ageing process and to protect the sensor itself from the oil and ageing respectively. Sensor mounting was made with olive type tube fitting (PTFE insulated). Temperature values are transferred via LAN into a MySQL database for easy access and statistical evaluations.

Temperature measurement at combined aged samples

A different measurement system has been set-up for the combined ageing vessels: A customized, 16 channel measurement system, based on thermocouples (TC type K) has been built. 8 channels have been used for the measurement of sample temperatures and vessel temperature respectively (Figure 5.11, b). The remaining 8 channels have been used to determine the temperature of the ovens (outside) as well as room temperature for safety reasons (malfunction detection). Temperature values are transferred via LAN into a MySQL database for easy access and statistical evaluations.

5.3 Electrical conductivity measurement set-ups

The utilized equipment and measurement set-ups for the determination of electrical conductivity of pressboard and insulating oils is described briefly in the following section.

5.3.1 General

The electrical conductivity of oil and pressboard was determined with voltage-current measurements in the style of applicable standards: IEC 60093 [52] (VDE 0303-30 [148]) for pressboard and IEC 60247 [53] (VDE 0380-2 [157]) for oils.

The set-ups are described in the following subsections, however an annotation is given in terms of electrode material: Although it is quite **common to use brass electrodes** for electrical measurements, they have some major disadvantages when it comes to HVDC applications. Especially when used for breakdown investigations or electrical conductivity measurements, the injections of free charge carriers can be troublesome. **Stainless steel electrodes seem to be a good alternative**, as already proposed by [14, 130] for example. In general, steel has a higher work function than brass⁸⁶. This solution was also employed for this work as all test cells for oil and pressboard have been made from stainless steel (1.4301).

⁸⁶In fact, the work function of copper is even higher than the one of steel.

Due to the large time constants (caused by large relaxation times) it takes 24 h or more at the oil and pressboard samples to reach a steady current at 20°C, a parallel measurement of several samples was aspired. With **multiplexers** (Keithley 705 scanner with adequate low-current switch cards Keithley 7058) it was eventually possible to measure 4 pressboard cells and 2 oil cells in parallel.

Care has to be taken when choosing switching times: Electrometers needs a certain time to deliver a stable reading of the current. This timespan is longer at small current values (e.g. pA range) and for a “large” $\frac{di}{dt}$. Therefore, after switching to a different test cell, a “**dead-time**” had to be await to reduce glitches and avoid “incorrect” current measurement values. Furthermore, the first measurement in each channel is longer than all subsequent measurements. As the voltage is switched on simultaneously, the current changes strongly shortly after voltage application (keyword: “*transient time*”), this “start measuring time” is necessary to record this process with confidence.

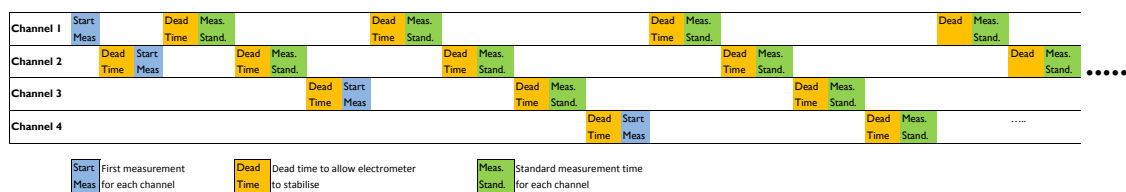


Figure 5.12: Measurement times and switching regime for multiplexers (schematically)

Protection circuits, based on low-leakage current diodes and a gas discharge tube, have been designed and applied at all measurements.

5.3.2 Set-up for mineral insulating oil

The electrical conductivity of mineral insulating oils has been determined with two different set-ups within this work:

- Customized set-up with Tettex 2903 test cells
- Standardized set-up: BAUR DTL

The customized set-up has the advantage, that one can **freely choose measurement parameters** (voltage, current measurement, time, etc.) However, the preparation process is time-consuming and measurements at elevated temperatures ($\geq 90^\circ\text{C}$) is tricky, as problems with the sealing and/or dielectric strength can occur. On the other hand, **simple and time-efficient measurements** are possible with a standardized measurement device BAUR DTL. The automated determination of ϵ_r , $\tan(\delta)$ and the specific resistivities for positive and negative voltages can be done in comparable short time. Therefore, both methods have been applied and are furthermore compared against each other.

Customized set-up with Tettex 2903 test cells

The schematic measurement chain of the customary set-up is pictured in Figure 5.13. A DanBridge DB604 has been used as stabilized voltage source. The applied voltage was 2 kV at maximum, as this was limited by the Tettex test cells. To improve the long-term behaviour of the test cells, the moisture level need to remain quite constant during a measurement cycle ($\geq 24\text{h}$). Therefore, cylindrical Viton gaskets have been introduced, which worked well at 20°C and partly also at 50°C. However, at 90°C the leakage current increased dramatically in several cases, which even lead to dielectric breakdown in some cases, which is why they have no been used at all at elevated temperatures. A placement of the equipment in an exsiccator with drying medium (e.g. silica gel) might solve the issue with moisture ingress.

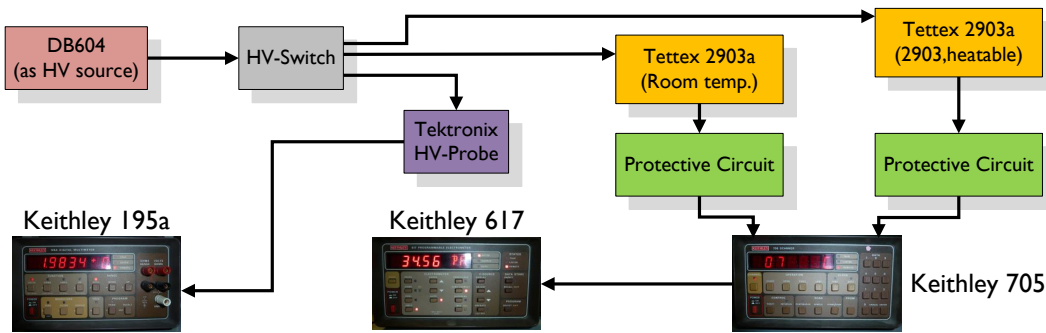


Figure 5.13: Schematic set-up for measurement of electrical conductivity of insulation oils

The electrical conductivity of insulating oils has been measured with voltages of 2 kV and 1 kV which results in electrical field strengths of 1 kV/mm and 0,5 kV/mm respectively. As the test cells can be heated only, the temperature is governed by room temperature if no heating is applied. However, by heating the room during winter season, it was possible to measure at 20°C ($\pm 1,0^\circ\text{C}$). Measurements at 50, 60 and 90°C could be made with a tolerance of $\pm 1^\circ\text{C}$

BAUR DTL

Measurement of electrical conductivity has been conducted with 500 V DC, which results in an electrical field strength of 0,25 kV/mm. Other dielectric parameters ($\tan(\delta)$, ϵ_r) have been determined with 2000 V AC. Both (maximum) voltages are given by device limitations. In terms of measurement time, no reasonable measurements could be made at 20°C. Therefore, the lowest possible temperature was 30°C during this work.

5.3.3 Set-up for pressboard

The test cells described in Appendix C have been used for the electrical conductivity determination of pressboard⁸⁷. The schematic measurement chain of the customary set-up is pictured in Figure 5.14. The applicable voltage is only limited by the dielectric strength of the sample, the HV switches (max. switching voltage 7 kV) and the bushing (20 kV). Measurements have been made between 250 V and 10 kV, however the voltage was not switched at 10 kV due to limitations of the relay switches.

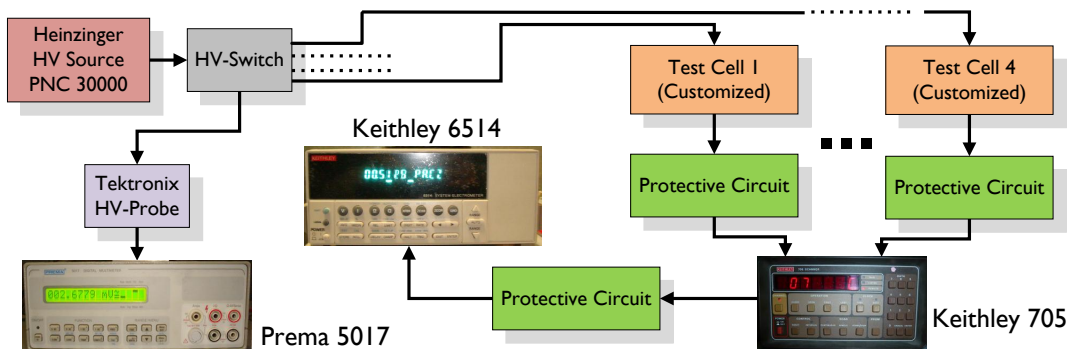


Figure 5.14: Schematic set-up for measurement of electrical conductivity of pressboard (with 4 test cells in parallel)

⁸⁷However, the influence of moisture content was determined with a slightly different set-up, which is described in [60].

5.4 Electrostatic charging tendency measurement set-up

To evaluate the **electrostatic charging tendency** (ECT), a spinning disc set-up has been used. A closed aluminium vessel (Volume of around 4,5 l), which is insulated by Teflon discs, serves as basis for this construction (Figure 5.15). A speed controllable DC motor (brushless) is connected on top of the vessel via an insulated clutch. A new and innovative current tap has been developed in [164]. The current is collected via 2 carbon brushes, which are supported with spring mounts to ensure a steady contact pressure and good electrical contact respectively. More details about the set-up and basic investigations can be found in [164].

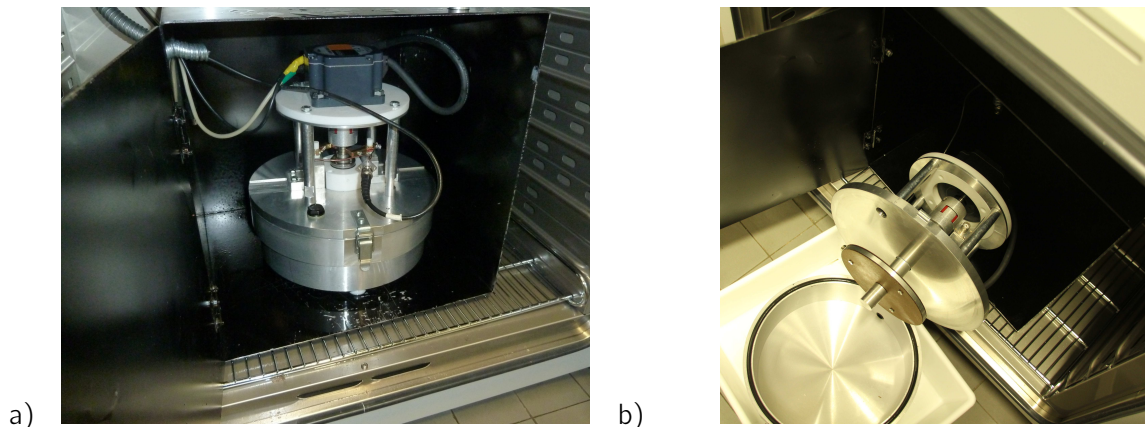


Figure 5.15: Spinning disc apparatus for ECT determination: a) Apparatus in thermal oven; b) Open cover with sample holder

5.5 Space charge measurement set-up

Space charge measurements have been carried out at the TU Delft (EWI, Institute of High Voltage Technology and Management) during research visits in 2010 and 2011. The set-up used is pictured in Figure 5.16 and described in detail in [13, 56, 105]. The whole set-up is located in a test chamber which can be climate controlled. Measurements have been carried out at 20 and 60°C with a poling voltage of 10 kV and a pulse voltage of 500 V with a width of 20 ns.

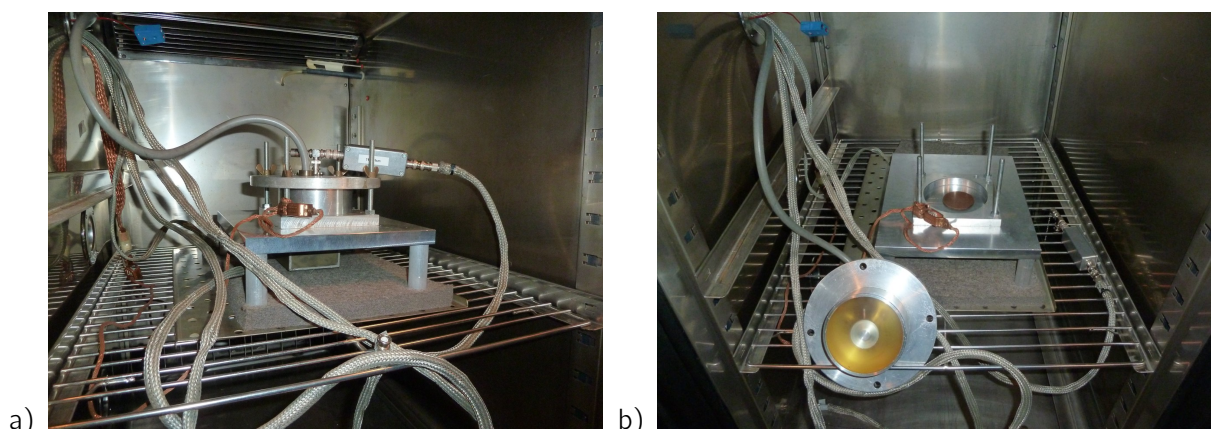


Figure 5.16: Space charge measurement set-up at TU Delft: a) Apparatus in thermal oven; b) HV electrode disassembled

Experimental results

» A philosopher once said: "It is necessary for the very existence of science that the same conditions always produce the same results." Well, they do not. «

Richard Feynman, 1965

6.1 General

The thermally aged samples, which have been available for further investigations are listed in Table 6.1. The planned durations are listed in the first column. It was not possible at every ageing sample to fulfil these times. This was owed to equipment/resources availability which lead to shortened or prolonged ageing times respectively. Eventually, **112 sample sets** (with 1,6l of oil, 7 pressboard discs and 10 spacers each) have been aged artificially successfully.

Table 6.1: Summary of thermally aged samples

Oil Type (Duration)	Nynas Nytro 4000 X		Shell Diala GX		Nynas Nytro 10 XN		Average
	samples	Duration	samples	Duration	samples	Duration	
1 w (168h)	4	262 h	4	195 h	4	128 h	195 h (+16%)
3 w (504h)	-	-	4	509 h	4	754 h	632 h (+25%)
5 w (840h)	4	842 h	4	864 h	8	1.090 h	932 h (+11%)
8 w (1344h)	4	1.590 h	-	-	4	1.343 h	1.467 h (+9%)
11 w (1848h)	4	1.876 h	4	1.891 h	4	1.985 h	1.917 h (+4%)
14 w (2352h)	4	2.356 h	4	2.403 h	4	2.615 h	2.458 h (+5%)
17 w (2856h)	4	2.923 h	-	-	4	2.997 h	2.960 h (+4%)
24 w (4032h)	8	4.042 h	8	4.305 h	4	4.089 h	4.145 h (+3%)
32 w (5376h)	4	5.608 h	4	5.383 h	4	5.437 h	5.476 h (+2%)
Sample Σ	36	-	32	-	40	-	-

However, not all of them could be used for further tests, due to issues during ageing process, for example moisture/oxygen ingress, etc. A repetition of the artificial ageing to fill the three missing durations was not possible however for resource availability reasons (pressboard samples, equipment,...).

6.2 Electrical conductivity of pressboard

Influence of moisture content, electrical field strength, temperature and thermal ageing onto the electrical conductivity of the investigated pressboard samples in dependence of oil type is described in the following chapter. The “step-functions”, that are visible in the conductivity and current diagrams originate from the loglog-plot and from the “rough” data sampling: As shown in section 5.3.1, data is sampled for a start time and then only for the shorter sampling time (approx 3 s). Between each sampling cycle, during nearly 90 s no data is available in each channel.

6.2.1 Moisture content

It was assumed, that moisture content has a strong influence onto electrical conductivity of pressboard. To evaluate this influence, exemplary measurements on pressboard discs⁸⁸ have been made, as described in [60]. As this was in the beginning of this work, the final set-up which was used for the following investigations had not been completed yet. Therefore, the influence of moisture has been determined with **a slightly different set-up** [60].

Dried and impregnated pressboard samples have been placed in a climate cabinet at 40°C and 70% relative humidity. To achieve a moisture increase of around 1 percentage point, a waiting time of approximately 1 hour was necessary each. However, most of the moisture was deposited on the surface and only a small part was assumed to have diffused into the pressboard. This is especially true for the very dry samples (around 1% moisture content) due to the comperable short residence time within the climate chamber. To achieve a more equal moisture distribution, much longer waiting times need to be adhered.

Moisture contents between 0,2 and 5,5% have been evaluated at 20°C, as pictured in Figure 6.1. It can be clearly seen, that **the electrical conductivity rises for each percentage point of moisture increase by one order of magnitude**. This relationship is valid for a moisture content between 0,2 and 3,5%. For higher moisture contents (in this case 5,5%), the current and electrical conductivity respectively increased also by one order of magnitude when compared to the conductivity at 3,5%. However, the current does not decrease with time, which means that polarisation effects are not dominating the current trend anymore. A possible reason for that might be found in conductive paths inside the pressboard which carry a significant conduction current (insulation current). In [99, 165] a “water shell” model based on percolation theory is discussed to explain similar effects on silica-filled epoxy-nanocomposites. Such conductive paths, caused by “monolayers” of water molecules are also reported there. This would also explain, why **this transient process happens so fast**: The current reaches a level, which is close to steady state, in shortly after 1 min. This is by far the fastest transient/polarisation process of all investigated samples. Dielectric heating can be excluded as the source of heating as demonstrated below:

The steady state current of the samples with 5,5% moisture content of $I = 393 \text{ nA}$ at the used voltage of $U = 3.130 \text{ V}$ results in

$$P = U \cdot I = 3.130 \cdot 393 \cdot 10^{-9} = 0,00123 \text{ W} \quad (6.1)$$

Even when considering that dielectric heating would only affect the sample in the area of the high voltage electrode ($\varnothing = 170 \text{ mm} \rightarrow V = 2,270 \cdot 10^{-5} \text{ m}^3$ at the 1 mm thick samples), the inserted power is much less ($0,03 \text{ W/cm}^3$) than for example the defined maximum value [149] of $0,1 \text{ W/cm}^3$. However, in [14] it is indicated, that discharge paths (in liquids) are quite sensitive to site and it follows »one or more filamentary tracks«. When considering this, the current would have to flow through a volume smaller than $12,3 \text{ mm}^3$ to exceed the limit of $0,1 \text{ W/cm}^3$. This would result in a diameter a single conducting path with less than 3,96 mm when assuming a circular one (through the bulk of the material).

⁸⁸Sample diameter $\varnothing = 190 \text{ mm}$, 1 mm thickness, ungrinded; impregnated with and measured in Nynas Nytro 4000X at $E = 3 \text{ kV/mm}$

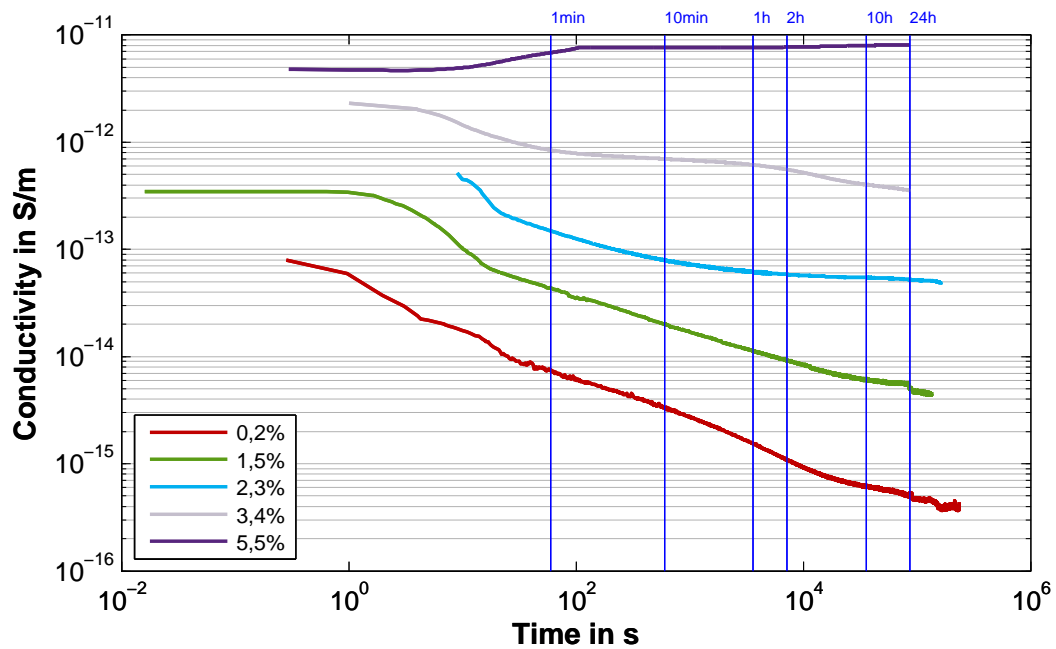


Figure 6.1: Influence of moisture content onto the electrical conductivity of pressboard (with Nynas Nytro 4000X)

These results are most likely only valid for pressboards (in combination with Nynas Nytro 4000X) at the used field strength. For example in [66, 72], the electrical conductivity of paper has been measured at varied temperature (at 20, 50 and 90°C) and moisture content at $E = 0,1 \text{ kV/mm}$. There, the increase of electrical conductivity by one order of magnitude was only observed between 0,4 and 1% moisture content. At higher moisture levels, the increase of electrical conductivity was much lower at all investigated temperatures when compared to the results of this work. These deviations can be explained by differences in the wetting procedure of the samples and probably in the type of materials tested.

However, the **reproducibility of the conductivity measurements is good in general**, as also indicated in Figure 6.2. There, the spread and the location of the mean is plotted for each investigated moisture level. The differences in electrical conductivity between the single levels are large enough to allow the secure determination of electrical conductivity at each level⁸⁹.

Table 6.2: Electrical conductivity in S/m of investigated pressboard samples with varied moisture content, determined at 20°C with $E = 3 \text{ kV/mm}$

Moisture	n	1min	10min	1h	2h	10h	24h	95% CI
0,2%	3	7,31E-15	3,33E-15	1,53E-15	1,10E-15	6,04E-16	5,23E-16	3,47...6,92E-16
1,5%	7	4,37E-14	2,01E-14	1,14E-14	9,22E-15	6,12E-15	4,96E-15	3,35...7,35E-15
2,3%	1	1,49E-13	7,90E-14	6,19E-14	5,84E-14	5,45E-14	5,20E-14	-
3,4%	2 ⁸⁹	8,42E-13	6,98E-13	6,16E-13	5,57E-13	4,02E-13	3,57E-13	3,50...3,65E-13
5,5%	3	6,85E-12	7,69E-12	7,67E-12	7,71E-12	7,98E-12	8,08E-12	7,20...8,97E-12

⁸⁹In [60], 3 samples of the sample set “3,4%” have been evaluated. However, when applying Dixon’s Q test, which is a simple test for small samples, one sample has to be discarded as an outlier with a probability of 99%.

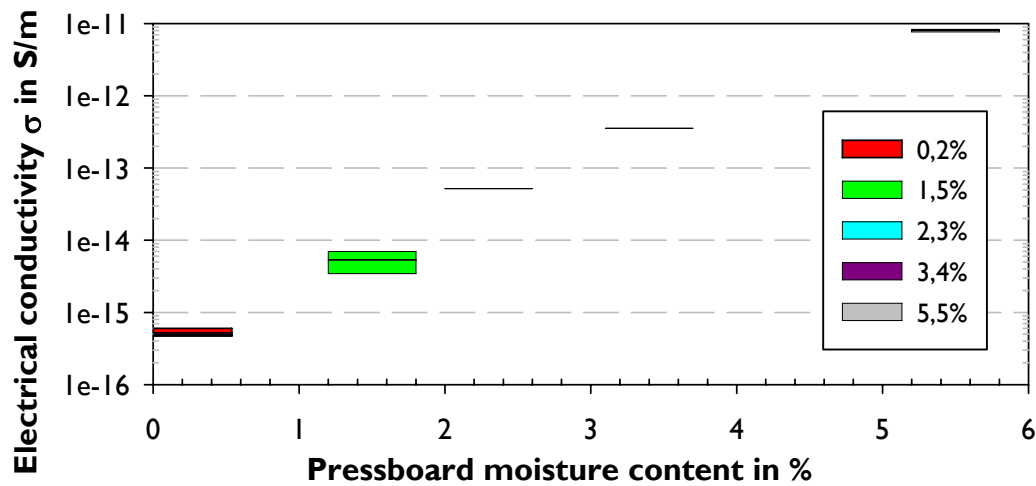


Figure 6.2: Spread of electrical conductivity measurements with varied moisture content

6.2.2 Electrical field strength

The influence of electrical field strength onto electrical conductivity was investigated for new pressboard samples with Shell Diala GX. Voltages of 250, 500, 1.000, 3.000, 6.000 and 10.000 V have been applied for > 24 h. **Basically, the electrical field strength does not have an influence on the steady state value** of the electrical conductivity of pressboard within the investigated voltage and field strength range respectively, as seen in Figure 6.4. As long as the voltage is “high” enough to produce a current, which can be measured with according confidence, the before mentioned statement is correct.

In this context, the measurement with 250 V at the Shell Diala GX impregnated samples actually needs to be discarded (Figure 6.3). At this “low” voltage, the steady-state current (<0,2 pA) is basically in the same region as the leakage currents and the noise of the set-up and the conduction current can not be determined with confidence.

However, it seems that the field strength has an influence on the time trend, as Figure 6.4 shows. With the exception of the trend at 0,25 kV/mm, the time gradient (decreasing) of conductivity is slightly higher with increasing field strengths. But it has to be doubted that this has any practical implications.

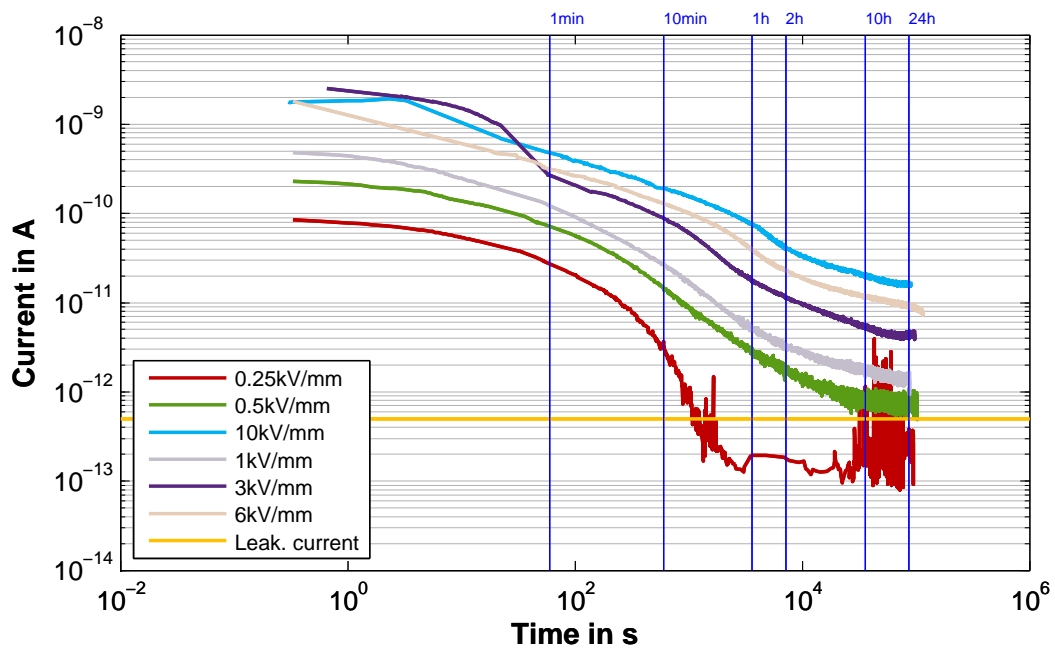


Figure 6.3: Influence of electrical field strength onto the measured current (time trend) of pressboard (with Shell Diala GX, measured at 20°C)

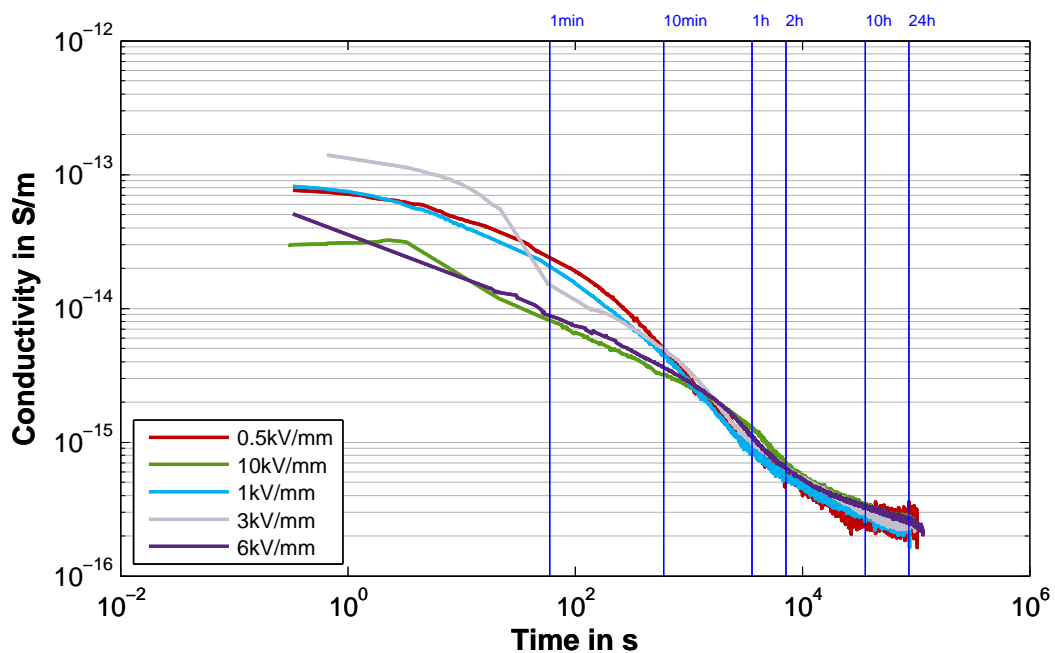


Figure 6.4: Influence of electrical field strength onto the electrical conductivity of pressboard (with Shell Diala GX, measured at 20°C)

6.2.3 Temperature

Temperature has a large influence onto the electrical conductivity of pressboard, as demonstrated in Figure 6.5. Here, new pressboard samples (moisture content <0,3%) have been measured at $E = 3\text{ kV/mm}$ at 20 and 90°C.

Steady state of the current is reached in less than 2 hours at 90°C, whereas it takes more than 24 h to reach a steady state at 20°C. Conductivity at 90°C is around two magnitudes higher when compared to

20°C. In fact, this is beneficial, as the ratio of conductivities (oil:board) decreases: The pressboard is relieved at HVDC operation when compared to 20°C, as it will be shown later.

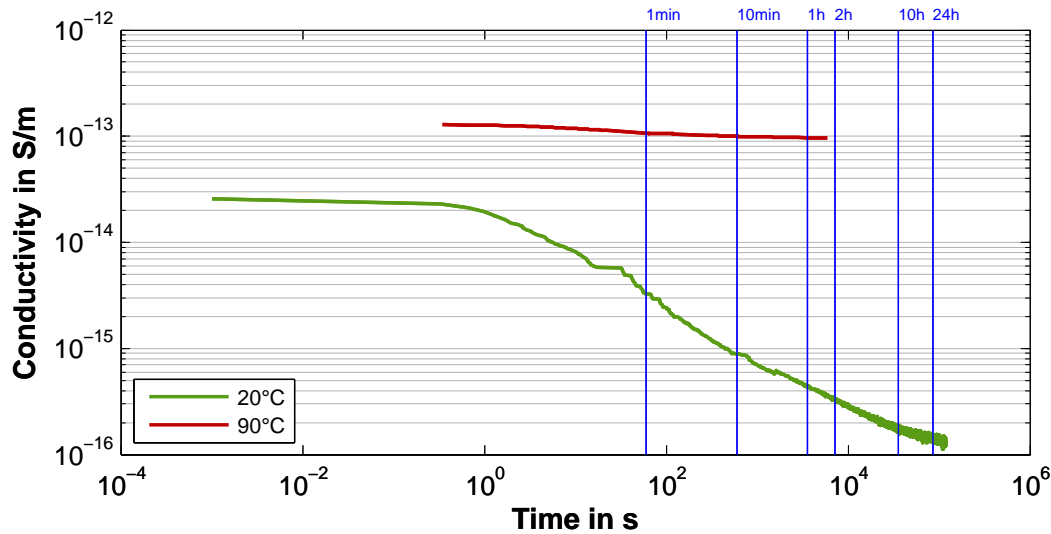


Figure 6.5: Influence of temperature onto the electrical conductivity of pressboard (with Nynas Nytro 4000X)

6.2.4 Ageing

The determination of ageing influence onto the electrical conductivity was a main target of this work. A multitude of measurements have been made for pressboard samples impregnated with three different mineral oils, which will be described in the following section. All conductivity plots are averaged time trends of several single measurements of comparably treated samples.

Pressboard impregnated with Nynas Nytro 4000X

The influence of ageing on the electrical conductivity of pressboard, which was impregnated with Nynas Nytro 4000X, is shown in the figure below. Interestingly, the steady state currents and the final conductivity values **do not differ significantly between the unaged and all the aged samples**.

This might be founded in the comparable low moisture content of the ageing samples due to sealed ageing vessels and a good preparation. As noted before, the oil was bubbled with nitrogen before the drying process and nitrogen atmosphere was present above the oil level in all the ageing vessels.

Clearly, the samples which have been aged for 32 weeks have the highest electrical conductivity shortly after voltage application and also at steady-state. However, all results are still easily within the typical range of reproducibility of different measurements ($\pm 10\%$ cot σ_0).

It is also interesting to note that in some cases the lowest currents (on average) in the early phase after voltage application (polarisation) could not be observed at the unaged but at samples which have been aged for 1 and 5 weeks. This was also reported in literature, for example in [68, 69] for OIP bushings. In this special case, deviations might originate from the set-up through remaining charges in the used insulators (PTFE), as the measured no-load currents have been different in these cases. Furthermore, oil properties (*oil conductivity*) are strongly governing these results.

The samples have been impregnated in several batches and the “same” oil has been used for all impregnation cycles. However it is very likely that different origins and manufacturing dates of the “same” oil result in varied different oil properties. Generally, this would also apply for the pressboard samples. In this case

however, they originate from a single batch, which is why the influence of oil property variation is much more likely.

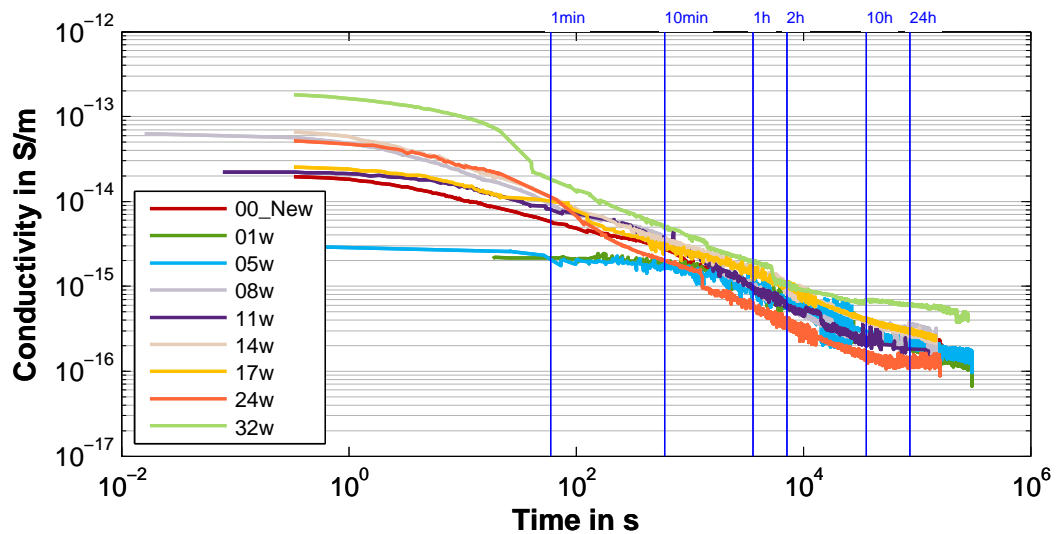


Figure 6.6: Electrical conductivity of pressboard (impregnated with Nynas Nytro 4000X) in variation of thermal ageing duration, measured at 20°C and $E = 3 \text{ kV/mm}$

Pressboard impregnated with Shell Diala GX

The investigation of thermal ageing behaviour of Shell Diala GX brought similar results like ageing in Nytro 4000X: A **clear distinction** of steady-state electrical conductivity can be made for unaged and **1 and 3 weeks aged samples only**. For longer ageing durations and therefore at samples with higher moisture content, quite similar steady-state conductivity values have been determined.

As already seen in the Nytro 4000X plots, the current and electrical conductivity **time trend in the initial stage** (10 min) after voltage application **is not a reliable indicator for steady-state estimations**.

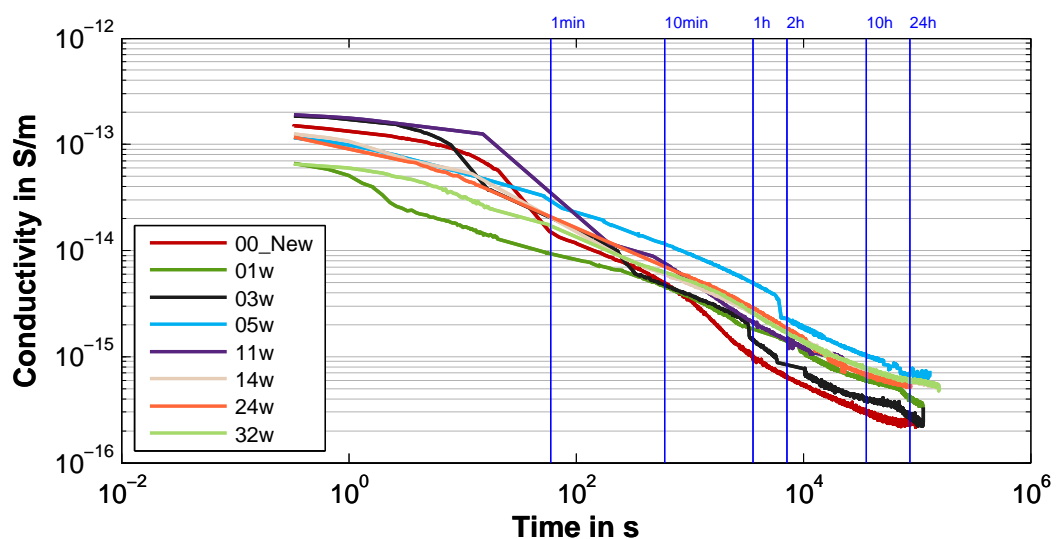


Figure 6.7: Electrical conductivity of pressboard (impregnated with Shell Diala GX) in variation of thermal ageing duration, measured at 20°C and $E = 3 \text{ kV/mm}$

Pressboard impregnated with Nynas Nytro 10XN

A distinction of aged samples just by electrical conductivity measurements is also tricky for the samples impregnated with Nynas Nytro 10XN. Only the new and unaged samples (00_New) have a distinctive “low” conductivity which separates them from the other family of curves.

It can be said that in general, the (capacitive/polarisation) current during the first 30 seconds after voltage application increases with increasing moisture and ageing condition. However it is not possible to conclude from the capacitive current, which dominates the current and conductivity respectively shortly after voltage application, to the ageing condition with confidence. For example, in Figure 6.8 the difference between the samples aged for 5 and 17 weeks respectively is only marginal. A reason for this can be found in the comparable low moisture content of all samples.

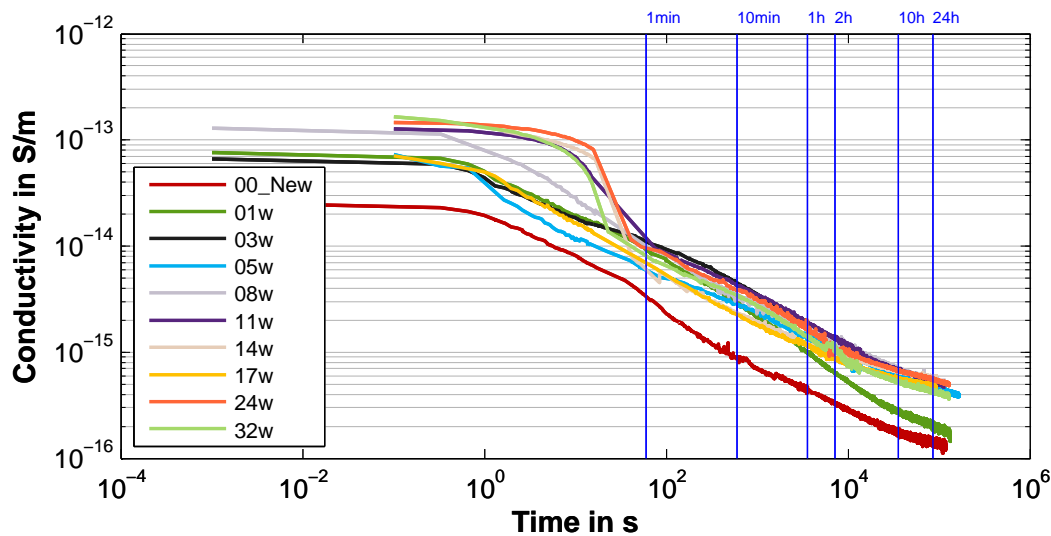


Figure 6.8: Electrical conductivity of pressboard (impregnated with Nynas Nytro 10XN) in variation of thermal ageing duration, measured at 20°C and $E = 3 \text{ kV/mm}$

6.2.5 Influence of combined ageing onto electrical conductivity of pressboard

The influence of combined ageing was investigated exemplary on 4 samples impregnated with Nynas Nytro 4000X. First, these samples had been subjected to a **temperature of 135°C for 1 week**. Afterwards, temperature has been reduced to **20°C** and a **stress of $E = 10 \text{ kV/mm}$** has been applied **for a further week**⁹⁰. The test cells have not been opened during this ageing cycle. Unfortunately, the simultaneous application of temperature and voltage was not possible to dielectric issues with the test cell (cabling and connectors). The averaged results of the conductivity time trend before and after the ageing process are shown in the figure below.

It can be seen that there is a negligible influence of combined ageing within this short time-scale. As also seen from Figure 6.9, polarisation processes are different in terms of time trend and duration. However, the conductivity end values are still within one order of magnitude. Here, to be precise, the value of electrical conductivity is still within the range of $\sigma = 2 \text{ to } 3 \cdot 10^{-16} \text{ S/m}$.

Ageing of Transformerboard due to combined electrical (AC) and thermal ageing has been investigated in [107]. Here, no significant ageing effects up to a (AC) field strength of $E \leq 10 \text{ kV/mm}$ could be determined. However, it has to be noted that this was determined merely on the basis of the dielectric loss factor $\tan(\delta)$. In [67, 72], similar results have been found by CDM investigations. There, oil impregnated paper samples

⁹⁰Rightly, one has to speak of subsequent ageing, as temperature and voltage have been applied subsequently.

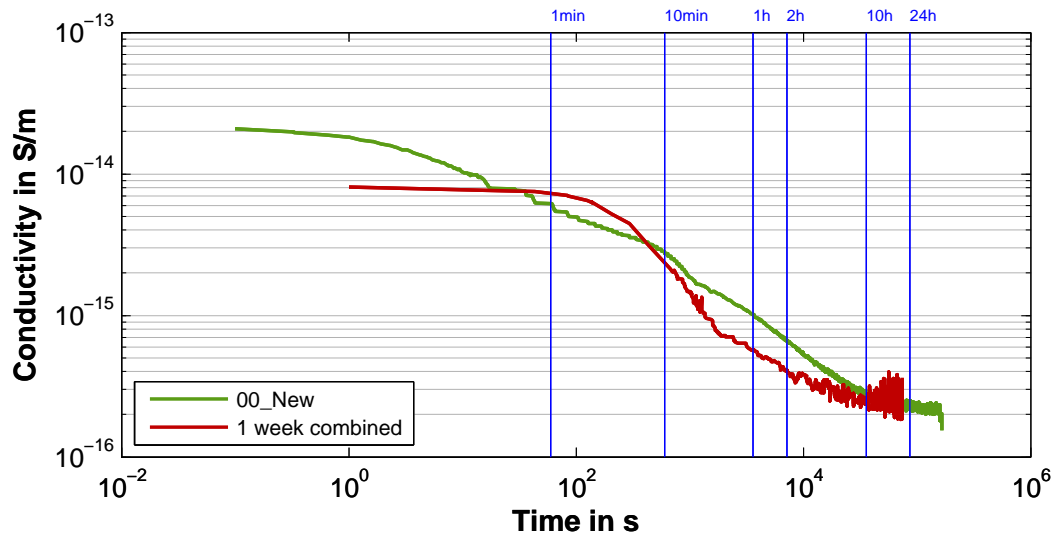


Figure 6.9: Electrical conductivity of combined aged pressboard samples (Nynas Nytro 4000X), measured at 20°C and $E = 3 \text{ kV/mm}$

from service aged (HVDC) bushings have been investigated and compared to results gained from new paper samples. It is demonstrated, that PDC measurements can reveal (severe) equipment ageing nevertheless.

6.2.6 Reproducibility of measurements

In IEC 60093 [52] (VDE 0303-30 [148]), deviances of factor 10 between subsequent measurements with the same preconditions are possible. Figure 6.10 shows exemplary the time trend of measured currents for new (unaged) pressboard samples, which have been prepared equally. Except for one measurement, the time trend in the beginning is very similar between around $2 \cdot 10^{-10}$ and $8 \cdot 10^{-10}$ A. The end values can't be determined easily from this figure, as no filtering was applied for this raw data. Therefore all sources of noise, glitches due to measurement point switching etc. are still present in these time trends. However, the current varies between $1 \cdot 10^{-12}$ and $5 \cdot 10^{-12}$ A at steady state, which is far below the factor of 10 as defined in the standard.

The electrical conductivity is determined by the measurement of voltage and current. Therefore, the dimensions of the electrodes (measurement electrode diameter) and sample thickness are needed to calculate electrical conductivity according to (4.33) and (4.34). So care has to be taken when determining these values.

Basically, such **a good reproducibility could be achieved for all conductivity measurements** of pressboard, independent of ageing state or moisture content. However, sometimes there have been deviations and "outliers" - But they were all caused by problems with the set-up: Broken or damaged cabling, misplaced electrodes, etc. and could be spotted easily, either visually or during data processing. It can be concluded that if the set-up is properly designed, electrical currents and conductivity can be determined with good reproducibility and confidence.

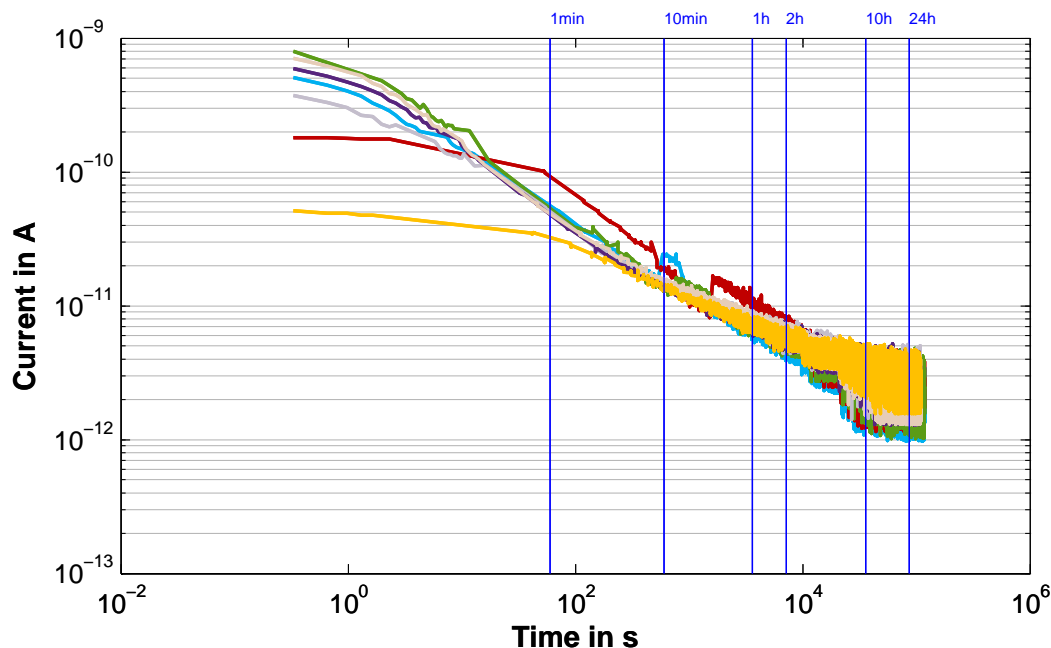


Figure 6.10: Reproducibility of current measurements shown exemplary for unaged pressboard with Nynas Nytro 10XN, measured at $E = 3 \text{ kV/mm}$ at 20°C (no filtering applied)

6.2.7 Polarisation processes

At 20°C it takes in general 24 h or more to reach steady-state conditions of the insulation current after the application of an external direct voltage. At 90°C , the polarisation time constant is significantly reduced, as steady state is reached in less than 2 h (see Figure 6.5).

It can be seen from Figure 6.11 that in terms of steady-state value of the conductivity of unaged pressboard,

the **oil type has only a minimal influence**. However, polarisation processes seem to be influenced which results in different time trends.

Now, when assuming a relative permittivity $\epsilon_r = 4$ and a (steady-state) conductivity $\sigma = 2 \cdot 10^{-16}$ S/m, the following dielectric relaxation time can be calculated:

$$\tau = \frac{\epsilon_r \cdot \epsilon_0}{\sigma} \rightarrow 177.084 \text{ s} = 46,37 \text{ h} \quad (6.2)$$

Relaxation processes are also temperature dependent - The time constant at a defined temperature τ can be calculated from the value τ_0 determined with [61]:

$$\tau = \tau_0 \cdot e^{\left(\frac{E_a}{k_B \cdot T}\right)} \quad (6.3)$$

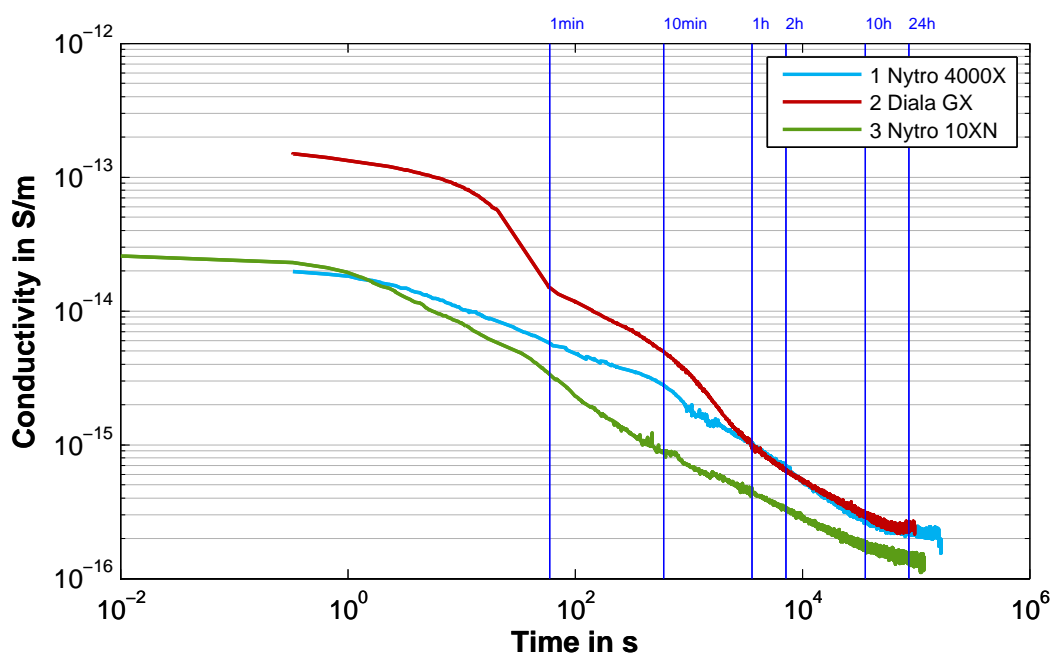


Figure 6.11: Electrical conductivity of unaged pressboard in variation of impregnation oil type, measured at $E = 3 \text{ kV/mm}$ at 20°C

6.3 Electrical conductivity of mineral insulating oils

Influence of oil type, temperature, electrical field strength, moisture content, measurement method and thermal ageing onto the electrical conductivity is described in the following chapter. In general, the results have been acquired through multiple measurements with a Tettex 2903 set-up at $E = 1 \text{ kV/mm}$ and subsequent averaging.

6.3.1 Oil type

The influence of oil type onto electrical conductivity can be clearly seen in Figure 6.12: Basically, the electrical conductivity of Nynas Nytro 10XN is around the factor of 10 lower than the one of Nynas Nytro 4000X and around factor 100 lower than the conductivity of the investigated Shell Diala GX. Measurement data has been gained for unaged oils at 22°C with Tettex 2903 test cells at $E = 1 \text{ kV/mm}$.

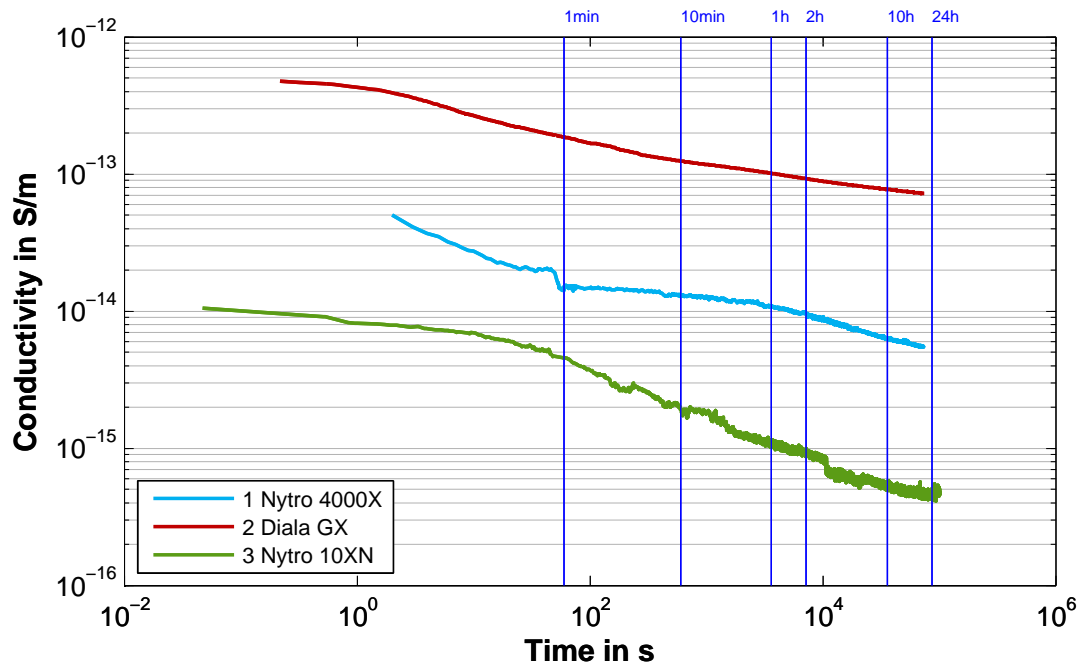


Figure 6.12: Electrical conductivity of 3 different mineral insulating oils at 22°C

For comparative reasons, time-trend values are listed below in Table 6.3 and are compared against IEC 60247.

Table 6.3: Electrical conductivity of (unaged) mineral oils at varied times at 22°C and 30°C (IEC 60247)

Oil type	1min	10min	1h	2h	10h	24h	IEC 60247 ⁹¹
Nytro 4000X	1,41E-14	1,30E-14	1,08E-14	9,60E-15	6,28E-15	5,49E-15	5,587E-14
Diala GX	1,86E-13	1,25E-13	1,01E-13	9,24E-14	7,73E-14	7,26E-14	8,565E-13
Nytro 10XN	4,57E-15	1,92E-15	1,09E-15	9,95E-16	5,29E-16	4,79E-16	5,000E-14

However, this comparison is hindered in two ways: First, measurement at 20°C (or 22°C) was not possible with the BAUR DTL, so these data has been acquired at 30°C. Secondly, even at 30°C, a determination of electrical conductivity was not possible for Nynas Nytro 10XN and is close at the measurement end range for Nynas Nytro 4000X.

To enable a basic comparison, the values determined with the Tettex set-up at 22 and 90°C (see Section 6.3.2) are **fitted to 30°C with the Arrhenius relationship** (3.4). Activation energies E_a can be calculated from measurement data gained at 2 different temperatures:

$$E_a = \frac{R \cdot T_1 \cdot T_2}{(T_1 - T_2)} \cdot \ln \left(\frac{k_1}{k_2} \right) \quad (6.4)$$

Electrical conductivity values are used for the rate constants k . Now this leads to conductivity values, which are shown in Table 6.4. The deviations for Nynas Nytro 10XN are shown in brackets, as the conductivity could not be determined with the used set-up (limitation to 20TΩm). It can be seen that the conductivity values determined with IEC 60247 are about 2,7 times higher than the conductivity values gained with the Tettex after 1 min and around 5 to 6 times higher than the 24 h values.

⁹¹10 Measurements had been made in a BAUR DTL at 30°C (average value 30,47°C, $\pm = 0,6^\circ\text{C}$) with $E = 0,25\text{ kV/mm}$ for each oil type

Table 6.4: Deviations between Tettex and IEC 60247 measurements

Oil type	1 min	24 h	IEC 60247	Δ 1 min	Δ 24 h
Nytro 4000X	2,46E-14	9,93E-15	5,587E-14	2,27	5,63
Diala GX	3,17E-13	1,33E-13	8,565E-13	2,70	6,46
Nytro 10XN	6,82E-15	8,46E-16	5,000E-14	(7,33)	(59,08)

6.3.2 Temperature

The influence of temperature onto the electrical conductivity of the three investigated oils is plotted in Figures 6.13 to 6.15. The temperature of 22°C ($\pm 1,5^\circ\text{C}$) was not chosen arbitrarily but was the room temperature during all (oil) measurement series. From the figures below it can be observed that the slope of conductivity is smaller at higher temperatures, which means the end value is reached sooner.

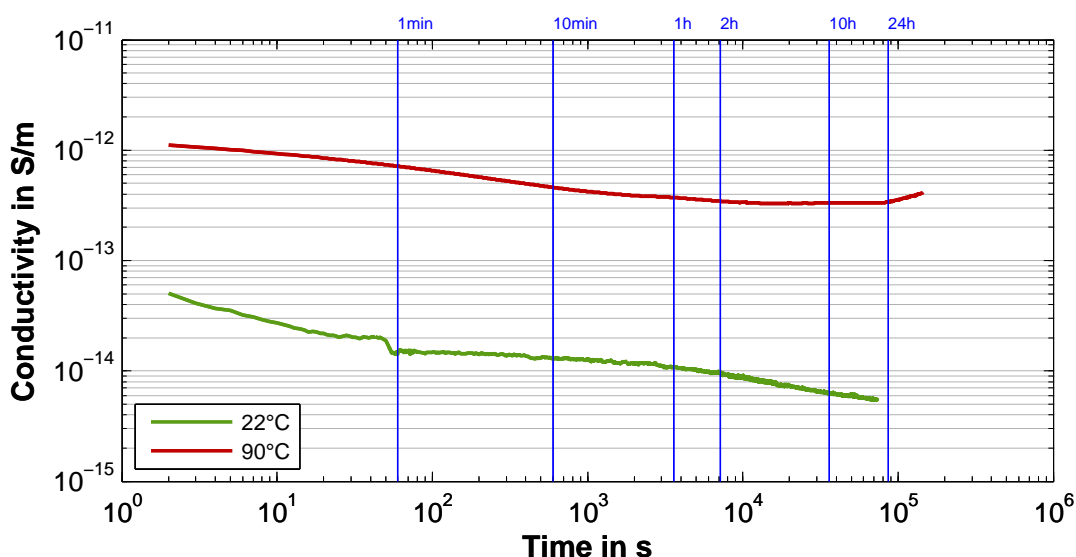
An increase of electrical conductivity could be noticed in some Nytro 4000X samples at 90°C. Actually, this was (most likely) a matter of moisture increase, which would be founded by the fact that no sealing could be used at this temperature (see Section 5.3.2).

The comparable large spread in conductivity at Nytro 10XN can be explained by the very low conductivity of this oil. The measured (steady-state) current is much less than 10 pA. At room temperature, the determined conductivity of 10XN is already in the same order of magnitude as pressboard (Figure 6.6 to 6.8).

The ratio of electrical conductivity between 22 and 90°C is given in Table 6.5. Generally, the ratio between both temperatures is increasing with increasing measurement time. This is caused by the strong decrease of electrical conductivity at lower temperatures when polarisation processes are decayed.

Table 6.5: Ratios of oil conductivity between 22 and 90°C

Oil type	22°C		90°C		Ratio 22:90°C		Ratio 1 min:24 h	
	1 min	24 h	1 min	24 h	1 min	24 h	22°C	90°C
Nytro 4000X	1,41E-14	5,49E-15	7,15E-13	3,66E-13	50,71	66,67	2,57	1,95
Diala GX	1,86E-13	7,26E-14	8,09E-12	5,22E-12	43,49	71,90	2,56	1,55
Nytro 10XN	4,57E-15	4,79E-16	7,80E-14	2,72E-14	17,07	56,78	9,54	2,87

**Figure 6.13:** Electrical conductivity of (unaged) Nynas Nytro 4000X in variation of temperature

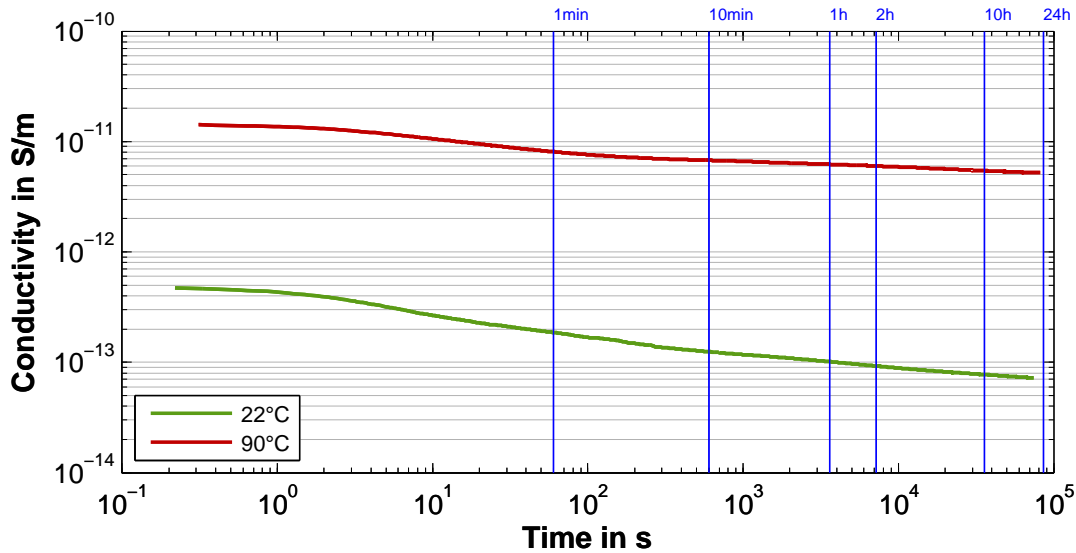


Figure 6.14: Electrical conductivity of (unaged) Shell Diala GX in variation of temperature

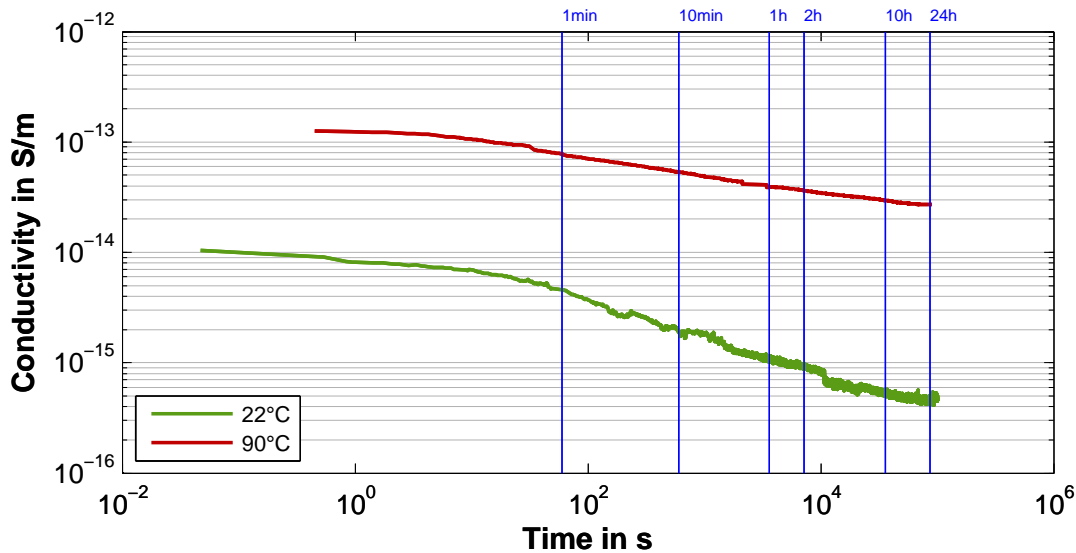


Figure 6.15: Electrical conductivity of (unaged) Nynas Nytro 10XN in variation of temperature

6.3.3 Electrical field strength

The influence of electrical field strength on the measured electrical conductivity was investigated for $E = 1 \text{ kV/mm}$ and $E = 0,5 \text{ kV/mm}$. A higher field strength was not possible due to limitations of the set-up in dielectric strength. Lower field strengths are problematically in terms of measurement accuracy, as the measured currents are very low in amplitude. Therefore, the Nynas Nytro 10XN was only measured at $E = 1 \text{ kV/mm}$ and no comparison can be made for this oil here.

The two investigated oils, Nynas Nytro 4000X and Shell Diala GX show quite **similar behaviour in terms of field strength dependency**, yet the time trend is (weakly) dependent on the oil type. The ratios between $E = 1$ and $0,5 \text{ kV/mm}$ are given in Table 6.8.

Here, the comparison to (1 min) conductivity values determined according to IEC 60247 with $E = 0,25 \text{ kV/mm}$ is also possible. The IEC values are taken from Section 5.1.4 on page 62. The results are summarized in Table 6.7. Generally, the **conductivities determined according to IEC 60247 are higher** than those determined with higher field strengths with the Tettex set-up. Although, one exception is the 90°C value of Diala GX - Here the conductivity was 1,14 times higher at the Tettex set-up (at $E = 1 \text{ kV/mm}$). As a rule, the differences are expected to decrease with increasing temperature, as the electrical conductivity

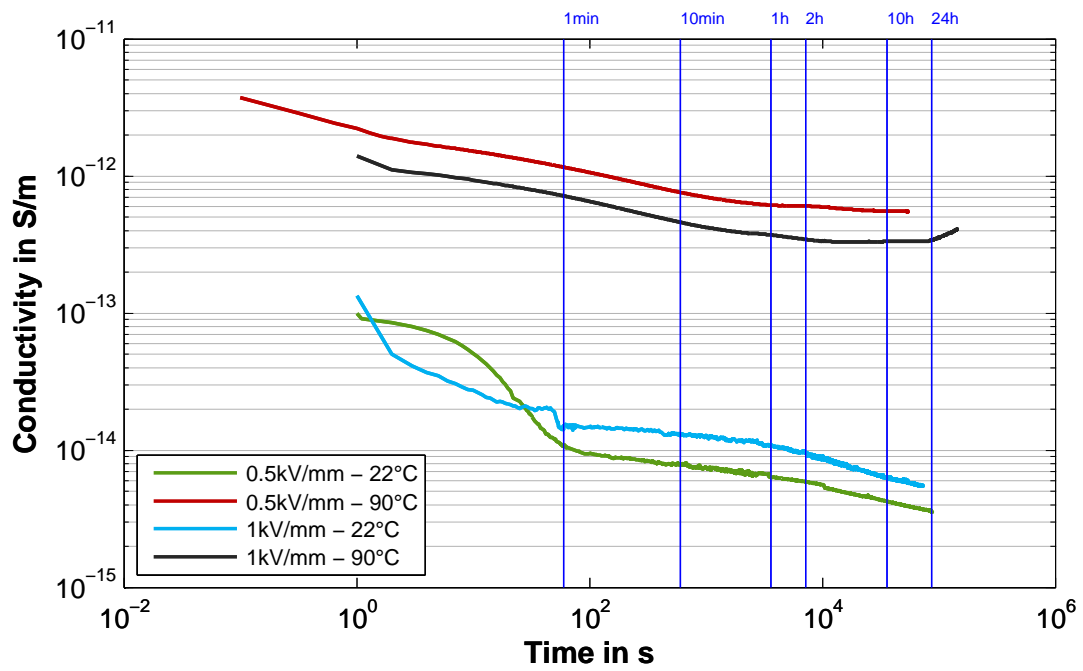


Figure 6.16: Electrical conductivity of (unaged) Nynas Nytro 4000X in variation of temperature and field strength

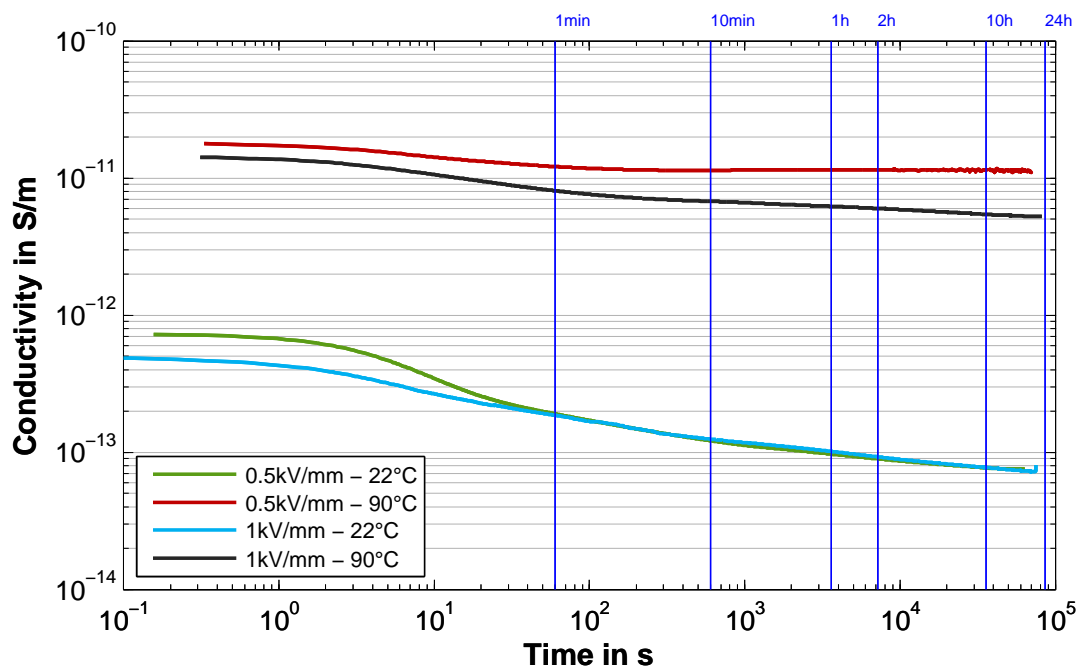


Figure 6.17: Electrical conductivity of (unaged) Shell Diala GX in variation of temperature and field strength

Table 6.6: Oil conductivity for varied field strength at 1 min and after 24 h

Oil type	22°C				90°C			
	E = 1 kV/mm		E = 0,5 kV/mm		E = 1 kV/mm		E = 0,5 kV/mm	
	1 min	24 h	1 min	24 h	1 min	24 h	1 min	24 h
Nytro 4000X	1,41E-14	5,49E-15	1,07E-14	3,55E-15	7,15E-13	3,66E-13	1,16E-12	5,52E-13
Diala GX	1,86E-13	7,26E-14	1,91E-13	7,54E-14	8,09E-12	5,22E-12	1,21E-11	1,11E-11

rises in general then. Furthermore, ion mobility is bigger which results in faster (decay of) polarisation processes.

Table 6.7: Oil conductivity for varied field strength at 1 min

Oil type	$E = 1 \text{ kV/mm}$		$E = 0,5 \text{ kV/mm}$		$E = 0,25 \text{ kV/mm}$	
	22°C	90°C	22°C	90°C	22°C ⁹²	90°C
Nytro 4000X	1,41E-14	7,15E-13	1,07E-14	1,16E-12	2,78E-14	3,98E-12
Diala GX	1,86E-13	8,09E-12	1,91E-13	1,21E-11	6,05E-13	7,11E-12

Table 6.8: Ratios of oil conductivity at varied temperatures and times

Oil type	Ratio 1:0,5 kV/mm				Ratio 1:0,25 kV/mm	
	22°C		90°C		1 min values	
	1 min	24 h	1 min	24 h	22°C	90°C
Nytro 4000X	1,32	1,55	0,62	0,66	0,51	0,18
Diala GX	0,97	0,96	0,67	0,47	0,31	1,14

6.3.4 Influence of moisture

To investigate the influence of moisture, insulation oil samples have been **artificially wetted** at room temperature (20°C). Exemplary, this was carried out for dried Nynas Nytro 4000X samples. Small amounts of distilled water have been introduced in a glass vessel with dry oil (<5 ppm) and sealed with a silicone plug. Then, the oil-water mix was stirred with a magnetic stirrer for at least 24 h. Eventually, water contents of 5, 11 and 36 ppm could be achieved⁹³. Afterwards, at least 3 measurements for each moisture content have been made before a new series was started. These dielectric measurements have been made with a BAUR DTL at 30°C at $E = 0,25 \text{ kV/mm}$. The results are pictured in Figure 6.18 below. It can be seen that the electrical conductivity rises naturally with moisture content. With a doubling of absolute water content (from 5 to 11 ppm) the conductivity rises by a factor of 2. Compared to the start value, the conductivity at 36 ppm is nearly 13 times higher.

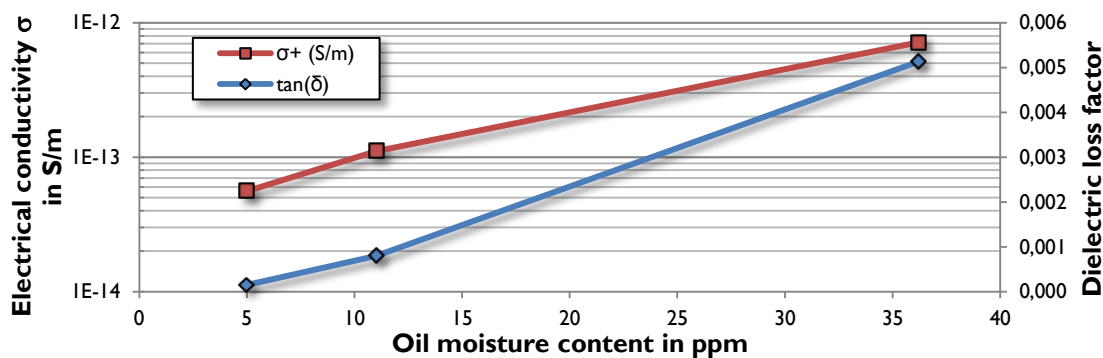


Figure 6.18: Electrical conductivity and dielectric loss factor of a mineral oil in dependence of moisture content

6.3.5 Measurement method

The electrical conductivity of insulating oils has been determined with test cells according to IEC 60247 (BAUR DTL) and with a customized set-up (Tettex 2903), where higher field strengths and longer measurement durations have been applied. The results of the electrical conductivity measurements with the Tettex 2903 set-up is pictured in Figure 6.19 below. For comparative reasons, in Figure 6.19 the most left blue line

⁹²The 22°C values have been extrapolated with Arrhenius equation (see also Section 6.3.1).

⁹³Spreads are as follows: $5 \pm 0,0 \text{ ppm}$, $11 \pm 0,7 \text{ ppm}$ and $36,2 \pm 2,2 \text{ ppm}$

marks 1 minute after voltage application, which is also approximately the moment, where the BAUR DTL conducts the measurement.

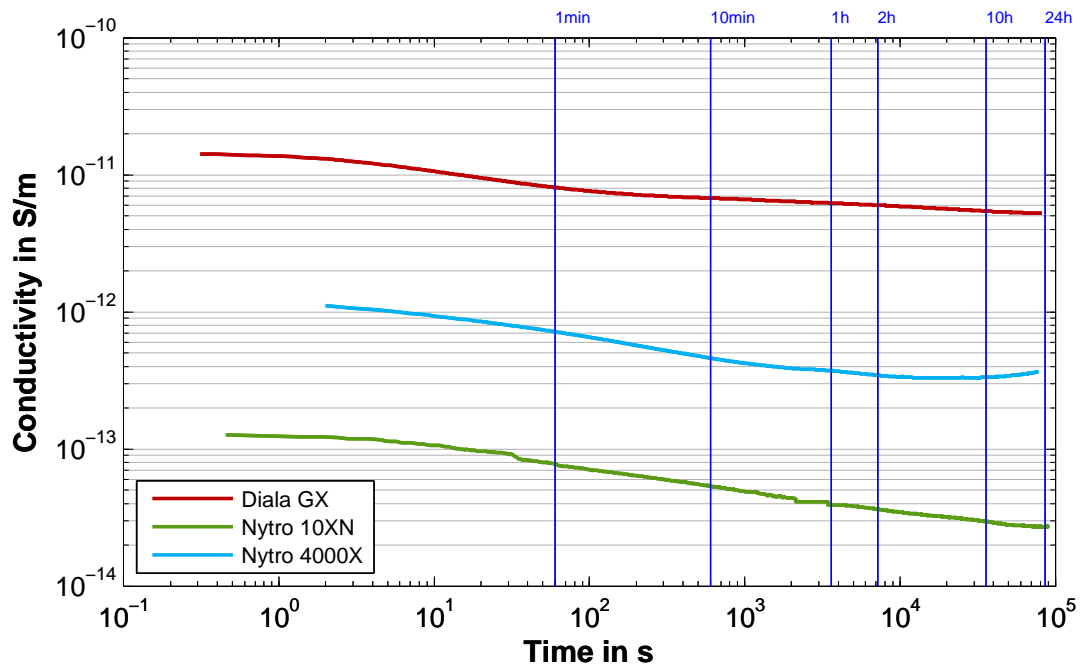


Figure 6.19: Electrical conductivity of 3 different mineral insulating oils at 90°C

At 20°C, the electrical conductivity can not be determined securely with the used BAUR DTL (see Table 6.3) as the specific resistance is way above measurement range there. For a better comparison, here the results at 90°C are used:

Table 6.9: Electrical conductivity of (unaged) mineral oils at varied times at 90°C in S/m

Oil type	1min	10min	1h	2h	10h	24h	IEC 60247 ⁹⁴
Nytro 4000X	7,15E-13	7,60E-13	3,73E-13	3,45E-13	3,33E-13	3,40E-13	3,979E-12
Diala GX	8,09E-12	6,76E-12	6,22E-12	5,99E-12	5,43E-12	5,22E-12	7,106E-12
Nytro 10XN	7,78E-14	5,36E-14	3,91E-14	3,63E-14	2,96E-14	2,72E-14	6,098E-13

For insulation oils with a comparable high electrical conductivity as the investigated Diala GX, the IEC 60247 (BAUR DTL) yields about the same result as the determination with higher field strengths ($E = 1 \text{ kV/mm}$ instead of $E = 0,25 \text{ kV/mm}$) and longer measurement times. The deviation between both methods in this case is in the range between -13% (1min) and +26% (24h) when taking the IEC 60247 value as a basis.

However, if the insulation oil has a much higher specific resistivity, the deviation is much larger. On the one hand, this is owed to larger relaxation times, as polarisation processes dominate the current time trend for a longer period. On the other hand, the large resistivities result in very low currents, which might be hard(er) to measure at lower field strengths. In these cases, the electrical conductivities determined with the Tettex set-up were between 5,5 (Nytro 4000X) and 7,8 (Nytro 10XN) times lower than those gained with the IEC 60247 method.

⁹⁴More than 10 Measurements had been made in a BAUR DTL at 90°C (average value 90,25°C, $\pm = 0,25^\circ\text{C}$) with $E = 0,25 \text{ kV/mm}$ for each oil type

6.3.6 Ageing

The influence of ageing was determined according to IEC 60247 only, due to experimental-economical reasons and equipment (non-)availability⁹⁵. Measurements have been conducted at 90°C and $E = 0,25 \text{ kV/mm}$. The results presented are average values of at least 3 single measurements. The parameters conductivity, relative permittivity and dielectric loss factor have been determined (see Section 6.5).

The electrical conductivity rises sharply already in the beginning stage of thermal ageing, which can be explained with the generation of water (and probably other ageing by-products). However, for Nynas Nytro 4000X an significant increase of electrical conductivity could be determined not until 5 weeks of ageing duration. Up to an ageing duration of 24 weeks, the electrical conductivity remains nearly constant at the according levels. At 32 weeks, a slight increase could be noticed.

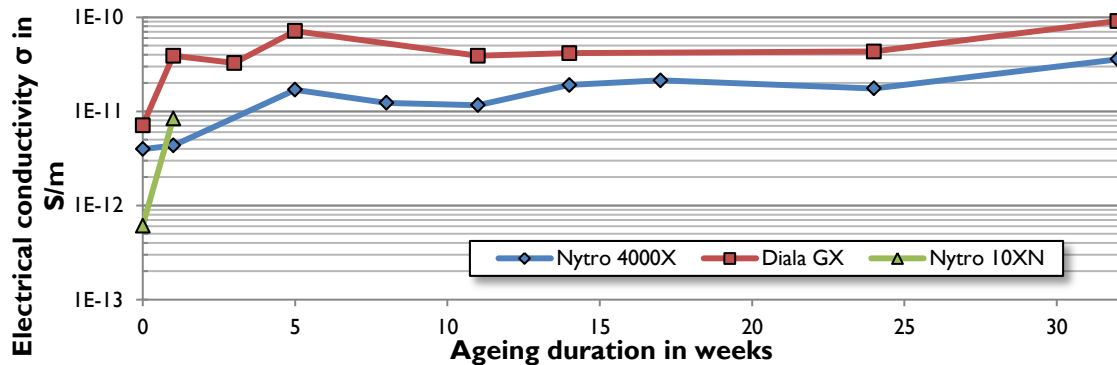


Figure 6.20: Influence of thermal ageing onto electrical conductivity of oil, measured at 90°C and $E = 0,25 \text{ kV/mm}$

6.4 Material parameters after ageing: Pressboard

The results of degree of polymerisation (DP) and moisture content measurements are described in this section.

6.4.1 Degree of polymerisation (DP)

The degree of polymerisation is an **important characteristic material parameter**. The determination was conducted according IEC 60450 (see Appendix D). The time trend of DP value is shown in Table 6.10 and Figure 6.21 respectively. Basically, the time trend is according to expectations, as the DP value is decreasing with increasing ageing temperature. However, there are some data points which deserve closer attention:

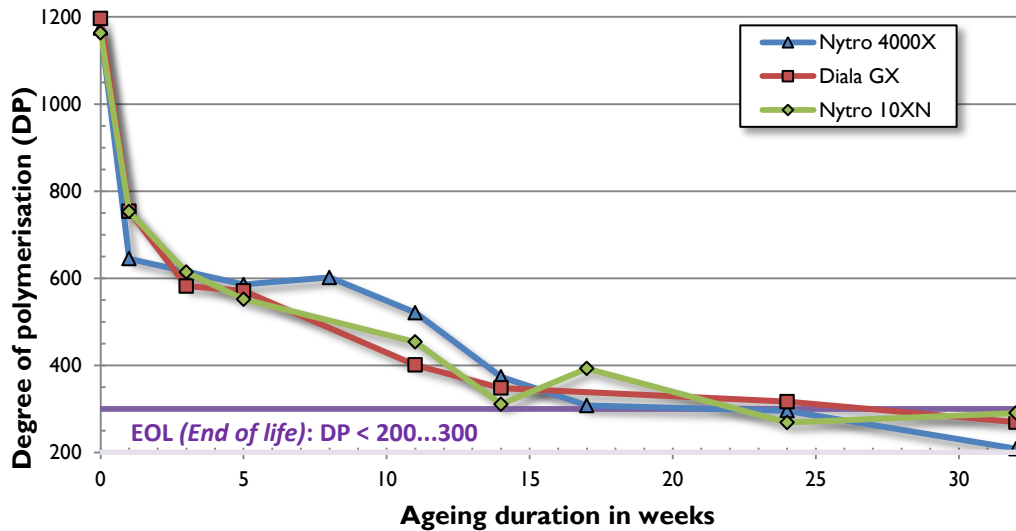
There are some data points (14w @ 10XN) which have a too low or too high (e.g. 1w @ 4000X, 32w @ 10XN) DP value when compared to the general trend. This can be explained when looking closer at the ageing process: The samples originate from different preparation batches and have been placed in different ovens at different positions. Further, there have also been deviations in ageing durations, as shown in Table 6.1.

When assuming an average activation energy E_a of 111 kJ/mol the data in Table 6.10 can be used to determine the ageing rate constant k with equation (6.4).

⁹⁵Values for aged Nytro 10XN samples except the 1 week samples could not be determined as these samples had been contaminated in the lab.

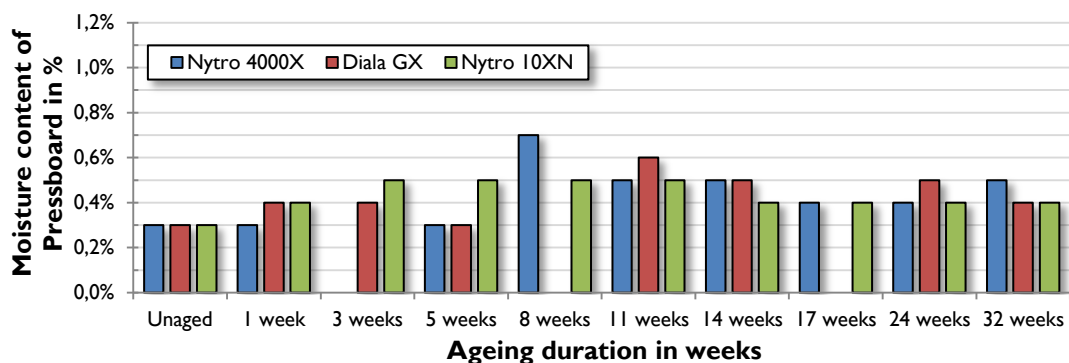
Table 6.10: Degree of polymerisation for aged pressboard samples

Duration	New	1 w	3 w	5 w	8 w	11 w	14 w	17 w	24 w	32 w
4000 X	1.175	645	-	586	602	521	374	308	296	209
Diala GX	1.196	754	582	571	-	401	348	-	317	270
10XN	1.163	753	614	552	391	454	311	393	269	291
Literature		573 [159]								

**Figure 6.21:** Degree of polymerisation (DP) of pressboard at varied ageing stages

6.4.2 Moisture content of pressboard

The pressboard samples (as well as the according insulation oils) have been subjected to a thoroughly preparation process as described in Appendix A. Therefore, the moisture levels for all unaged pressboard samples have been quite low with around 0,2% moisture content. As the ageing vessels have been sealed and furthermore the vessels had a nitrogen atmosphere, it was expected that ageing through oxidation was hindered quite efficiently. The moisture levels are furthermore comparable with similar experiments described in literature, e.g. in [42, 159]. None of the three investigated insulation oils showed a particularly different behaviour. **Moisture levels remained quite constant between 1 and 32 weeks.**

**Figure 6.22:** Moisture content of pressboard with varied ageing stages

6.4.3 Impulse voltage strength

Measurements have been made in the style of IEC 60243-3 (VDE 0303-23 [147]) with a 1,2/50 μ s normative lightning impulse shape (LI) with negative polarity on Nynas Nytro 4000X samples. The negative test voltage was chosen to avoid flashovers or other related problems which can happen at positive

polarity, especially at such a compact set-up. The following average values were observed during the ($n = 97$) tests:

- Rise time $t_1 = 1,08 \mu s$ ($\sigma = 0,012 \mu s$)
- Time-to-half $t_2 = 47,83 \mu s$ ($\sigma = 0,233 \mu s$)

A waiting time of at least 1 minute between subsequent impulses was chosen. However, only 1 impulse per voltage level was carried out, instead of the 3 shots, which are required in [147]. Typical electrodes (brass, polished) with diameters of $\varnothing_1 = 75 \text{ mm}$ and $\varnothing_2 = 25 \text{ mm}$ according IEC 60243-1 (VDE 0303-21 [146]) have been used. In literature, (lightning) impulse voltage field strengths of high density pressboard of around 100 kV/mm are reported, for example in [12, 107].

The influence of ageing onto the (lightning) impulse voltage strengths can be practically neglected, under the precondition that moisture levels are low (lower than 4% according to [30]), as the following results show:

- New (unaged) samples: $U_{BDS} = -102,89 \text{ kV}$, moisture content $< 0,3\%$, DP ≈ 1200
- Aged 24 weeks: $U_{BDS} = -98,23 \text{ kV}$, moisture content $< 0,6\%$, DP ≈ 300
- Aged 32 weeks: $U_{BDS} = -98,16 \text{ kV}$, moisture content $< 0,6\%$, DP ≈ 200

This equates a decrease in impulse voltage breakdown strength by 4,5% from the unaged to the 32 weeks aged condition. The influence of ageing onto breakdown strength of aged samples, as reported for example in [30, 107], can be confirmed in such a way that there is no or a negligible decrease when the moisture content in the pressboard is low. **Surface condition** has definitely an influence on impulse strength, but this was not investigated here. In [93] an increase of around 25% in impulse voltage strength of machined samples when compared to (unmachined) samples with sieve structure is reported. The **mechanical strength** - which can be linked to DP value - has, if at all, only a **minor influence onto impulse strength**.

However, the results of the breakdown process are strongly different between new and aged samples, as shown in Figure 6.23: The impact area of the breakdown is comparable small at new samples, whereas **at the aged samples larger parts of pressboard are expelled** due to the reduced mechanical strength. The electrical discharge at the unaged samples leads to a small discharge channel with a length of several mm whereas at the pictured 32 week sample a blast off over a length of more than 18 mm (Figure 6.23 b) could be observed⁹⁶.

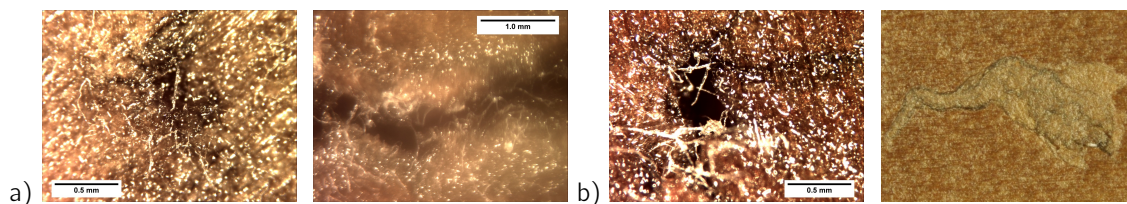


Figure 6.23: Pressboard samples after breakdown during lightning impulse voltage tests (front and back-sides): a) Unaged sample b) Thermally aged at 135°C for 32 weeks

6.5 Material parameters after ageing: Insulating oils

6.5.1 Colour (VDEW scale)

Although the colour alone is not suitable for a solely classification of an oil, it can still give an indication if and how strong ageing has been taken place. Generally, new oils possess a colour between “1” and “2”

⁹⁶This picture has been taken with a Nikon D90, therefore no scale could be added.

according to VDEW colour sheet⁹⁷ [145], which was used here. Colour range for used oils is between yellow (Colour "3"), dark brownish (Colour between "4" and "7") to black (Colour ">"8"). Exemplary, this is shown in Figure 6.24 with colours of "1", "2", "6" and "10".

Up to ageing durations of 5 weeks, no (significant) increase in colour occurred. However, in some oil samples sludge and particles could be found. They originated, as far as they could be traced, from non-cured silicon glue. In some samples, oil oxidation due to non-functioning sealing took place which resulted in high colour numbers (7 to 10). In the end, all these samples had been excluded from further investigations.



Figure 6.24: Colour of varied mineral oil samples

Table 6.11: Colour of aged mineral oil samples (VDEW scale)

Duration	New	1 w	3 w	5 w	8 w	11 w	14 w	17 w	24 w	32 w
4000 X	1	1	-	1	1	1	2	3	3	3
Diala GX	1	1	1	1	-	1	1	-	2	3
10XN	1	1	1	1	3	2	2	3	3	2

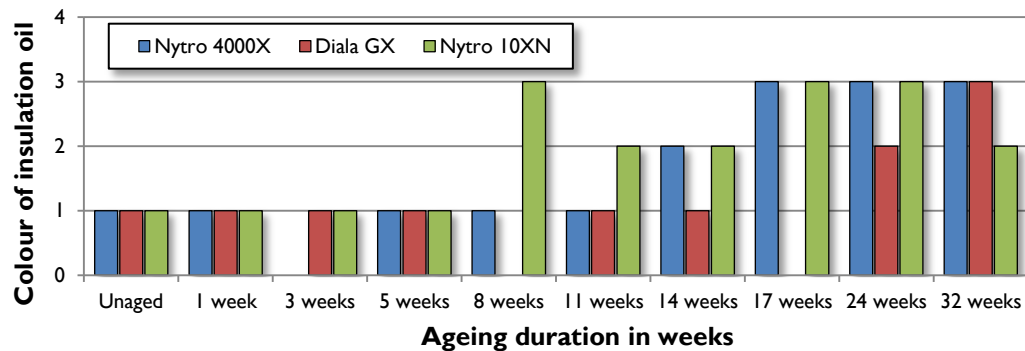


Figure 6.25: Colour of mineral insulating oils in different ageing stages

6.5.2 Dielectric loss factor $\tan(\delta)$

The dielectric loss factor $\tan(\delta)$ generally increases with progressing ageing as ageing by-products are increasing the conductivity and (ohmic) losses. The dielectric loss factor has been determined with a BAUR DTL C at 90°C.

Table 6.12: Dielectric loss factor $\tan(\delta)$ of aged mineral oil samples (measured at 90°C), scaled to 10^{-3}

Duration	New	1 w	3 w	5 w	8 w	11 w	14 w	17 w	24 w	32 w
4000 X	1,20	1,46	-	6,44	5,12	4,98	8,06	11,87	7,33	14,05
Diala GX	4,93	9,38	14,81	14,33	-	11,09	15,61	-	19,18	48,26
10XN	0,76	2,79	-	-	-	-	-	-	-	-

⁹⁷There are also other methods of colour determination, e.g. in ISO 2049. The values can be converted between VDEW and ISO though [145].

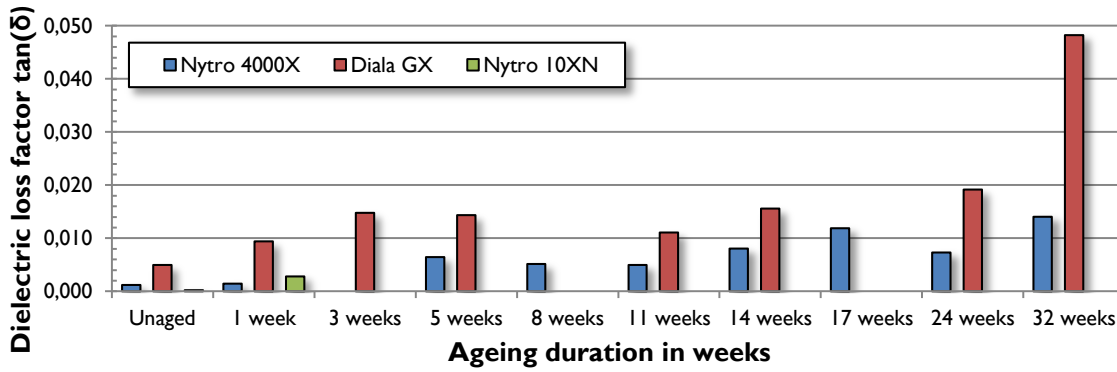


Figure 6.26: Dielectric loss factor $\tan(\delta)$ of mineral insulating oils in different ageing stages

6.5.3 Moisture content

The moisture content of insulation oils has been determined promptly after the separation oil and board at the end of each ageing stage. Measurements have been conducted with Karl-Fischer-Titration (direct injection) at the according oil temperature, which was generally around 40°C. From the values and Figure 6.27 below **an increase of oil moisture content with progressing ageing** can be observed. Comparable high moisture contents have been determined in this investigation, which is mainly caused by the elevated temperature, at which oil and pressboard has been separated (90°C). Further, some “outliers” (e.g. 10XN at 11 weeks) can be observed. In this case, the sample series had been flawed insofar that the sealing and the silicone adhesive were not applied correctly. As other parameters (oil color, board conductivity) have been within expectation, this single sample has been kept. For other samples, similar reasons could be identified and partly, such samples have been excluded from further measurements and classified as outliers.

Table 6.13: Moisture content of aged mineral oil samples

Duration	New	1 w	3 w	5 w	8 w	11 w	14 w	17 w	24 w	32 w
4000 X	4	10	-	14	14	14	14	19	15	18
Diala GX	7	9	11	13	-	14	17	-	19	18
10XN	5	9	17	14	13	23	16	16	14	21
Literature ⁹⁸										
[162]	11	14	14	17	17					

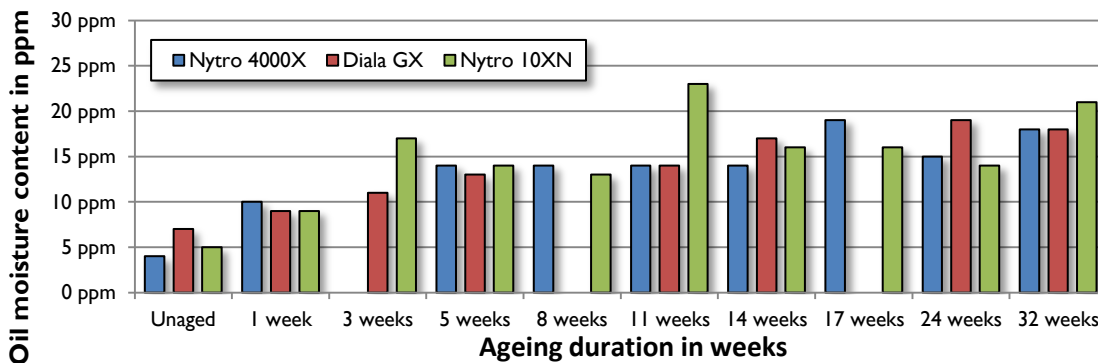


Figure 6.27: Moisture content of mineral insulating oils in different ageing stages

6.5.4 Relative permittivity ϵ_r

The relative permittivity ϵ_r has been determined with a BAUR DTL C at 90°C. It can be seen that the three investigated mineral insulating oils have small differences in their relative permittivity. In terms of

⁹⁸Intermediate values have been linear interpolated.

temperature, there is a slight and nearly linear decrease of relative permittivity with increasing temperature. The maximum difference between 30 and 105°C has been determined for Shell Diala GX and Nynas Nytro 10 XN (-5,5% each). The difference between 90 and 105°C is very low (around 1%) for all three oils, so the practical outcome of this will be also low.

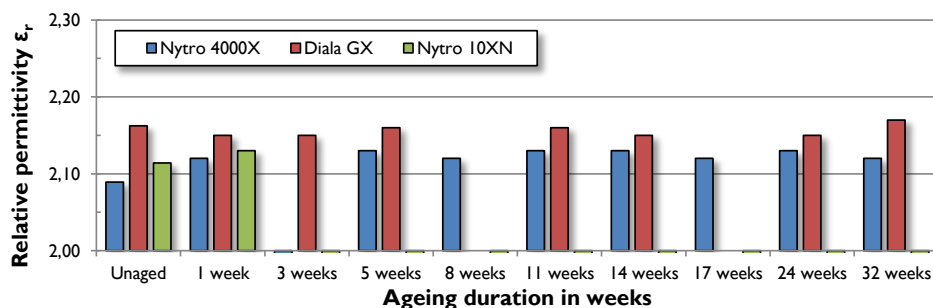


Figure 6.28: Relative permittivity ϵ_r of mineral insulating oils in different ageing stages

Table 6.14: Relative permittivities ϵ_r of aged mineral insulating oil samples (measured at 90°C)

Duration	New	1 w	3 w	5 w	8 w	11 w	14 w	17 w	24 w	32 w
4000 X	2,09	2,12	-	2,13	2,12	2,13	2,13	2,12	2,13	2,12
Diala GX	2,15	2,15	2,15	-	-	2,16	2,15	-	2,15	2,17
10XN	2,09	2,13	-	-	-	-	-	-	-	-
Literature ⁹⁹										
[162] ¹⁰⁰	2,19	2,21	2,20	2,20	2,20					

6.6 Electrostatic charging behaviour of oil-cellulose insulation systems

The electrostatic charging behaviour of new and aged pressboard samples has been investigated. Here, the influence of temperature, oil type and ageing are pictured. Generally, ECT increases with increasing rotational speed. Therefore, all results of aged samples presented here have been acquired at 400 min⁻¹. More details about this and the set-up can be found in [164].

The (absolute) peak value of the charging and discharging currents is not a reliable parameter for ECT determination with the set-up used. As the charging and discharging currents change very strongly within the first seconds after a state change (motor switch-on/off), it can not be guaranteed that the peak is determined securely with the measurement equipment used. Therefore it is not possible to draw a direct conclusion from the peak value alone, the time trend must be considered as well. Partly, peak currents are not shown in the following figures for the sake of a clear plot (of the transient processes).

6.6.1 Temperature

The influence of temperature onto ECT is shown exemplary for Nynas Nytro 4000X samples in Figure 6.29. **With increasing temperature the peaks of charging and discharging currents increase.** This is in consistence with results from literature [91]. Temperature dependence is the result of two contrary processes: On the one hand, due to a temperature increase, the electrical conductivity (of the oil) increases, which causes a reduction of the relaxation time constant τ . Further, this causes a reduction of the Debye length and therefore a reduction of the area¹⁰¹, at which charge separation can occur.

¹⁰⁰Intermediate values have been linear interpolated.

¹⁰⁰Measured at 600V ($E = 400$ V/mm) and 20°C

¹⁰¹Correctly, the distance between electrode and undisturbed bulk - the stern layer - is reduced.

On the other hand, viscosity decreases with increasing temperature and therefore ion mobility increases. This causes an increase of the Debye length. In the overall view, a temperature increase causes an increase in ECT, as the excess charge carriers are not transported out of the double layer.

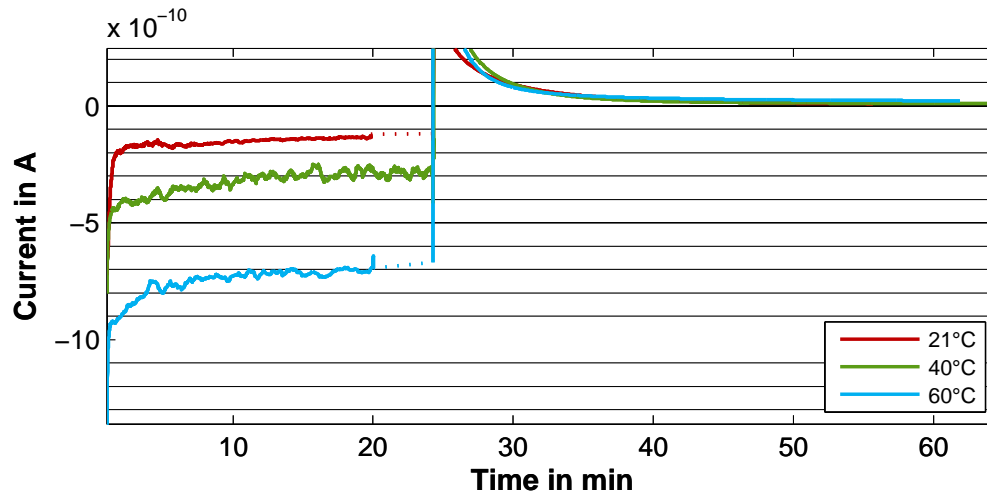


Figure 6.29: Current time-trend of Nynas Nytro 4000X sample at 400 min^{-1} at varied temperature

6.6.2 Oil type

Oil type has a significant influence on ECT, as this was also reported in literature. Problems in transformers could be directly linked to certain oil types in the past [119, 137]. The results for the investigated oils are pictured below. These measurements have been conducted in a temperature controlled environment (thermal oven) at 60°C with varied rotational speed.

The most interesting outcome is the difference in polarity of the charging and discharging currents: Whereas for Nynas Nytro 4000X and 10XN the charging current had a negative peak for each single measurement and the discharging current always a positive peak, these relations have been exactly the opposite for Shell Diala GX. In literature it was reported [137] that a **change in polarity** can be an indication for oil ageing. However, only unaged oils and samples have been investigated here. The reason for polarity change is therefore to be sought in the oil composition only.

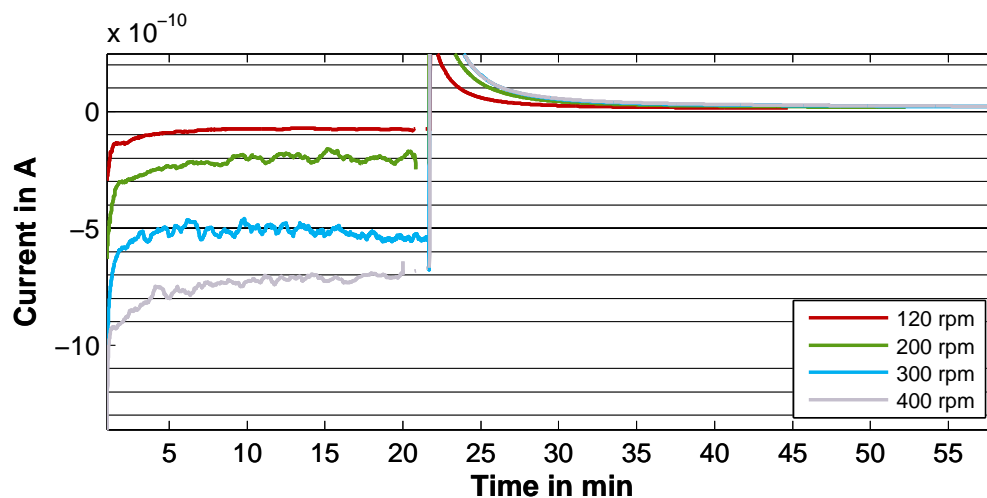


Figure 6.30: Current time-trend of Nynas Nytro 4000X sample at 60°C and varied rotational speed

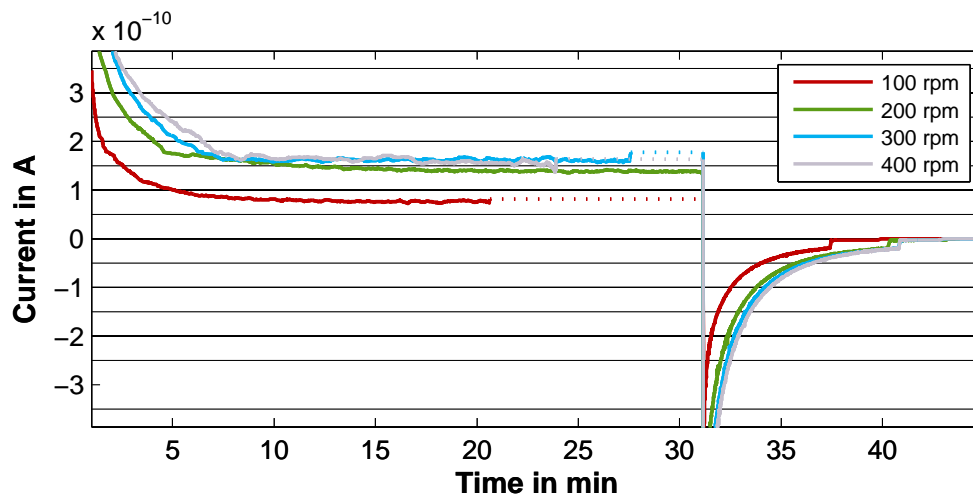


Figure 6.31: Current time-trend of Shell Diala GX sample at 60°C and varied rotational speed

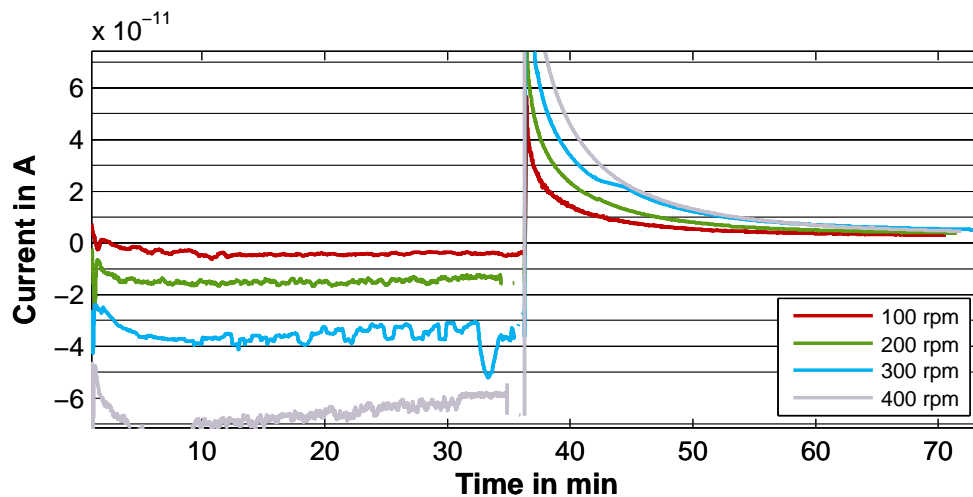


Figure 6.32: Current time-trend of Nynas Nytro 10XN sample at 60°C and varied rotational speed

6.6.3 ECT of thermally aged samples

A comparison of thermally aged samples - 11 and 32 weeks at 135°C - to new and unaged samples is shown in this section. These measurements have been conducted in a temperature controlled environment (thermal oven) at 60°C and with a disc rotational speed of 400 min⁻¹. Regarding the influence of ageing no concurrent results could be achieved. With progressive ageing (**Nytro 4000X** samples) the charging currents are reduced in amplitude and decrease faster when compared to the unaged samples.

For the **Diala GX** no significant influence of ageing could be determined at all, the measured currents are quite similar between the investigated aged samples. An increase in ECT could be determined for the **Nytro 10XN** samples. With progressive ageing an increase in charging and discharging currents could be determined reproducible. However, it has to be noted that the absolute values of these currents are still lower than the ones of 4000X and in the same region as of Diala GX.

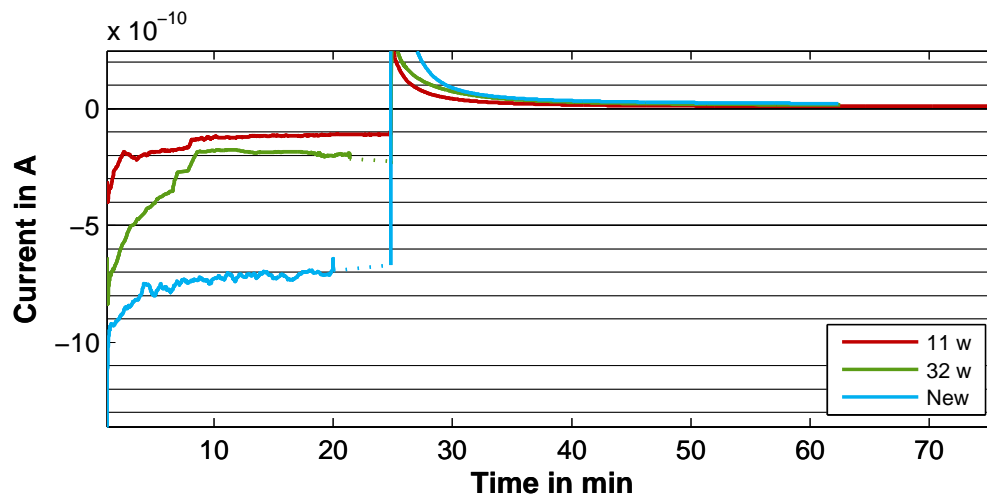


Figure 6.33: Current time-trend of new and aged Nynas Nytro 4000X samples at 60°C and 400 min⁻¹

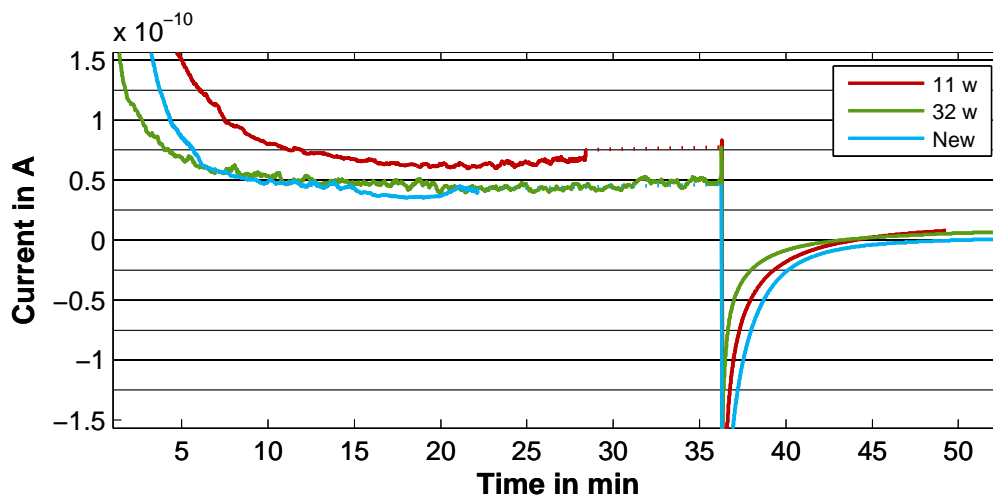


Figure 6.34: Current time-trend of new and aged Shell Diala GX samples at 60°C and 400 min⁻¹

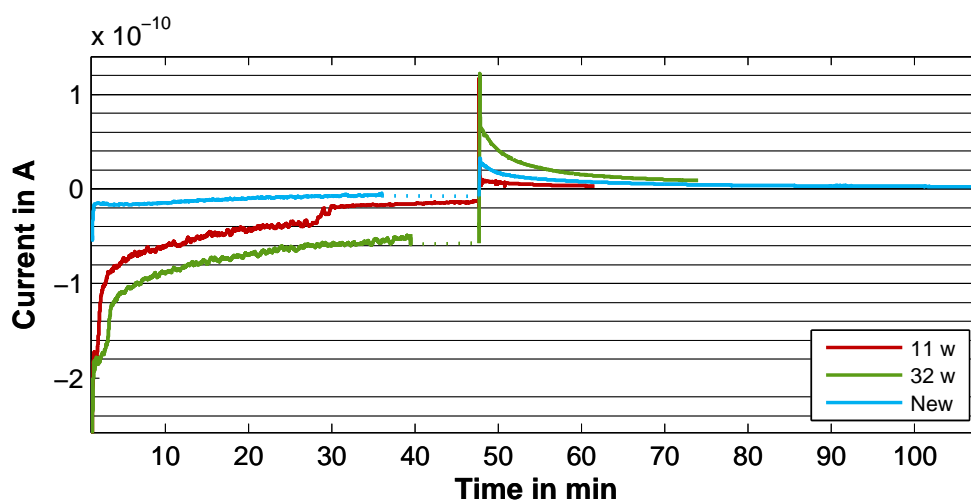


Figure 6.35: Current time-trend of new and aged Nynas Nytro 10XN samples at 60°C and 400 min⁻¹

6.7 Space charges in cellulose

Space charge distribution has been determined experimentally with the PEA method (see Section 5.5) at 20 and 60°C with the following, new and (thermally) aged pressboard samples:

Table 6.15: Pressboard samples for space charge (PEA) measurements

ID	Material	Impregnated with	Condition	Moisture content
N1	T IV	Nynas Nytro 4000X	New	< 0,3%
N2	T IV	Shell Diala GX	New	< 0,3%
N3	T IV	Nynas Nytro 10XN	New	< 0,3%
A1	T IV	Nynas Nytro 4000X	Thermally aged for 11 weeks	< 0,6%
A2	T IV	Shell Diala GX	Thermally aged for 11 weeks	< 0,6%
A3	T IV	Nynas Nytro 10XN	Thermally aged for 11 weeks	< 0,6%
N10	K-Buffer	Nynas Nytro 4000X	New	< 0,3%
N20	K-Buffer	Shell Diala GX	New	< 0,3%
A0	T IV	Shell Diala GX	Thermally aged for 12 weeks	< 0,6%

A poling voltage of 10 kV and a pulse voltage of 500 V (pulse width 10 and 20 ns respectively) has been used. Poling and depoling was applied for around 2 h each, which was chosen arbitrary by the means of equipment availability. The results are pictured as space charge plots which have been obtained through filtering and processing of raw measurement data. More details about this process can be found in [3]. In each diagram, space charge distribution at the beginning of poling (black dotted line), at end of measurement (pink line) and at an intermediate moment (green line) is plotted. The high voltage electrode is on the left side of the horizontal axis ("0 mm") and the ground electrode on the right side ("1" or "0,5 mm") respectively.

6.7.1 Oil type and ageing

The influence of oil type and ageing was investigated for the samples A1-A3 and N1-N3 at 20°C and the results are presented in the figures below. It was found that for every investigated oil type and ageing condition only homocharges are generated at both dielectric interfaces. This is also consistent with results of measurements on insulation paper reported in literature, e.g. in [56]. **No significant influence of ageing** onto the space charge distribution nor on the amplitude could be determined at 20°C. However, the measured amplitude of the homocharge at the high voltage electrode increases at the aged samples. This is explained by changes in material properties (DP value) and therefore a different acoustic behaviour when compared to new samples which has no practical implications nevertheless.

However, from these results it is not possible to deduct the kind of charge carrier, although in [56], where similar measurements have been made on insulation paper, it is assumed that the negative charges are electrons and the positive ones are holes. At least the origin of charges is clearer - They originate either from the electrode (electrode injection) or from the oil layer (interface or surface charge injection). If the latter would be the dominant process, space charge generation would be nearly independent of electrode material, which was not investigated within this work though. From the literature [84] it is known, that the electrode material can have a significant influence on measured space charge distribution in several materials. But this is not the case for paper, as reported also in [56].

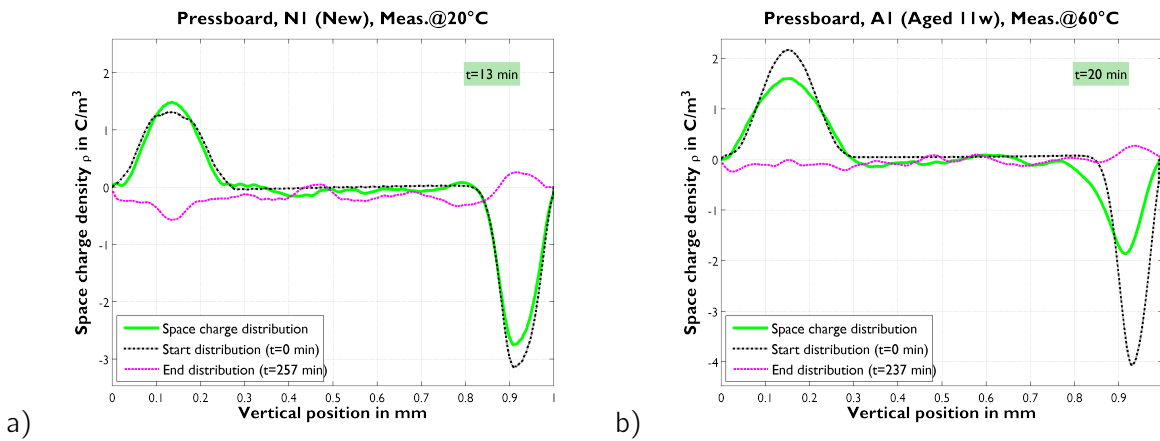


Figure 6.36: Space charge profile of pressboard with Nynas Nytro 4000X measured at 20°C: a) Unaged b) Aged for 11 weeks at 135°C

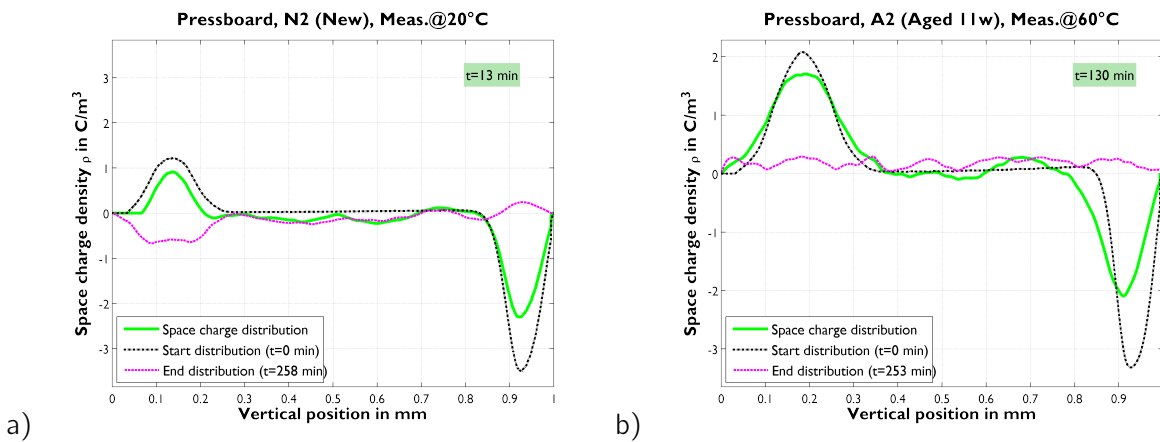


Figure 6.37: Space charge profile of pressboard with Shell Diala GX measured at 20°C: a) Unaged b) Aged for 11 weeks at 135°C

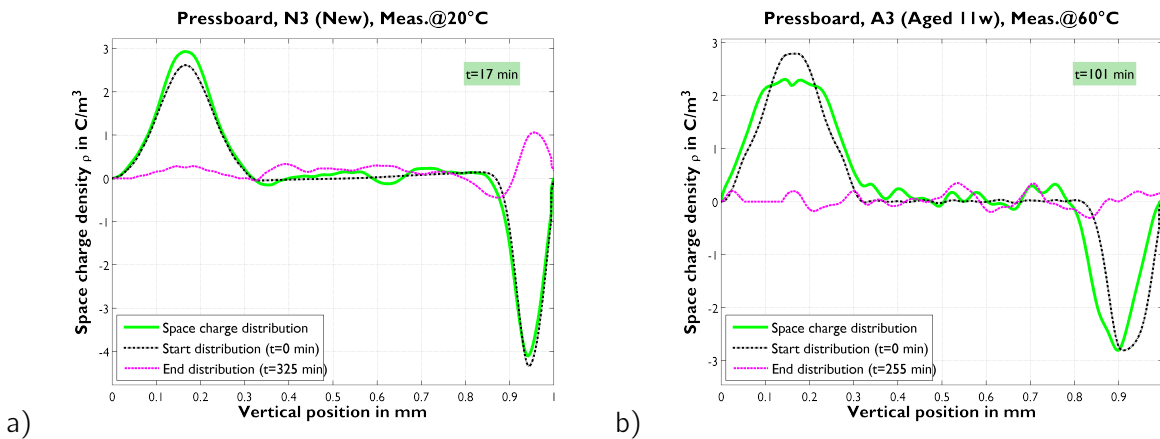


Figure 6.38: Space charge profile of pressboard with Nynas Nytro 10XN measured at 20°C: a) Unaged b) Aged for 11 weeks at 135°C

6.7.2 Temperature

The influence of temperature was studied on the aged samples A1-A3 at 20 and 60°C. Interestingly, **no significant difference** could be observed at all samples when comparing both temperatures. The only exception to that extent is the sample A3 (Nytro 10XN), which showed an increase of space charge density at the high voltage electrode which was around 2,6 times higher at 60°C than at 20°C.

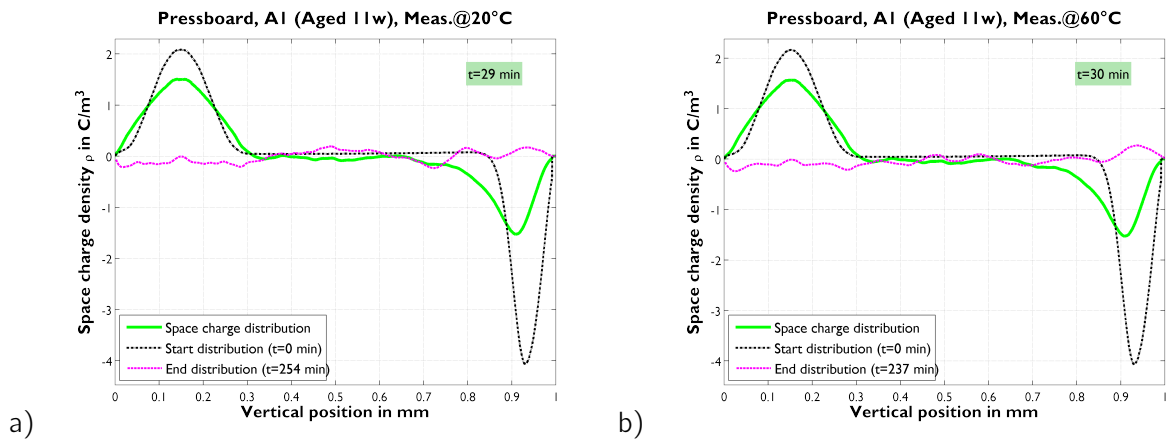


Figure 6.39: Space charge profile of aged pressboard with Nynas Nytro 4000X measured at 20 a) and 60°C b)

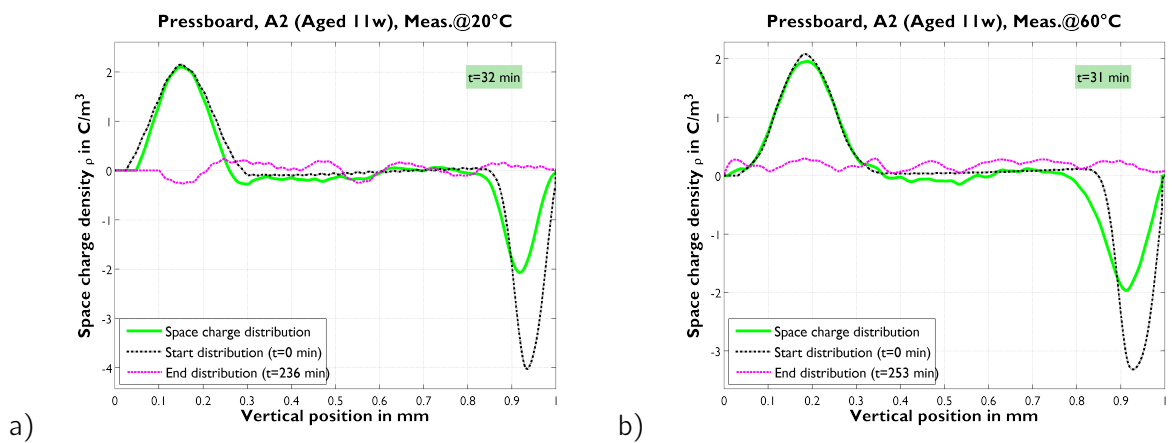


Figure 6.40: Space charge profile of aged pressboard with Shell Diala GX measured at 20 a) and 60°C b)

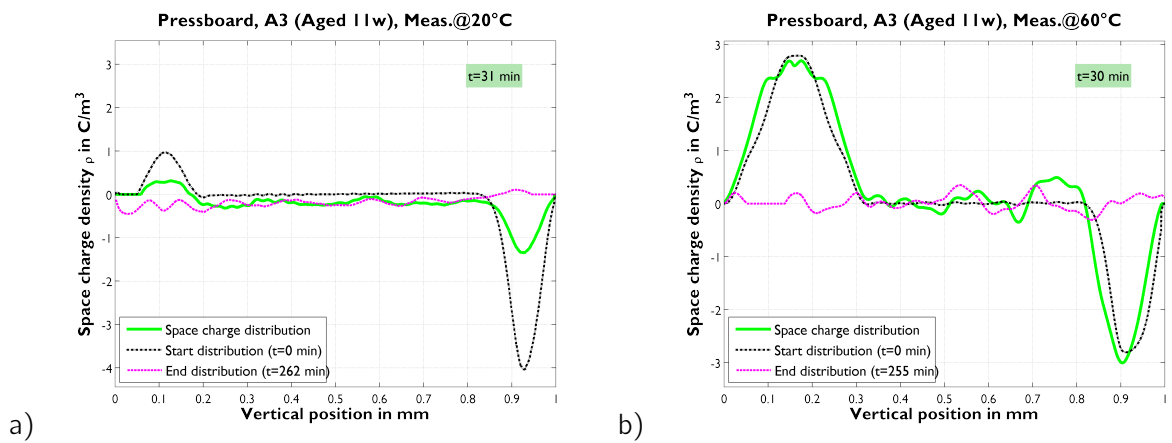


Figure 6.41: Space charge profile of aged pressboard with Nynas Nytro 10XN measured at 20 a) and 60°C b)

6.7.3 Influence of sample surface

In the beginning of this work, it was not known if oil-impregnated pressboard samples can be used for PEA measurements¹⁰² at all. One of the concerns is the heavy damping of measurement signals, as already reported in [56]: There, the amplitude of a 10 ns pulse passing through a 100 μm paper layer is reduced by a factor between approximately 1,25 and 1,6. If the same applies to the 1 mm pressboard samples, only around 10% of the original impulse are detected at best under ideal conditions.

Therefore, preliminary works had been carried out to test the method beforehand. For this reason, several pressboard samples had been aged in a similar way like all the other samples described within this work have been aged later on. Pressboard discs ($\varnothing 140$ mm, thickness 1 mm, unmachined) have been artificially aged at 135°C in and Shell Diala GX for 3 months.

However, there was one significant difference between these samples and the samples from the ageing tests: The former were not grinded and had therefore a sieve structure at the surface (see also Figure 5.1).

A comparison of **space charge measurements of grinded and unmachined samples** is shown in the figures below. Several assumptions had been made to explain these distributions: Influence of partial discharges or even the single cellulose layers within the pressboard have been investigated. This was also the reason to measure the space charge distribution of paper later on: If there is an influence of the material layers, it should not be present in the paper samples as they are manufactured with significant less layers (4 layers) as Transformerboard.

However, these results could not be replicated with the machined pressboard samples that had been aged for 11 weeks in subsequent measurements. It is now assumed that the previous results had been **caused by the surface roughness** (sieve structure) only. Reflections in the cavities on both sides of the sample could be responsible for the “odd” space charge distribution due to acoustic reflections of the HF (10 ns and 20 ns respectively) pulses.

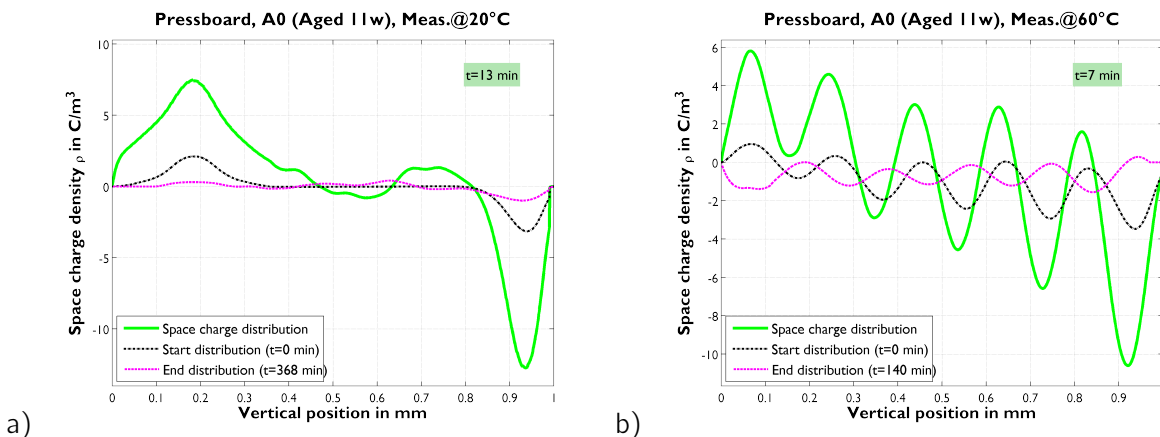


Figure 6.42: Space charge profile of aged pressboard with unmachined surface with Shell Diala GX at 20 a) and 60°C b)

6.7.4 K-Buff paper

K-Buff paper was investigated as reference samples due to interim issues with aged pressboard at 60°C as stated before. Measurements have been done at samples N10 at 20 and 60°C. As these samples are only 0,5 mm thick, the poling voltage was reduced to 5 kV to keep the field strength constant throughout these investigations ($E = 10$ kV/mm).

It can be clearly seen in the figures below, that in all cases homocharges are generated at the beginning. Similar results have been found in [56]. In terms of space charge distribution, the behaviour of the investigated

¹⁰²With the available set-up at Delft University of Technology and its limits in terms of dielectric strength and maximum voltage respectively.

paper samples is slightly different compared to pressboard: First, **a migration of charge into the bulk** of the material can be observed. Further, this effect is also temperature dependent, as at 60°C charges in the bulk can be determined already directly after voltage application. This is typical, as with increasing stress (electrical and/or thermal), more charges are injected into a material and the penetration depth is increasing [11].

The influence of single paper layers on the space charge distribution could not be determined. However, the conclusion that they do not have an influence at thicker samples or at high density material (pressboard) can not be drawn from these results.

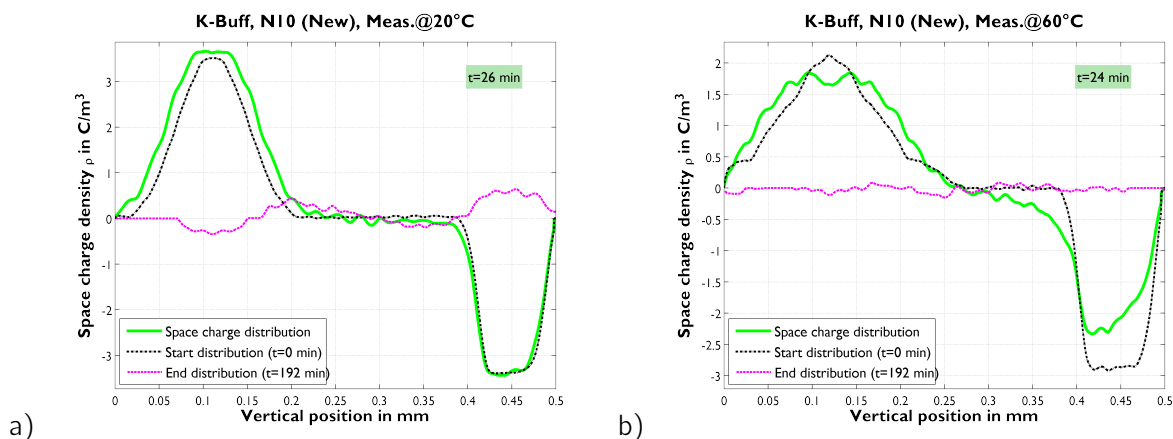


Figure 6.43: Space charge profile of unaged K-Buff paper with Nynas Nytro 4000X at 20 a) and 60°C b)

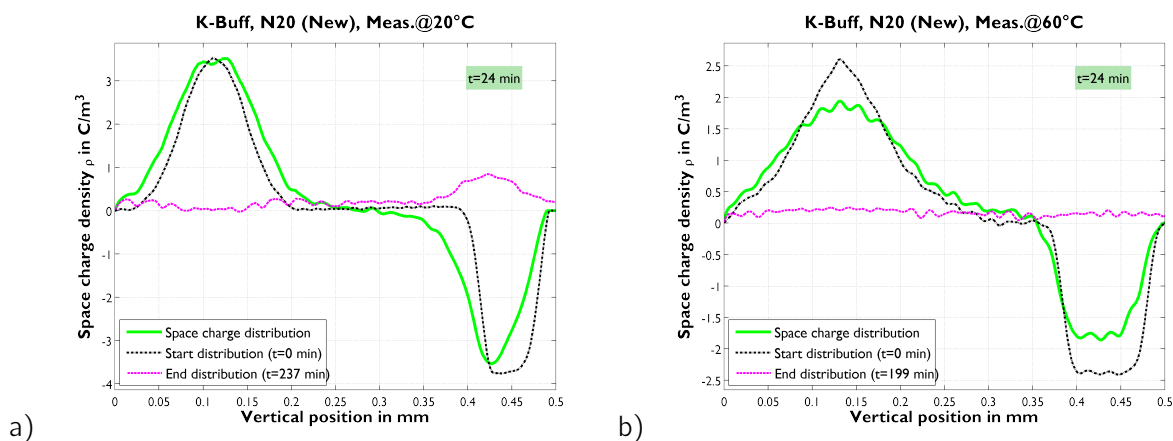


Figure 6.44: Space charge profile of unaged K-Buff paper with Shell Diala GX at 20 a) and 60°C b)

» *I may not have gone where I intended to go, but I think I have ended up where I needed to be* «

Douglas Adams, 1988

7.1 Electrical conductivity and ageing behaviour

It was assumed that ageing has an significant influence onto the electrical conductivity of pressboard an insulation oil. The verification of this proposition was a main goal of this work. While this proposition could be confirmed for the latter, **the influence of (artificial) ageing of pressboard onto its electrical conductivity seems to be small**. The conductivity was still within one order of magnitude at all oil types at all ageing conditions (unaged up to 32 weeks of ageing).

As long as the moisture level within the equipment is low, the electrical conductivity of pressboard will not rise significantly as demonstrated on numerous samples. In the scope of this work, moisture content levels between $<0,3\%$ and $<1\%$ have been investigated in terms of ageing and electrical conductivity. Further, the relation between three different impregnation oil types and pressboard conductivity was researched. Here, no significant difference between the oil types were observed. However, higher moisture contents can have significant impacts.

The **main influences onto electrical conductivity of pressboard are therefore temperature and moisture content**. If the moisture content rises over $1,5\%$, electrical conductivity will increase by a factor of around 10 when compared to the unaged samples with a moisture content of $<0,3\%$. For each percentage point of pressboard moisture content increase, the electrical conductivity will rise by a factor of around 10 compared to the "drier" sample. This relation holds - and was determined experimentally - up to a moisture content of around $3,5\%$.

A major **influence of the degree of polymerisation (DP) onto the electrical conductivity of pressboard could not be observed** within this work. Such an influence might be possible, as for example in [92] it is proposed that relaxation processes of polymers (in [92]: PE - *Polyethylene*) are influenced by the chain length or more precise, chain mobility. For pressboard this could not be confirmed as DP values between 1.200 for new samples and less than 300 for the most severely aged samples have been investigated and no significant difference could be observed nor attributed to the change of DP.

An **influence of electrical field strength onto the electrical conductivity of pressboard could not be observed**. Field strengths between 0,5 and 10 kV/mm have been investigated and they all yielded similar results.

Ageing by-products, like acids for example might influence the electrical conductivity of oil but also of pressboard, as they could be also accumulate on or in the pressboard. This could not be verified within this work, as the acidity of the oil did not raise significantly during the ageing process. Further, the pressboard samples have not been investigated in terms of material deposits (e.g. pH and conductivity of aqueous extract). The **current** (and electrical conductivity respectively) **time trend in the initial stage** (around 10 min) after voltage application **is not a reliable indicator for steady-state estimations**. In these specific cases:

- sample handling (electrostatic charging while wiping samples carefully dry)
- oil handling (electrostatic charging due to filling process, bubbling,...)
- test cell charging (remaining charge from previous measurements, e.g. in the PTFE spacers¹⁰³)

have been identified as main causes for the **large spread** in current measurements at the initial stage. Also in literature, interesting deviations between new and aged samples in terms of polarisation current time trend have been reported. In [68, 70], polarisation currents of aged OIP bushings are below those of new bushings. If, however, the polarisation current in the early phase after voltage application is much higher than this would be expected for new and dry samples, this is still a vital indicator for severe ageing [68]. Within this work this such high initial currents could not be observed for the artificially aged samples.

Ageing of oil-cellulose insulation system generally affects the oil stronger than the paper. Moisture levels of both oil and pressboard did not significantly increase in this work, as long as the vessels sealing was intact. Several oil samples needed to be discarded from further investigations, as their sealing was defective. As a consequence, heavy oxidation occurred in these samples, which resulted in high moisture content of both oil and cellulose, high dielectric loss factors and a strong increase in oil colour (up to 10).

The influence of combined ageing¹⁰⁴ was researched with a small sample size of $n = 4$ pressboard samples, impregnated with Nynas Nytro 4000X. There, no **actual impact of combined ageing** could be demonstrated when ageing 1 week at 135°C with following 1 week at 20°C and application of $E = 10$ kV/mm. However, with slight modifications of the set-up used, a concurrent application of voltage and temperature stress (at 135°C) seems possible and is further also strongly recommended. Longer ageing durations should be investigated also.

The situation for the investigated insulation oils in terms of electrical conductivity is different when compared to pressboard. **The electrical conductivity of oil rises (relatively) stronger with ageing** due to the increased moisture content. In contrast to the pressboard, the increase of moisture is small in absolute numbers, however it is still considerable large in relative terms. Comparable large amounts of moisture have been determined for the aged oil samples. They are (mainly) the result of sample treatment: Oil and cellulose have been separated at 90°C after the artificial ageing. Therefore, large(r) amounts of moisture migrate from the pressboards into the oil when compared to other investigations (literature), which is severe for the latter. Generally, this separation is commonly done at lower temperatures, resulting in lower moisture levels in the oil.

Electrical conductivity of all three oils rose around one order of magnitude after 1 week of ageing (Nytro 10XN and Diala GX) and slightly less than one order at Nytro 4000X after 5 weeks. Then, the conductivity

¹⁰³A possible remedy could be achieved by switching the polarity of the voltage source. This is described in [74] as *Alternating Voltage Method*.

¹⁰⁴Actually, subsequent ageing was conducted, as first temperature and afterwards voltage was applied.

remains quite constant over the ageing duration up to 24 weeks with a slight increase at 32 weeks. An electrical field strength between 0,5 and 1 kV/mm has a negligible influence onto the electrical conductivity of insulation oils. However, for much lower field strengths a different behaviour is expected. The main parameters for electrical conductivity of insulating oils is moisture content and temperature. When oil moisture content rises above 15 ppm the conductivity doubles when compared to the “dry” values.

In terms of conductivity measurement either a lower or a much higher field strength is desirable. In terms of “real” conductivity a small field strength (several V/mm only) is beneficial as described in literature. However, this poses massive requirements to the measuring method and instruments as the currents are very small then. The usage of higher field strengths for measurements, which are comparable to those occurring at actual operation, replicates the situation in HV equipment better and might yield more precise material specification data.

A **relation between electrical conductivity σ and dynamic viscosity η** was often drawn in literature [2, 139, 160]. Generally speaking, the product of σ and η should remain constant within a smaller temperature range, say within 30 to 60°C. This relationship can be found for example in [160]. There, this proportion holds for several different oils. Yet, there are some differences to the results of this work: For example, the investigations in [160] were made in the 1920's and 30's so it can be assumed that oil composition is not comparable to current oils. This can be seen from the absolute conductivity and especially viscosity values. Further, in [139, 160] short-time conductivity values instead of “steady-state” as used herein, are taken. Within this work (Figure 7.1 b) it is demonstrated that **the product of viscosity and conductivity is increasing with temperature** - This bakes up the fact that additional ions are generated due to endothermic dissociation with rising temperature, which is also an explanation for the rising conductivity. This is also consistent with the results presented and discussed in [2]. Further, the relationship in terms of conductivity still holds for all three oils as seen from Figure 7.1 below: The Nytro 10XN has the (absolute) lowest electrical conductivity and so is the product $\sigma \cdot \eta$ the lowest of all three oils.

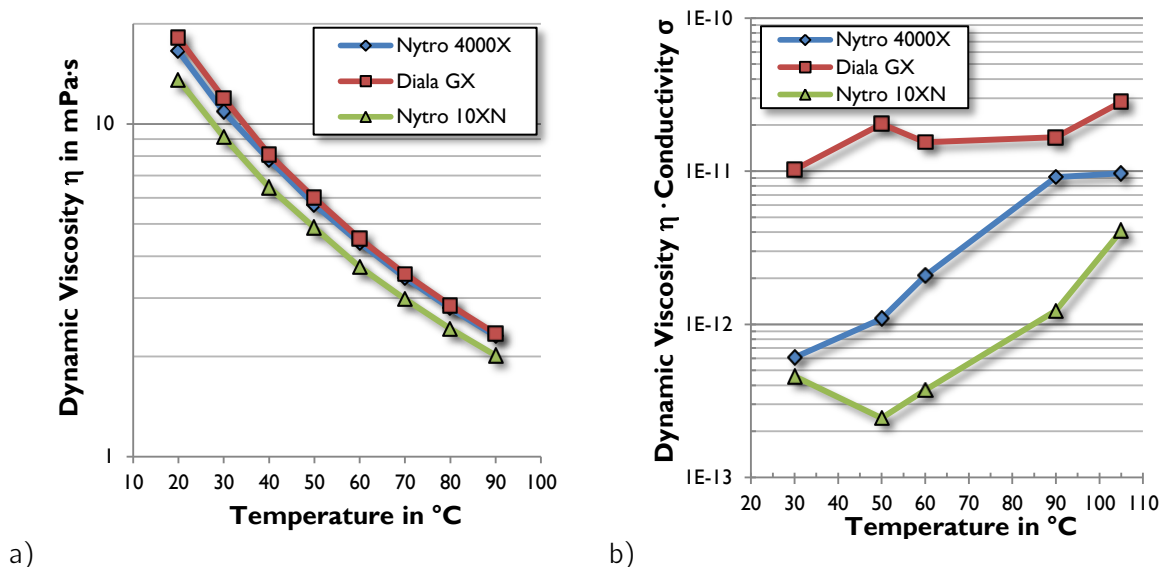


Figure 7.1: a) Dynamic viscosity η and b) product of $\eta \cdot \sigma$ of (unaged) investigated mineral oils

7.2 Charging tendency

Charging tendency of pressboard was investigated in terms of electrostatic charging behaviour and space charge distribution. Firstly, it is possible to measure the space charge density of pressboard samples up to a thickness of roughly 1 mm with the presented PEA set-up. Larger thicknesses would require stronger pulses,

as the damping inside the pressboard is higher than at other polymers (plastics). This would actually require higher (pulsing) voltages, which can not be applied to the currently used set-up.

Space charge distribution within pressboard is in total **unremarkable** and according to expectations: **Homocharges** have been formed at all investigated samples at 20 and 60°C. Temperature has also only a minor influence at pressboard, however at K-Buff paper samples the influence is significant: There, charge packets are present in the bulk already directly or shortly after voltage application.

Ageing processes seem to change little on charge distribution. The oil type and therefore oil conductivity has a negligible influence on space charge distribution. This is reasonable as the influence on electrical conductivity of pressboard does, if at all, depend only weakly on impregnation oil type. However, in terms of insulation design an important parameter might have been “overlooked” in the past: As homocharges are formed, the electrical field stress might be increased in the dielectric (bulk) as demonstrated for example in [56] on HVDC cable samples. If this is not considered in FEM simulations this could result in calculated field strengths which are lower than those in practice.

Surface properties seem to have an influence onto measured space charge distribution. This was demonstrated in the preliminary investigation at pressboard samples with sieve structure. There, no useful measurement data could be gained at elevated temperatures, which is assumed to be the result of reflections in the cavities of the sieve structure.

In terms of **electrostatic charging tendency (ECT)** several measurements have been made at unaged and aged samples in different oil types. With the spinning disc apparatus only relative measurements can be made and no absolute results in terms of a critical oil flow speed could be gained. It could be demonstrated that the **oil type has significant influence on the ECT**. This is founded mainly in the different oil viscosities and furthermore to their varied oil conductivity. A problematic influence of pressboard ageing onto ECT, as partly reported in literature, could not be validated in this work. However, here the aged samples have been tested in unaged oil only. The combination of aged oil and aged pressboard might yield different results. It can be concluded that the main influences are still the rotational speed (=flow rate), oil type and temperature.

7.3 Recommendations and consequences

It can be seen as the ultimate objective to keep HVDC equipment as dry as possible at any circumstances during their whole equipment life. Not only that moisture can speed up ageing processes, it can also increase the conductivities of oil and cellulosic components, of which the former will be stronger affected. The drier an insulation system can be kept, the nearer design values in terms of electrical field strengths and field distribution can be obeyed.

But also a different conclusion can be drawn: For the dielectric stress at an oil-cellulose insulation system - besides the electrical conductivity of the materials used - also the ratio of cellulose to oil conductivity is of importance. Now, **if the cellulose is not dried thoroughly** - say with moisture contents of around 1% - and a highly insulating oil is used (like the Nytro 10XN in this investigation), the **ratio of both conductivities can reach values of nearly 1** at 20°C. This is insofar interesting, as typically ratios of 10 to 100 (or even more) can be easily reached. In the case of such a low conductivity ratio, the dielectric stress is shared much better between oil and cellulose as this would be the case when the cellulose would be very dry (<0,5%), resulting in a higher ratio. In that sense, **a field grading** seems to be easily possible by “adjusting” moisture level contents, especially those of pressboard. However, besides from “adjusting” these levels exactly, the long-term impact of such a method is questionable as moisture levels might change during equipment lifetime.

In terms of ageing, field distribution can change during ageing process, when the conductivity of pressboard remains nearly constant but the conductivity of oil increases. This results in a further relief of stress for the oil gaps at stationary DC stress. Simultaneously, additional load is put to the cellulosic parts which basically retain their original electrical conductivity values up to moisture contents of around 1%.

7.4 Further steps and outlook

In this work, the basic influencing parameters onto the electrical conductivity of oil and pressboard have been identified and investigated. Now the field is open for further investigations. Solely from this work, the following steps might be worth investigating:

Plywood is a common material in transformer construction. The addition of plywood certainly changes the ageing behaviour of closed samples as it can release acids during ageing. They can therefore pose an influence onto the electrical conductivity of oil and cellulose. However, little is known about this issue. Further, the ageing behaviour of **low density pressboard** (e.g. Transformerboard T III) in connection with electrical conductivity might be of interest. In connection with such investigations, a research in terms of **dissolved gasses (DGA)** can be worth trying. With simple modifications of the thermal ageing samples this can be easily achieved. The artificial ageing process applied within this work was “comparable mild” to the materials due to thoroughly preparation and drying process and furthermore the sealing from ambient with an additional nitrogen cover. The ageing of a small sample set in **open containers** can be interesting insofar as the oil properties are then expected to change significantly. This would exemplify simulate problems with the sealing in practical applications.

Combined ageing (simultaneous application of temperature and dielectric stress) could be covered only briefly in this work. Longer ageing durations and the test of several oils is definitely worth trying, as a working set-up was successfully designed and tested in this work. In this connection, the HV switchbox needs to be redesigned as such high voltages used there (10 kV) could not be switched. Also at “lower” voltages (around 6 kV) EMC issues occurred which makes a new solution necessary for further investigations.

Although the (combined) vessels for ageing and conductivity measurements of pressboard proved well in this investigations, several improvements can be made: First, sample changing and cleaning is a very time consuming and tedious task. A **vessel redesign** in terms of usability is therefore recommended. These test cells can be also used to investigate the behaviour of **layered insulation set-ups**. If spacers, for example made from ceramics or pressboard are used, the set-up may be also utilized to measure polarisation and depolarisation currents of insulation oils. However, special attention needs to be paid in the conversion from current measurement data to electrical conductivity of such layered set-ups.

Alternative insulating liquids (e.g. esters) are more common in high-voltage products nowadays as this was the case several years ago. The determination of electrical conductivity of such liquids in dependency of the parameters identified in this work seems to be also interesting.

» *I think if you do something and it turns out pretty good, then you should go do something else wonderful, not dwell on it for too long. Just figure out what's next.* «

Steve Jobs, 2006

Within this work, artificially ageing of three mineral oil types and pressboard samples in a representative combination has been conducted in thermal ovens at 135°C for 9 different ageing durations between 1 and 32 weeks. Furthermore, combined ageing has been evaluated for a small number of samples. In total, more than 700 samples have been aged thermally and thermally-electrically. Main target of this work was to find a relationship between ageing, electrical conductivity and charging behaviour of new and unaged (pressboard) samples. Within the scope of this work, customized test-cells for the determination of electrical conductivity of pressboard and the possibility to conduct combined, thermal-electrical ageing on these samples have been successfully designed and constructed.

Now, does ageing influence the electrical conductivity of oil-cellulose insulation system? Well, the answer is *yes and no*. As long as the moisture content of pressboard is below 1%, the electrical conductivity of the investigated pressboard samples is reproducible between 10^{-16} and 10^{-15} S/m at 20°C ($E = 3$ kV/mm). Up to typical technical field strengths of $E = 10$ kV/mm a similar behaviour can be expected from the results gained with unaged samples.

The conductivity depends mainly on the temperature and only weakly on the ageing condition at the investigated samples. The influence of the impregnation oil used is also negligible. So, as long as there are no excessive ageing processes taking place (formation of water, acids,...), **thermal ageing will not substantially increase the electrical conductivity of pressboard**. Further, it could be demonstrated that a decreasing degree of polymerisation (DP) is not an indicator for changed (=increased) electrical conductivity. Yet, the electrical conductivity of oil depends more distinctive on the ageing condition, as already comparable small amounts of water increase the electrical conductivity. An increase by a factor of around 10 between dry oil (< 6 ppm) and aged oil (around 10 ppm and more) could be observed.

So if moisture levels are quite constant during equipment operation, the electrical conductivity and therefore the electrical field distribution is still in the range of the design values. However, if only the moisture content in the cellulose rises (due to ageing or when the insulation system is not dried thoroughly), also its conductivity rises which would equal the field distribution between oil and board to a certain extent. This depends on the ratios between the conductivities of the cellulosic parts and oil.

The **electrostatic charging tendency (ECT)** was also investigated with a spinning-disc set-up. **No significant influence of ageing could be detected**, neither after 11 nor 32 weeks of thermal ageing.

Although it could be demonstrated that the oil type has an influence on ECT behaviour, no dramatic ECT levels have been observed at these investigations.

It was also shown within this work, that the **space charge distribution** within pressboard samples with a thickness of 1 mm can be measured with a compact pulsed electro-acoustic (PEA) set-up. Homocharges have been observed in all investigated cases of new and 11 weeks aged samples at 20 and 60°C. Space charge is mainly concentrated on the surface/interfaces due to electrode and/or interface charge injection. **No charge build-up in the bulk material could be determined for the pressboard samples**, although such processes have been witnessed at the K-Buffer paper samples. **Temperature does not pose a major influence** (when comparing the 20 to 60°C results) in terms of space charge distribution within pressboard.

For the practical operation of HVDC equipment it is of particular importance that the moisture levels remain quite constant during operational lifetime to keep conductivities and field stress near the design values. On the other hand it is necessary to consider changes of (electrical) material parameters during equipment (operational) lifetime already at the insulation system design stage.

There is still a wide field of unanswered questions: Further work could and should be done with different materials for example. The addition of plywood to the ageing samples and the investigation of low density pressboard are promising tasks. Moreover, research should be done in terms of combined ageing as now a working set-up is available. Longer combined ageing durations of more than 1 week should be carried out. With small modifications of the ageing vessels it shall be possible to conduct DGA investigations as well.

List of Figures

1.1	Evolution of transmission voltages	2
1.2	AC/DC Test installation in Berlin (1942) between suburbs of Charlottenburg and Moabit; Valve hall of Gotland I Line; Pulling the Gotland cable ashore	2
1.3	Comparison of AC and DC transmission line costs	4
1.4	Transmissible Power with a 1100 kV (uncompensated) AC Overhead line	4
1.5	Transmissible power with different line technologies	5
1.6	Electrical field plot of a converter transformer (end distance) during AC, DC and PR stress	6
1.7	Active part of an HVDC converter transformer during manufacturing & Assembled HVDC converter transformer	6
1.8	Schematic view of a HV condenser bushing core	7
1.9	Modern HV bushing manufacturing	7
1.10	HVDC bushings for 800 kV during testing at Graz University of Technology	7
1.11	Insulation system of XLPE and mass-impregnated HV cables	8
1.12	FEM model of a HV bushing for AC application	10
1.13	FEM model of a HV bushing with applied DC voltage	10
1.14	Electrical conductivity of various insulation oils	10
2.1	800 kV HVDC Converter transformer during HV-test & Cross-sectional view of a 220/400 kV (AC) transformer	14
2.2	Schematic insulation system of a power transformer	15
2.3	Cellulose in its structural form (D-glucopyranose with 1,4 β -linkages)	16
2.4	Schematic production of paper and pressboard	16
2.5	Cellulosic insulation products	16
2.6	Structures of hydrocarbons in a typical mineral insulation oil	20
3.1	Factors influencing performance and degradation of transformer oil/paper insulation and resulting breakdown mechanisms	23
3.2	Distribution of water content between cellulose and oil for a new transformer	24
3.3	Correlation between DP-Value and tensile strength; Ageing rates due to different ageing mechanisms	25
4.1	Schematic of an insulation system and time trend of currents after voltage application	33
4.2	Polarisation mechanisms caused by a step-function of the electric field E	35
4.3	Simplified band model of electrical conductivity in solids	38
4.4	Discrete electron energy states with energy bands and gaps in variation of atom proximity	38

4.5	Electrical conductivity of pressboard and oil	42
4.6	Conduction mechanisms in liquid dielectrics	42
4.7	Conductivity-time characteristics: Theoretical behaviour and actual measurement of a mineral oil	44
4.8	Influence of temperature onto polarisation currents	44
4.9	Electrical conductivity and influence of electrical field strength	45
4.10	Electrical conductivity of a mineral insulating oil with varied moisture content	47
4.11	Influence of moisture content on electrical conductivity of cellulose	47
4.12	Voltage trend during typical PR-Test	48
4.13	Transient creep stress on bushing barrier surface at polarity reversal	48
4.14	Electrodes and measurement set-up for determination of specific resistance of solid materials, according to IEC 60093	49
4.15	Space charge measurement with PEA method	55
4.16	Schematic spinning disc apparatus set-up	57
5.1	Magnified views of unimpregnated pressboard samples	60
5.2	Relative permittivity ϵ_r and dielectric loss factor $\tan(\delta)$ of unaged pressboard samples	60
5.3	Relative permittivity ϵ_r and dielectric loss factor $\tan(\delta)$ of (unaged) investigated mineral oils	63
5.4	Electrical conductivity of (unaged) investigated mineral oils	64
5.5	Kinematic viscosity ν and density ρ of (unaged) investigated mineral oils	65
5.6	Composition of an ageing sample	65
5.7	Schematic set-up for electrical conductivity measurement	68
5.8	Schematic of conductivity measurement and practical set-up	68
5.9	Delivery of Portakabin	69
5.10	Inside view of ageing container	69
5.11	Thermal ovens with ageing vessels	69
5.12	Measurement times and switching regime for multiplexers	71
5.13	Schematic set-up for measurement of electrical conductivity of insulation oils	72
5.14	Schematic set-up for measurement of electrical conductivity of pressboard (with 4 test cells in parallel)	72
5.15	Spinning disc apparatus for ECT determination	73
5.16	Space charge measurement set-up at TU Delft	73
6.1	Influence of moisture content onto the electrical conductivity of pressboard	77
6.2	Spread of electrical conductivity measurements with varied moisture content	78
6.3	Influence of electrical field strength onto the measured current of pressboard	79
6.4	Influence of electrical field strength onto the electrical conductivity of pressboard	79
6.5	Influence of temperature onto the electrical conductivity of pressboard	80
6.6	Electrical conductivity of pressboard (Nynas Nytro 4000X, aged)	81
6.7	Electrical conductivity of pressboard (Shell Diala GX, aged)	81
6.8	Electrical conductivity of pressboard (Nynas Nytro 10XN, aged)	82
6.9	Electrical conductivity of combined aged pressboard samples	83
6.10	Reproducibility of current measurements	84
6.11	Electrical conductivity of unaged pressboard in variation of impregnation oil type	85
6.12	Electrical conductivity of 3 different mineral insulating oils at 22°C	86
6.13	Electrical conductivity of (unaged) Nynas Nytro 4000X in variation of temperature	87
6.14	Electrical conductivity of (unaged) Shell Diala GX in variation of temperature	88
6.15	Electrical conductivity of (unaged) Nynas Nytro 10XN in variation of temperature	88
6.16	Electrical conductivity of Nynas Nytro 4000X in variation of field strength	89
6.17	Electrical conductivity of Shell Diala GX in variation of field strength	89

6.18	Electrical conductivity and dielectric loss factor of a mineral oil in dependence of moisture content	90
6.19	Electrical conductivity of 3 different mineral insulating oils at 90°C	91
6.20	Influence of thermal ageing onto electrical conductivity of oil	92
6.21	Degree of polymerisation (DP) of pressboard at varied ageing stages	93
6.22	Moisture content of pressboard with varied ageing stages	93
6.23	Pressboard samples after breakdown during lightning impulse voltage tests	94
6.24	Colour of varied mineral oil samples	95
6.25	Colour of mineral insulating oils in different ageing stages	95
6.26	Dielectric loss factor $\tan(\delta)$ of mineral insulating oils in different ageing stages	96
6.27	Moisture content of mineral insulating oils in different ageing stages	96
6.28	Relative permittivity ϵ_r of mineral insulating oils in different ageing stages	97
6.29	Current time-trend of Nynas Nytro 4000X sample at 400 min ⁻¹ at varied temperature	98
6.30	Current time-trend of Nynas Nytro 4000X sample at 60°C and varied rotational speed	98
6.31	Current time-trend of Shell Diala GX sample at 60°C and varied rotational speed	99
6.32	Current time-trend of Nynas Nytro 10XN sample at 60°C and varied rotational speed	99
6.33	Current time-trend of new and aged Nynas Nytro 4000X samples	100
6.34	Current time-trend of new and aged Shell Diala GX samples	100
6.35	Current time-trend of new and aged Nynas Nytro 10XN samples	100
6.36	Space charge profile of pressboard with Nynas Nytro 4000X measured at 20°C	102
6.37	Space charge profile of pressboard with Shell Diala GX measured at 20°C	102
6.38	Space charge profile of pressboard with Nynas Nytro 10XN measured at 20°C	102
6.39	Space charge profile of pressboard (aged/Nynas Nytro 4000X), 20 & 60°C	103
6.40	Space charge profile of pressboard (aged/Shell Diala GX), 20 & 60°C	103
6.41	Space charge profile of pressboard (aged/Nynas Nytro 10XN), 20 & 60°C	103
6.42	Space charge profile of aged pressboard with varied unmachined surface	104
6.43	Space charge profile of K-Buffer paper (unaged/Nynas Nytro 4000X) at 20 and 60°C	105
6.44	Space charge profile of K-Buffer paper (unaged/Shell Diala GX) at 20 and 60°C	105
7.1	Dynamic viscosity η and $\eta \cdot \sigma$ of (unaged) investigated mineral oils	109
A.1	Schematics of vacuum processing equipment for sample preparation	A.1
A.2	Impregnation of pressboard samples	A.2
A.3	Filling of thermal ageing samples	A.7
B.1	Pyrex 1490 dish (Image supplied by manufacturer)	B.1
B.2	Original Pyrex Dish and grinded sealing surface)	B.2
B.3	Temperature monitoring system for thermal ageing samples	B.2
D.1	Impulse voltage tests	D.2
D.2	Moisture determination of pressboard	D.3
E.1	Determining the colour of insulating oils	E.1

List of Tables

1.1	Dependence of (relative) permittivity ϵ and electrical conductivity σ on several factors . . .	9
2.1	Important properties of insulation liquids for various electrical equipment	19
2.2	Important properties of mineral insulation oils	19
2.3	Classification of crude petroleum	20
3.1	Duration needed to reduce the DP of paper from 1.300 to 150	25
4.1	Electrical conductivity of Transformerboard at varied electrical field strength	45
4.2	Electrical conductivity of insulation oils at varied electrical field strength	46
4.3	Time intervals for typical PR test	48
5.1	Electrical properties of Nynas Nytro 4000 X (unaged)	63
5.2	Electrical properties of Shell Diala GX (unaged)	63
5.3	Electrical properties of Nynas Nytro 10XN (unaged)	63
5.4	Viscosity and density of investigated oils	65
5.5	Water content in oil and pressboard for ageing sample ratios	66
6.1	Summary of thermally aged samples	75
6.2	Electrical conductivity of investigated pressboard samples with varied moisture content . . .	77
6.3	Electrical conductivity of (unaged) mineral oils at varied times	86
6.4	Deviations between Tettex and IEC 60247 measurements	87
6.5	Ratios of oil conductivity between 22 and 90°C	87
6.6	Oil conductivity for varied field strength at 1 min and after 24 h	89
6.7	Oil conductivity for varied field strength at 1 min	90
6.8	Ratios of oil conductivity at varied temperatures and times	90
6.9	Electrical conductivity of (unaged) mineral oils at varied times at 90°C	91
6.10	Degree of polymerisation for aged pressboard samples	93
6.11	Colour of aged mineral oil samples (VDEW scale)	95
6.12	Dielectric loss factor $\tan(\delta)$ of aged mineral oil samples	95
6.13	Moisture content of aged mineral oil samples	96
6.14	Relative permittivities ϵ_r of aged mineral insulating oil samples	97
6.15	Pressboard samples for space charge (PEA) measurements	101
A.1	Composition of Nynas Nytro 4000 X	A.6
A.2	Composition of Shell Diala GX	A.6

A.3	Composition of Nynas Nytro 10 XN	A.6
-----	--	-----

Bibliography

- [1] ABB AB. *The NorNed HVDC connection, Norway - Netherlands*. 2008. 2 pages. (Cited on page 8).
- [2] Ignacy Adamczewski. *Ionization, conductivity and breakdown in dielectric liquids*. Taylor & Francis, 1969. 439 pages. ISBN: 978-0850660272. (Cited on pages 37, 64, 109).
- [3] Thomas Andritsch. "Epoxy Based Nanodielectrics for High Voltage DC Applications: Synthesis, Dielectric Properties and Space Charge Dynamics". Dis. Delft: TU Delft, 2010. 204 pages. (Cited on pages 37, 101).
- [4] Jos Arrillaga. *High Voltage Direct Current Transmission*. 2nd edition. 1998. ISBN: 978-0852969410. (Cited on pages 1, 4).
- [5] Gunnar Asplund. "Ultra high voltage transmission". In: *ABB Review*, Vol. 2 (2007), page 27. (Cited on page 4).
- [6] Ray Bartnikas. *Engineering Dielectric Volume III: Electrical Insulating Liquids*. Edited by American Society for Material Testing and Materials (ASTM). 1994. ISBN: 0-8031-2055-9. (Cited on pages 18–20, 27, 36, 42).
- [7] Ray Bartnikas. *Engineering Dielectrics Volume IIA: Electrical properties of Solid Insulating Materials: Molecular structure and electrical behaviour*. Philadelphia: ASTM, 1983. 724 pages. ISBN: 978-0-8031-0228-6. (Cited on page 35).
- [8] Ray Bartnikas. *Engineering Dielectrics Volume IIB: Electrical properties of Solid Insulating Materials: Measurement Techniques*. Philadelphia: ASTM, 1987. 589 pages. ISBN: 0-8031-0491-X. (Cited on page 50).
- [9] Thomas Benz. "320 kV Extruded Cables for HVDC Transmission - Experience and Development Trends". In: *ETG Fachtagung Isoliersysteme, 27.-28.09.2010* (2010). (Cited on page 8).
- [10] John Desmond Bernal. *A history of classical physics: from antiquity to the quantum*. Barnes & Noble Books, 1997. ISBN: 0-76070-601-8. (Cited on page 1).
- [11] Jens Beyer. "Space Charge and Partial Discharge Phenomena in HVDC Devices". PhD Thesis. Delft: TU Delft, 2002. 223 pages. (Cited on pages 8, 12, 33, 39, 53–55, 105).

- [12] Manfred Beyer et al. *Hochspannungstechnik*. Berlin: Springer-Verlag, 1986. ISBN: 3-540-16014-0. (Cited on pages 14, 40, 45, 94).
- [13] Riccardo Bodega. "Space Charge Accumulation in Polymeric High Voltage DC Cable Systems". PhD Thesis. Delft: TU Delft, 2006. 196 pages. (Cited on pages 2, 8, 73).
- [14] A. Bradwell. *Electrical Insulation*. Edited by N. Parkman. Volume 2. IEE Electrical and Electronics Materials and Devices Series. Exeter: Peter Peregrinus Ltd. on behalf of the Institution of Electrical Engineer, 1983. 283 pages. ISBN: 0-86341-007-3. (Cited on pages 14, 20, 27, 28, 32, 33, 36, 41, 43, 47, 48, 70, 76).
- [15] CIGRÉ Joint Working Group 12/15.13. *CIGRÉ Brochure 170: Static electrification in power transformers*. Paris: CIGRÉ, 2000. 83 pages. (Cited on pages 11, 55, 56).
- [16] CIGRÉ Joint Working Group A2/B4.28. *CIGRÉ Brochure 406: HVDC Converter Transformers: Design Review, Test Procedures, Ageing Evaluation and Reliability in Service*. Paris: CIGRÉ, 2010. 37 pages. ISBN: 978-2-85873-093-3. (Cited on pages 10, 48).
- [17] CIGRÉ Task Force D1.01.10. *CIGRÉ Brochure 323: Ageing of cellulose in mineral-oil insulated transformers*. Paris: CIGRÉ, 2007. 87 pages. ISBN: 978-2-85873-018-6. (Cited on pages 13–16, 19, 23–27, A.6, D.1).
- [18] CIGRÉ Task Force D1.12.01. *CIGRÉ Brochure 288: Space Charge Measurement in Dielectrics and insulating materials*. Paris: CIGRÉ, 2006. 51 pages. (Cited on page 54).
- [19] CIGRÉ Working Group 14.32. *CIGRÉ Brochure 215: HVDC Converter stations for voltages above ± 600 kV*. Paris: CIGRÉ, 2002. 41 pages. (Cited on page 66).
- [20] CIGRÉ Working Group A2.32. *Brochure 378 - Copper sulphide in transformer insulation*. Paris: CIGRÉ, 2009. 37 pages. ISBN: 978-2-85873-065-0. (Cited on page 18).
- [21] CIGRÉ Working Group B1.07. *Statistics of AC underground cables in power networks*. Paris: CIGRÉ, 2007. 148 pages. ISBN: 978-2-85873-026-1. (Cited on page 7).
- [22] Aake Carlson. "Specific requirements on HVDC converter transformers". In: (1996). URL: [http://www05.abb.com/global/scot/scot221.nsf/veritydisplay/5f6d61425208b604c1256fda004aeada/\\$file/specificrequirementsonhvdconvertertransformers.pdf](http://www05.abb.com/global/scot/scot221.nsf/veritydisplay/5f6d61425208b604c1256fda004aeada/$file/specificrequirementsonhvdconvertertransformers.pdf). (Cited on page 6).
- [23] Jen-Shih Chang, Arnold J. Kelly, and Joseph M. Crowley. *Handbook of electrostatic processes*. 1st edition. New York: Marcel Dekker Inc., 1995. 763 pages. ISBN: 0-8247-9254-8. (Cited on pages 31, 32, 34–36, 56).
- [24] Frank M. Clark. *Insulating Materials for Design and Engineering Practice*. 1st edition. John Wiley and Sons, Inc., 1962. 1218 pages. ISBN: 0471158550. (Cited on pages 14, 17, 34).
- [25] Roland Coelho. *Physics of dielectrics for the engineer*. 1st edition. Amsterdam: Elsevier Scientific Publishing Company, 1979. 175 pages. ISBN: 0-444-41755-9. (Cited on pages 33–35, 61).
- [26] D. W. Crofts. "The static electrification phenomena in power transformers". In: *Electrical Insulation, IEEE Transactions on*, Vol. 23.no. 1 (1988), pages 137–146. DOI: 10.1109/14.2347. (Cited on pages 11, 55–57).
- [27] Ansgar Dais. "Hochspannungsdurchführungen". In: WEIDMANN Seminar Transformatoren 2010, Rapperswil. 2010. (Cited on page 6).

- [28] Thomas W. Dakin. "Electrical Insulation Deterioration Treated as a Chemical Rate Phenomenon". In: *American Institute of Electrical Engineers, Transactions of the*, Vol. 67.no. 1 (1948), pages 113–122. DOI: 10.1109/T-AIEE.1948.5059649. (Cited on page 29).
- [29] Deutsches Institut für Normung. *DIN 50035 (1989-04): Begriffe auf dem Gebiet der Alterung von Materialien - Polymere Werkstoffe (Terms and definitions used on ageing of materials; examples concerning polymeric materials)*. Beuth Verlag, 1989. (Cited on page 21).
- [30] H. Z. Ding, Z. D. Wang, and P. N. Jarman. "Effect of ageing on the impulse breakdown strength of oil-impregnated pressboard used in power transformers". In: *Electrical Insulation and Dielectric Phenomena, 2006 IEEE Conference on*. Electrical Insulation and Dielectric Phenomena, 2006 IEEE Conference on. 2006, pages 497–500. (Cited on page 94).
- [31] Len A. Dissado and John C. Fothergill. *Electrical Degradation and Breakdown in Polymers*. Stevenage: Peter Peregrinus Ltd. on behalf of the Institution of Electrical Engineers, 1992. 620 pages. ISBN: 0-86341-196-7. (Cited on pages 37–40, 53).
- [32] Institute of Electrical and Electronics Engineers. *IEEE Std 43-2000 (R2006): IEEE Recommended Practice for Testing Insulation Resistance of Rotating Machinery*. New York, 2000. 21 pages. DOI: 10.1109/IEEESTD.2000.91301. (Cited on page 33).
- [33] Institute of Electrical and Electronics Engineers. *IEEE Std C57.129-2007 (Revision of IEEE Std C57.129-1999): IEEE Standard for General Requirements and Test Code for Oil-Immersed Hvdc Converter Transformers*. New York, 2008. 47 pages. DOI: 10.1109/IEEESTD.2008.4444831. (Cited on pages 47, 48).
- [34] Institute of Electrical and Electronics Engineers. *IEEE Std C57.91: IEEE guide for loading mineral-oil-immersed transformers*. New York, 1996. 100 pages. ISBN: 1-55937-569-8. DOI: 10.1109/IEEESTD.1996.79665. (Cited on pages 15, 22, 23, 25, 28, 29).
- [35] Alan M. Emsley, Richard John Heywood, and Gary C. Stevens. "Ultra-Accelerated Thermal Ageing Tests". In: edited by Leslie G. Mallinson. 1st edition. *Ageing Studies and Lifetime Extension of Materials*. New York: Kluwer Academic/Plenum Publishers, New York, 2001, pages 277–282. ISBN: 0-306-46477-2. (Cited on page 28).
- [36] Alan M. Emsley and G. C. Stevens. "Review of chemical indicators of degradation of cellulosic electrical paper insulation in oil-filled transformers". In: *Science, Measurement and Technology, IEE Proceedings -*, Vol. 141; 141.no. 5 (1994), pages 324–334. DOI: 10.1049/ip-smt:19949957. (Cited on pages 23, 27).
- [37] Herbert G. Erdman. *Electrical insulating oils*. 1st edition. Philadelphia: American Society for Testing and Materials (ASTM), 1988. 151 pages. ISBN: 0-8031-1179-7. (Cited on pages 18, 20, 55, 56).
- [38] J. Fabre and A. Pichon. "Deteriorating Process and Products of paper in oil application to transformers". In: *CIGRÉ Session 1960, Paper 137* (1960). (Cited on pages 13, 24, 25).
- [39] Gerhard Fasching. *Werkstoffe für die Elektrotechnik*. 4th edition. Wien: Springer Verlag, 2005. 679 pages. ISBN: 3-221-22133-6. (Cited on page 38).
- [40] Wilhelm Füßl. *Oskar von Miller 1855 - 1934. Eine Biographie*. 1st edition. München: Beck, 2005. 452 pages. ISBN: 978-3406529009. (Cited on page 1).

- [41] René Flosdorff and Günther Hilgarth. *Elektrische Energieverteilung*. 8th edition. Stuttgart/Leipzig/Wiesbade: B.G. Teubner GmbH, 2003. 390 pages. ISBN: 3-519-26424-2. (Cited on pages 3, 4).
- [42] Hans Peter Gasser et al. "Aging of Pressboard in Different Insulating Liquids". In: *International Conference on Dielectric Liquids (ICDL)*, 27. - 30.06.2011 (2011). DOI: 10.1109/ICDL.2011.6015450. (Cited on page 93).
- [43] Uno Gäfvert. "Dielectric response analysis of real insulation systems". In: *Solid Dielectrics, 2004. ICSD 2004. Proceedings of the 2004 IEEE International Conference on*, Vol. 1 (2004), pages 1–10. DOI: 10.1109/ICSD.2004.1350276. (Cited on page 15).
- [44] Ernst Gockenbach. "Spannungsformen in HGÜ-Systemen - Statische und dynamische Beanspruchungen". In: *Isoliersysteme bei Gleich- und Mischfeldbeanspruchung*, Presentation at the ETG-Fachtagung, Cologne. Köln, 2010. (Cited on page 9).
- [45] Wolfgang Hauschild. "Die Entwicklung der Hochspannungs-Prüftechnik in den letzten 50 Jahren". In: *50 Jahre Hochspannungstechnik in Stuttgart*; 23.06.2005. 2005. (Cited on page 2).
- [46] Peter Heinzig. "Geschichte, Funktion und Einsatzgebiete von Transformatoren". In: *WEIDMANN Seminar Transformatoren 2010*. Rapperswil, 2010. (Cited on page 5).
- [47] Klaus Heuck, Klaus-Dieter Dettmann, and Detlef Schulz. *Elektrische Energieversorgung*. 7th edition. Wiesbaden: Friedr. Vieweg und Sohn Verlag, 2007. 762 pages. ISBN: 978-3-8348-0217-0. (Cited on pages 3, 4).
- [48] Richard John Heywood. "The degradation models of cellulosic transformer insulation". Dissertation. University of Surrey, 1997. (Cited on pages 15, 27, 29, D.1).
- [49] M. Hilaire, C. Marteau, and R. Tobazeon. "Apparatus developed for measurement of the resistivity of highly insulating liquids". In: *Electrical Insulation, IEEE Transactions on*, Vol. 23.no. 4 (1988), pages 779–789. DOI: 10.1109/14.7352. (Cited on pages 32, 33, 41–43).
- [50] M. Häusler and D. Retzmann. "Vom Smart Grid zum Supergrid - Effiziente Lösungen mit UHV DC Höchstleistungsübertragung "Grüner Energien"". In: *Präsentation bei der ETG Fachtagung Isoliersysteme, 27.-28.09.2010* (2010). (Cited on pages 3, 5).
- [51] International Electrotechnical Commission. *IEC 60076-7: Power transformers - Part 7: Loading guide for oil-immersed power transformers*. 1st edition. Geneva, 2005. (Cited on pages 22, 23, 25).
- [52] International Electrotechnical Commission. *IEC 60093: Methods of test for volume resistivity and surface resistivity of solid electrical insulating materials*. 2nd edition. Geneva, 1980. (Cited on pages 11, 49, 51, 67, 70, 84).
- [53] International Electrotechnical Commission. *IEC 60247: Insulating liquids - Measurement of relative permittivity, dielectric dissipation factor ($\tan d$) and d.c. resistivity*. 3rd edition. Geneva, 2004. (Cited on pages 50, 70).
- [54] International Electrotechnical Commission. *IEC 60296: Fluids for electrotechnical applications - Unused mineral insulating oils for transformers and switchgear*. 4th edition. 2012. 43 pages. ISBN: 978-2-88912-928-7. (Cited on page 62).

- [55] International Electrotechnical Commission. *IEC 61620: Insulating liquids - Determination of the dielectric dissipation factor by measurement of the conductance and capacitance - Test method*. 1st edition. Geneva, 1998. (Cited on page 50).
- [56] Marc Jan Petrus Jeroense. "Charges and discharges in HVDC cables; in particular in mass-impregnated HVDC cables". Dissertation. Delft: TU Delft, 1997. 223 pages. (Cited on pages 8, 12, 53, 73, 101, 104, 110).
- [57] G. R. Jones, M. A. Laughton, and M. G. Say. *Electrical Engineer's Reference Book*. 15th edition. Oxford: Butterworth-Heinemann, 1993. 1000 pages. ISBN: 0-7506-1202-9. (Cited on page 18).
- [58] Lars Jonsson and Rutger Johansson. "High-voltage bushings". In: *ABB Review* no. 3 (2009), pages 66–70. URL: <http://www.abb.com/abbreview>. (Cited on page 7).
- [59] Thomas Judendorfer, Alexander Pirker, and Michael Muhr. "Conductivity measurements of electrical insulating oils". In: *Dielectric Liquids (ICDL), 2011 IEEE International Conference on*. Dielectric Liquids (ICDL), 2011 IEEE International Conference on. Trondheim, 2011. ISBN: 2153-3725. DOI: 10.1109/ICDL.2011.6015456. (Cited on pages 10, 11).
- [60] Thomas Judendorfer et al. "Electrical conductivity of pressboard and the influence of moisture content". In: *CIGRÉ Transformer Colloquium 2012, Dubrovnik (2012)*. (Cited on pages 72, 76, 77).
- [61] Manfred Kahle. *Elektrische Isoliertechnik*. Berlin: VEB Verlag Technik, 1988. 360 pages. ISBN: 3-341-00492-0. (Cited on pages 14, 33, 40–43, 85).
- [62] Karl-Werner Kanngießner. "Hochspannungs-Gleichstrom-Übertragung". In: *BBC-Nachrichten*, Vol. 48.no. September/Oktober (1966), pages 583–591. (Cited on pages 1, 2, 4).
- [63] Kwan Chi Kao. *Dielectric phenomena in solids: With emphasis on physical concepts of electronic processes*. 1st edition. San Diego, California: Elsevier Academic Press, 2004. 581 pages. ISBN: 0-12-396561-6. (Cited on pages 31–41, 61).
- [64] Michael Käßberger. "Vorgänge im Papier bei dynamisch beschleunigter Alterung". Dissertation. Graz: TU Graz, Fakultät für Maschinenbau, 1998. 205 pages. (Cited on pages 21, 24–26).
- [65] Andreas Küchler. *Hochspannungstechnik*. 3rd edition. Springer Berlin Heidelberg, 2009. 607 pages. ISBN: 978-3-540-78412-8. DOI: 10.1007/978-3-540-78413-5. (Cited on pages 7, 14, 15, 19, 42, 51).
- [66] Andreas Küchler et al. "Charakterisierung von Isolierstoffen und Isoliersystemen durch Polarisations- und Depolarisationsstromanalysen (PDC-Analysen)". In: *1. Burghauser Isolierstoff Kolloquium (2007)*. (Cited on pages 43, 44, 47, 51, 77).
- [67] Andreas Küchler et al. "Condition Assessment of aged transformer bushing insulations". In: *CIGRÉ Session 2006, Paper A2-104 (2006)*. (Cited on page 82).
- [68] Andreas Küchler et al. "Das dielektrische Verhalten von Öl-Papier-Isolationen unter der Wirkung von Grenzflächen-, Material- und Prüfparametern". In: *ETG-Fachtagung Grenzflächen in elektrischen Isoliersystemen (2005)*. (Cited on pages 46, 80, 108).

- [69] Andreas KÜchler et al. "Dielektrische Eigenschaften von Öl-Board- und Öl-Papier- Isolierungen als Kenngrößen für die Diagnose von Transformatoren und Durchführungen". In: *ETG Fachtagung Diagnostik elektrischer Betriebsmittel, 19.-20.09.2006* (2006). (Cited on pages 46, 47, 52, 80).
- [70] Andreas KÜchler et al. "Einfluss äußerer Grenzflächen auf die dielektrische Diagnose betriebsgealterter Hochspannungsdurchführungen". In: edited by Energietechnische Gesellschaft im VDE (ETG). Hanau, 2005, pages 223–228. ISBN: 3-8007-2879-6. (Cited on page 108).
- [71] Andreas KÜchler et al. "Evaluation of Conductivities and Dielectric Properties for Highly Stressed HVDC Insulating Materials". In: *CIGRÉ Session 2010, Paper D1-106-2010* (2010). (Cited on pages 9, 11, 45, 49).
- [72] Andreas KÜchler et al. "Parameters determining the dielectric properties of oil impregnated pressboard and presspaper in AC and DC power transformer applications". In: *ISH 07 International Symposium on High Voltage Engineering* (2007). (Cited on pages 44, 47, 51, 77, 82).
- [73] J. Kedzia. "Investigation of transformer oil electrification in a spinning disk system". In: *Electrical Insulation, IEEE Transactions on*, Vol. 24; 24.no. 1 (1989), pages 59–65. DOI: 10.1109/14.19866. (Cited on pages 12, 57).
- [74] Keithley. *Low Level Measurements Handbook*. 6th edition. No. 1559 - 80450KSI. Cleveland, Ohio, 2004. (Cited on page 108).
- [75] Thomas Kern. "System- und Technologievergleich von UHV-Übertragungssystemen". Diplomarbeit. Graz: TU Graz, 2010. 159 pages. (Cited on pages 2, 4).
- [76] Friedrich Kießling, Peter Nefzger, and Ulf Kaintzyk. *Freileitungen: Planung, Berechnung, Ausführung*. 5th edition. Springer, 2001. 611 pages. ISBN: 3540422552. (Cited on page 2).
- [77] Chan-Ki Kim et al. *HVDC Transmission: Power conversion applications in power systems*. Singapore: John Wiley and Sons (Asia), 2009. 439 pages. ISBN: 978-0-470-82295-1. (Cited on pages 5, 6).
- [78] Edward Wilson Kimbark. *Direct current transmission, Volume 1*. 1st edition. New York: John Wiley & Sons, Inc., 1971. 508 pages. ISBN: 0-471-47580-7. (Cited on pages 1, 2).
- [79] Dieter Klemm et al. *Comprehensive Cellulose Chemistry; Volume 1: Fundamentals and Analytical Methods*. Weinheim: Wiley-VCH Verlag GmbH, 1998. 263 pages. ISBN: 3-527-29413-9. (Cited on pages 15, 16).
- [80] Dieter Klemm et al. *Comprehensive Cellulose Chemistry; Volume 2: Functionalization of Cellulose*. 1st edition. Weinheim: Wiley-VCH Verlag GmbH, 1998. 389 pages. ISBN: 3-527-29489-9. (Cited on page 15).
- [81] T. Kobayashi et al. "Major factors influencing static electrification in an aged transformer". In: *Electrical Insulation and Dielectric Phenomena, 2005. CEIDP '05. 2005 Annual Report Conference on*. Electrical Insulation and Dielectric Phenomena, 2005. CEIDP '05. 2005 Annual Report Conference on. 2005, pages 474–477. DOI: 10.1109/CEIDP.2005.1560723. (Cited on page 11).
- [82] Christoph Krause. "Zellulose und Mineralöl: Die (fast) perfekte Hochspannungsisolation". In: *FKH-/VSE Fachtagung* (2007). (Cited on pages 5, 14–16, 24).

- [83] Michael Kreienberg. "50 Jahre Hochspannungs-Gleichstromübertragung (HGÜ)". In: *etz - Elektrotechnik + Automation* no. 10 (2004), pages 58–59. (Cited on page 2).
- [84] Frederik H. Kreuger. *Industrial High DC Voltage*. 1st edition. Delft: Delft University Press, 1995. 198 pages. ISBN: 90-407-1110-0. (Cited on pages 9, 12, 53, 101).
- [85] A. Kurita et al. "DC Flashover Voltage Characteristics and Their Calculation Method for Oil-Immersed Insulation Systems in HVDC Transformers". In: *Power Delivery, IEEE Transactions on*, Vol. 1.no. 3 (1986), pages 184–190. DOI: 10.1109/TPWRD.1986.4307991. (Cited on page 42).
- [86] Edelhard Kynast. "Isolationskoordination und Hochspannungstechnik in den UHV-Technologien". Dissertation. Graz: TU Graz, 2011. 166 pages. (Cited on pages 2, 4).
- [87] P. Lair, S. Lelaidier, and A. Marzin. "Converter transformers for 500 kV HVDC links". In: *CIGRÉ Session 1996, Paper 12-201* (1996). (Cited on page 13).
- [88] W. Lampe and E. Spicar. "Influence of different stress factors on the dielectric and mechanical strength of oil-cellulose insulation". In: *CIGRÉ Session 1978, Paper 15-05* (1978). (Cited on page 26).
- [89] G. M. Lanfranconi, G. Maschio, and E. Occhini. "Self-Contained Oil-Filled Cables for High Power Transmission in the 750-1200 kV Range". In: *Power Apparatus and Systems, IEEE Transactions on*, Vol. PAS-93.no. 5 (1974), pages 1535–1545. DOI: 10.1109/TPAS.1974.293884. (Cited on page 7).
- [90] Thomas Leibfried and Adolf J. Kachler. "Insulation diagnostics on power transformers using the polarisation and depolarisation current (PDC) analysis". In: *Electrical Insulation, 2002. Conference Record of the 2002 IEEE International Symposium on*. Electrical Insulation, 2002. Conference Record of the 2002 IEEE International Symposium on. 2002, pages 170–173. (Cited on page 11).
- [91] Gerhard Lemesch. "Methoden zur Beurteilung der elektrischen Aufladungsneigung von flüssig/festen Isolierungssystemen". Dissertation. Graz: TU Graz, 1996. (Cited on pages 37, 56, 97).
- [92] T. J. Lewis. "Polyethylene under electrical stress". In: *Dielectrics and Electrical Insulation, IEEE Transactions on*, Vol. 9.no. 5 (2002), pages 717–729. DOI: 10.1109/TDEI.2002.1038659. (Cited on page 107).
- [93] Werner Lick and Michael Muhr. "Prebreakdown behaviour of oil-board-arrangements under lightning impulse stress". In: *Electrical Insulation and Dielectric Phenomena, 2004. CEIDP '04. 2004 Annual Report Conference on*. Electrical Insulation and Dielectric Phenomena, 2004. CEIDP '04. 2004 Annual Report Conference on. 2004, pages 519–521. DOI: 10.1109/CEIDP.2004.1364301. (Cited on page 94).
- [94] David R. Lide. *CRC Handbook of Chemistry and Physics*. 87th edition. Boca Raton: Taylor and Francis, 2007. 2608 pages. ISBN: 978-0849304873. (Cited on page 38).
- [95] Marcus Liebschner. "Interaktion von Ölspalten und fester Isolation in HVDC-Barriersystemen". Dissertation. Illmenau: Technische Universität Illmenau, 2009. 139 pages. (Cited on pages 41, 43, 45, 46, 51).

- [96] Qiang Liu et al. "Experimental research on the streaming electrification of transformer oil under aging". In: *Condition Monitoring and Diagnosis, 2008. CMD 2008. International Conference on* (2008), pages 243–246. DOI: 10.1109/CMD.2008.4580272. (Cited on pages 11, 56).
- [97] Y. Liu and M. M. A. Salama. "Applying simulation model to uniform field space charge distribution measurements by the PEA method". In: *Electrical Insulation, 1996., Conference Record of the 1996 IEEE International Symposium on*. Electrical Insulation, 1996., Conference Record of the 1996 IEEE International Symposium on. Volume 2. 1996, 466–469 vol.2. DOI: 10.1109/ELINSL.1996.549383. (Cited on pages 53, 54).
- [98] Pierre Lorin et al. "Increase transformer reliability and availability: From condition assessment to site repair". In: *Petroleum and chemical industry committee (PCIC) Conference 2010* (2010). (Cited on page 22).
- [99] Bernhard Lutz. "Einflussfaktoren auf die elektrische Feldverteilung in Isoliersystemen mit polymeren Isolierstoffen bei Gleichspannungsbelastung". Shaker Verlag. Dissertation. Munich: TU München, 2011. 242 pages. (Cited on pages 32, 37, 40, 45, 54, 76).
- [100] Riccardo Maina et al. "Copper dissolution and deposition tendency of insulating mineral oils related to dielectric properties of liquid and solid insulation". In: *Dielectric Liquids (ICDL), 2011 IEEE International Conference on*. Dielectric Liquids (ICDL), 2011 IEEE International Conference on. 2011, pages 1–6. ISBN: 2153-3725. DOI: 10.1109/ICDL.2011.6015423. (Cited on page 18).
- [101] James R. Melcher. *Continuum Electromechanics*. Cambridge, MA: The MIT Press, 1981. 640 pages. ISBN: 978-0262131650. URL: http://ocw.mit.edu/ans7870/resources/melcher/resized/cem_811.pdf. (Cited on pages 37, 42).
- [102] D. Meurer and M. Stürmer. "Kabelsysteme für Mittel- und Hochspannung - Alterungsdiagnose: notwendig und hilfreich?" In: *ETG Fachtagung Diagnostik elektrischer Betriebsmittel, 26-27.02.2002* (2002). (Cited on page 7).
- [103] Gian Carlo Montanari and Luciano Simoni. "Aging phenomenology and modeling". In: *Electrical Insulation, IEEE Transactions on*, Vol. 28.no. 5 (1993), pages 755–776. DOI: 10.1109/14.237740. (Cited on pages 22, 28).
- [104] Vincent M. Montsinger. "Loading Transformers By Temperature". In: *American Institute of Electrical Engineers, Transactions of the*, Vol. 49.no. 2 (1930), pages 776–790. DOI: 10.1109/T-AIEE.1930.5055572. (Cited on pages 23, 25, 28).
- [105] Peter Morshuis and Marc Jan Petrus Jeroense. "Space charge measurements on impregnated paper: a review of the PEA method and a discussion of results". In: *Electrical Insulation Magazine, IEEE*, Vol. 13; 13.no. 3 (1997), pages 26–35. DOI: 10.1109/57.591529. (Cited on pages 54, 73).
- [106] Hans Peter Moser. *Transformerboard*. Special print of Scientia Electrica; Translated by W. Heidemann, EHV-Weidmann Lim., St. Johnsbury, Vermont, U.S.A. 1979. 120 pages. (Cited on pages 13, 14, 16).
- [107] Hans Peter Moser and Vincenz Dahinden. *Transformerboard II: Properties and application of Transformerboard of different fibres*. 2nd edition. 1999. 222 pages. (Cited on pages 13, 82, 94).

- [108] Hans Peter Moser et al. "Static Electrification in power transformers". In: *3rd EPRI Workshop* (1992). (Cited on page 57).
- [109] Gerfrid Newesely. "Isolieröle". In: *WEIDMANN Seminar Transformatoren 2010* (2010). (Cited on pages 18, 20).
- [110] Nexans Deutschland GmbH. *Cables for High Voltage Underground Power Transmission*. Hannover, 2009. 12 pages. (Cited on page 8).
- [111] Nynas Naphtenics AB. *Nynas Nytro 10 XN Safety Data Sheet*. Stockholm, 2010. 5 pages. URL: [https://nyport.nynas.com/Apps/1112.nsf/wnsds/SE_EN_Nytro_10_XN/\\$File/Nytro_10_XN_SE_EN_SDS.pdf](https://nyport.nynas.com/Apps/1112.nsf/wnsds/SE_EN_Nytro_10_XN/$File/Nytro_10_XN_SE_EN_SDS.pdf). (Cited on pages 20, A.6).
- [112] Nynas Naphtenics AB. *Nynas Nytro 4000 X Safety Data Sheet*. Stockholm, 2010. 5 pages. URL: [https://nyport.nynas.com/Apps/1112.nsf/wnsds/SE_EN_Nytro_4000_X/\\$File/Nytro_4000_X_SE_EN_SDS.pdf](https://nyport.nynas.com/Apps/1112.nsf/wnsds/SE_EN_Nytro_4000_X/$File/Nytro_4000_X_SE_EN_SDS.pdf). (Cited on pages 20, A.6).
- [113] Nynas Naphtenics AB. *Transformatorenöl Handbuch*. Solna, Schweden, 2000. 70 pages. (Cited on pages 19, 20, 56).
- [114] E. Occhini and G. Maschio. "Electrical Characteristics of Oil-Impregnated Paper as Insulation for HV DC Cables". In: *Power Apparatus and Systems, IEEE Transactions on*, Vol. PAS-86; PAS-86.no. 3 (1967), pages 312–326. DOI: 10.1109/TPAS.1967.291959. (Cited on pages 9, 11, 43).
- [115] H. Ohno et al. "Construction of the world's first long-distance 500 kV XLPE cable line". In: *CIGRÉ Session 2000, Paper 21-106* (2000). (Cited on page 7).
- [116] S. Okabe, M. Kohtoh, and T. Amimoto. "Investigation of electrostatic charging mechanism in aged oil-immersed transformers". In: *Dielectrics and Electrical Insulation, IEEE Transactions on*, Vol. 17.no. 1 (2010), pages 287–293. DOI: 10.1109/TDEI.2010.5412029. (Cited on page 56).
- [117] John III Olmsted and Gregory M. Williams. *Chemistry - The molecular science*. 2nd edition. Wm. C. Brown Publishers, 1997. 1056 pages. ISBN: 0-8151-8450-6. (Cited on page 28).
- [118] Lars Onsager. "Deviations from Ohm's Law in Weak Electrolytes". In: *The Journal of chemical physics*, Vol. 2.no. 9 (1934), pages 599–615. DOI: 10.1063/1.1749541. URL: <http://dx.doi.org/10.1063/1.1749541>. (Cited on page 43).
- [119] T. V. Oommen. "Static electrification properties of transformer oil". In: *Electrical Insulation, IEEE Transactions on*, Vol. 23.no. 1 (1988), pages 123–128. DOI: 10.1109/14.2345. (Cited on pages 56, 98).
- [120] K. R. Padiyar. *HVDC Power Transmission Systems: Technology and System Interactions*. 2nd edition. 2009. 289 pages. ISBN: 978-81-224-0102-8. (Cited on pages 4–6).
- [121] Stanley H. Pine et al. *Organische Chemie*. 1st edition. Braunschweig: Vieweg, 1987. 1189 pages. ISBN: 3-528-08530-4. (Cited on page 16).
- [122] Ugo Piovan. "HVDC converter transformers: Polarity reversal impact on dielectric design". In: *IEEE/PES Transformers Committee, Fall 2004 Meeting, Technical presentation* (2004). (Cited on pages 6, 48).
- [123] Ugo Piovan and Guido Schenk. "Effects of variability of mineral oil electrical conductivity on reliability of HVDC converter transformers". In: *Trafotech, 8th International Conference* (2010). (Cited on page 11).

- [124] Gerhard Praxl and Gerhard Lemesch. "Measurement of ECT with the CIGRE test cell, Status Report". In: *CIGRÉ Study Committee SC12 Colloquium* (1993). (Cited on pages 12, 57).
- [125] T. O. Rouse. "Mineral insulating oil in transformers". In: *Electrical Insulation Magazine, IEEE*, Vol. 14.no. 3 (1998), pages 6–16. DOI: 10.1109/57.675572. (Cited on pages 19, 20).
- [126] W. W. Satterlee and R. D. Reed. "Controlled Temperature and Insulation Protection in the Operation Of Power Transformers". In: *American Institute of Electrical Engineers, Transactions of the*, Vol. 68.no. 1 (1949), pages 753–760. DOI: 10.1109/T-AIEE.1949.5060006. (Cited on pages 15, 24, 29).
- [127] Mario Schenk and Frank Trautmann. "HVDC Transformer Technology for Voltages >800 kV: Recent projects and future trends". In: *IEEE Transformer Committee, HVDC Converter Transformers and Smoothing Reactors Subcommittee - Toronto meeting (25.10.2010)* (2010). (Cited on page 3).
- [128] Werner F. Schmidt. "Electronic Conduction Processes in Dielectric Liquids". In: *Electrical Insulation, IEEE Transactions on*, Vol. EI-19.no. 5 (1984), pages 389–418. DOI: 10.1109/TEI.1984.298767. (Cited on page 42).
- [129] Tim Schnitzler et al. "Condenser controlled bushings for applications in Direct Voltages Systems (HVDC)". In: *Presentation at the ETG Fachtagung Isoliersysteme 2010* (2010). (Cited on page 7).
- [130] A. H. Sharbaugh, J. C. Devins, and S. J. Rzad. "Progress in the Field of Electric Breakdown in Dielectric Liquids". In: *Electrical Insulation, IEEE Transactions on*, Vol. EI-13.no. 4 (1978), pages 249–276. DOI: 10.1109/TEI.1978.298076. (Cited on page 70).
- [131] Amir Abbas Shayegani et al. "PDC measurement evaluation on oil-pressboard samples". In: *Solid Dielectrics, 2004. ICSD 2004. Proceedings of the 2004 IEEE International Conference on. Solid Dielectrics, 2004. ICSD 2004. Proceedings of the 2004 IEEE International Conference on. Volume 1. 2004, 51–54 Vol.1.* (Cited on page 51).
- [132] Shell UK Products Ltd. *Safety Data Sheet: Shell Diala Oil GX*. 2005. 8 pages. URL: [https://nyport.nynas.com/Apps/1112.nsf/wnsds/SE_EN_Nytro_4000_X/\\$File/Nytro_4000_X_SE_EN_SDS.pdf](https://nyport.nynas.com/Apps/1112.nsf/wnsds/SE_EN_Nytro_4000_X/$File/Nytro_4000_X_SE_EN_SDS.pdf); . (Cited on page 20).
- [133] Mohammad Mahdi Saei Shirazi, Hossein Borsi, and Ernst Gockenbach. "Influence of ionic impurity on loss factor, permittivity and breakdown voltage of cellulosic insulation paper". In: 16th International Symposium on High Voltage Engineering (ISH), Paper C-53. Capetown, South Africa, 2009, pages 803–806. ISBN: 978-0-620-44584-9. (Cited on page 59).
- [134] John Shrimpton. *Charge Injection Systems - Physical principles, Experimental and Theoretical Work*. 1st edition. Springer-Verlag Berlin Heidelberg, 2009. 196 pages. ISBN: 978-3-642-00293-9. DOI: 10.1007/978-3-642-00294-6. (Cited on pages 34, 36–38, 41, 42, 53).
- [135] D. H. Shroff and A. W. Stannett. "A review of paper aging in power transformers". In: *Generation, Transmission and Distribution, IEE Proceedings*, Vol. 132.no. 6 (1985), pages 312–319. DOI: 10.1049/ip-c:19850052. (Cited on pages 24, 29).

- [136] Siemens AG PTD High Voltage Division. *High Voltage Direct Current Transmission - Proven Technology for Power Exchange*. Order No. E5001-U131-A92-V2-7600, 2003. 48 pages. URL: <http://www.siemens.com/hvdc>. (Cited on page 4).
- [137] A. Sierota, R. G. Heydon, and J. Rungis. *Diagnosis of transformer oils by the measurement of their electrostatic charging tendency*. English. 1994. (Cited on pages 98, E.1).
- [138] Jan Erik Skog and Nils Henrik Jendal. "NorNed kabel HVDC Project". In: *NorNed Seminar 2006 - Statnett SF Presentation (6. December 2006) in Oslo* (2006). (Cited on page 24).
- [139] A. W. Stannett. "The conductivity of hydrocarbon transformer oil containing water and solid conducting particles". In: *British Journal of Applied Physics*, Vol. 2.no. 4 (1951), page 110. DOI: doi:10.1088/0508-3443/2/4/304. (Cited on pages 42, 46, 47, 109).
- [140] T. Takada et al. "Comparison between the PEA method and the PWP method for space charge measurement in solid dielectrics". In: *Dielectrics and Electrical Insulation, IEEE Transactions on*, Vol. 5.no. 6 (1998), pages 944–951. DOI: 10.1109/94.740780. (Cited on page 54).
- [141] Tatsuo Takada. "Acoustic and optical methods for measuring electric charge distributions in dielectrics". In: *Dielectrics and Electrical Insulation, IEEE Transactions on*, Vol. 6.no. 5 (1999), pages 519–547. DOI: 10.1109/94.798112. (Cited on page 54).
- [142] R. Tobazeon, J. C. Filippini, and C. Marteau. "On the measurement of the conductivity of highly insulating liquids". In: *Dielectrics and Electrical Insulation, IEEE Transactions on*, Vol. 1 (1994), pages 1000–1004. DOI: 10.1109/94.368663. (Cited on page 41).
- [143] Daniel Tschudi and Peter Heinzig. "State of the art solid insulation after 125 years of transformer practice". In: *International Colloquium Transformer Research and Asset Management* (2009). (Cited on pages 9, 14).
- [144] S. Tsukao et al. "Increase of Static Electrification in Aged Transformers". In: *Power Engineering Society General Meeting, 2007. IEEE* (2007), pages 1–5. DOI: 10.1109/PES.2007.386077. (Cited on pages 11, 56–58).
- [145] VDEW - Vereinigung Deutscher Elektrizitätswerke. *Ölbuch Teil 2: Isolierflüssigkeiten*. 6th edition. 1983. ISBN: 3-8022-0063-2. (Cited on pages 27, 95).
- [146] Verband der Elektrotechnik, Elektronik und Informationstechnik. *VDE 0303-21: Elektrische Durchschlagsfestigkeit von isolierenden Werkstoffen (IEC 60243-1:1998)*. Berlin, 1999. 21 pages. (Cited on page 94).
- [147] Verband der Elektrotechnik, Elektronik und Informationstechnik. *VDE 0303-23: Elektrische Durchschlagsfestigkeit von isolierenden Werkstoffen - Prüfverfahren (IEC 60243-3:2001)*. Berlin, 2002. 8 pages. (Cited on pages 93, 94, D.1).
- [148] Verband der Elektrotechnik, Elektronik und Informationstechnik. *VDE 0303-30: Prüfverfahren für Elektroisierstoffe: Spezifischer Durchgangswiderstand und spezifischer Oberflächenwiderstand von festen, elektrisch isolierenden Werkstoffen (IEC 93:1980)*. Berlin, 1993. 16 pages. (Cited on pages 11, 49, 70, 84).
- [149] Verband der Elektrotechnik, Elektronik und Informationstechnik. *VDE 0303-3/05-83: Prüfung von Werkstoffen für die Elektrotechnik: Messung des elektrischen Widerstandes von nichtmetalenen Werkstoffen (Zurückgezogen 1993-12)*. Berlin, 1983. 29 pages. (Cited on page 76).

- [150] Verband der Elektrotechnik, Elektronik und Informationstechnik. *VDE 0311-20: Zellulosepapiere für elektrotechnische Anwendungen - Teil 2: Prüfverfahren (IEC 60554-2:2001)*. Berlin, 2002. 33 pages. (Cited on page 60).
- [151] Verband der Elektrotechnik, Elektronik und Informationstechnik. *VDE 0315-2: Tafel- und Rollenpressspan für elektrotechnische Anwendungen - Teil 2: Prüfverfahren (IEC 60641-2:2004)*. Berlin, 2005. 27 pages. (Cited on page A.1).
- [152] Verband der Elektrotechnik, Elektronik und Informationstechnik. *VDE 0315-3-1: Tafel- und Rollenpressspan für elektrotechnische Anwendungen - Teil 3: Bestimmungen für einzelne Werkstoffe - Blatt 1: Anforderungen für Tafelpressspan, Typen B.0.1, B.0.3, B.2.1, B.2.3, B.3.1, B.4.1, B.4.3, B.5.1, B.5.3 und B.6.1*. Berlin, 2009. 11 pages. (Cited on pages IV, 17).
- [153] Verband der Elektrotechnik, Elektronik und Informationstechnik. *VDE 0370-16: Bestimmung des Permittivitäts-Verlustfaktors durch Messung der Konduktanz und Kapazität*. Berlin, 1999. 19 pages. (Cited on page 50).
- [154] Verband der Elektrotechnik, Elektronik und Informationstechnik. *VDE 0370-2: Richtlinie zur Überwachung und Wartung von Isolierölen auf Mineralölbasis in elektrischen Betriebsmitteln (DIN IEC 60422)*. Berlin, 2007. 48 pages. (Cited on pages 18, 24, A.2, E.1).
- [155] Verband der Elektrotechnik, Elektronik und Informationstechnik. *VDE 0370-20: Isolierflüssigkeiten - Ölimprägniertes Papier und ölimprägnierter Preßspan - Bestimmung von Wasser mit automatischer Karl-Fischer-Titration*. Berlin, 1999. 19 pages. (Cited on pages D.2, E.2).
- [156] Verband der Elektrotechnik, Elektronik und Informationstechnik. *VDE 0370-5: Bestimmung der Durchschlagspannung bei Netzfrequenz - Prüfverfahren*. Berlin, 1996. 10 pages. (Cited on page 18).
- [157] Verband der Elektrotechnik, Elektronik und Informationstechnik. *VDE 0380-2: Isolierflüssigkeiten - Messung der Permittivitätszahl, des dielektrischen Verlustfaktors ($\tan d$) und des spezifischen Gleichstromwiderstandes (IEC 60247:2004)*. Berlin, 2005. 25 pages. (Cited on pages 50, 51, 70, E.1).
- [158] Verband der Elektrotechnik, Elektronik und Informationstechnik. *VDE 0532-76-7: Leistungstransformatoren Teil 7: Leitfaden für die Belastung von ölgefüllten Leistungstransformatoren*. Berlin, 2008. 55 pages. (Cited on pages 17, 29).
- [159] Shiqiang Wang et al. "Research on Aging Characteristics of Oil Impregnated Pressboard under Combined Thermal and Electrical Stresses". In: *Condition Monitoring and Diagnosis, 2010. CMD 2010. International Conference on* (2010). (Cited on page 93).
- [160] John B. Whitehead. *Impregnated Paper Insulation: The Inherent Electrical Properties*. Volume 4. Monographs of the National Research Council, Committee on Electrical Insulation. New York: John Wiley & Sons, Inc., 1935. 221 pages. (Cited on pages 13, 14, 20, 41, 42, 61, 109).
- [161] A. C. M. Wilson. *Insulating liquids: their uses, manufacture and properties*. Stevenage: Peter Peregrinus Ltd. on behalf of the Institution of Electrical Engineers, 1980. 221 pages. ISBN: 0-906048-23-0. (Cited on pages 19, 20).

- [162] Endah Yulastuti. "Analysis of Dielectric Properties Comparison between Mineral Oil and Synthetic Ester Oil". Master Thesis. Delft: TU Delft, 2010. 72 pages. (Cited on pages 96, 97).
- [163] W. S. Zaengl. "Applications of dielectric spectroscopy in time and frequency domain for HV power equipment". In: *Electrical Insulation Magazine, IEEE*, Vol. 19.no. 6 (2003), pages 9–22. DOI: 10.1109/MEI.2003.1266348. (Cited on page 34).
- [164] Andreas Zlodnjak. "Untersuchung der elektrostatischen Aufladungsneigung von Isolierölen und Pressspan mittels Spinning-Disc-Anordnung". Diplomarbeit. Graz: TU Graz, 2012. (Cited on pages 12, 73, 97).
- [165] C. Zou et al. "The influence of water on dielectric behavior of silica-filled epoxy nanocomposites and percolation phenomenon". In: *Electrical Insulation and Dielectric Phenomena, 2007. CEIDP 2007. Annual Report - Conference on*. Electrical Insulation and Dielectric Phenomena, 2007. CEIDP 2007. Annual Report - Conference on. 2007, pages 372–375. DOI: 10.1109/CEIDP.2007.4451502. (Cited on page 76).

Appendices

List of appendices:

- A. Investigated materials and their preparation
- B. Ageing vessels for thermal ageing
- C. Ageing vessels for combined ageing
- D. Ageing diagnosis: Pressboard
- E. Ageing diagnosis: Oil
- F. Summarized list of equipment and materials used

A Investigated materials and their preparation

Before cellulosic and oil samples could be used, they had to be impregnated and dried respectively. This has been done manually at Graz University of Technology for all samples within this work with a set-up that is pictured in Figure A.1.

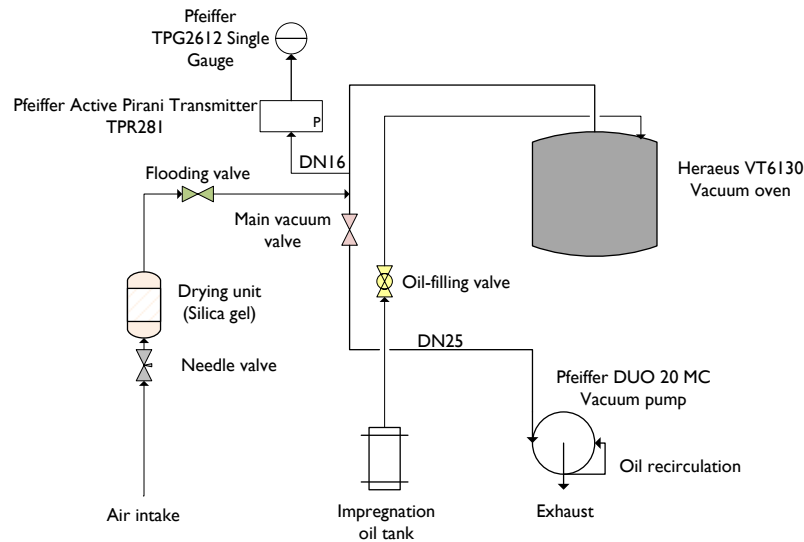


Figure A.1: Schematics of vacuum processing equipment for sample preparation

A.1 Pressboard preparation

All pressboard samples (and also the K-Buff paper samples) have been prepared according to the following procedure. The time durations are median values of all impregnation cycles (23 in total):

1. Drying of samples at 105°C for at least 48 hours in a (forced convection)¹ thermal oven (average value: 55,83 h).
2. Application of vacuum (< 1 mbar) for at least 24 hours at 105° C (average value: 36,42 h)
3. Reduction of temperature to 90°C
4. Impregnation process: Filling of the sample holders with reprocessed mineral oil. Samples are kept under vacuum at 90°C for at least 24 hours (average value: 33,46 h).
5. Breaching of vacuum through a drying unit. Rest period of typically 24 hours.
6. Removing of samples and immediate use or shrink-wrap in gas tight foil

Moisture levels of $\leq 0,3\%$ for the unaged cellulose have been achieved with this method. In IEC 60641-2 (VDE 0315-2 [151]), the pressure during drying needs to be <1 kPa (10 mbar). During impregnation with preheated oil (70 to 90°C), the pressure needs to be <1,5 kPa (=15 mbar).

A.2 Mineral oils and their preparation

Before using mineral oil samples, they have been reprocessed according the following procedure:

¹if available

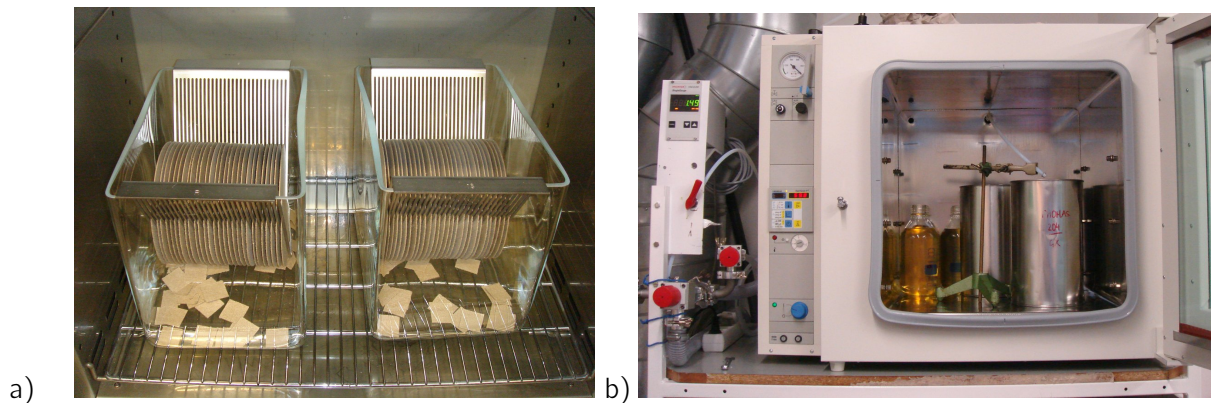


Figure A.2: Impregnation process: a) Pressboard samples during drying cycle; b) Oil drying in vacuum oven

1. Oil for ageing samples: Bubbling dry nitrogen through the oil vessel (at room temperature) for at least 1 hour
2. Drying of the oil in a vacuum oven for at least 24h at 60°C at a vacuum of <1 mbar (typically <0,3 mbar)
3. Breaching of vacuum removing of oil and immediate use or storage in gas-tight aluminium containers

Care has to be taken when using the terms **reclamation** and **reprocessing**. The former is used to describe the elimination of (soluble and insoluble) polar contaminants in the insulation oil by using physical and chemical processes. The latter describes a physical process only, in which water and solid particles are removed (see IEC 60422 or VDE 0370-2 [154]). Here, only reprocessing could be conducted: Vacuum drying and (mechanical) filtering.

Material datasheet: Nynas Nytro 4000X²PRODUCT DATA SHEET
Nytro 4000X

PROPERTY	UNIT	TEST METHOD IEC	GUARANTEED DATA		TYPICAL DATA
			MIN	MAX	
Physical					
Appearance		IEC 60296	Clear, free from sediment		complies
Density, 20°C	kg/dm ³	ISO 12185		0,895	0,872
Viscosity, 40°C	mm ² /s	ISO 3104		12,0	9,2
Viscosity, -30°C	mm ² /s	ISO 3104		1800	850
Pour point	°C	ISO 3016		-40	-60
Chemical					
Acidity	mg KOH/g	IEC 62021		0,01	<0,01
Corrosive sulphur		DIN 51353	non-corrosive		non-corrosive
Corrosive sulphur		ASTM D 1275 B	non-corrosive		non-corrosive
Corrosive sulphur		IEC 62535	non-corrosive		non-corrosive
Sulphur content	%	ISO 14596		0,15	0,01
Aromatic content	%	IEC 60590			4
Antioxidant, phenols	Wt %	IEC 60666	0,08	0,40	0,38
Water content	mg/kg	IEC 60814		30	<20
Furfural content	mg/kg	IEC 61198		0,1	<0,1
Electrical					
Dielectric dissipation factor (DDF) at 90°C		IEC 60247		0,005	<0,001
Interfacial tension	mN/m	ISO 6295	40		52
Breakdown voltage					
- Before treatment	kV	IEC 60156	30		40-60
- After treatment	kV		70		>70
Oxidation stability					
At 120°C, 500 h		IEC 61125 C			
Total acidity	mg KOH/g			0,30	<0,01
Sludge	Wt %			0,05	<0,01
DDF/90°C				0,050	<0,010
Health, safety and environment					
Flash point, PM	°C	ISO 2719	135		148
DMSO extractable compounds	Wt %	IP 346		3	<3
PCB		IEC 61619	not detectable		not detectable

Nytro 4000X is an inhibited insulating oil with extremely good electrical and excellent ageing properties meeting IEC 60296 (03), special applications.

Severely Hydrotreated Insulating Oil
Issuing date: 2008-03-28



²This data sheet is part of the document available at [https://nyport.nynas.com/Apps/1112.nsf/wnpds/Nytro_4000X_IEC/\\$File/PDS_Nytro_4000X_EN.pdf](https://nyport.nynas.com/Apps/1112.nsf/wnpds/Nytro_4000X_IEC/$File/PDS_Nytro_4000X_EN.pdf), checked at 29.06.2011

Material datasheet: Shell Diala GX³

Technical Data Sheet

- **Low water content of delivered oil**

Diala GX is available in drums (and in restricted regions in bulk) as "Shell Diala GX dried", specially handled to retain a high breakdown voltage as delivered. This enables the product to be used in many applications without further treatment.

Typical Physical Characteristics

Property	Units	Method	IEC 60296 Requirement	Shell Diala GX
Appearance		IEC 60296	Clear, free from sediment and suspended matters	Complies
Density at 20 °C	kg/m ³	ISO 3675	Max. 895	886
Kinematic viscosity at 40 °C	mm ² /s	ISO 3104	Max. 12	8,0
Kinematic viscosity at -30 °C	mm ² /s	ISO 3104	Max. 1.800	1.100
Flashpoint P.M.	°C	ISO 2719	Min. 135	136
Pourpoint	°C	ISO 3016	Max. -40	-57
Neutralisation value	mg KOH/g	IEC 62021-1	Max. 0,01	< 0,01
Corrosive Sulphur		DIN 51353	Not corrosive	Not corrosive
Corrosive Sulphur		IEC 62535	-	Not corrosive
Corrosive Sulphur		ASTM D 1275 B	-	Not corrosive
Breakdown voltage Untreated After treatment	kV	IEC 60156	Min. 30 Min. 70	>30 >70
Dielectric Dissipation Factor (DDF) at 90 °C		IEC 60247	Max. 0,005	0,002
Gassing	mm ³ /min	IEC 60628 A	-	-14
Oxidation Stability (500 h /120 °C)		IEC 61125 C		
Total acidity	mg KOH/g		Max. 1,2	1,0
Sludge	%m		Max. 0,8	0,45
DDF at 90 °C		IEC 60247	Max. 0,5	0,12
Oxidation Stability Baader (28 d /110 °C)		DIN 51554	-	
Neutralisation value	mg KOH/g			0,1
Sludge content	%m			0,01
DDF at 90 °C				0,01

These characteristics are typical of current production.

Whilst future production will conform to Shell's specification, variations in these characteristics may occur.

³This data sheet is part of the document available at http://www.epc.shell.com/Docs/GPCDOC_X_cbe_24855_key_140002725133_3371.pdf, checked at 29.06.2011

Material datasheet: Nynas Nytro 10XN⁴PRODUCT DATA SHEET
Nytro 10XN

PROPERTY	UNIT	TEST METHOD IEC	GUARANTEED DATA		TYPICAL DATA
			MIN	MAX	
Physical					
Appearance		IEC 60296	Clear, free from sediment		complies
Density, 20°C	kg/dm ³	ISO 12185		0,895	0,877
Viscosity, 40°C	mm ² /s	ISO 3104		8,0	7,6
Viscosity, -30°C	mm ² /s	ISO 3104		800	730
Pour point	°C	ISO 3016		-45	-63
Chemical					
Acidity	mg KOH/g	IEC 62021		0,01	<0,01
Corrosive sulphur		DIN 51353	non-corrosive		non-corrosive
Corrosive sulphur		ASTM D 1275 B	non-corrosive		non-corrosive
Corrosive sulphur		IEC 62535	non-corrosive		non-corrosive
Sulphur content	%	ISO 14596		0,15	<0,01
Aromatic content	%	IEC 60590			7
Antioxidant, phenols	Wt %	IEC 60666		0,4	0,3
Water content	mg/kg	IEC 60814		30	<20
Furfural content	mg/kg	IEC 61198		0,1	<0,1
Electrical					
Dielectric dissipation factor (DDF) at 90°C		IEC 60247		0,005	<0,001
Interfacial tension	mN/m	ISO 6295	40		49
Breakdown voltage					
- Before treatment	kV	IEC 60156	30		40-60
- After treatment	kV		70		>70
Oxidation stability					
At 120°C, 500 h		IEC 61125 C			
Total acidity	mg KOH/g			0,30	0,04
Sludge	Wt %			0,05	<0,02
DDF/90°C				0,050	0,03
Health, safety and environment					
Flash point, PM	°C	ISO 2719	140		144
DMSO extractable compounds	Wt %	IP 346		3	<3
PCB		IEC 61619	not detectable		not detectable

Nytro 10XN is an inhibited insulating oil with extremely good electrical and low temperature properties and excellent ageing properties. This product meets IEC 60296 (03), special applications and ASTM D3487 type II (excluding gassing tendency).

Severely Hydrotreated Insulating Oil
Issuing date: 2008-03-28



⁴This data sheet is part of the document available at [https://nyport.nynas.com/Apps/1112.nsf/wnpds/Nytro_10XN_IEC/\\$File/PDS_Nytro_10XN_EN.pdf](https://nyport.nynas.com/Apps/1112.nsf/wnpds/Nytro_10XN_IEC/$File/PDS_Nytro_10XN_EN.pdf), checked at 29.06.2011

Oil composition

The oil composition has been taken from the according oil data and safety data sheets.

Table A.1: Composition of Nynas Nytro 4000 X[112]

Chemical Name	CAS#	EC#	Weight-%
Hydrotreated Light Naphthenic Distillate	64742-53-6	265-156-6	70 - 90%
Lubricating oils, petroleum, C20-50, hydrotreated neutral oil-based	72623-87-1	276-738-4	10 - 30%
2,6-ditertiary Butyl-4-Methyl Phenol	128-37-0	204-881-4	<0,4%

Table A.2: Composition of Shell Diala GX⁵

Chemical Name	CAS#	EC#	Weight-%
Highly refined mineral oil	-	-	60 - 100%
Naphtenic solvent (petroleum), heavy aromatic; Kerosene - unspecified	64742-94-5	265-198-5	0,1 - 1%
Other additives	-	-	0 - 1%

Table A.3: Composition of Nynas Nytro 10 XN[111]

Chemical Name	CAS#	EC#	Weight-%
Distillates (petroleum), hydrotreated light naphthenic	64742-53-6	265-156-6	>99%
2,6-di-tert-butyl-p-cresol	128-37-0	204-881-4	<0,3%

A.3 Steel and copper stripes

Both steel and copper stripes have been carefully cleaned before their usage in the ageing tests. They have been immersed in 2-Propanol and wiped dry afterwards. Before putting the stripes into the ageing vessels, they have been dried in thermal ovens at 115° C for at least 6 hours.

A.4 Sample filling

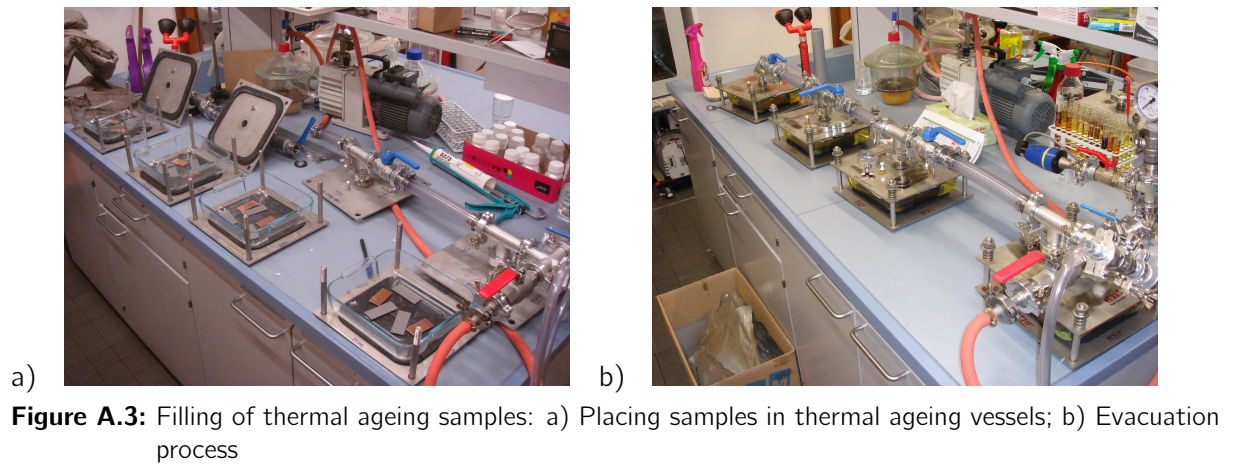
Dried and impregnated pressboard samples are placed in glass vessels with dry oil and steel and copper stripes. Prepared vessels are shown in the figure below. After putting the pressboard samples, spacers and mineral oil into the vessel, the vessel was closed immediately. Also, the seal was glued onto the glass vessel and the steel cover.

After a setting time of >24 hours, the vessels are evacuated to < 1 mbar and then filled with dried nitrogen (+0,3bar). This is just enough to leave nitrogen in when putting a cover on the vacuum flange. When this procedure is finished the samples are ready for the thermal ageing process.

Sample conditioning after ageing

After removing the (thermal) ageing vessels from the artificial ageing process, they have been kept in an oven at 90°C for at least 24h. The time should be sufficient to achieve a moisture equilibrium between oil and cellulose [17]. After this waiting period, the ageing vessel was opened and oil and cellulose have

⁵This information was found in the Norwegian version of the Safety Data Sheet ("VERNEBLAD"), available online at <http://logichem.netpower.no/verneblad.aspx?iId=10688>, accessed 31.07.2011



been separated. It is important to do this task identically for the whole ageing sample range - Different temperatures can lead to a changed moisture distribution between oil and cellulose.

B Ageing vessels for thermal ageing

Standard PYREX laboratory glass dishes made from borosilicate glass are used as vessels for the thermal ageing tests. These vessels can withstand temperatures up to 150°C constantly and up to 500°C for short term stress according to manufacturer's specification. The glass dish is furthermore covered with a stainless steel (1.4301) plate. A FKM (Viton®) sealing, which is additionally secured with an adhesive, is used to seal the gap between the glass dish and the cover plate. Figure B.3 b) shows a complete vessel with mounted temperature sensor.

This design has three main advantages:

1. Large samples (diameter of >140 mm) can be accommodated
2. Transparent vessel: Ageing process can be constantly visually "monitored"
3. Reduced cost when compared to other solutions (like complete stainless steel vessels)

The complete vessel consists of the following parts:

1. Glass dish (Pyrex; borosilicate glass)
2. Sealing (FKM)
3. Bottom and cover plate (stainless steel, 1.4301)
4. Screw connection with springs (stainless steel, 1.4301)
5. Connection for temperature sensor (stainless steel, 1.4301 with PTFE sealing)
6. Small-flange (DN25) as access bore (stainless steel, 1.4301 with FKM sealing)



- Type: Pyrex 1490/04
- Volume: . . . 2000 ml
- Length: 200 mm
- Width: 210 mm
- Height: 60 mm

Figure B.1: Pyrex 1490 dish (Image supplied by manufacturer)

The dimensions of the dish are approximate and differ slightly from batch to batch. The frame of the dish was also not perfectly suited for a sealing surface in factory condition. Several tests and preliminary investigations had to be carried out until a suitable solution was found: First, the glass was grinded (see Figure B.2) and a Viton sealing was glued (silicone adhesive) onto the dish. Glue was also applied between sealing and stainless steel cover. So a secure sealing (tightness) could be achieved in the (absolute) pressure range between < 1 mbar and 1,5 bar.

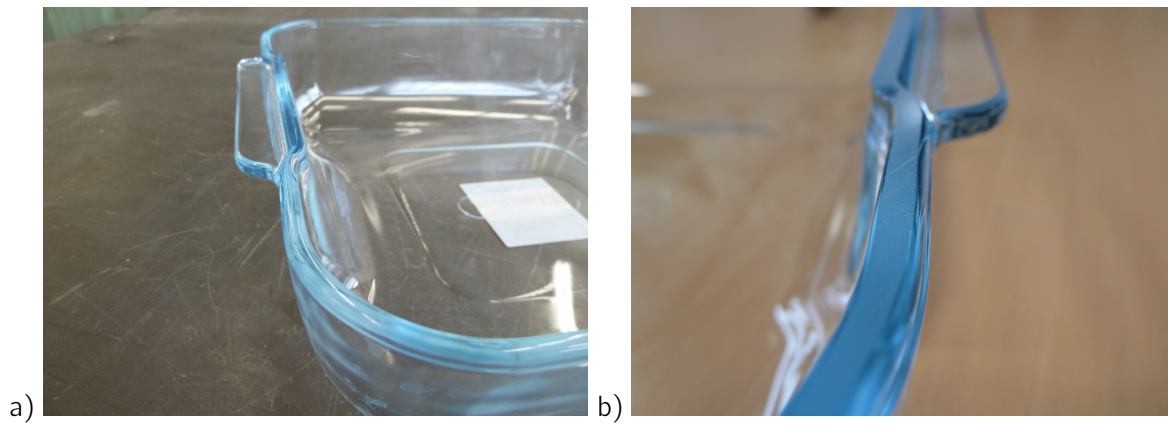


Figure B.2: a) Original Pyrex Dish b) Grinded sealing surface

A temperature monitoring system was also developed to monitor the ageing vessels and samples respectively throughout the ageing process. This was achieved with a customized 30 channel Pt100 system with PTFE insulated temperature sensors. Temperature values have been sampled every second and transferred into a MySQL database via LAN connection.

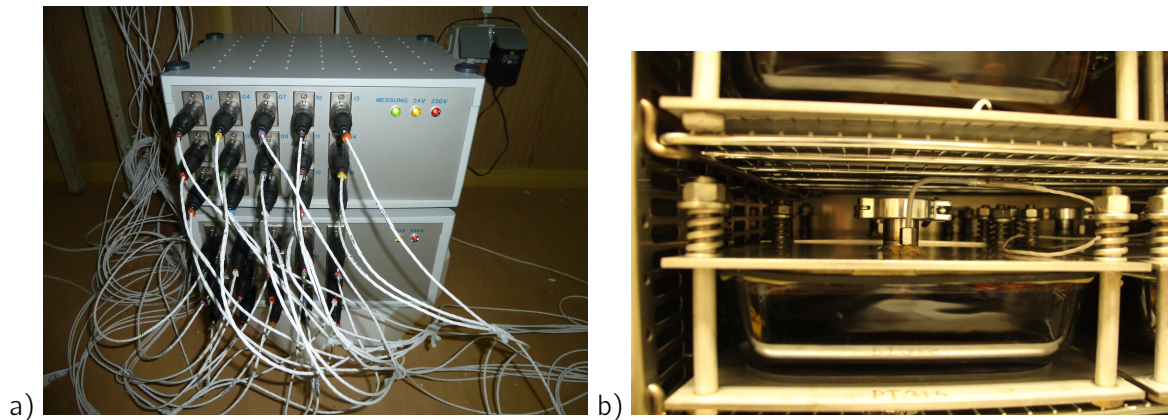
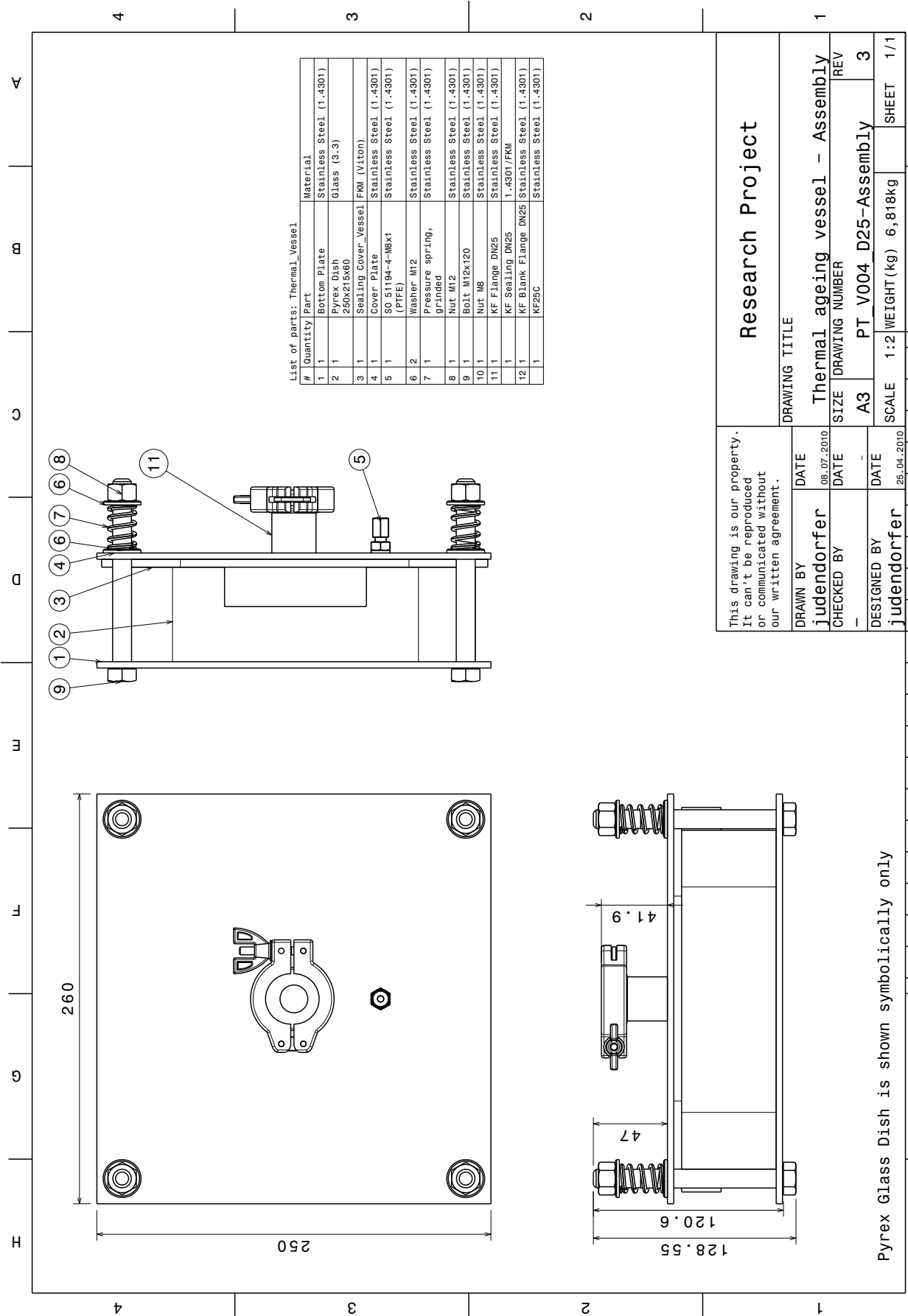


Figure B.3: Temperature monitoring system for thermal ageing samples: a) Signal acquisition units and data logger b) sensor mounted in thermal ageing vessel



List of parts: Thermal_Vessel

#	Quantity	Part	Material
1	1	Bottom Plate	Stainless Steel (1.4301)
2	1	Pyrex Dish 250x215x60	Glass (3.3)
3	1	Sealing Cover_Vessel	FKM (Viton)
4	1	Cover Plate	Stainless Steel (1.4301)
5	1	SO 51194-4-M8x1 (PIPE)	Stainless Steel (1.4301)
6	2	Washer M12	Stainless Steel (1.4301)
7	1	Pressure spring, grinded	Stainless Steel (1.4301)
8	1	Nut M12	Stainless Steel (1.4301)
9	1	Bolt M12x120	Stainless Steel (1.4301)
10	1	Nut M8	Stainless Steel (1.4301)
11	1	KF Flange DN25	Stainless Steel (1.4301)
		KF Sealing DN25	1.4301/FKM
12	1	KF Blank Flange DN25	Stainless Steel (1.4301)
		KF25C	Stainless Steel (1.4301)

This drawing is our property. It can't be reproduced or communicated without our written agreement.

Research Project

DRAWING TITLE

Thermal ageing vessel - Assembly

DRAWN BY: judendorfer DATE: 08.07.2010
 CHECKED BY: DATE: -
 DESIGNED BY: judendorfer DATE: 25.04.2010

SIZE: A3 DRAWING NUMBER: PT V004 D25-Assembly REV: 3
 SCALE: 1:2 WEIGHT(kg): 6,818kg SHEET: 1/1

Pyrex Glass Dish is shown symbolically only

C Ageing vessels for combined ageing

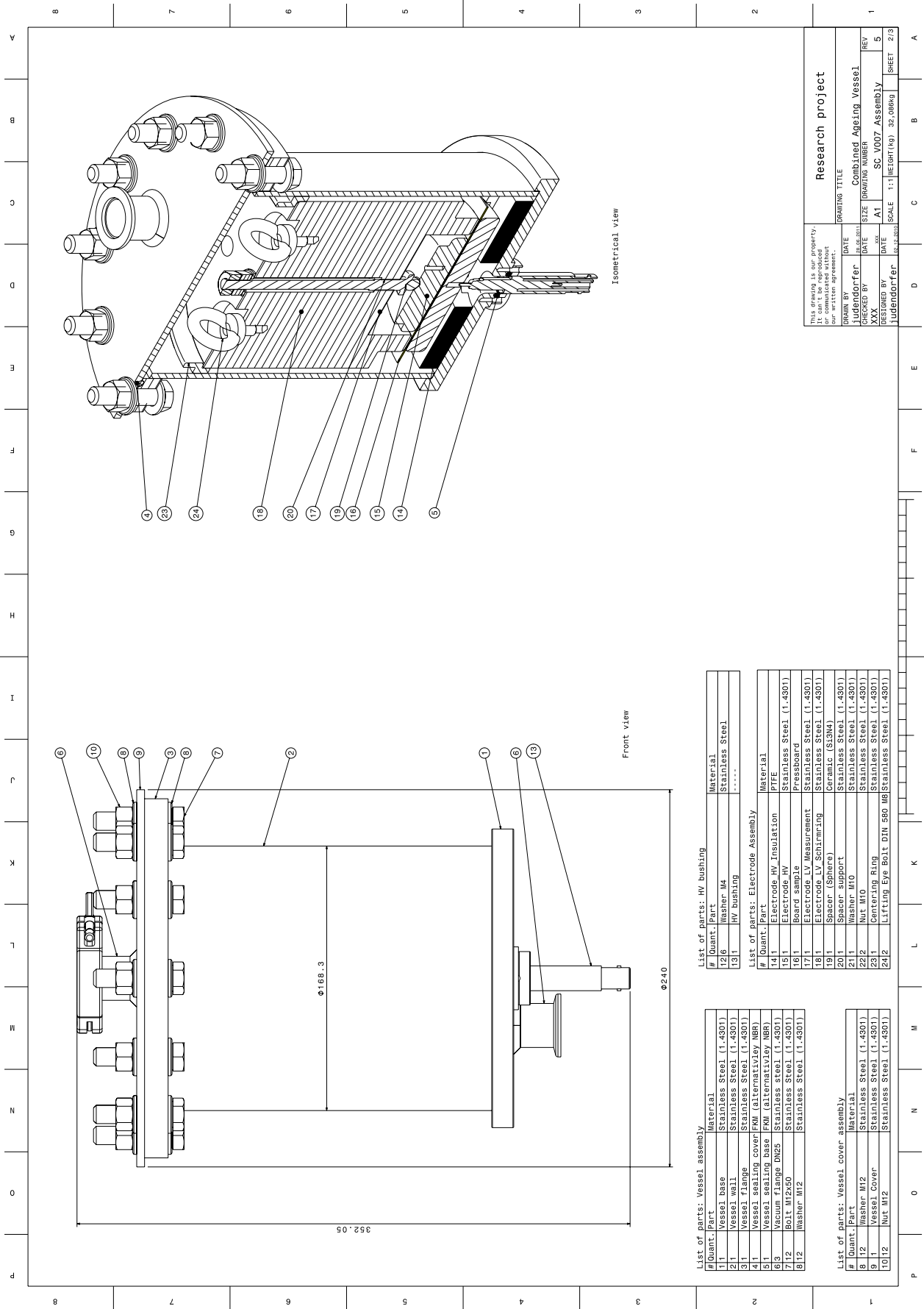
Customized test vessels have been designed and constructed to allow a (combined) ageing and the determination of electrical conductivity of pressboard sample in the same vessel without the need to open it. Most of the components have been made from stainless steel (1.4301). The only exceptions are the HV insulation ring, which is made from PTFE, sealing (Viton), insulation spacer (ceramic sphere) and the HV bushing, which has a ceramic inlay. All components can withstand temperatures of at least 135°C constantly.

Temperature resistant PTFE (measurement cabling) and silicone (HV cabling) cables have been utilized. A ceramic sphere (“#19”) is used to insulate the measurement electrode (“#17”) from the grounded weight (“#18”).

Main dimensions of the test vessel are as follows:

- Measurement electrode, outer diameter $\varnothing = 84$ mm
- Guard electrode, inner diameter $\varnothing_i = 90$ mm
- Electrode gap $g = 3$ mm
- Measurement electrode, weight $m_{ME} = 0,755$ kg
- Guard electrode, weight $m_{GE} = 17,669$ kg

An assembly drawing and a list of parts is shown at the following page.



This drawing is our property. It can't be reproduced without our written agreement.		DRAWING TITLE	
DRAWN BY	DATE	DATE	DATE
XXX	10.06.2011	10.06.2011	10.06.2011
CHECKED BY	SIZE	SCALE	REV
Judendorfer	A1	1:1	5
Judendorfer	SC_V007	ASSEMBLY	SHEET
	1:1	WEIGHT(kg)	2/3

List of parts: HV bushing

#	Quant.	Part	Material
12	6	Washer M4	Stainless Steel
13	1	HV bushing	-----

List of parts: Electrode Assembly

#	Quant.	Part	Material
14	1	Electrode HV Insulation	PIFE
15	1	Electrode HV	Stainless Steel (1.4301)
16	1	Board sample	Pressboard
17	1	Electrode LV Measurement	Stainless Steel (1.4301)
18	1	Electrode LV Schirmring	Stainless Steel (1.4301)
19	1	Spacer (Sphere)	Ceramic (Si3N4)
20	1	Spacer support	Stainless Steel (1.4301)
21	1	Washer M10	Stainless Steel (1.4301)
22	1	Nut M10	Stainless Steel (1.4301)
23	1	Centering Ring	Stainless Steel (1.4301)
24	1	Lifting Eye Bolt DIN 560 M6	Stainless Steel (1.4301)

List of parts: Vessel assembly

#	Quant.	Part	Material
1	1	Vessel base	Stainless Steel (1.4301)
2	1	Vessel wall	Stainless Steel (1.4301)
3	1	Vessel flange	Stainless Steel (1.4301)
4	1	Vessel sealing cover	Stainless Steel (1.4301)
5	1	Vessel sealing cover	Stainless Steel (1.4301)
6	1	Vacuum flange DN25	Stainless Steel (1.4301)
7	1	Bolt M12x50	Stainless Steel (1.4301)
8	1	Washer M12	Stainless Steel (1.4301)

List of parts: Vessel cover assembly

#	Quant.	Part	Material
8	1	Washer M12	Stainless Steel (1.4301)
9	1	Vessel cover	Stainless Steel (1.4301)
10	1	Nut M12	Stainless Steel (1.4301)

D Ageing diagnosis: Pressboard

The methods and processes used for sample taking and ageing diagnosis within this work are documented in this appendix. Generally, all processes are following current standards (IEC, VDE), but in several cases they have been adopted to specific needs. Pressboard samples have been kept either in vacuum (new samples) or sealed in aluminium foil (Climafoil; for new and aged samples) to keep their moisture levels.

D.1 Degree of polymerisation (DP)

The degree of polymerisation (DP) is one of the most important material properties to assess the ageing of cellulose and pressboard respectively. As already described in Chapter 3, the DP can be directly linked to mechanical strength, which is very important for the integrity of the insulation system.

Sufficient mechanical strength⁶ is necessary to keep the insulation system intact and enables it to withstand operational and failure conditions (e.g. short-circuits).

It is more convenient to determine the degree of polymerisation than mechanical strength, especially for samples taken from aged transformers [17]. This is possible because both quantities can be related to each other. Nevertheless, the determination of the degree of polymerisation (DP) is not an easy task and takes several hours to complete. Furthermore, there are different methods to actually determine the degree of polymerisation from viscosity measurements [48].

All DP values have been determined by WEIDMANN Electrical Technology AG according to IEC 60450. Each sample has been measured twice and the mean was determined.

D.2 Dielectric parameters

The dielectric loss factor ($\tan(\delta)$) and the relative permittivity ϵ_r have been determined for unaged pressboard and paper samples. Electrode set-ups (stainless steel) in the style of IEC 60093 have been used. A weight of 17 kg was used for all measurements. The measurement set-up itself consisted of a Tettex 2904 set-up with a digital bridge-vector set-up (LDIC LDV-6). Measurements have been made at a voltage of $U = 1$ kV (AC).

D.3 Impulse strength

The impulse voltage strength of pressboard samples has been determined in the style of IEC 60243-3 (VDE 0303-23 [147]). The major divergence from that procedure used here was the fact that only one voltage application (lightning impulse voltage with $1,2/50\mu\text{s}$) per stage/level was conducted. This was mainly due to experimental-economical reasons (equipment availability). An oil-filled⁷ plexiglass test vessel was used with brass electrodes according to IEC 60243-3 (75/25 mm). The test set-up is pictured in Figure D.1 below.

⁶In most cases, the tensile strength is meant in this respect

⁷Nynas Nytro 4000X, moisture content <5 ppm

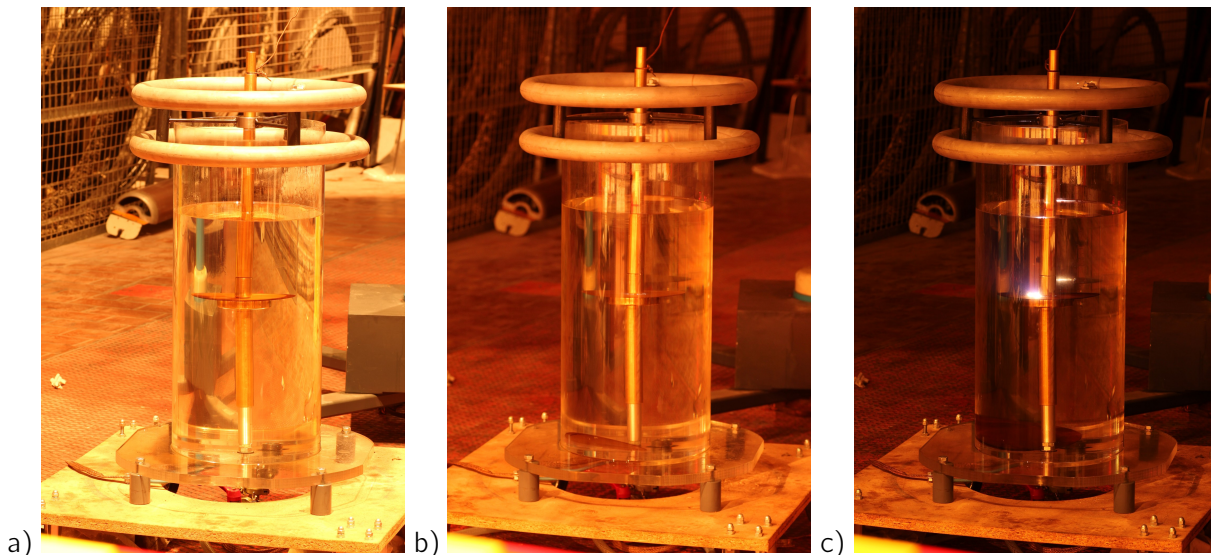


Figure D.1: Impulse voltage tests (BIL) on pressboard samples: a) Test set-up b) Surface discharges (no breakdown) c) Dielectric breakdown

D.4 Moisture content of pressboard

The moisture content of pressboard has been determined by Karl-Fischer-Titration with oven method. Pressboard is heated in a thermal oven and the moisture is transferred into the measurement cell with a dry nitrogen gas stream. The following equipment and items have been used:

- Titration stand: Metrohm 831 KF Coulometer
- Oven: Metrohm 688 KF Oven
- Titration reagent: Hydranal Coulomat AG Oven
- Titration solution: 2-Propanol alcohol (J.T.Baker 8175)
- Laboratory scale: A&D GR-300

The Standards IEC 60814 and VDE 0370-20 [155] respectively have been followed, but adapted as listed below:

1. Oven is preheated to around 200°C (instead of 135°C, as indicated in [155]). The nitrogen stream is adjusted around 8 litres per hour⁸
2. Wait until the drift has stabilized, currently a drift between 7 up to around 15 $\mu\text{g}/\text{min}$ can be achieved when using the oven method with this set-up.
3. Place a weighed pressboard sample of 0.3 to 0.5 g inside the weighing boat and introduce it into the oven. Sample weight has to be adapted to achieve a (measured) water content between 1.000 and 10.000 μg .
4. End of titration is reached, when the relative drift is below 5 $\mu\text{g}/\text{min}$ (device dependent).
5. Remove sample and weighing boat.
6. Weigh the sample again.
7. Put sample in hexane solvent to remove the impregnation oil (for around 15 minutes) and shake the flask constantly. Afterwards, the pressboard sample is placed in a thermal oven (115° C) for at least 30 minutes to securely remove the hexane from the pressboard.

⁸The standard defines a flow rate of 50 cm³ to 100 cm³ per minute = 3 to 6 l/h. The slightly higher volumetric flow rate was chosen to ensure a secure transportation of moisture out of the oven and into the titration vessel.

8. Weigh the sample again.
9. Calculate moisture content of the sample according the standard with the corrected weight.
10. The boat is put in an acetone bath, washed, dried and cleaned with a non-fuzzing tissue. Afterwards, the boat is placed into a thermal oven to remove the moisture and is transferred for cooling down and storing into an desiccator with silica gel.
11. Measurement is repeated at least twice (within this work) with a new sample and a new boat.



a)



b)

Figure D.2: Moisture determination of pressboard: a) Measurement set-up with KF Coulometer b) Weighing boat with sample in detail

E Ageing diagnosis: Mineral insulating oils

In the following section, the diagnostic methods which have been carried out for (mineral) insulating oils within this work are described in alphabetical order below.

E.1 Colour and appearance

The colour and the appearance of an insulation oil are not a critical parameter. However, they can give indication of possible oil ageing and property changes. The colour itself has no direct expressiveness, however, a change of colour can be the evidence for material ageing and/or for contaminants. The colour is determined by comparing small oil samples in test tubes against standardized colour sheets. In this case the “Farbtafel” which is part of the “VDEW Ölbuch” [137] was used.

Oil samples were placed in Duran FIOLAX test tubes with a thickness of 0,5 mm. All images have been taken with a Nikon D90 (ISO 640, 1/125s, F5,6) with a 18-200 mm lens (at 200 mm) against ambient light, as indicated in the specifications. Due to varied ambient lightning during the measurements, aperture and exposure time had to be changed for some images.

Appearance is also determined by visual inspection and checks the presence of sediments or sludge for example. For a detailed analysis, e.g. IEC 60422-Annex C (or VDE 0370-2 [154]) or ISO 2049 gives details.

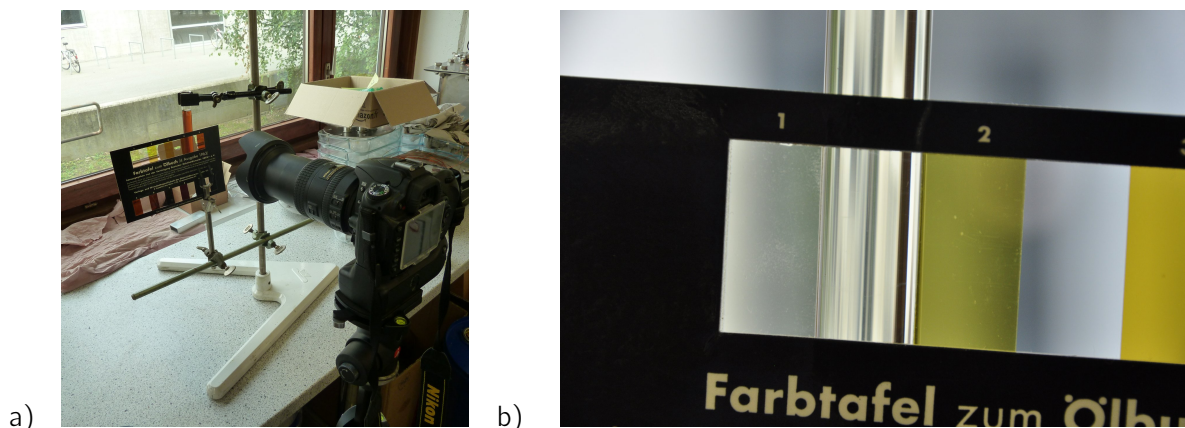


Figure E.1: Determining the colour of insulating oils: a.) Set-up b.) Exemplary image (new oil)

E.2 Dielectric parameters

The dielectric parameters relative permittivity ϵ_r and dielectric loss factor ($\tan(\delta)$) of insulations oils have been determination with a BAUR DTL within a temperature range between 30 and 105°C. The $\tan(\delta)$ and ϵ_r have been determined at AC with $U = 2000\text{ V}$.

Furthermore, specific resistivity of insulation oils has been determined also in the same procedure at $U = 500\text{ V DC}$. Before filling a new or different oil type, the complete measurement cell has been disassembled and thoroughly cleaned. After assembling and calibrating, the cell has been flushed up to 10 times with clean oil before starting a measurement series.

Details about the measurement procedure can be found in the standard IEC 60247 and VDE 0380-2 [157] respectively.

E.3 Moisture content of oil

Moisture content of oils has been determined with (coulometric) Karl-Fischer-Titration. Hereby, the following equipment has been used:

- Titration stand: Metrohm 831 KF Coulometer
- Analyte Hydranal Coulomat AG-H
- Catholyte Hydranal Coulomat CG
- Titration solution: 2-Propanol alcohol (J.T.Baker 8175)
- Laboratory scale A&D GR-300

Direct determination of oil moisture is achieved by injecting around 1 ml of oil into the KF titration vessel. This is done at least three times and the average moisture value is calculated. The process is carried out in the style of IEC 60814 (VDE 0370-20 [155]) with adoptions.

1. Flushing of the syringe : The syringe⁹ (capacity 5 ml) is filled (with around 3 ml; between half and full capacity) and shaken well. Afterwards, the whole content is disposed.
2. Filling of the syringe: The syringe is filled again with 5 ml, of which around 1 ml are disposed again and weighed afterwards. The standard VDE 0370-20 [155] requires a precision of 0,1 g at weighing, the available scale has a resolution of 0,1 mg.
3. Injection of sample into the titration vessel. A drift of less than 10 $\mu\text{g}/\text{min}$ is recommended by the coulometer manufacturer, in general the drift was below 3 $\mu\text{g}/\text{min}$.
4. Weigh the syringe again to determine the amount of liquid injected into the titration vessel.
5. Calculate the amount of moisture in the sample (done automatically by the Coulometer)
6. Repeat this process at least twice. Syringe will be flushed only once then in between and only for new oil samples; this is in contrary to the standard, where it is flushed twice. For aged samples, flushing is not conducted to use as little oil as possible. The syringe is kept sealed with the original cap when not in use (e.g. during titration cell stabilisation/conditioning).

⁹In contradiction to the standard, disposable plastic syringes instead of glass syringes are used

F Summarized list of equipment and materials used

This section lists briefly all equipment used within the scope of this work at the Institute of High Voltage Engineering and System Management at Graz University of Technology.

F.1 Apparatus

Current measurement

- Electrometer Keithley 617
- Electrometer Keithley 6514
- Protective circuits (customized)
- Multiplexer: Keithley 705 Scanner with 7058 Low Current Card

Voltage measurement

- Keithley 195A Digital Multimeter
- Prema 5014 Digital Multimeter
- Tektronix HV probe P6015 and P6015A
- Fluke 80K - 40 H.V. probe

Voltage sources

- Danbridge DB604 megohmmeter, 0... + 5 kV
- fug HCE 7 - 12500 POS, 0... + 12,5 kV
- Heinzinger HNCs, 0... + 30 kV
- Heinzinger PNC 30000-2, 0... ± 30 kV

Dielectric test cells and equipment

- Tettex 2903a + Heating 2903
- Tettex 2904
- BAUR DTL
- Customized test cells (also used for combined ageing)
- Customized temperature controller (PID with Pt100 input)
- Digital bridge-vector LDIC LDV-6

Chemical diagnosis

- KFT: Metrohm 831 KF Coulometer, Oven: Metrohm 688 KF Oven
- Scale: A&D GR-300

Vacuum apparatus

- Oven: Heraeus VT6130
- Vacuum pump: Pfeiffer DUO20MC
- Vacuum sensor: Pfeiffer TPR281 (Pirani) and TPG2612 (Display)
- Other vacuum equipment: Pumps: Leybold-Heraeus LH D8A, LH D2A; Sensor: LH 16202 B3; Display: LH Thermovac TM 211
- All tubing and connections are realised either in stainless steel or PTFE

Temperature measurement

- IR: Raytek Raynger ST2
- For Tettex test cells: Yokogawa DX1006 with thermocouples (Type K) + Internal Pt100 sensor (Tettex 2903)
- For Ageing: Customized Pt100 (30 channels) and TC (Type T, 16 channels) systems

Impulse voltage testing

- Haefely Impulse Generator 800 kV
- Siemens voltage divider SMCF 1000/800
- Impulse voltage recorder Dr. Strauß Stoßspannungsmesssystem TR-AS 100-10
- Yokogawa DL 9040 (5 GS/s, 500 MHz)
- PMK PHV 641-L 1:100 probe

Protection circuit testing

- Haefely Impulse Generator 47 Ib
- Customized protection circuit
- Yokogawa DLM 2054 DSO
- PMK PHV 621 probe (1:100)
- LEM PR50 Current probe

Colour determination of mineral oils

- Colour chart according to VDEW
- Duran FIOLAX test tube, 16x130 (0,5 mm thickness)
- Camera Nikon D90 with 18-200 mm, F5,6, 1/125s, ISO 640

Microscope

- Reichert Biovar, Type 300404
- Lenses: SPI 40/065, 10/0,25 and 2,5/0,08
- Camera Bresser MikroCam 9

F.2 Vessels

- Glass vessels for thermal ageing: Pyrex 1490/04 (see Appendix B)
- Oil storage for samples: Duran bottles (0,5 and 1,0 litres), Aluminium containers (around 5 litres)
- Combined ageing and pressboard conductivity measurements: customized (stainless steel; see Appendix C)

F.3 Materials handling

- Syringes: B.Braun Injekt[®]5 ml / Luer Solo; HenkeSassWolf Norm-Ject [®]5 ml / Luer Lock
- Needles: B.Braun Sterican[®]Hypodermic-needle (0,90x40mm BI/BB), Size 1
- Pressboard holder during drying and impregnation process: Customized (stainless steel)
- Pressboard impregnation vessel: Glass vessel ("Aquarium Assistent", 220 x 250 x 180 mm)
- Whatman TE 37 (PTFE supported filter with 1 μ m pore size) in Schleicher & Schuell FP 050/1 filter holder (Polysulfone)

F.4 Pressboard

- Pressboard: WEIDMANN T IV, cylindrical discs, \varnothing 140 mm, thickness 1 mm (grinded); plain material for spacers; supplied by WEIDMANN Electrical Technology AG, Rapperswil
- Paper samples for additional PEA measurements: K-Buffer, \varnothing 55 mm, thickness 0,5 mm, supplied by WEIDMANN Electrical Technology AG, Rapperswil

F.5 Mineral oils

- Nynas Nytro 4000X, supplied by TU Graz (IHS) and Siemens Transformers Austria (Weiz), Datasheet on page A.3
- Shell Diala GX, supplied by TU Graz (IHS), Datasheet on page A.4
- Nynas Nytro 10XN, supplied by Nynas Austria, Datasheet on page A.5

F.6 Liquids

- 2-Propanol (99,5%; HPLC), Roth CP41.4, J.T.Baker 8175
- Acetone, 99,5%, Roth 5025.6, J.T.Baker 8002
- Cyclohexane, 99,5%, Roth 6570.3
- Ethanol, 99,8%, Roth K928.1
- Hexane (n-Hexane), Sigma-Aldrich 208752
- Hydranal Coulomat AG-H, Fluka 34843
- Hydranal Coulomat CG, Fluka 34840
- Hydranal AG Oven, Fluka 34739
- Hydranal Water Standard Oil, Fluka 34694
- KOH in 2-Propanol, Fluka 35008
- Methanol (HPLC), Roth X948.1

F.7 Other Materials

- Steel sheets for ageing tests: 105-30H (Manufacturer Euro-Mit Staal B.V.), supplied by Siemens Transformers Austria GmbH & Co KG (Weiz)
- Copper sheets for ageing tests: Cu-DHP Nr. 2.0090 DIN 1787, supplied by Siemens Transformers Austria GmbH & Co KG (Weiz)

F.8 Other equipment

- Lint-free paper: Kimtech Science, Kimberly-Clark Professional 7552
- Cleaning paper: Roth cleaning tissues
- Soda lime, Roth 8652.1

Curriculum Vitae



Thomas Judendorfer was born in Steyr, Upper Austria in 1982. He received his secondary school degree from HTL Steyr in 2001 in the field of mechanical engineering. In 2002 he started his studies of electrical engineering at Graz University of Technology. In 2007 he received his master's degree (Dipl.-Ing.) in Energy Management Technology - *High Voltage Engineering* with distinction. Thereby, his master thesis took him to a research exchange lasting several months at the University of Edinburgh and Heriot-Watt University (Edinburgh Campus) between 2006 and 2007.

From 2006 to 2008 he was working as a part-time employee at the *Test institution of high voltage engineering Graz Ltd.* Since 2008 he is with the Institute of High Voltage Engineering and System Management, where he works as university research assistant.

He started his Ph.D. (Dissertation) work on the topic of oil-cellulose insulation systems in 2009. This project is conducted in cooperation with WEIDMANN Electrical Technology AG, Switzerland. Further, the project took him several times to Delft University of Technology, The Netherlands. These stays between 2009 and 2012 were particularly used for practical research in the field of space charges in cellulose.